

17-22
JULY
2016



19TH CONFERENCE ON DYNAMICAL PROCESSES IN EXCITED STATES OF SOLIDS

Book of Abstracts



Table of contents

1	Program	2
2	Monday 18th July 2016: Presentations	8
	Exceptional Excited State Dynamics in Lead Halide Perovskites for Light Emission and Solar Energy Conversion Applications, Zhu Haiming	8
	Laser Cooling of Solids: a journey into the cryogenic regime, Sheik-Bahae Mansoor	10
	Excitation of Local Centers in the Long-Wavelength Tail of Electron-Phonon Bands: Feasibility of Laser Cooling and Observation of Spontaneous Fluorescence Oscillations, Feofilov Sergey	11
	The Eu^{3+} charge transfer energy and position of Eu^{2+} ground level, an exception of the rule, Deren Przemyslaw	12
	Intervalence Coupling and Persistent Charge-transfer Luminescence in f-element Compounds, Liu Guokui	13
	Single-Molecule Study of Conformation-Related Photophysics in Conjugated Molecular Complexes and Organic Dye-Gold Nanoparticle Structures, Vacha Martin	14
	Transient two-dimensional infrared spectroscopy in a vibrational ladder, Kemlin Vincent [et al.]	15
	Coherent Energy Transfer in Light Harvesting Complexes: addressing single	

molecules on fs time scale, Van Hulst Niek F.	16
Vibrational dynamics of metal carbonyl complexes trapped in CH ₄ : a novel witness of solid methane's phase transition, Thon Raphael [et al.]	17
On the Fenna-Matthews-Olson Protein Complex of Green Sulfur Bacteria, Kell Adam [et al.]	18
3 Tuesday 19th July 2016: Presentations	19
The quantum realm of nanoplasmonics for active control of optoelectronics and ultraresolved spectroscopy, Aizpurua Javier	19
Raman Sensing and Imaging by Interference and Surface Enhancement Processes, Alvarez-Fraga Leo [et al.]	21
Effect of aggregates of silver nanostructures on the optical properties of Yb ³⁺ -doped RbTiOPO ₄ , Sanchez-Garcia Laura [et al.]	22
Plasmonic nanoantennas: bright and efficient nanosources, Esparza J. U.	23
Ultrafast size-dependent electronic interactions in small metal nanoparticles and clusters, Maioli Paolo [et al.]	24
Controlling energy transfer and radiative lifetimes in luminescent lanthanide complexes and materials, Bunzli Jean-Claude	25
Lanthanide-Doped Luminescent Nano-Bioprobes for In Vitro Detection of Tumor Markers, Chen Xueyuan [et al.]	26
Energy transfer processes in organic-sensitized Yb-doped NaYF ₄ nanoparticles, Lu Haizhou [et al.]	27
Engineering Core/Shell Rare Earth Nanoparticles for Ultimate Control Over Light Emitting Processes, Sun Lingdong [et al.]	28
NIR Nanomaterials for disease diagnostics and therapy, Zhang Fan	29

Nd ³⁺ Contactless Fluorescent Temperature Sensor, Orlovskii Yurii [et al.]	30
Mapping of local fields in solids by phononless fluorescence spectromicroscopy of single dye molecules, Andrey Naumov [et al.]	31
Optical microscopy and spectroscopy of single molecules and single plasmonic gold nanoparticles, Orrit Michel	32
Correlative atomic force and confocal fluorescence microscopy: Single molecule imaging and force induced spectral shifts, Basche Thomas [et al.]	33
Superradiance of molecular monolayers on insulating surfaces, Eisfeld Alexander [et al.]	34
Charge dynamics in organo-metal-halide perovskite nano-crystals probed by super-resolution optical micro-spectroscopy at the individual crystal level, Scheblykin Ivan [et al.]	35
Intrinsic optical properties of organic-inorganic hybrid perovskite MAPbI ₃ and its multiple stages of spontaneous and photo-induced structure transformation, Zhang Yong	36
Harvesting light through upconversion for photocatalysis applications, Ledoux Gilles	37
Exciton dynamics in perovskite CH ₃ NH ₃ PbI ₃ single crystals, Phuong Le Quang [et al.]	38
Dynamics of the Photoexcited States in Octahedral Mo ₆ Cluster Halides, Wada Yoshiki [et al.]	39
4 Wednesday 20th July 2016: Presentations	40
Photon conversion in the mid-infrared for gas sensing, Camy Patrice	40
Investigation of Thermal Quenching for Y ₃ Al ₅ O ₁₂ :Ce ³⁺ by Thermoluminescence Excitation Spectroscopy, Ueda Jumpei [et al.]	42

Controlled Electron-Hole Trapping and Detrapping Process in GdAlO ₃ by Valence Band Engineering, Luo Hongde [et al.]	43
Red phosphors based on hexafluorides doped with Mn ⁴⁺ . The new act of old game with 3d ³ system, Grinberg Marek [et al.]	44
Mn ⁴⁺ doped aluminate phosphors for warm white LEDs, Peng Mingying	45
Degradation processes in the red emitting phosphors Na ₂ MF ₆ -Mn ⁴⁺ (M = Si, Ti) exposed to thermal and blue LED irradiation stresses, Barros Anthony [et al.]	46
Ionoluminescence as a Tool to Investigate the Dynamics of Electronic Excitations in Dielectrics: the Case of SiO ₂ , Bachiller-Perea Diana [et al.]	47
Qubits in diamond: solid state quantum registers and nanoscale sensors, Jelezko Fedor	48
Lineshape in Spectra of Xe Center in Diamond: From Helium to Room Temperatures, Deshko Yury [et al.]	49
Ultra-narrow linewidth stoichiometric rare earth crystals for quantum information applications, Ahlefeldt Rose [et al.]	50
Optical pumping in Neodymium-doped yttrium orthosilicate, Cruzeiro Emmanuel [et al.]	51
High Resolution Spectroscopy of Single Erbium Sites in Silicon, Rancic Milos [et al.]	52
Smarter Modelling of Energy Levels of Rare-Earth Quantum-Information Candidates, Reid Michael	53
5 Thursday 21st July 2016: Presentations	54
Spin dynamics of charged and neutral excitons in colloidal nanocrystals, Yakovlev Dmitri	54

Local density of states and energy transfer in nanophotonics, Carminati Remi	56
Modification of phonon processes in nano-structured rare-earth-ion-doped materials, Veissier Lucile [et al.]	57
Spectroscopic properties of $\text{La}_{1-x}\text{Gd}_x\text{AlO}_3$ nanocrystals doped with Pr^{3+} ions, Lemanski Karol [et al.]	59
Hot intraband luminescence under different types of excitation, Omelkov Sergey [et al.]	60
Collective Higgs amplitude mode in superconductors studied by strong terahertz pulse, Matsunaga Ryusuke	61
Nonlinear optical spectroscopy on exciton states in model semiconductors GaAs and ZnO, Pisarev Roman	62
Exciton interband relaxation observed by time-resolved cyclotron resonance in diamond, Akimoto Ikuko [et al.]	64
Exciton dynamics in solid ZnO: UV luminescence of ZnO crystal and nanoparticles excited by femtosecond IR, UV and VUV laser pulses, Martin Patrick	65
Study of Exciton Dynamics in Multifunctional Oxides, Selim Farida [et al.]	66
Optical quantum memory based on rare-earth-ion doped crystals, Afzelius Mikael	67
Spin-wave storage of heralded single photons in a crystal, Seri Alessandro [et al.]	68
Rare-earth-activated Materials for Optical Frequency References, Thiel Charles [et al.]	69
Acousto-optic imaging using spectral holeburning in $\text{Tm}^{3+}:\text{YAG}$ crystals, Laureau Jean-Baptiste [et al.]	70

Towards quantum frequency conversion between atoms and light using rare earth ion dopants using cavity enhanced Raman heterodyne spectroscopy, Longdell Jevon [et al.]	71
Slow light based optical frequency shifter, Li Qian [et al.]	72
Energy Migration Upconversion in Spatially Separated Doping Nanostructures, Zhang Hong [et al.]	73
Controlling Photon Upconversion in Lanthanide-doped Nanocrystals, Liu Xiaogang	74
Modelling Blue to UV Upconversion in β -NaYF ₄ : 0.3% Tm ³⁺ , Villanueva-Delgado Pedro [et al.]	75
Design rules for multiple d-f emission bands in lanthanides, De Jong Mathijs [et al.]	76
High pressure study of cooperative luminescence of CaAl ₄ O ₇ :Yb ³⁺ , Suchocki Andrzej [et al.]	77
6 Friday 22nd July 2016: Presentations	78
Novel Optical Excited States of Nano-carbon and Atomically Thin Two-dimensional Materials, Matsuda Kazunari	78
Mid-infrared absorption imaging of a quantum degenerate exciton gas in cuprous oxide at 100 mK, Yoshioka Kosuke	80
Polariton-condensation effects on photoluminescence dynamics in a CuBr microcavity, Nakayama Masaaki [et al.]	81
Is there inter-valley Auger recombination in InGaAs/InP quantum wells?, Pusep Yuri [et al.]	82
Emission properties of GaN/AlN multi-quantum-wells under high hydrostatic pressure – experimental and ab-initio comparative study, Kaminska Agata [et al.]	83

Pressure induced mechano-chemistry in molecular solids, Chronister Eric	84
Excitation-induced processes in model molecular solid N ₂ , Savchenko Elena	85
Vibronic Spectra of Frenkel Excitons in a 2-Dimensional Polyacene Lattice, Hartmann Thomas [et al.]	86
Experimental Evidence of Enhancement of Optical Magnetization by Magnetic Torque, Rand Stephen [et al.]	87
7 Poster Session I	88
Tunable luminescence from silico-carnotite type double silicates doped with Tb ³⁺ and Eu ³⁺ , Bettinelli Marco	94
Divalent bismuth doped deep red scintillating materials for X-ray detection, Li Liyi [et al.]	95
Photoluminescence properties and energy transfer via multi luminescent centers of Sr ₂ MgAl ₂₂ O ₃₆ :Ce ³⁺ phosphor for near UV-pumped white LEDs, Bingfu Lei	96
Spectroscopic properties of Ce ³⁺ in the cuspidine-type oxide nitride compound Y ₄ Si _{2-x} Al _x O _{7+x} N _{2-x} , Lazarowska Agata [et al.]	97
Photoluminescence evolution with illumination time in CH ₃ NH ₃ PbI _{3-x} Cl _x thin films and MAPbI ₃ crystals, Coya Carmen [et al.]	98
New phosphor MgCa ₃ Si ₂ O ₈ : Eu ²⁺ , energy level location of Ln ³⁺ and Ln ²⁺ in MgCa ₃ Si ₂ O ₈ , Stefanska Dagmara [et al.]	99
Cr ³⁺ -Nd ³⁺ energy transfer in novel whitlockite phosphor Ca ₉ Cr(PO ₄) ₇ :Nd ³⁺ ions, Watras Adam [et al.]	100
Synthesis and spectroscopic characterization of Ca ₉ Al _{1-x} Cr _x (PO ₄) ₇ (x = 0,1-1) powders, Miniajluk Natalia [et al.]	101

Meta-stability of silicate phosphors, Jeon Byungjoo [et al.]	102
Single crystal phosphors for high-power laser lighting, Kang Taewook [et al.]	103
Strong blue absorption in heavy Mn-doped phosphors, Park Kwangwon [et al.]	104
Temperature-Dependent Photoluminescence Lifetimes of Cu-Doped Zn-In-S Quantum Dots, Zhao Jialong	105
High density excitation with alpha particles, Wolszczak Weronika [et al.]	106
The Vacuum Referred Binding Energies of Bi ³⁺ in wide band gap compounds, Awater Roy [et al.]	107
Luminescence of defective monoclinic zirconia prepared in a solar furnace, Sildos Ilmo [et al.]	108
Luminescence investigations of ZnGa ₂ O ₄ : Mn ²⁺ and ZnGa ₂ O ₄ : Mn ²⁺ , Eu ³⁺ compounds with spinel structure, Kravets Oleg [et al.]	109
Dynamics of electron photoexcited states on the TiO ₂ – xanthene dyes interface, Ibrayev Niyazbek [et al.]	110
Luminescent properties of Eu ³⁺ doped SrKB ₅ O ₉ , Bondzior Bartosz [et al.]	111
Optical spectroscopy and EPR studies of Mn ²⁺ ions in YAlO ₃ , Zhydachevskii Yaroslav [et al.]	112
Optical and Electron Paramagnetic Resonance Spectroscopy of Yb ³⁺ :Y ₂ SiO ₅ , Welinski Sacha [et al.]	113
Mechanism of luminescence enhancement of SrSi ₂ O ₂ N ₂ :Eu phosphor via manganese addition, Barzowska Justyna [et al.]	114
Eu(II) luminescence properties in hydrides and hydride fluorides, Kunkel Nathalie [et al.]	115

The luminescence of electronic excitations in alkali halide crystals at lattice symmetry lowering, Shunkeyev Kuanyshbek [et al.]	116
Morphology Control and Upconversion Luminescence Properties of Monoclinic $\text{Y}_2\text{WO}_6:\text{Yb}^{3+}/\text{Er}^{3+}$, Chen Cuili [et al.]	117
Combustion Synthesis and Luminescence Properties of $\text{Sr}_3\text{La}_2(\text{BO}_3)_4:\text{Eu}^{3+}$ Phosphors, Cai Peiqing [et al.]	118
Spectroscopic study of materials doped rare-earth ions, Bitam Adel [et al.]	119
Confined Excitons in $\text{CdF}_2\text{-CaF}_2$ Superlattices, Ivanovskikh Konstantin	120
High-pressure photoluminescence spectroscopy of codoped $\text{LiNbO}_3:\text{Cr}^{3+}; \text{W}^{4+}$ crystals., Sanchez-Alejo Marco [et al.]	121
Luminescence properties of different Eu sites in $\text{Ba}_2\text{K}(\text{PO}_3)_5$ doped with Eu^{2+} and Eu^{3+} , Baran Anna [et al.]	122
Luminescence Properties of Silicate Apatite Phosphors $\text{M}_2\text{La}_8\text{Si}_6\text{O}_{26}:\text{Eu}$ ($\text{M} = \text{Mg}, \text{Ca}, \text{Sr}$), Khaidukov Nikolai [et al.]	123
Optically Properties of K_2SO_4 Doped by Transition Metal Ions, Tussupbekova Ainura [et al.]	124
Energy transfer and Spectroscopic Properties of UV Active Media $\text{Ce}^{3+}:\text{LiCa}_{1-x}\text{Sr}_x\text{AlF}_6$, Shavelev Alexey [et al.]	125
Theoretical study on photoinduced nucleation dynamics by injection of THz optical pulses, Ishida Kunio [et al.]	126
Ultra-short Pulse Lasing from $\text{LiLu}_{0.7}\text{Y}_{0.3}\text{F}_4:\text{Ce}^{3+}$, Nizamutdinov Alexey [et al.]	127
$\text{YAG}:\text{Ce}^{3+}$ nanoceramics: spectroscopy, dynamics and TSL, Shi Q. [et al.]	128
Radiative and nonradiative recombination in Si-doped InN thin films, Jang	

Dynamics of changes in optical absorption induced by exposition to short- and long-wavelength radiation in the BTO:Al crystal, Shandarov Stanislav [et al.] 130

Basic Principles of Ion Beam Induced Luminescence and its Application to the Study of Electronic Excitation in Insulators, Bachiller-Perea Diana [et al.] 131

Theoretical modeling of transition metals tetroxoanions adsorption on N(B)-doped single-walled carbon nanotubes and graphene, Hizhnyi Yuriy [et al.] 132

Luminescence and Upconversion spectroscopy of Er³⁺/Yb³⁺-doped Y₃Ga₅O₁₂ nano-garnets for optical nano-devices, Monteseuro Virginia [et al.] 133

Blue upconversion emission of Cu²⁺ ions sensitized by Yb³⁺-trimers in CaF₂, Weiping Qin [et al.] 135

Energy migration in doped crystals, Rabouw Freddy [et al.] 136

Luminescent properties of Ce³⁺-activated germanate scintillating glasses, Qian Shan [et al.] 137

The Influence of Point Defects on Amplification and Spectral Characteristics of InGaAs-based Laser Diode Arrays, Platnitskaya Katsiaryna [et al.] 138

The Excited States of Gallium and Nitrogen Vacancies in the GaN/AlN Heterointerface and Its Relaxation, Lebiadok Yahor [et al.] 139

Photonic Effects on Magnetic Dipole Transition Probabilities, Wang Z. J. [et al.] 140

Carbon segregation phenomena on Fe_{0.85}Al_{0.15}(110) : a STM, LEED and XPS study, Dai Z. 141

Quantum wells based structures tested by polarized photoreflectance at room temperature, Gonzalez-Fernandez J. V. 142

Narrowing of excitation band in nanophosphors, Kim Hyojun [et al.]	143
Towards cavity-enhanced single rare earth ion detection, Casabone Bernardo [et al.]	144
Towards bulk crystal coherence times in $\text{Eu}^{3+}:\text{Y}_2\text{O}_3$ nanocrystals, Bartholomew John [et al.]	145
Persistent optical hole-burning spectroscopy of nano-confined dye molecules in liquid at room temperature: optical memory in liquid?, Murakami Hiroshi	146
Fluorescence microscopy of single organo-metal halide perovskite nanowires: effect of crystal-phase transition, Dobrovolsky Alexander [et al.]	147
Optical properties of quantum dots coupled to cone-shaped nanoantennas, Scherzinger Kerstin	148
Polarized photoluminescence of carbon dots, Nelson Dmitrii [et al.]	149
Investigation of highly efficient energy transfer in porphyrin molecules/ carbon nanotubes nanoassemblies, Delport Geraud	150
Optical Properties of Graphene Nanoribbons, Delport Geraud [et al.]	151
Lanthanide-ion-doped NaYF_4 upconversion nanophosphores: optical spectroscopy of single particles, Vainer Yuri [et al.]	152
Influence of plasmon silver films on photoinduced electronic processes in polymeric films of poly (3-hexylthiophene), Afanasyev Dmitriy [et al.]	153
Anomalous exciton diffusion in disordered wire-like materials, Giorgis Valentina [et al.]	154
Photodynamic antimicrobial chemotherapy using zinc phthalocyanines in the treatment of bacterial infection, Chen Zhuo [et al.]	155
Thermoelectric properties of disordered molecular wires with electron-vibron	

interaction, Diaz Elena [et al.]	156
Mechanisms of Protoporphyrin IX Delayed Fluorescence, Vinklarek Ivo [et al.]	157
Study of the thermal stability of the green fluorescent protein in the range 20-100C, Han T. P. J. [et al.]	158
Dephasing mechanisms in transparent ceramics with narrow optical linewidths, Kunkel Nathalie [et al.]	159
An Infrared Pump-Probe Measurement of the $6H7/2$ Lifetime of Sm^{3+} in $LiYF_4$, Wells Jon-Paul [et al.]	160
Time Evolution of Softening of Coherent Phonon in Antimony, Nakayama Sho	161
Robust photon-echo generation in quantum dots using a pair of chirp pulses, Sato Yoshitaka [et al.]	162
Complex Quantum Beats of Excitons in Quantum Dots observed using Three-Pulse Photon Echo, Yuto Arai [et al.]	163
Appearance of coherent LO phonons during the decay of LO-phonon-plasmon coupled mode in an undoped GaAs/n-type GaAs epitaxial structure, Sumioka Takahiro [et al.]	164
Compact ultrafast X-ray and gamma-ray source driven by intense femtosecond laser pulses, Li Ruxin [et al.]	165
Role of dynamical symmetry in an effective time-independent Hamiltonian for a laser-driven system, Inoue Jun-Ichi	166
8 Poster Session II	167
Pulse photoconductivity and light-induced absorption in undoped photorefractive $Bi_{12}SiO_{20}$ and $Bi_{12}TiO_{20}$ crystals, Kornienko Tatiana [et al.]	173

Spectroscopic properties of $\text{Eu}^{3+}:\text{GdBO}_3$ nanopowders obtained by the sol-gel method, Seraiche Mourad [et al.]	174
Energy relaxation processes in $\text{Zn}_x\text{Mg}_{1-x}\text{WO}_4$ mixed crystals, Krutyak Nataliya [et al.]	175
Spectroscopy of Er^{3+} ions in $\text{Li}_5\text{La}_3\text{Nb}_2\text{O}_{12}$ garnets., Munoz-Santiuste Juan E.	176
Photoluminescence properties of nanoporous anodic alumina alloyed with manganese ions, Mukhurov Mikolai	177
Influence of crystal field on optical properties of $\text{KNaSiF}_6:\text{Mn}^{4+}$ phosphor at ambient and high hydrostatic pressure, Lesniewski Tadeusz [et al.]	178
Influence of the compensation defects on the luminescence of $\text{Sr}_2\text{SiO}_4:\text{Eu}^{3+}$ and $\text{Sr}_2\text{SiO}_4:\text{Eu}^{2+}$, Szczodrowski Karol [et al.]	179
Investigating the thermal stability of luminescence from some w-LED phosphors, Sharma Suchinder [et al.]	180
Up-conversion luminescence – a new property in tenebrescent Hackmanites, Norrbo Isabella [et al.]	181
Research the centers of electron capture in K_2SO_4 , Tussupbekova Ainura [et al.]	182
Green Emitting $\text{Ca}_3\text{SiO}_4\text{Cl}_2:\text{Eu}^{2+}$ Phosphor for Blue Converted White LEDs, Joshi Charusheela	183
Scintillation properties of alkaline metal doped LiCaAlF_6 , Yanagida Takayuki [et al.]	184
$\text{ZnGa}_2\text{O}_4:\text{Cr}$ and $\text{ZnGa}_2\text{O}_4:\text{Cr},\text{Bi}$ as new temperature sensing phosphors, Glais Estelle [et al.]	185
Defect luminescence and relaxation kinetics in amorphous yttrium-alumino-borate (α -YAB) phosphors, Sontakke Atul [et al.]	186

Dynamics of Sensitization in (Cr,Nd,Yb):YAG Ceramics, Lupei Voicu [et al.]	187
Electron-phonon interaction of Pr ³⁺ and Sm ³⁺ in YAG, Lupei Aurelia [et al.]	189
Effects of Si Codoping on Optical Properties of Ce-doped Ca ₆ BaP ₄ O ₁₇ from First-Principles Calculations, Ning Lixin [et al.]	190
Ponderomotive forces mediate UV solid-state laser operation, Semashko Vadim [et al.]	191
Propagating, Confined and Interface Acoustic Phonon Modes in GaN/AlN Quantum Wells, Zan Yuhai [et al.]	192
Luminescence Properties of Organic-Inorganic Layered Perovskite-Type Compounds under Vacuum Ultraviolet Irradiation, Kawano Naoki [et al.]	193
Cyclical Changes in Optical Properties of SrTiO ₃ Structure, Gorbenko Vitaliy [et al.]	194
Polariton-like propagation of photoluminescence from exciton-exciton scattering in a GaAs/AlAs multiple-quantum-well structure, Furukawa Yoshiaki [et al.]	195
X-ray excited luminescence of Ba ₂ MgSi ₂ O ₇ :Eu ²⁺ , Liang Hongbin [et al.]	196
Ce ³⁺ to Tb ³⁺ Energy Transfer in Ce ₂ (SO ₄), Iyer Muley Aarti [et al.]	197
Luminescence Study of SrB ₄ O ₇ : Sm ²⁺ as Multimode Temperature Sensor with High Sensitivity, Cao Zhongmin	198
Pathways of relaxation excited states of Pr ³⁺ in Y ₂ Si ₂ O ₇ : Pr ³⁺ , Yb ³⁺ , Grzeszkiewicz Karina [et al.]	199
Chromium Pairs in Combustion Synthesized alpha-Alumina, Krebs John [et al.]	200

Energy Transfer between Different Transitions within Rare-earth Ions, Zhong Jiuping	201
Peculiarities of $\text{Er}^{3+} \leftrightarrow \text{Yb}^{3+}$ energy transfer in $\text{CaSc}_2\text{O}_4:\text{Er}:\text{Yb}$, Stefan Angela [et al.]	202
Initial process of photoluminescence dynamics in a β - Ga_2O_3 single crystal, Yamaoka Suguru [et al.]	203
Luminescence of Ce^{3+} ion Activated Potassium Gadolinium Pyrosilicates Phosphor under Vacuum Ultraviolet and X-Rays Excitation, Haiyong Ni [et al.]	204
Near-infrared Spectroscopy of Lattice Defects in Anion-defective Sapphire at 4-300 K, Mamytbekov Zhayloo [et al.]	205
Influence of synthesis parameters on the spectroscopic properties of $\text{Ca}_9\text{Y}(\text{PO}_4)_7$ doped with $\text{Eu}^{3+}, \text{Eu}^{2+}$, Gorecka Natalia [et al.]	206
Photoemission Calculations using Projection Operator Method for Metals and Semiconductors., Bawitlung Zoliana [et al.]	207
Luminescence properties and energy transfer of $\text{GdBO}_3:\text{Ce}^{3+}, \text{Tb}^{3+}$ phosphor, Zhang Qihong [et al.]	208
MREI-model Calculation of Two-mode Property of Bulk Transverse Optical Phonons and Its Influence on Electronic Mobility in $\text{Al}_x\text{Ga}_{1-x}\text{N}/\text{GaN}$ Quantum Well, Zhuo Gu [et al.]	209
Anomalous Polaritonic Luminescence from Rare-Gas Solids, Ogurtsov Alexander [et al.]	210
Nonlinear composition dependent optical spectroscopy of $\text{Ba}_2\text{xSr}_{2-2\text{x}}\text{V}_2\text{O}_7$, Fang Hongwei [et al.]	211
The environmental factor model: a tool for the design of Eu^{2+} -doped orthophosphate phosphors?, Amer Mariam [et al.]	212

Relaxation through conical intersection: quantum friction of pseudorotation and Slonczewki resonances, Pae Kaja	213
Electroluminescence of PLZT Relaxor Ceramics at Fast-rising Electric Fields, Kallaev Suleyman [et al.]	214
Green Emission of U ⁶⁺ activated Lithium based Tungstates, Pote Swapnil	216
Tunable and White-Light Emission nitride phosphors Ca ₂ Si ₅ N ₈ :Ce ³⁺ ,Na ⁺ , Eu ²⁺ , Jiao Huan [et al.]	217
TDDFT study of thiocarbonyl compounds in RAFT polymerization, Ouddai Nadia	218
Thermoluminescence of novel lanthanum oxide obtained by a glycine-based solution combustion method, Orante-Barron Victor [et al.]	219
Thermoluminescence of novel zinc oxide nanophosphors obtained by glycine-based solution combustion synthesis, Orante-Barron Victor [et al.]	220
Plasmon-assisted upconversion energy-transfer in Er ³⁺ ,Yb ³⁺ :LiNbO ₃ , Hernandez-Pinilla David [et al.]	221
Investigation on Emission and Topological Phase Transition of Individual NaREF ₄ Nanoparticle, Yan Chun-Hua [et al.]	222
Photon avalanche upconversion in rare-earth doped nanoparticles, Kornher Thomas [et al.]	224
Towards better understanding of the persistent luminescent properties of Cr-doped and Cr, Bi-doped ZnGa ₂ O ₄ nanoparticles, Pellerin Morgane [et al.]	225
Influence of optical phonons on the electronic mobility in Al ₂ O ₃ /AlGa _N /Ga _N double heterojunctions, Zhou Xiaojuan	226
Optical Properties of CdTe Quantum Dot Superlattices Self-Organized with Electrostatic Interaction, Watanabe Taichi [et al.]	227

Single Donor-Acceptor Pair Attached to a Protein Molecule as a Tool for Studying Folding/Unfolding Fluctuations in the Protein, Osad'ko Igor	228
Synthesis and spectroscopic properties of cage-like SrAl ₂ O ₄ :Eu ²⁺ microspheres via a sol-gel method, Qiao Xusheng	229
Au Islands Enhanced Luminescence of Er ³⁺ /Yb ³⁺ Co-Doped Gd ₂ (MoO ₄) ₃ Thin Films and Application in Temperature Sensing, Hao Haoyue [et al.]	230
Enhance the sensitivity of optical thermometer based on non-thermally coupled levels of Tm ³⁺ , Lu Hongyu [et al.]	231
Metal transition ion implantation on Ga ₂ O ₃ nanowires, Gonzalo Alicia [et al.]	232
Formation of chelated rare earth clusters in porous sol-gel silicate materials, Silversmith Ann [et al.]	233
Transport and recombination of photo-injected electrons in Dye-sensitized solar cells based ZnO nanostructures, Ilyassov Baurzhan [et al.]	234
Study of surface effect on photoassisted field emission from Ta(112) and Ti(0001) by using the Transfer Hamiltonian method, Chawngthu Rosangliana	235
Light induced toxicity of rare earth doped trifluoride crystalline nanoparticles, Pudovkin Maksim [et al.]	236
Optical thermometry of Er ³⁺ -doped transparent NaYb ₂ F ₇ glass-ceramics, Hu Fangfang [et al.]	237
Enhanced near-infrared response of c-Si solar cell using YVO ₄ : Bi ³⁺ , Ln ³⁺ (Ln = Yb and Nd) phosphors, Joshi Charusheela	238
Photo-Physical Properties of Spin-Coated Lead Halide Perovskite Thin Films, Sun Kien Wen	239
Frequency selective transient and permanent spectral hole burning processes in Ce:YSO at liquid helium temperatures, Karlsson Jenny [et al.]	240

Intersubband optical absorption between multi energy levels in InGaN/GaN spherical core-shell quantum dots, Liu Wen-Hao [et al.]	241
Directionally solidified Ce:LaBr ₃ / CaBr ₂ eutectic scintillator for radiation imaging applications, Kamada Kei [et al.]	242
Electronic Structure of Optical Properties of Host Material (Gd ₂ O ₂ S, Gd ₂ O ₃ and Gd ₂ O _{3-x} S _x)for Upconversion Phosphor Computational Modeling, Fei Wang	243
Giant negative magnetoresistance in oxygen-deficient Mn-substituted ZnO, Ruotolo Antonio	244
Epitaxial Seeded Growth of Rare Earth Nanocrystals with Efficient 800 nm Near-Infrared to 1525 nm Short-Wavelength Infrared Downconversion Photoluminescence for in vivo Bioimaging, Wang Rui [et al.]	245
Single-band upconversion nanoprobe for multiplexed simultaneous in situ molecular mapping of cancer biomarkers, Lei Zhou [et al.]	247
A many-particle quantum-kinetic formalism for describing emission properties of single quantum objects in frozen environments, Gladush Maxim [et al.]	248
Author Index	249

Chapter 1

Program

Sunday, 17 July	
16:00-19:00	Registration
Monday, 18 July	
8:00-9:30	Registration
9:30 -10:00	Opening Ceremony
10:00-10:45	<p style="text-align: center;">Sturge Prize Ceremony and Lecture Exceptional Excited State Dynamics in Lead Halide Perovskites for Light Emission and Solar Energy Conversion Applications Haiming Zhu</p>
10:45-11:15	Coffee break
Session: Doped Insulators	
11:15-12:00	<p style="text-align: center;">Laser Cooling of Solids: a journey into the cryogenic regime Mansoor Sheik-Bahae (Tutorial)</p>
12:00-12:15	<p style="text-align: center;">Excitation of Local Centers in the Long-Wavelength Tail of Electron-Phonon Bands: Feasibility of Laser Cooling and Observation of Spontaneous Fluorescence Oscillations, S.P. Feofilov, A.B. Kulinkin, V.A. Konyushkin, A.N. Nakladov</p>
12:15-12:30	<p style="text-align: center;">The Eu³⁺ charge transfer energy and position of Eu²⁺ ground level, an exception of the rule, P.J. Dereń, G. Banach, B. Brzostowski, K. Lemański, W. Walerczyk</p>
12:30-12:45	<p style="text-align: center;">Intervalence Coupling and Persistent Charge-transfer Luminescence in f-element Compounds, Guokui Liu, Shuao Wang, Thomas E. Albrecht-Schmitt</p>
12:45-14:45	Lunch
Session: Molecular Systems	
14:45-15:15	<p style="text-align: center;">Single-Molecule Study of Conformation-Related Photophysics in Conjugated Molecular Complexes and Organic Dye-Gold Nanoparticle Structures Martin Vacha (Invited)</p>
15:15-15:45	<p style="text-align: center;">Transient two-dimensional infrared spectroscopy in a vibrational ladder Vincent Kemlin, Adeline Bonvalet, Louis Daniault, Manuel Joffre (Invited)</p>
15:45-16:15	<p style="text-align: center;">Coherent Energy Transfer in Light Harvesting Complexes: addressing single molecules on fs time scale Niek van Hulst (Invited)</p>
16:15-16:30	<p style="text-align: center;">Vibrational dynamics of metal carbonyl complexes trapped in CH₄: a novel witness of solid methane's phase transition, Raphael Thon, Wutharath Chin, Didier Chamma, Jean-Pierre Galaup, Claudine Crépin</p>
16:30-16:45	<p style="text-align: center;">On the Fenna-Matthews-Olson Protein Complex of Green Sulfur Bacteria Adam Kell, Robert Blankenship, Ryszard Jankowiak</p>
16:45-17:15	Coffee break
17:15-19:15	Poster Session I

Tuesday, 19 July	
	Session: Plasmonics
8:30-9:15	The quantum realm of nanoplasmonics for active control of optoelectronics and ultra-resolved spectroscopy, Javier Aizpurua (Tutorial)
9:15-9:45	Raman Sensing and Imaging by Interference and Surface Enhancement Processes, Leo Alvarez-Fraga, Felix Jimenez-Villacorta, Esteban Climent-Pascual, Rafael Ramirez-Jimenez, Carlos Prieto, Alicia de Andres (Invited)
9:45-10:00	Effect of aggregates of silver nanostructures on the optical properties of Yb³⁺ doped RbTiOPO₄, Laura Sanchez-García, Christos Tserkezis, Maria O Ramirez, Pablo Molina, Joan Carvajal, Magdalena Aguiló, Francesc Díaz, Javier Aizpurua, Luisa Bausá
10:00-10:15	Plasmonic nanoantennas: bright and efficient nanosources A. Raj Dhawan, J. U. Esparza, C. Belacel, C. Schwob, M. Nasilowski, B. Dubertret, L. Coolen, P. Senellart, A. Maître
10:15-10:30	Ultrafast size-dependent electronic interactions in small metal nanoparticles and clusters, Paolo Maioli, Tatjana Stoll, Denis Mongin, Michel Pellarin, Matthias Hillenkamp, Michel Broyer, Aurélien Crut, Fabrice Vallée, Natalia Del Fatti
10:30-11:00	Coffee break
	Session: Sensors
11:00-11:30	Controlling energy transfer and radiative lifetimes in luminescent lanthanide complexes and materials, Jean-Claude Bünzli (Invited)
11:30-12:00	Lanthanide-Doped Luminescent Nano-Bioprobes for In Vitro Detection of Tumor Markers, Xueyuan Chen, Wei Zheng, Shanyong Zhou, Datao Tu, Ping Huang, Jin Xu (Invited)
12:00-12:15	Energy transfer processes in organic-sensitized Yb-doped NaYF₄ nanoparticles, Haizhou Lu, Yu Peng, Huanqing Ye, Xianjin Cui, Mark Green, Philip Blower, Peter Wyatt, William Gillin, Ignacio Hernandez
12:15-12:30	Engineering Core/Shell Rare Earth Nanoparticles for Ultimate Control Over Light Emitting Processes, Lingdong Sun, Hao Dong, Yang Li, Chun-Hua Yan
12:30-12:45	NIR Nanomaterials for disease diagnostics and therapy, Fan Zhang
12:45-13:00	Nd³⁺ Contactless Fluorescent Temperature Sensor, Yurii Orlovskii, Kaarel Kaldvee, Stanislav Fedorenko, Laurits Puust, Alexander Vanetsev, Elena Orlovskaya, Martti Pärs, Ilmo Sildos
13:00-14:30	Lunch
	Session: Single Centers
14:30-15:00	Mapping of local fields in solids by phononless fluorescence spectromicroscopy of single dye molecules, Andrey Naumov, Tatiana Anikushina, Alexey Gorshelev, Maxim Gladush, Ivan Eremchev, Alina Golovanova, Lothar Kador, Jürgen Köhler (Invited)
15:00-15:30	Optical microscopy and spectroscopy of single molecules and single plasmonic gold nanoparticles, Michel Orrit (Invited)
15:30-15:45	Correlative atomic force and confocal fluorescence microscopy: Single molecule imaging and force induced spectral shifts, Thomas Basché, Sven Stöttinger, Gerald Hinze
15:45-16:00	Superradiance of molecular monolayers on insulating surfaces, Alexander Eisfeld, Alexander Paulheim, Christian Marquardt, Markus Müller, Moritz Sokolowski
16:00-16:15	Charge dynamics in organo-metal-halide perovskite nano-crystals probed by super-resolution optical micro-spectroscopy at the individual crystal level, Ivan Scheblykin, Yuxi Tian, Alexander Dobrovolsky, Daniela Täuber
16:15 16:45	Coffee break
	Session: Photovoltaic and Photocatalysis Materials
16:45-17:15	Intrinsic optical properties of organic-inorganic hybrid perovskite MAPbI₃ and its multiple stages of spontaneous and photo-induced structure transformation, Yong Zhang (Invited)
17:15-17:45	Harvesting light through upconversion for photocatalysis applications, G. Ledoux, B. Mahler, Y. Chen, S. Mishra, E.Jeanneau, M. Daniel, J. Zhang, S. Daniele (Invited)
17:45-18:00	Exciton dynamics in perovskite CH₃NH₃PbI₃ single crystals, Le Quang Phuong, Yumi Nakaike, Atsushi Wakamiya, Yoshihiko Kanemitsu
18:00-18:15	Dynamics of the Photoexcited States in Octahedral Mo₆ Cluster Halides, Yoshiki Wada, Norio Saito, Fabien Grasset, Stephane Cordier, Karine Costuas, Naoki Ohashi
18:15-20:15	Poster Session II

Wednesday, 20 July

Session: Doped Insulators and Defects	
8:30-9:00	Photon conversion in the mid-infrared for gas sensing, A. Braud, A.L. Pelé, J.L. Doualan, R. Chahal, V. Nazabal, B. Bureau, R. Moncorgé, P. Camy (Invited)
9:00-9:15	Investigation of Thermal Quenching for $Y_3Al_5O_{12}:Ce^{3+}$ by Thermoluminescence Excitation Spectroscopy, Jumpei Ueda, Pieter Dorenbos, Adrie Bos, Andries Meijerink, Tanabe Setsuhisa
9:15-9:30	Controlled Electron-Hole Trapping and Detrapping Process in $GdAlO_3$ by Valence Band Engineering, Hongde Luo, Adrie Bos, Pieter Dorenbos
9:30-9:45	Red phosphors based on hexafluorides doped with Mn^{4+}. The new act of old game with $3d^3$ system, Marek Grinberg, Sebastian Mahlik, Tadeusz Lesniewski, Agata Lazarowska, Ye Jin, Ru-Shi Liu
9:45-10:00	Mn^{4+} doped aluminate phosphors for warm white LEDs, Mingying Peng
10:00-10:15	Degradation processes in the red emitting phosphors $Na_2MF_6-Mn^{4+}$ (M = Si, Ti) exposed to thermal and blue LED irradiation stresses, Anthony Barros, Philippe Boutinaud, Geneviève Chadeyron, Rachid Mahiou
10:15-10:30	Ionoluminescence as a Tool to Investigate the Dynamics of Electronic Excitations in Dielectrics: the Case of SiO_2, Diana Bachiller-Perea, David Jiménez-Rey, Angel Muñoz-Martín, Fernando Agulló-López
10:30-11:00	Coffee break
Session: High Resolution and Coherent Spectroscopy	
11:00-11:45	Qubits in diamond: solid state quantum registers and nanoscale sensors, Fedor Jelezko (Tutorial)
11:45-12:00	Lineshape in Spectra of Xe Center in Diamond: From Helium to Room Temperatures, Yury Deshko, Anshel Gorokhovskiy
12:00-12:15	Ultra-narrow linewidth stoichiometric rare earth crystals for quantum information applications, Rose Ahlefeldt, Michael Hush, Matthew Sellars
12:15-12:30	Optical pumping in Neodymium-doped yttrium orthosilicate, Emmanuel Cruzeiro, Imam Usmani, Alexey Tiranov, Cyril Laplane, Jonathan Lavoie, Nicolas Gisin, Mikael Afzelius
12:30-12:45	High Resolution Spectroscopy of Single Erbium Sites in Silicon, Milos Rancic, Michael Reid, Matthew Sellars, Sven Rogge, Sebastian Horvath, Chunming Yin, Gabriele DeBoo, Qi Zhang
12:45-13:00	Smarter Modeling of Energy Levels of Rare-Earth Quantum-Information Candidates, M.F. Reid, S.P. Horvath, J.S. Stewart, J.-P.R. Wells
Free afternoon	

Thursday, 21 July	
	Session: Nanostructured Materials
8:30-9:00	Spin dynamics of charged and neutral excitons in colloidal nanocrystals, Dmitri Yakovlev (Invited)
9:00-9:30	Local density of states and energy transfer in nanophotonics Rémi Carminati (Invited)
9:30-9:45	Modification of phonon processes in nano-structured rare-earth-ion-doped materials, Lucile Veissier, Thomas Lutz, Charles Thiel, Philip Woodburn, Rufus Cone, Paul Barclay, Wolfgang Tittel
9:45-10:00	Spectroscopic properties of $\text{La}_{1-x}\text{Gd}_x\text{AlO}_3$ nanocrystals doped with Pr^{3+} ions K. Lemański, B. Bondzior, P.J. Dereń
10:00-10:30	Coffee break
	Session: Ultrafast Processes
10:30-11:00	Hot intraband luminescence under different types of excitation Sergey Omelkov, Vitali Nagirnyi, Marco Kirm (Invited)
11:00-11:30	Collective Higgs amplitude mode in superconductors studied by strong terahertz pulse, Ryusuke Matsunaga (Invited)
11:30-12:00	Nonlinear optical spectroscopy on exciton states in model semiconductors GaAs and ZnO, Roman Pisarev (Invited)
12:00-12:15	Exciton interband relaxation observed by time-resolved cyclotron resonance in diamond, Ikuko Akimoto, Nobuko Naka
12:15-12:30	Exciton dynamics in solid ZnO: UV luminescence of ZnO crystal and nanoparticles excited by femtosecond IR, UV and VUV laser pulses, P. Martin, A. Belsky, M. Dumergue, S. Petit, D. Descamps, A. Vasil'ev
12:30-12:45	Study of Exciton Dynamics in Multifunctional Oxides, Farida Selim, Pooneh Saadatkia, Buguo Wang, David Look
12:45-14:30	Lunch
	Session: Classical and Quantum Processing
14:30-15:00	Optical quantum memory based on rare-earth-ion doped crystals, Mikael Afzelius (Invited)
15:00-15:15	Spin-wave storage of heralded single photons in a crystal, Alessandro Seri, Daniel Rieländer, Andreas Lenhard, Margherita Mazzera, Hugues de Riedmatten
15:15-15:30	Rare-earth-activated Materials for Optical Frequency References, Charles Thiel, Thomas Böttger, Roger Macfarlane, Rufus Cone
15:30-15:45	Acousto-optic imaging using spectral holeburning in Tm^{3+}:YAG crystals, J.- B. Laudereau, A. Chauvet, A. Ferrier, Ph. Goldner, T. Chanelière, F. Ramaz
15:45-16:00	Towards quantum frequency conversion between atoms and light using rare earth ion dopants using cavity enhanced Raman heterodyne spectroscopy, Jevon Longdell, Xavier Fernandez-Gonzalvo, Yu-Hui Chen, Chunming Yin, Sven Rogge
16:00-16:15	Slow light based optical frequency shifter, Qian Li, Yupan Bao, Axel Thuresson, Adam Nilsson, Lars Rippe, Stefan Kröll
16:15-16:45	Coffee break
	Session: Rare Earth Doped Materials
16:45-17:15	Energy Migration Upconversion in Spatially Separated Doping Nanostructures, Hong Zhang, Langping Tu, Fei Wu, Jing Zuo, Xiaomin Liu, Xianggui Kong (Invited)
17:15-17:45	Controlling Photon Upconversion in Lanthanide-doped Nanocrystals, Xiaogang Liu (Invited)
17:45-18:00	Modelling Blue to UV Upconversion in $\beta\text{-NaYF}_4: 0.3\% \text{Tm}^{3+}$ Pedro Villanueva-Delgado, Karl W. Krämer, Rafael Valiente
18:00-18:15	Design rules for multiple d-f emission bands in lanthanides, Mathijs de Jong, Daniel Biner, Karl Krämer, Zoila Barandiarán, Luis Seijo, Andries Meijerink
18:15-18:30	High pressure study of cooperative luminescence of $\text{CaAl}_4\text{O}_7:\text{Yb}^{3+}$, Andrzej Suchocki, Dawid Jankowski, Małgorzata Puchalska, Artem Bercha, Witold Trzeciakowski
19:30	Conference Dinner

Friday, 22 July	
	Session: Semi-Conductors
8:45-9:30	Novel Optical Excited States of Nano-carbon and Atomically Thin Two-dimensional Materials Kazunari Matsuda (Tutorial)
9:30-10:00	Mid-infrared absorption imaging of a quantum degenerate exciton gas in cuprous oxide at 100 mK, Kosuke Yoshioka (Invited)
10:00-10:15	Polariton-condensation effects on photoluminescence dynamics in a CuBr microcavity, Masaaki Nakayama, Katsuya Murakami, Yoshiaki Furukawa
10:15-10:30	Is there inter-valley Auger recombination in InGaAs/InP quantum wells?, Yuri Pusep, Marco Tito, Alfred Gold, Marcio Teodoro, Gilmar Marques, Ray LaPierre
10:30-10:45	Emission properties of GaN/AlN multi-quantum-wells under high hydrostatic pressure – experimental and ab-initio comparative study, Agata Kaminska, Dawid Jankowski, Pawel Strak, Krzysztof Korona, Jolanta Borysiuk, Ewa Grzanka, Mark Beeler, Konrad Sakowski, Eva Monroy, Stanislaw Krukowski
10:45-11:15	Coffee break
	Session: Molecular Systems
11:15-11:45	Pressure induced mechano-chemistry in molecular solids, Eric L. Chronister, Andrew Rice, Sebastian Jezowski (Invited)
11:45-12:00	Excitation-induced processes in model molecular solid N₂, E.V. Savchenko, I.V. Khyzhniy, S.A. Uytunov, M.A. Bludov, A.P. Barabashov, G.B. Gumenchuk and V.E. Bondybey
12:00-12:15	Vibronic Spectra of Frenkel Excitons in a 2-Dimensional Polyacene Lattice, Thomas Hartmann, Christoph Warns, Ivan Lalov, Peter Reineker
12:15-12:30	Experimental Evidence of Enhancement of Optical Magnetization by Magnetic Torque Stephen Rand, E.F.C. Dreyer, P. Anisimov, A.A. Fisher
12:30-13:00	Closing Ceremony

Chapter 2

**Monday 18th July 2016:
Presentations**

Exceptional Excited State Dynamics in Lead Halide Perovskites for Light Emission and Solar Energy Conversion Applications

Haiming Zhu

Department of Chemistry, Zhejiang University

38 Zheda Road, Hangzhou, Zhejiang, China, 310027

Organic-inorganic hybrid lead halide perovskites have attracted intense research interests in last few years as low cost and high performance solar cell materials. In parallel with their rapid development in photovoltaics, here we focus on their emerging light emission, especially the lasing emission properties from perovskite nanostructures. We show room temperature lasing from solution grown perovskite nanowires with near unity quantum yield, high quality factor and broad wavelength tunability. Now, a major puzzle emerging from these results is why such solution grown defective semiconductors exhibit carrier properties expected from defect-free and nonpolar inorganic semiconductors. By combining different time-resolved spectroscopy techniques, we systematically investigated the hot carrier cooling, band edge carrier trapping and electron-hole radiative recombination process in perovskites with different cations. We show the unique role played by the organic cation and general positive properties for this family of materials. All these results point to an important design principle for new optoelectronic materials: introducing dynamic disorder and polaronic screening to make a defective semiconductor behave as a perfect one.

Laser Cooling of Solids: a journey into the cryogenic regime

Mansoor SHEIK-BAHAE

Department of Physics and Astronomy, University of New Mexico, United States
msb@unm.edu

Laser cooling of solids (also known as optical refrigeration) has advanced tremendously since its first experimental observation in 1995. Most recently, crystals doped with Yb ions have cooled to an absolute temperature of about 90K starting from room temperature, with even lower temperatures possible. Optical refrigeration is currently the only available technique for realizing an all-solid-state cryocooler. In this tutorial, I will present an overview of the recent advances in laser cooling of rare-earth doped crystals. I will also discuss the prospects of laser cooling in semiconductors including CdS nanostructures as well as bulk semiconductors such as GaAs.

Excitation of Local Centers in the Long-Wavelength Tail of Electron-Phonon Bands: Feasibility of Laser Cooling and Observation of Spontaneous Fluorescence Oscillations

S.P. Feofilov¹, A.B. Kulinkin¹, V.A. Konyushkin², A.N. Nakladov²

¹*Ioffe Institute, St. Petersburg, 194021, Russia*

²*Prokhorov General Physics Institute, Moscow, 119991, Russia*

Various insulating materials containing fluorescent local centers of different nature with electric dipole allowed transitions were studied under excitation in the long-wavelength tail of the absorption spectrum (“laser cooling regime”). The materials used include alkali halides with aggregate color centers, Eu^{2+} -doped crystals and fluorescent organic dye-doped polymers. The goal of our experiments was to find out whether it is possible to employ electric dipole allowed radiative transitions of local centers for optical refrigeration via the phonon-assisted anti-Stokes emission in the broad electron-phonon bands of the emission spectra. The concept proposed here is to cool via allowed electronic transitions with moderate vibronic coupling. The experimental observations support the possibility of using broad electron-phonon emission bands of electric dipole allowed radiative transitions for optical refrigeration of solids. All studied groups of materials are of interest for further studies aimed at finding new laser cooling media. The mechanisms responsible for the absence of observable optical refrigeration are discussed.

The electric dipole allowed $4f^65d^1-f^7$ fluorescence of CaS:Eu^{2+} crystals was studied under excitation in the long-wavelength tail of the absorption spectrum (the regime typical for laser cooling experiments). Optical bistability as well as transients/oscillations of fluorescence and temperature with characteristic times of about seconds were observed in thermally-isolated samples optically heated by the strong laser excitation. This peculiar oscillations may be considered as “relaxational oscillations” that occur in a strongly nonlinear system. The mechanism responsible for the observed bistability and transients is different from that reported for rare earth ions-doped insulators, semiconductor films and ferroelectrics.

References

- [1] S.P. Feofilov, A.B. Kulinkin, V.A. Konyushkin, A.N. Nakladov, *Opt. Mater.* **48** (2015) 75.
- [2] S.P. Feofilov, A.B. Kulinkin. *J. Lumin.* **170** (2016) 121.

The Eu^{3+} charge transfer energy and position of Eu^{2+} ground level, an exception of the rule

P.J. Dereń^a, G. Banach^b, B. Brzostowski^c, K. Lemański^a and W. Walerczyk^a

^a *Institute of Low Temperature and Structure Research, Polish Academy of Sciences, Okólna Street 2, 50-422 Wrocław, Poland,*

^b *DATA Sp. z o.o., ul. Fabryczna 10 53-609, Wrocław, Poland*

^c *Institute of Physics, University of Zielona Góra, ul. Prof. Szafrana 4a, 65-516 Zielona Góra, Poland*

corresponding author. P.Deren@int.pan.wroc.pl

It seems that a simple method for determination of the position of the Eu^{2+} ground level as the maximum of the $\text{O}^{2-} \rightarrow \text{Eu}^{3+}$ Charge Transfer (CT) transition [1] may not always be valid in the hosts where Eu^{3+} replaces for Ca^{2+} , Sr^{2+} , or Ba^{2+} .

Recently we published the results of spectroscopic investigations of $\text{CaAl}_2\text{SiO}_6$ doped with Eu^{3+} and Eu^{2+} [2]. This aluminosilicate has an energy band gap of 5.5 eV, the energy of the CT transition is as high as 5.1 eV. Accordingly to the so far applied formalism, the Eu^{2+} ground level lies just 0.4 eV below the conduction band. In spite of this, it is possible to observe strong transitions between the 4f and 5d electronic configurations i.e. broad emission with maximum at 2.36 eV and excitation spectrum with first maximum at 3.35 eV.

Our previous work [3], turned out to be very helpful in understanding of this phenomenon. This paper shows the results of the experiments and thorough discussion on the basis of exact structural analysis, and ab-initio calculations.

References:

- [1] P. Dorenbos, *The Eu^{3+} charge transfer energy and the relation with the band gap of compounds*, *J. Lumin.* 111 (2005) 89–104.
- [2] K. Lemański, W. Walerczyk, P. J. Dereń, *Luminescent properties of europium ions in $\text{CaAl}_2\text{SiO}_6$* *J. All. Comp.* Available online 26 February 2016
- [3] A. Watras, A. Matraszek P. Godlewska, I. Szczygieł, J. Wojtkiewicz, B. Brzostowski, G. Banach, J. Hanuza and P. J. Dereń, *The role of the Ca vacancy in the determination of the europium position in the energy gap, its valence state and spectroscopic properties in $\text{KCa}(\text{PO}_3)_3$* , *Phys. Chem. Chem. Phys.*, 2014, **16**, 5581-558,

Intervallence Coupling and Persistent Charge-transfer Luminescence in f-element Compounds

Guokui Liu^a, Shuao Wang^b, and Thomas E. Albrecht-Schmitt^c

^a *Chemical Sciences and Engineering Division, Argonne National Laboratory, Argonne, Illinois 60439, USA*

^b *School for Radiological and Interdisciplinary Sciences, Soochow University, Suzhou 215123, China*

^c *Department of Chemistry and Biochemistry, Florida State University, Tallahassee, Florida 32306, USA*

Charge transfer transitions are commonly observed in the absorption spectra of f-elements (lanthanides and actinides) ions in complexes and compounds within the visible and near UV region. However, charge transfer photoluminescence does not occur except in a few special cases such as Yb^{3+} and UO_2^{2+} where below the lowest charge transfer state there is no electronic state to quench the charge transfer state. Here in this presentation, we discuss unusual metastable charge transfer states, including that of Eu^{3+} in the metal-organic frameworks (MOFs) of $\text{Sr}(\text{HCOO})_2$ and Cf^{3+} in the lattice of $\text{Cf}(\text{HDP A})_3\text{-H}_2\text{O}$.^{1,2} In both systems, charge transfer luminescence with ms lifetime has been observed even though the low-lying $4f^6$ ($5f^9$) states of Eu^{3+} (Cf^{3+}) locate very close below the emitting charge transfer states. The radiative relaxation in the process of charge-hole recombination is primarily enabled by the increased stability of divalent oxidation state in these compounds. Temperature dependence of the charge transfer luminescence indicates the dual channels of charge-transfer relaxation, and suggests the competition between the nonradiative relaxation through the excited states and the radiative relaxation directly into the ground state of Eu^{3+} (Cf^{3+}). In the framework of charge transfer vibronic exciton (CTVE) interaction, we have developed a phenomenological model to provide a theoretical interpretation and characterization of the metastable charge transfer states and persistent luminescence emission.

References:

[1] Guokui Liu, Samantha K. Cary and Thomas E. Albrecht-Schmitt, *Phys. Chem. Chem. Phys.* 17, (2015)16151-16157

[2] Samantha Cary et. al., *Nature Communication* 6, (2015)6827

Single-Molecule Study of Conformation-Related Photophysics in Conjugated Molecular Complexes and Organic Dye-Gold Nanoparticle Structures

Martin Vacha

*Department of Organic and Polymeric Materials, Tokyo Institute of Technology, Ookayama
2-12-1-S8-44, Meguro-ku, Tokyo 152-8552, Japan*

Understanding the photoresponse of conjugated complexes on molecular level is important both from the point of basic knowledge of the molecular photophysics as well as from the point of potential applications as photo-driven nanoscale devices. We study molecular complexes, either as assemblies composed of conjugated small molecules such as molecular aggregates, or as covalently linked chromophores such as conjugated polymers. Using different modes of electronic excitation, such as linear absorption, plasmonic near-field enhancement, energy transfer or charge recombination, we investigate the resulting excited state, the conformational states of the molecular complex and their cooperative dynamics. As one example, conformational changes of a conjugated polymer polyfluorene are studied on single-chain level upon excitation by linear absorption of light and by charge recombination. Both excitation mechanisms lead to dramatically different photophysical properties that reflect different intramolecular aggregation processes [1]. In photoluminescence the emission spectra are dominated by either singlet excitons or excimers formed via neutral ground-state aggregates. In electroluminescence the singlet exciton emission is absent and the spectra are either due to formation of charged ground-state aggregates or excimers. In both photoluminescence and electroluminescence, thermally induced conformational dynamics of the polyfluorene chains leads to strong spectral dynamics on timescales of seconds. As another example of conjugated polymer photophysics we study the effect of polymer chain topology on its properties by comparing on single-molecule level cyclic and linear chains of poly(phenylene vinylene). Further, in the structures of organic dyes attached to gold nanorods, single particle dark-field imaging is used to determine orientation of each nanorod. Selective excitation of the longitudinal plasmon by polarized laser light is then used to study enhancement of Förster resonant energy transfer between donor and acceptor dye molecules randomly attached to the nanorod by monitoring changes in the acceptor fluorescence, with observed enhancement factors on the order of 100.

References:

[1] Y. Honmou, S. Hirata, H. Komiyama, J. Hiyoshi, S. Kawauchi, T. Iyoda, M. Vacha, *Nature Commun.* 5 (2014) 4666

Transient-two-dimensional infrared spectroscopy in a vibrational ladder

Vincent Kemlin*, Adeline Bonvalet, Louis Daniault, and Manuel Joffre

LOB, Ecole Polytechnique, CNRS, INSERM, Université Paris-Saclay, 91128 Palaiseau, France

*vincent.kemlin@polytechnique.edu

Two-dimensional infrared spectroscopy (2DIR) is the transposition of two-dimensional nuclear magnetic resonance (2D NMR) to nonlinear infrared spectroscopy. It is now a well-established technique that can be implemented even on biomolecules in an excited state, as demonstrated previously for a UV excitation [1] or a temperature jump [2].

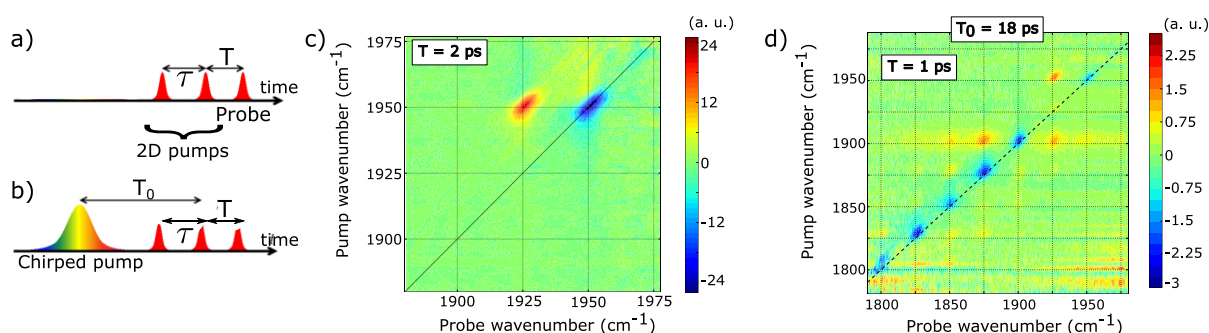


Figure 1: Three (a) and four (b) pulse sequences used to measure equilibrium 2D-IR spectrum and transient 2D-IR spectra following vibrational ladder climbing in HbCO by use of a negatively chirped infrared pulse. The equilibrium 2D-IR spectrum (c) is shown for a waiting time $T = 2$ ps, while the transient 2D-IR spectrum (d) is obtained for $T_0 = 18$ ps after the chirped pulse and a waiting time $T = 1$ ps.

In this talk, we will start by discussing the main features of 2DIR spectroscopy of carboxy-hemoglobin at equilibrium (Fig. 1c). Then, we will explain how adiabatic vibrational ladder climbing [3] allows us to prepare and control the vibrational excited state of the CO molecule. Our latest transient-2DIR experiments on such a strongly excited vibrational state (Fig. 1d) will be presented and discussed.

Because of the greater number of levels populated after vibrational ladder climbing, many more peaks in the 2D spectrum can be detected when the system is strongly displaced from equilibrium. The rich dynamics of these new peaks will be shown to yield a direct measurement of the vibrational lifetimes of the excited states. We measured the lifetimes of HbCO up to level $n=6$, thus confirming the interest of this method to explore new regions of the potential energy surface.

References:

- [1] C. Kolano, J. Helbing, M. Kozinski, W. Sander and P. Hamm, Nature 444, 469 (2006)
- [2] H. S. Chung, Z. Ganim, K. C. Jones and A. Tokmakoff, Proceedings of the National Academy of Sciences 104, 14237 (2007)
- [3] C. Ventalon, J. M. Fraser, M. H. Vos, A. Alexandrou, J.-L. Martin and M. Joffre, Proceedings of the National Academy of Sciences 101, 13216 (2004)

Coherent Energy Transfer in Light Harvesting Complexes: addressing single molecules on fs time scale

Niek van Hulst

ICFO – the Institute of Photonic Sciences, Castelldefels, Barcelona
ICREA – Institució Catalana de Recerca i Estudis Avançats, Barcelona
e-mail: Niek.vanHulst@ICFO.eu Web: www.ICFO.eu

Nature has developed photosynthesis to power life. Surprisingly, quantum coherences are observed in the energy transfer of photosynthetic complexes, even at room temperature. Does nature exploit quantum concepts? Does the coherence help to find an optimal path for robust or efficient transfer? How are the coherences sustained? What is their spatial extent in a real light-harvesting network?

Specializing on femto-nano toolboxes our goal is to look ultrafast into the nanoscale, to see individual molecules in action. Recently we succeeded in the first detection of coherent oscillations of a single photo-synthetic complex at physiological conditions [1, 2], and non-classical photon emission of individual complexes [3, 4]. Using resonant plasmonic antennas we managed to enhance the emission 500 times, while enhancing the observed photon number to 10^8 . In parallel we developed direct single molecule excitation spectroscopy [5]. These results, pave the way to address photosynthetic networks in real nano-space and on femtosecond timescale. Specific objectives are: Ultrafast single protein detection: tracing the fs coherent energy transfer path within an individual complex and throughout the network of antenna complex; addressing the very nature of the persistent coherences. Detection beyond fluorescence: light harvesting complex are designed for light transport, not emission. To this end we explore innovative alternatives: optical antennas to enhance quantum efficiency; detection of stimulated emission; and others.

Recent advances and ideas will be discussed.

References:

- [1] Hildner, Brinks, Nieder, Cogdell, van Hulst, *Science***340**, 1448-1451 (2013).
- [2] Brinks, Hildner, van Dijk, Stefani, Hernando, van Hulst, *Chem. Soc. Rev.***43**, 2476 (2014).
- [3] Wientjes, Renger, Curto, Cogdell, van Hulst, *Nature Comm.***5**: 4236 (2014).
- [4] Wientjes, Curto, Renger, Cogdell, van Hulst, *Phys. Chem. Chem. Phys.***16**, 24739 (2014).
- [5] Piatkowski, Gellings, van Hulst, *Nature Comm.***7**: 10411 (2016)

Vibrational dynamics of metal carbonyl complexes trapped in CH₄: a novel witness of solid methane's phase transition

R. Thon¹, W. Chin¹, D. Chamma^{1,2}, J.-P. Galaup³, C. Crépin¹

*1 Institut des Sciences Moléculaires d'Orsay (ISMO), CNRS,
Université Paris-Saclay, 91405 Orsay (France)*

*2 Laboratoire de Mathématiques et Physique (LAMPS) EA 4217
Université de Perpignan, 66860 Perpignan (France)*

*3 Laboratoire Aimé Cotton UMR 9188, CNRS,
Université Paris-Saclay, 91405 Orsay (France)*

The phase transition of solid methane is observed through vibrational spectroscopy and non-linear time-resolved spectroscopy of W(CO)₆ guest molecules. The specificities of each solid methane phases are highlighted by remarkable features due to the guest-host coupling in the 5-35 K temperature range.

Solid methane undergoes a phase transition at $\Theta^{\circ}=20.4$ K under low pressure. In phase I, above Θ° , methane molecules exhibit random reorientations due to thermal orientational fluctuations (orientational diffusion). In phase II, below Θ° , 75% of the molecules are orientationally ordered due to a moderate molecular octupole-octupole interaction. The resulting anisotropic field almost cancel out in 25% of the sublattices where the molecules behave as weakly hindered rotators [1]. The vibrational dynamics of the antisymmetric CO stretching mode of W(CO)₆ complexes trapped in solid methane is investigated and show interesting features related to the solid methane structural changes. Specific interactions of the complexes with the surrounding methane molecules contribute, by affecting their partial ordering, to the observed lowering of the phase transition temperature down to 18-19 K. The existence of different types of trapping sites is revealed by the complex structure of the linear absorption spectra which display a drastic motional narrowing from phase II to phase I. Further informations come from the population dynamics and dephasing studied by photon echo technique (time resolved non linear spectroscopy using 1-color 4-waves mixing) and its theoretical modeling. Although dephasing dynamics vary smoothly in the range 5-35 K, a significant shortening (from ~200 to 10 picoseconds) of the population lifetime at the phase transition is observed for some category of trapped complexes. It suggests that in phase I some additional fast transfer is occurring whose nature has to be investigated by additional studies. Our results in CD₄ solid, and comparison with our previous work in N₂ and rare gas cryogenic matrices [2], highlights solid methane specific dynamics.

References:

- [1] Press, W. *Single-Particle Rotations in Molecular Crystals*; Springer V.; Berlin, Heidelberg, New York vol. 92 (1981)
- [2] R. Thon, W. Chin, J.-P. Galaup, A. Ouvrard, B. Bourguignon, C. Crépin, *J. Phys. Chem. A* 117 (2013) 8145

On the Fenna-Matthews-Olson Protein Complex of Green Sulfur Bacteria

Adam Kell,¹ Robert E. Blankenship² and Ryszard Jankowiak^{1,3}

¹Department of Chemistry and Department of ³Physics, Kansas State University, Manhattan, KS, USA; ²Departments of Chemistry and Biology, Washington University in St. Louis, Saint Louis, MO, USA

The Fenna-Matthews-Olson (FMO) trimer (composed of identical subunits) from green sulfur bacteria is an important protein model system to study exciton dynamics and excitation energy transfer (EET) in photosynthetic complexes. In addition, FMO is a popular model for excitonic calculations, with many theoretical parameter sets reported describing different linear and nonlinear optical spectra. In spite of homologous X-ray structures, different bacteria can exhibit one of two types of absorption spectra,¹ for which *Prosthecochloris aestuarii* and *Chlorobaculum tepidum* are two well-studied examples. While it has been speculated that the coordination state of BChl *a* 8 plays a role in determining the spectral class,² no consensus exists as of yet. However, it is likely that small structural differences can modify excitonic interactions and optical spectra.³ Using an experimentally determined shape for the spectral density for the lowest-energy state ($J_{ph}(\omega)$), simulated optical spectra are obtained from structure-based calculations for entire FMO trimers. For higher energy pigments, the effect of a broader $J_{ph}(\omega)$ shape with a different *S* factor and/or variable Γ_{inh} are also tested for comparison. We show that the presence of uncorrelated EET between monomers of the trimer, must be considered to explain various linear optical spectra. Results for *Chlorobaculum tepidum*, *Prosthecochloris aestuarii* and *Pelodictyon phaeum* are compared and contrasted. Simultaneous fits of experimental low-temperature (5 K) absorption, fluorescence and hole-burned spectra place constraints on the determined pigment site energies; providing new Hamiltonians that should be further tested to improve modeling of 2D electronic spectroscopy data and our understanding of coherent and dissipation effects in this important protein complex.

References:

- [1] C. Francke, J. Amesz, Photosynth. Res. 52 (1997) 137
- [2] D. E. Tronrud, J. Wen, L. Gay, R. E. Blankenship, Photosynth. Res. 100 (2009) 79
- [3] C. R. Larson, C. O. Seng, L. Lauman, H. J. Matthies, J. Wen, R. E. Blankenship, J. P. Allen, Photosynth. Res. 107 (2011) 139

Chapter 3

**Tuesday 19th July 2016:
Presentations**

The quantum realm of nanoplasmonics for active control of optoelectronics and ultraresolved spectroscopy

Javier Aizpurua

*Center for Materials Physics CSIC-UPV/EHU
and Donostia International Physics Center DIPC
Paseo Manuel Lardizabal 5, Donostia-San Sebastián 20018, Spain*

The optical response of plasmonic nanosystems has been traditionally well described within the framework of the local dielectric response theory. However, practical configurations in surface-enhanced microscopies and spectroscopies are reaching the possibility to establish sub-nanometric control of morphologies and architectures, which expose the importance of addressing the quantum nature of electrons and photons to correctly describe a complex variety of optoelectronic processes, including active control of the optical response, nonlinearities, and ultraresolution.

In this tutorial, I will show the importance of considering quantum effects in the description of canonical plasmonic cavities [1] in connection with electronic transport [2] and molecular spectroscopy [3]. This description, based on the Time-dependent Density Functional Theory (TDDFT), shows how nanoplasmonics can be pushed to the extreme, reaching a situation of dialogue between optics and the atomic scale.

The relationship between electron transport across a plasmonic nanocavity and its optical response can be exploited at the quantum level with a remarkable precision. The migration and motion of single atoms can induce substantial changes in the transport properties that allow for modulation of optical signals with the minimum investment of energy and in an active fashion [4]. Another strategy of active control of a plasmonic resonance in a gap relies on the possibility to actively modify the tunneling barrier between the interfaces by means of the application of an external bias. This modifies the electron transmission across the gap producing changes in the electronic current at optical frequencies, and thus modulating the optical response of the system [5]. These are some examples of quantum active control of plasmonics that can be exploited in practical optoelectronic devices.

Furthermore, the importance of a precise atomistic description of a plasmonic cavity will be revealed with calculations of the local field distributions associated to atomic-scale features. These results reveal the remarkable possibility of accessing effective modal volumes down to 1 nm^3 , thus reaching the quantum limit of field localization [6]. This effect can be understood as an atomic-scale lightning rod effect which might be partially responsible for the ultraresolution reported in single-molecule spectroscopy experiments [3].

References:

- [1] R. Esteban, A.G. Borisov, P. Nordlander, and J. Aizpurua, *Nat. Comm.* 3 (2012) 825.
- [2] K. Savage et al. *NATURE* 491 (2012) 574.
- [3] R. Zhang et al., *NATURE* 498 (2012) 82.
- [4] F. Marchesin, P. Koval, P. M. Barbry et al., *ACS Photonics* 3 (2016) 269.
- [5] D.C. Marinica et al., *Science Advances* 1 (2015) e1501095.
- [6] M. Barbry, P. Koval, F. Marchesin, et al., *Nano Lett.* 15 (2015) 3410.

Raman Sensing and Imaging by Interference and Surface Enhancement Processes

Leo Álvarez-Fraga¹, Félix Jimenez-Villacorta¹, Esteban Climent-Pascual¹
Rafael Ramírez-Jiménez^{2, 1}, Carlos Prieto¹ and Alicia de Andrés¹

1 Instituto de Ciencia de Materiales de Madrid, Consejo Superior de Investigaciones Científicas. Cantoblanco 28049 Madrid, Spain

2 Departamento de Física, Escuela Politécnica Superior, Universidad Carlos III de Madrid, Avenida Universidad 30, Leganés, 28911 Madrid, Spain

Raman spectroscopy meets the required specificity criterion required for the detection of low concentrations of different agents in complex media, such as protein biomarkers in blood, since the vibrational spectrum of every component is a specific signature that can be used for its identification. Moreover, compared to magnetic resonance, Raman imaging has the ability of visualizing morphological details in cells and tissues on a much higher spatial resolution. Also, no external markers are required, it has a sub-micron resolution and quite good penetration depth. Nevertheless, Raman spectroscopy is strongly limited by its sensitivity. For the last years, a great effort is underway to increase Raman intensity mainly by localized surface plasmon resonance from metal nanoparticles (NPs). These SERS platforms still deals with problems such as the NPs stability, their interaction with the analyte and the adsorption, distribution and arrangement of the probed molecules on the substrate. Another enhancement process is the use of excitation wavelengths in resonant conditions for the sensed molecule, in general using ultra-violet lasers. Our aim is the fabrication of different architectures of SERS substrates that combine different Raman enhancement mechanisms in one multilayered hybrid system based on graphene. Graphene has several roles to play in optical sensing since it provides a biocompatible surface adequate for many organic and bio materials and also a protection of the metal NPs increasing the stability of the system. We will present our approaches to the different Raman enhancement processes. Graphene protected ruthenium ultrathin films with controlled size and shape of the particles present different characteristics of the Ru plasmon resonance adequate for UV-SERS. We will show that the intensification mechanism of Raman signal due to constructive interference produced in adequately designed dielectric films is very promising. Also we have explored the limit of ultrasmall Ag nanoparticles (4 nm) to study their interaction with graphene and its SERS amplification capabilities. The results of these approaches pave the way to the design and fabrication of extremely sensitive graphene based bio-compatible platforms by combining the different Raman enhancement processes.

Effect of aggregates of silver nanostructures on the optical properties of Yb³⁺ doped RbTiOPO₄

L. Sánchez-García,¹ C. Tserkezis,^{2,3} M. O. Ramírez,¹ P. Molina,¹ J. J. Carvajal,⁴ M. Aguiló,⁴ F. Díaz,⁴ J. Aizpurua,² and L. E. Bausá¹

¹Dept. Física de Materiales, Universidad Autónoma de Madrid, Madrid 28049, Spain

²Center for Materials Physics (CSIC-UPV/EHU) and Donostia International Physics Center (DIPC), Paseo Manuel Lardizabal 5, Donostia-San Sebastián 20018, Spain

³Technical University of Denmark, Department of Photonics Engineering, Ørsteds Plads, Building 343, 2800 Kgs. Lyngby, Denmark

⁴Física i Cristal·lografia de Materials i Nanomaterials (FiCMA-FiCNA) Universitat Rovira i Virgili, Tarragona 43005, Spain

RbTiOPO₄ (RTP) is a relevant electro-optic and nonlinear crystal which shows a very high optical damage threshold and relatively high nonlinear coefficients useful for quadratic frequency conversion. Additionally, previous reports have demonstrated efficient continuous-wave lasing of Yb³⁺ in RTP at around 1 μm [1], highlighting the system as a good candidate for highly stable, frequency doubled lasers [2].

With the aim of designing coherent sources with improved performance at the nanoscale, large aggregates of silver nanostructures have been tailored to match the emission spectra of Yb³⁺ ions and deposited onto the polar surface of Yb³⁺:RTP single crystals.

The role of the metallic aggregates on the photoluminescence of Yb³⁺ ions, as well as on the second harmonic generation (SHG) of the RTP host, is analyzed. The results show a remarkable enhancement of the Yb³⁺ f-f emission by a factor of 5, higher than that reported for other hybrid plasmon/rare-earth systems [3], and an extraordinary 60-fold enhancement of the SHG response.

The experimental results can be explained considering the spatial and spectral response of the near field enhancement calculated in the vicinity of the plasmonic structures. The effect of charge delocalization associated with the large size of the aggregates generates a broad plasmonic response in the near infrared region which is responsible for the observed improvement of the optical response.

The study points out the role of metallic aggregates to enhance both luminescence from rare earth ions and weak nonlinear processes at metal/dielectric interfaces and opens up an alternative route for the development of efficient nanosized optically active frequency-converter devices.

References:

- [1] X. Mateos et al. Optics Letters 32 (2007) 1929.
- [2] L. Deyra et al. in Advanced Solid-State Lasers Congress. OSA Technical Digest (2013), AM4A.39.
- [3] E. Yraola et al. Advanced Materials 25 (2013) 910.

PLASMONIC NANOANTENNAS: BRIGHT AND EFFICIENT NANOSOURCES

A. Raj Dhawan ¹, J. U. Esparza ¹, C. Belacel, C. Schwob ^{1,2}, M. Nasilowski ³, B. Dubertret ³,
L. Coolen ^{1,2}, P. Senellart ⁴, A. Maître ^{1,2}

1. Université Pierre et Marie Curie-Paris 6, UMR 7588, INSP, 4 place Jussieu, PARIS cedex 05, France

2. CNRS, UMR7588, INSP, Paris cedex 05, France

3. Laboratoire de Physique et d'Etude des Matériaux, ESPCI, UPMC, CNRS, 10 rue Vauquelin, 75005 Paris, France

4. Laboratoire de Photonique et de Nanostructures, CNRS, route de Nozay, 91460 Marcoussis, France

agnes.maitre@insp.upmc.fr

In the last decades the accelerated improvements of the techniques for nanofabrication have conducted to develop new structures and re-discover new electromagnetic effects in the optical wavelength scale. The term “optical nanoantennas” can be defined as a device to efficiently convert free propagating optical radiation to localized energy, and vice versa [1].

A patch nanoantenna consists of a nanoemitter embedded in a very thin dielectric layer enclosed with an optically thin gold nanodisk and a thick gold layer [2]. The patch nanodisk is positioned deterministically centered on the nanoemitter using an in-situ optical lithographic process (Figure 1). The nanoemitters under investigation are core/shell CdSe/CdS nanocrystals with 3-nm core diameter and 5-nm shell thickness. The fluorescence peak emission lays in the visible (around 630nm) at room temperature.

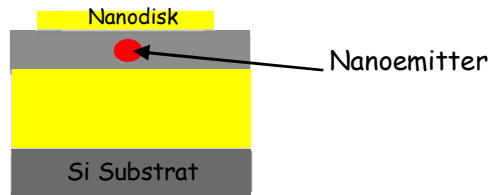


Fig 1. Scheme of a patch nanoantenna

The patch nanoantennas structure has demonstrated strong acceleration of spontaneous emission and controlled radiation pattern when aggregates of nanocrystals (around 50) were coupled to a plasmonic patch antenna. Several nanoantennas are fabricated with diameters varying from 1.4 to 2.1 μm . The dielectric spacing layer was set to 30 nm and high Purcell factor (defined as the ratio between the decay rate emission of nanoemitter with patch antenna and the one in a dielectric homogeneous medium) of 80 has been obtained [3].

In recent studies new techniques to couple an individual single nanocrystal to a patch antenna have permitted the deterministic position of a single emitter in the center of a patch antenna whose diameter size is between 150nm to 2 μm . By configuration the influence of a patch antenna up above a single emitter exhibit two kind of behavior depending of the size of the patch. For large diameter patch antennas a small Purcell factor is obtained, nevertheless for small antennas (150nm diameter) a significant factor of 23 is achieved. In the former case, the antenna acts as a single photon source whereas in the latter, thanks to Purcell effects. multiexcitons become radiative.

REFERENCES

- [1] P. Bharadwaj et al., *Advances in Optics Photonics* **1**, 438-483 (2009)
- [2] R. Esteban, T.V. Teperik, J.J. Greffet, “Optical patch antennas for single photon emission using plasmonic resonance”, *Phys. Rev. Lett.* **104**, 026802 (2010).
- [3] C. Belacel, B. Habert, F. Bigourdan, F. Marquier, J-P. Hugonin, S. Michaelis de Vasconcellos, X. Lafosse, L. Coolen, C. Schwob, C. Javaux, B. Dubertret, J-J. Greffet, P. Senellart, A. Maître, Controlling spontaneous emission with plasmonic optical patch antennas, *Nanoletters* **13** 1516 (2013).

Ultrafast size-dependent electronic interactions in small metal nanoparticles and clusters

P. Maioli, T. Stoll, D. Mongin, M. Pellarin, M. Hillenkamp, M. Broyer, A. Crut, F. Vallée, N. Del Fatti

*Institut Lumière Matière (iLM), Université Lyon 1 – CNRS,
10 Rue Ada Byron, 69622 Villeurbanne, France*

Reduction of the size of a material to a few nanometer scale leads to drastic modifications of its physical and catalytic properties. In the case of metal nano-objects with sizes larger than a few nanometers, these modifications are mostly due to classical effects. In contrast, for smaller clusters with sizes below about 2 nm (less than about 250 atoms), quantization plays an important role, leading to an evolution from a bulk-like behavior of the electronic properties (i.e., ruled by quasi-continuum of electronic states in the conduction band) to a molecular one (discrete energy states). Though the impact of quantization on static properties (ionization threshold, melting temperature, linear optical absorption, ...) of free clusters has been extensively investigated, their dynamical processes, e.g. ultrafast induced changes of electronic interactions, have been much less studied. This is due to the difficulty both in the synthesis of clusters with well controlled size and environment, and in the experiments.

Using high-sensitivity femtosecond pump-probe spectroscopy, we have measured the time-resolved optical response of silver nanoparticles in the 3 to 1 nm size range. Investigations have been performed in surfactant-free glass-embedded clusters, to limit surface effects. Using different probe wavelengths, the relaxation of photoexcited nonequilibrium electrons was followed in the time-domain, yielding information on the electron-electron and electron-vibration energy exchange processes. The efficiency of the electronic interactions is shown to increase with size reduction down to about 2 nm (consistently with previous results in larger particles [1-3]). It is then shown to further decrease at smaller sizes, although with a non monotonic behaviour. This effect is ascribed to quantization of the electronic states, whose energy level spacing becomes larger than the thermal energy and maximum phonon energy in that size range.

Modifications of the acoustic vibrational response of metal clusters in this size range will also be discussed [4].

References:

- [1] T. Stoll, P. Maioli, A. Crut, N. Del Fatti, and F. Vallée, *Eur. Phys. J. B* 87 (2014), 260
- [2] A. Arbouet, C. Voisin, D. Christofilos, P. Langot, N. Del Fatti, F. Vallée, J. Lermé, G. Celep, E. Cottancin, M. Gaudry, M. Pellarin, M. Broyer, M. Maillard, M. P. Pileni, and M. Treguer, *Phys. Rev. Lett.* 90 (2003), 177401
- [3] C. Voisin, D. Christofilos, N. Del Fatti, F. Vallée, B. Prével, E. Cottancin, J. Lermé, M. Pellarin, and M. Broyer, *Phys. Rev. Lett.* 85 (2000), 2200
- [4] A. Crut, P. Maioli, N. Del Fatti, and F. Vallée, *Phys. Rep.* 549 (2015), 1

Controlling energy transfer and radiative lifetimes in luminescent lanthanide complexes and materials

Jean-Claude G. Bünzli

Swiss Federal Institute of Technology, Lausanne (EPFL), Institute of Chemical Sciences & Engineering, CH 1015 Lausanne Switzerland

Hong Kong Baptist University, HKBU (Haimen) Institute of Science & Technology, Hong Kong, SAR, P. R. China

One third of the total value of the lanthanides used worldwide lies in phosphors and other luminescent materials which are ubiquitous in lighting devices, telecommunications, displays, security inks, counterfeiting tags, luminescent sensors, photocatalysis, bioanalysis, and bioimaging [1]. Luminescent lanthanide compounds have yet to yield their ultimate secrets. Indeed, interplay between f-states, charge-transfer states, ligand singlet and triplet states is governed by several energy transfer mechanisms. This renders difficult the task of designing efficient luminescent edifices with properties targeted at a specific application [2].

In this presentation, the current status of the design of highly luminescent lanthanide compounds and probes is discussed with respect to (i) optimizing energy transfer from the matrix to the lanthanide ion (antenna effect, Figure), (ii) minimizing non-radiative de-activations, and (iii) enhancing photophysical properties through insertion into polymeric matrixes and/or tuning of the radiative lifetime [3]. Recent examples from the authors' laboratories are presented [4,5].

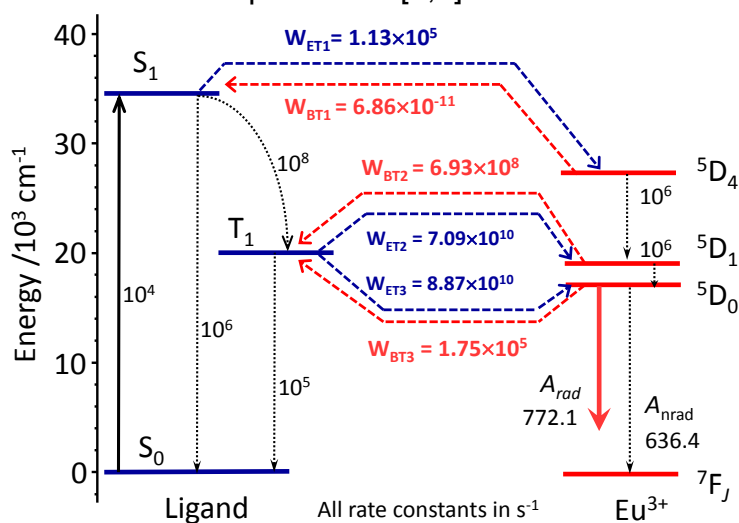


Figure. Energy transfer processes in a dimeric Eu(III) complex.

References

- [1] J.-C. G. Bünzli and S. V. Eliseeva, *Chem. Sci.* 4 (2013) 1939-1949.
- [2] J.-C. G. Bünzli, *Coord. Chem. Rev.* 293-294 (2015) 19-47.
- [3] J.-C. G. Bünzli, A.-S. Chauvin, H. K. Kim, E. Deiters and S. V. Eliseeva, *Coord. Chem. Rev.* 254 (2010) 2623-2633.
- [4] S. Biju, R. O. Freire, Y. K. Eom, R. Scopelliti, J.-C. G. Bünzli and H. K. Kim, *Inorg. Chem.* 53 (2014) 8407-8417.
- [5] N. M. Shavaleev, S. V. Eliseeva, R. Scopelliti and J.-C. G. Bünzli, *Inorg. Chem.* 54 (2015) 9166-9173.

Lanthanide-Doped Luminescent Nano-Bioprobes for In Vitro Detection of Tumor Markers

Wei Zheng, Shanyong Zhou, Datao Tu, Ping Huang, Jin Xu, Xueyuan Chen*

Key Laboratory of Optoelectronic Materials Chemistry and Physics, Fujian Institute of Research on the Structure of Matter, Chinese Academy of Sciences, Fuzhou, Fujian 350002, China

Lanthanide-doped inorganic nanoparticles possess superior physicochemical features such as long-lived luminescence, large antenna-generated Stokes or anti-Stokes shifts, narrow emission bands, high resistance to photobleaching and low toxicity, and thus are regarded as a new generation of luminescent bioprobes as compared to conventional molecular probes like organic dyes and lanthanide chelates. These functional nanoparticles, albeit most of their bulk counterparts were well studied previously, have attracted reviving interest for their biomedical applications in areas as diverse as biodetection, bioimaging, and disease diagnosis and therapeutics. In this talk, we shall focus on the latest advances made in developing lanthanide-doped inorganic nanoparticles as potential luminescent bioprobes, which cover from their chemical and physical fundamentals to bioapplications including the controlled synthesis, surface modification, electronic structure, optical properties, and their promising applications in diverse fields, with an emphasis on heterogeneous and homogeneous in-vitro biodetection of tumor markers [1-7].

References

- [1] Xueyuan Chen, Yongsheng Liu, and Datao Tu. *Lanthanide-Doped Luminescent Nanomaterials: From Fundamentals to Bioapplications*, Springer-Verlag Berlin Heidelberg, **2014**.
- [2] Wei Zheng, Ping Huang, Datao Tu, En Ma, Haomiao Zhu, and Xueyuan Chen*, *Chem. Soc. Rev.***2015**, *44*, 1379-1415 (**Inside Front Cover**).
- [3] Shan Lu, Datao Tu, Ping Hu, Jin Xu, Renfu Li, Meng Wang, Zhuo Chen, Mingdong Huang, and Xueyuan Chen*, *Angew. Chem. Int. Ed.* **2015**, *54*, 7915-7919.
- [4] S. Y. Zhou, W. Zheng, Z. Chen, D. T. Tu, Y. S. Liu, E. Ma, R. F. Li, H. M. Zhu, M. D. Huang*, and X. Y. Chen*, *Angew. Chem. Int. Ed.***2014**, *53*, 12498-12502.
- [5] Ping Huang, Wei Zheng, Shanyong Zhou, Datao Tu, Zhuo Chen, Haomiao Zhu, Renfu Li, En Ma, Mingdong Huang, and Xueyuan Chen*, *Angew. Chem. Int. Ed.***2014**, *53*, 1252.
- [6] Yongsheng Liu, Datao Tu, Haomiao Zhu, and Xueyuan Chen*, *Chem. Soc. Rev.***2013**, *42*, 6924.
- [7] Wei Zheng, Shanyong Zhou, Zhuo Chen, Ping Hu, Yongsheng Liu, Datao Tu, Haomiao Zhu, Renfu Li, Mingdong Huang, and Xueyuan Chen*, *Angew. Chem. Int. Ed.***2013**, *52*, 6671.

Energy transfer processes in organic-sensitized Yb-doped NaYF₄ nanoparticles

H. Lu¹, Y. Peng², H. Ye³, X. Cui⁴, J. Hu², M. A. Green⁵, P. J. Blower⁵, P. B. Wyatt²,
W. P. Gillin² and I. Hernández⁶

1) State Key Laboratory of ASIC and System, SIST, Fudan University, China

2) Materials Research Institute, Queen Mary University of London, UK

3) School of Physical and Mathematical Science, Nanyang Technological University

4) School of Environmental Sciences, University of Birmingham

5) Centre of Excellence in Medical Engineering, King's College London, UK

6) Dept. of Earth Sciences and Condensed Matter Physics, Universidad de Cantabria, Spain

Rare Earth doped materials suffer from limited excitation due to the low oscillator strength of intraconfigurational f-f transitions, which in turn favour long photoluminescence lifetimes which are interesting for a number of laser and biological applications, particularly in the infra-red (IR) range [1].

Sensitization from organic chromophores has been proved as a successful strategy for enhancing rare-earths' optical properties. However, organics often contain groups showing high frequency vibrations which can quench the lanthanides' luminescence, especially severely in the IR range. Although perfluorinated or halogenated organics can decrease the quenching and allow for efficient sensitization resulting in extraordinary optical properties in the infra-red range [2,3], this typically entails complex chemistry and limited possibilities for "wet" applications.

An alternative strategy involves the use organic antennae in combination with small inorganic nanoparticles doped with lanthanides and has allowed sensitization in IR emitting Yb³⁺ and Nd³⁺-doped NaYF₄ [4] and even broad band sensitized Up-conversion in Er³⁺, Yb³⁺ doped NaYF₄ [5]. These hybrid composites in which the IR-based lanthanide is kept and protected from the environment in an inorganic environment and excited from the external organic chromophores in the proximities [3], can show relatively long lifetimes.

Here we present the sensitized infra-red emission of sub small Yb³⁺-doped NaYF₄ nanoparticles through 2-hydroxy-perfluoroanthraquinone chromophore (1,2,3,4,5,6,7-heptafluoro-8-hydroxyanthracene-9,10-dione) [6], which allows excitation at wavelengths in the range 400-600 nm. This allows an overall increase of the Yb³⁺ luminescence by a factor 300 with respect to direct excitation. We study the lifetime of the Yb³⁺ emission and the dynamical processes involving the lanthanide ions and the perfluorinated chromophore at the surface of the nanoparticles.

References:

- [1] J.C.G. Bünzli, and S.V. Eliseeva, *Journal of Rare Earths* 28 (2010) 824
- [2] Ye et al. *Nature Materials* Authors, *Journal volume (year) page*
- [3] I. Hernández and W.P. Gillin in *Handbook on the Physics and Chemistry of Rare earths*, vol. 47, p. 1, Editors: JCG Bünzli and VKK Pecharsky, Elsevier (2015).
- [4] J.Zhang et al., *Journal of the American Chemical Society* 129 (2007)14834
- [5] W. Zou et al., *Nature Photonics* 6 (2012) 560
- [6] Y. Peng, et al. *The Journal of Physical Chemistry Letters* 5 (2014)1560

Engineering Core/Shell Rare Earth Nanoparticles for Ultimate Control Over Light Emitting Processes

Ling-Dong Sun, Hao Dong, Yang Li, Chun-Hua Yan

Beijing National Laboratory for Molecular Sciences, State Key Laboratory of Rare Earth Materials Chemistry and Applications, College of Chemistry and Molecular Engineering, Peking University, Beijing, 100871, China

Light emission from rare earth nanocrystals, ranged from ultraviolet to visible and even the near infrared, are attractive for a broad field of Stokes and anti-Stokes photon conversion applications. Thanks to the abundant energy levels of rare earth ions, resonance energy transfer, cross relaxation and phonon related nonradiation mechanism are important for control over light emitting processes. Combined with nanostructure, which is able to localize the energy transfer in nanoscale domain, the transition within typical rare earth ions could be confined and even combined via various layers. Based on this consideration, core/shell nanostructure are introduced as an ideal platform to realize selective or combinatorial light emitting from rare earth.

$\text{Nd}^{3+} \rightarrow \text{Yb}^{3+}$ energy transfer with an efficiency higher than 90% were also designed to combine with upconverting rare earth pairs ($\text{Yb}^{3+}/\text{Er}^{3+}$, Tm^{3+}) via a core/shell structure. Benefit from this design, upconversion emissions from Er^{3+} or Tm^{3+} could be sensitized both from Yb^{3+} (970 nm, $^4\text{F}_{5/2} \rightarrow ^4\text{F}_{7/2}$) and Nd^{3+} (808 nm, $^4\text{I}_{9/2} \rightarrow ^4\text{F}_{5/2}$) excitation.^[1] Furthermore, with the excitation of Nd^{3+} at 730 or 808 nm, downshifting emission from Nd^{3+} (1064 nm, $^4\text{F}_{3/2} \rightarrow ^4\text{I}_{13/2}$) and Yb^{3+} (970 nm, $^4\text{F}_{5/2} \rightarrow ^4\text{F}_{7/2}$) could be observed selectively or simultaneously. Together with a higher quantum efficiency, these emitting rare earth nanocrystals could be used as NIR excited and emitted nanoprobe for imaging and detection.

Ultimate control over light emitting were also realized with emitted shell layers and multiphoton upconverting selection.^[2,3] Emissions in the visible and near infrared combined with tunable lifetime were used for high signal to background imaging studies, and excitation density modulated optical switch investigations.

References:

- [1] Y.F. Wang, G. Y. Liu, L. D. Sun, J. W. Xiao, J. C. Zhou, *ACS Nano* 7 (2013) 7200.
- [2] H. Dong, L. D. Sun, Y.F. Wang, J. Ke, R. Si, J. W. Xiao, G. M. Lyu, S. Shi, C. H. Yan, *J. Am. Chem. Soc.* 137(2015), 6569.
- [3] L. Wang, H. Dong, Y. Li, R. Liu, Y.F. Wang, H. K. Bisoyi, L. D. Sun, C. H. Yan, and Q. Li, *Adv. Mater.* 27(2015), 2065.

NIR Nanomaterials for disease diagnostics and therapy

Fan Zhang*

Department of chemistry, Fudan University, Shanghai 200433, China

Email: zhang_fan@fudan.edu.cn

Upconverting nanoparticles (UCNPs) present a new technology for optical imaging/detection which is a growing field with both diagnostic and drug discovery uses. Currently, fluorophores including fluorescent dyes/proteins and quantum dots (QDs) are used for fluorescence-based imaging and detection. These are based on 'downconversion fluorescence', emitting low energy fluorescence when excited by high energy light (such as UV or short wavelength visible light). Fluorophores in current use have several drawbacks: photobleaching, autofluorescence, short tissue penetration depth and tissue photo-damage. UCNPs emit detectable photons of higher energy in the visible range upon irradiation with near-infrared (NIR) light based on a process termed 'upconversion'. UCNPs show absolute photostability, negligible autofluorescence, high penetration depth and minimum photodamage to biological tissues. They can be used for ultrasensitive interference-free biodetection because most biomolecules do not have upconversion properties.

Acknowledgements

The work was supported by NSFC (grant No. 21322508), China National Key Basic Research Program (973 Project) (No. 2013CB934100, 2012CB224805).

References

1. L. Zhou, R. Wang, C. Yao, X. M. Li, D. Y. Zhao and F. Zhang*, *Nature.Comm.*, **6**, 6938 (2015)
2. X. M. Li, F. Zhang*, and D. Y. Zhao *Chem. Soc. Rev.*, **44**, 1346 (2015)
3. R. Wang, X. M. Li, L. Zhou and F. Zhang*, *Angewand.Chem.Int. Ed.*, **53**, 12068 (2014)
4. L. Chen, L. Zhou, D. Zhu, C. H. Fan and F. Zhang*, *Anal. Chem.*, **87**, 1346 (2015)
5. X. M. Li, R. Wang, F. Zhang* and D. Y. Zhao, *Nano. Lett.*, **14**, 3634 (2014)
6. C. Yao, X. M. Li, D. Y. Zhao and F. Zhang*, *Anal. Chem.*, **86**, 9749 (2014)
7. F. Zhang*, R. C. Che, P. Hu, X. M. Li, J. P. Yang, D. K. Shen, W. Li and D. Y. Zhao, *Nano. Lett.*, **12**, 2852 (2012)

Nd³⁺ Contactless Fluorescent Temperature Sensor

K. Kaldvee¹, S.G. Fedorenko², L. Puust¹, A.S. Vanetsev^{1,3}, E.O. Orlovskaya³,
M. Pärss¹, I. Sildos¹, Yu.V. Orlovskii^{1,3}

¹Institute of Physics, University of Tartu, W. Ostwaldi str. 1, 50411, Tartu, Estonia

²Institute of Chemical Kinetics and Combustion SB RAS, 630090, Novosibirsk, Russia

³Prokhorov General Physics Institute RAS, Vavilov str. 38, 119991, Moscow, Russia

Recently we proposed to use the Nd³⁺: YPO₄ nanocrystals synthesized by the hydrothermal microwave treatment as fluorescent imaging agent in the near IR spectral range [1]. Here we discuss the possibility to use them as a contactless optical temperature sensor. The imaging can be merged with temperature controlled hyperthermia treatment using the core-shell Nd³⁺:YPO₄@DyPO₄ nanocrystals. The fluorescence is excited by 805 nm of OPO laser and the fluorescence kinetics of the ⁴F_{3/2} manifold of Nd³⁺ on temperature is measured. The ⁴F_{3/2} manifold has only two doubly degenerated crystal-field (CF) levels with the energy gap $\Delta E = 52 \text{ cm}^{-1}$. We solved the system of rate equations for three level system. The fluorescence of both level decays according to exponential law with equal rates determined by

$$W(T) = \frac{n_1(T)}{\tau_1} + \frac{n_2(T)}{\tau_2}, \quad (1)$$

where τ_1 and τ_2 are the lifetimes of the low and upper CF levels, respectively, and the equilibrium population of each level at specific temperature is set according to Boltzman distribution

$$n_1(T) = \left[1 + \exp\left(-\frac{\Delta E}{kT}\right) \right]^{-1}, \quad n_2(T) = n_1(T) \exp\left(-\frac{\Delta E}{kT}\right) = 1 - n_1(T). \quad (2)$$

We measured the lifetime $\tau_1 = 312.7 \text{ }\mu\text{s}$ of the low CF level at 10K when the upper CF level is practically not populated. The temperature dependence from 10K up to 373K of the fluorescence kinetics measured at 873.4 and 877.3 nm (the ⁴F_{3/2}(1) → ⁴I_{9/2}(1) and ⁴F_{3/2}(2) → ⁴I_{9/2}(1) transition, respectively) confirmed that the decay rate is independent on the detection wavelength. The measured lifetime $\tau = 1/W(T)$ is decreased from 312.7 μs to 282.2 μs in the range from 10 to 77K and then increase up to 308.1 μs at 373K. We calculated the spontaneous emission lifetime τ_2 of the upper CF level using Eqs. (1, 2) and the value of τ_1 measured at 10K. We found that τ_2 is much shorter than τ_1 . However, the calculated value of τ_2 depends on the temperature. For example, it is $\tau_2 = 201.8 \text{ }\mu\text{s}$ at 40K, $\tau_2 = 223.9 \text{ }\mu\text{s}$ at 77K, and $\tau_2 = 302.6 \text{ }\mu\text{s}$ at 373K. We explain this fact by a change of the spontaneous emission rate A for both CF levels with the temperature due to temperature dependent term originated from admixture of configuration of opposite parity into the ⁴fⁿ configuration. In the physiological temperature range 37 - 45°C the kinetic method of temperature measurement provides the sensitivity $\Delta\tau/\tau/\Delta T = 0.03\% \text{ K}^{-1}$, more than one order of magnitude less than the spectral method $\Delta(I_2/I_1)/(I_2/I_1)/\Delta T = 0.6\% \text{ K}^{-1}$ employing the spectral lines areas ratio I_2/I_1 dependence on temperature measured at the same transitions. The latter we propose for fluorescent contactless temperature sensor.

References:

[1] E. Samsonova, A.V. Popov, A.S. Vanetsev, K. Keevend, E.O. Orlovskaya, V. Kiisk, S. Lange, U. Joost, K. Kaldvee, U. Mäeorg, N.A. Glushkov, A.V. Ryabova, I. Sildos, V.V. Osiko, R. Steiner, V.B. Loschenov, and Yu.V. Orlovskii, Physical Chemistry Chemical Physics, 16 (2014) 26806

Optical microscopy and spectroscopy of single molecules and single plasmonic gold nanoparticles

Michel Orrit

Huygens-Kamerlingh Onnes Laboratory, LION, Leiden University
2300 RA Leiden (Netherlands)

<http://www.monos.leidenuniv.nl>; E-mail: orrit@physics.leidenuniv.nl

Optical signals provide unique insights into the dynamics of nano-objects and their surroundings [1]. I shall present some of our experiments of the last few years.

i) We study single gold nanoparticles by photothermal and pump-probe microscopy. We recently studied the dynamics of vapornanobubbles created in the liquid surrounding a single immobilized gold nanosphere. We found that these nanobubbles form in an instable, explosive process before collapsing. Nanobubbles can react to reflected sound waves such as those released in the explosion [2].

ii) Photothermal microscopy opens the study of non-fluorescent absorbers, down to single-molecule sensitivity [3]. Combining this contrast with photoluminescence, we can measure the luminescence quantum yield on a single-particle basis. The high signal-to-noise ratio of this technique enables uses of individual gold nanoparticles for local plasmonic and chemical probing [4] (see Fig. 1).

iii) Gold nanorods generate strong field enhancements near their tips. Matching the rods' plasmon to a dye's spectra, we observe enhancements in excess of thousand-fold for the fluorescence of single Crystal Violet molecules [5]. This method generalizes single-molecule fluorescence to a broad range of weak emitters.

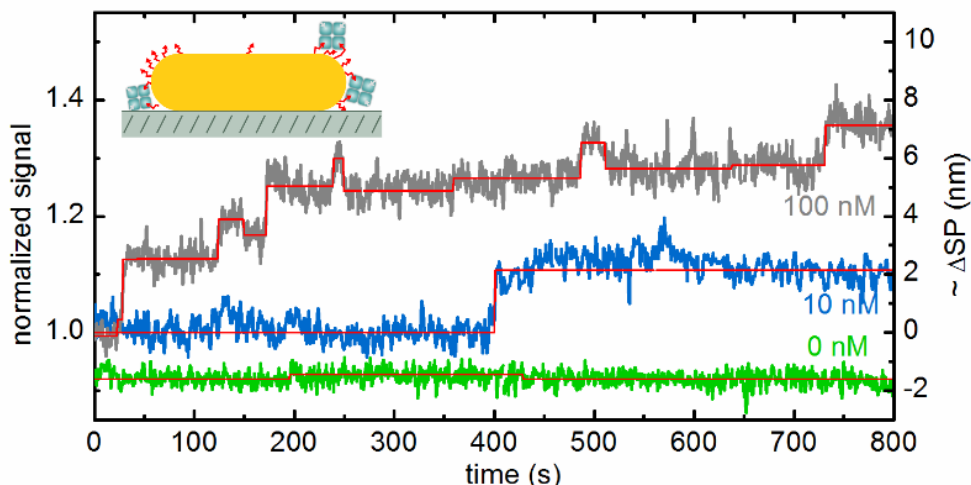


Figure 1: Example of an absorption trace of a single gold nanorod showing binding and unbinding events of single proteins [4].

References:

- [1] F. Kulzer et al., *Angew. Chem. Int. Ed.* **49** (2010) 854.
- [2] L. Hou et al., *New J. Phys.* **17** (2015) 013050
- [3] A. Gaiduk et al. *Science* **330** (2010) 353
- [4] P. Zijlstra et al., *Nature Nanotech.* **7** (2012) 379.
- [5] H. Yuan et al., *Angew. Chem. Int. Ed.* **52** (2013) 1217.

Correlative Atomic Force and Confocal Fluorescence Microscopy: Single Molecule Imaging and Force Induced Spectral Shifts

Sven Stöttinger, Gerald Hinze, Klaus Müllen, Thomas Basché

Institut für Physikalische Chemie, Johannes Gutenberg-Universität, Mainz, Germany

A grand challenge in nanoscience is to correlate structure or morphology of individual nano-sized objects with their photo-physical properties. An early example have been measurements of the emission spectra and polarization of single semiconductor quantum dots as well as their crystallographic structure by a combination of confocal fluorescence microscopy and transmission electron microscopy.[1] Recently, the simultaneous use of confocal fluorescence and atomic force microscopy (AFM) has allowed for correlating the morphology/conformation of individual nanoparticle oligomers or molecules with their photo-physics.[2, 3] In particular, we have employed the tip of an AFM cantilever to apply compressive stress to single molecules adsorbed on a surface and follow the effect of the impact on the electronic states of the molecule by fluorescence spectroscopy.[3] Quantum mechanical calculations corroborate that the spectral changes induced by the localized force (Figure 1) can be associated to transitions among the different possible conformers of the adsorbed molecule.

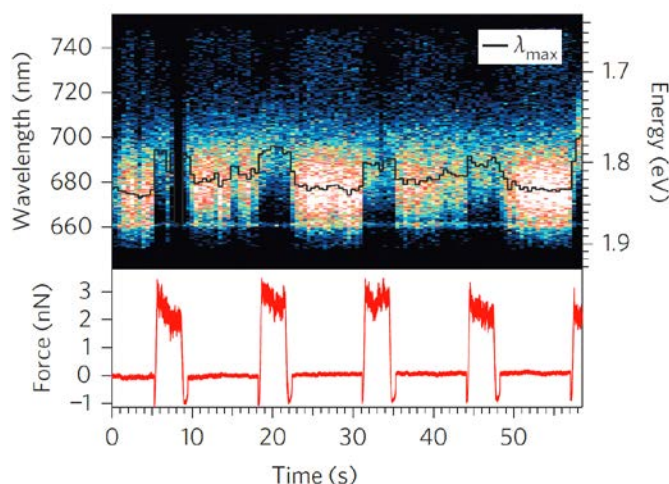


Figure 1: Fluorescence emission maxima (λ_{\max} , black curve) of a single terrylenediimide chromophore as a function of time while periodically applying force (red curve). Spectra are reversibly redshifted under compressive stress. [3]

References:

- [1] F. Koberling, U. Kolb, G. Philipp, I. Potapova, Th. Basché, A. Mews, J. Phys. Chem. B 107 (2003) 7463.
- [2] X. Xu, S. Stöttinger, G. Battagliarin, G. Hinze, E. Mugnaioli, C. Li, K. Müllen, Th. Basché, J. Am. Chem. Soc. 133 (2011) 18062.
- [3] S. Stöttinger, G. Hinze, G. Diezemann, I. Oesterling, K. Müllen, Th. Basché, Nature Nanotechnology 9 (2014) 182.

Superradiance of molecular monolayers on insulating surfaces

A. Eisfeld¹, M. Müller², A. Paulheim², C. Marquardt², M. Sokolowski²

¹Max Planck Institute for the Physics of Complex Systems

²University of Bonn

In recent experiments PTCDA molecules deposited on a KCl surfaces arrange in a well ordered two-dimensional layer (see Fig 1a,b). In this arrangement the molecules can exchange excitation energy via transition-dipole-dipole interaction. This leads to the formation of Frenkel excitons, i.e. states for which the electronic excitation is coherently delocalized over many molecules. The arrangement of the molecules is such that a so-called J-aggregate is formed, i.e. the dominant absorption is red-shifted with respect to the non-interacting molecules (see Fig 1c). This J-band also shows superradiant emission. Due to improved preparation conditions this superradiance is strongly enhanced compared to previous experiments [1].

In this contribution we discuss the temperature dependent superradiant emission, its relation to the coherence size of the exciton and its dependence on finite size effects. One peculiar feature of the present system is related to the width of the J-band. Usually the absorption line-shape of the J-band is much narrower than that of the individual molecules. However, in the experiment a considerable broadening is observed. We will discuss possible mechanisms responsible for this broadening.

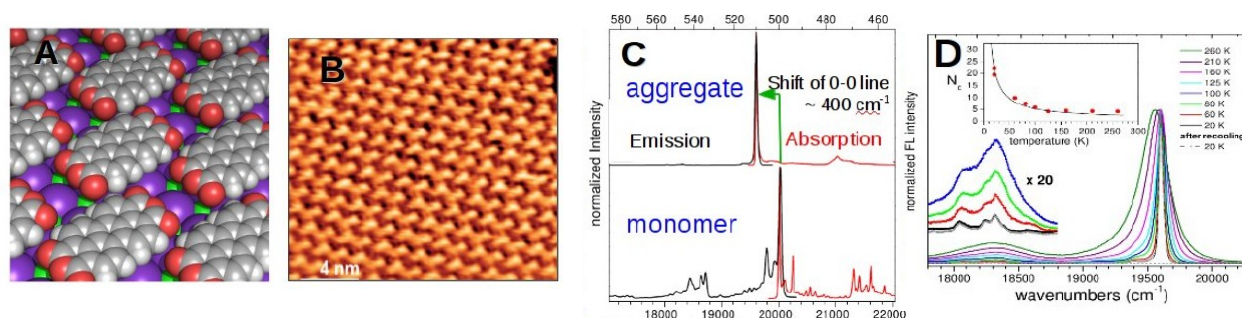


Figure 1: (A) Sketch of a PTCDA monolayer (aggregate) on KCl surface. (B) AFM image of PTCDA monolayer on bulk KCl (from T. Dienel et al., Adv. Mater. 20, 959). (C) Measured aggregate and single molecule spectra at 20K. (D) Temperature dependence of the spectra. The inset shows the temperature dependent coherence size of the exciton.

References:

- [1] M. Müller, A. Paulheim, A. Eisfeld and M. Sokolowski, J. Chem. Phys. 139 (2013) 044302
- [2] M. Müller et al. Phys. Rev. B 92 (2015) 121408(R)

Charge dynamics in organo-metal-halide perovskite nanocrystals probed by super-resolution optical microspectroscopy at the individual crystal level.

Aboma Merdasa, Yuxi Tian, Alexander Dobrovolsky, Daniela Täuber,
Ivan G. Scheblykin

Chemical Physics, Lund University, Box 124, SE-22100, Lund, Sweden

**e-mail: ivan.scheblykin@chemphys.lu.se*

Organo-metal halide (OMH) perovskites are the most studied materials for solar-cell applications during the last couple of years. Despite of the great progress in devices, fundamental questions including the nature of photoluminescence and mechanisms of charge recombination are far from been understood. OMH perovskites are direct semiconductors, however, presence of defects, mechanical softness, ion migration, unusual dielectric properties due to the organic molecule in the crystal structure, formation of crystals of different sizes and topology makes their optical and electrical properties quite peculiar. Here we present several phenomena observed by analysis of luminescence of micro- and nanocrystals of $\text{CH}_3\text{NH}_3\text{PbI}_3$.

We employed luminescence microscopy and spectroscopy, super-resolution optical imaging based on localization of emitting sites (SUPERLUMS - super-resolution luminescence micro-spectroscopy[1]), and electron microscopy for the very same sample in order to correlate the sample morphology and properties. We found a huge spatial inhomogeneity of the PL intensity and lifetime at the scales from nanometers and above and assigned it to a vast distribution of the PL quenching trap concentration.[2,3] The trap concentration can be changed by light irradiation which can lead to several orders of magnitude increase of the PL yield.[4]

We found that luminescence of ~100-nm crystals enhances much faster than that of larger, micrometer-sized ones. This crystal-size dependence of the photochemical light-passivation of charge traps responsible for PL quenching allowed us to conclude that traps are present in the entire crystal volume, rather than at the surface only. Due to this effect, “dark” micrometer sized perovskite crystals can be converted into highly luminescent smaller ones just by mechanical grinding.[2]

For crystals of less than one micrometer in size we observed PL blinking which shows that a single photoconvertible trap can control PL of the whole crystal.[3] Luminescence intensity blinking correlates with the corresponding luminescence lifetime change. It means that the quenching is dynamic rather than static and it is limited by the long diffusion length of the charge carriers in the material. Most probably the “super-trap” that induces blinking has a different nature than the others, much less efficient traps leading to decreased luminescence quantum yield in general.

References:

- [1] A. Merdasa, Á.J. Jiménez, R. Camacho, M. Meyer, F. Würthner, I.G. Scheblykin, , **Nano Lett.** 14 (2014) 6774–6781.
- [2] Y. Tian, A. Merdasa, ..., Scheblykin, **J. Phys. Chem. Lett.** 6 (2015) 4171–4177
- [3] Y. Tian, A. Merdasa, ... , Scheblykin, **Nano Lett.** 15 (2015) 1603–1608
- [4] Y. Tian, M. Peter, E. Unger, ..., Scheblykin, **Phys. Chem. Chem. Phys.** 17 (2015) 24978–24987

Intrinsic optical properties of organic-inorganic hybrid perovskite MAPbI₃ and its multiple stages of spontaneous and photo-induced structure transformation

Yong Zhang*

The University of North Carolina at Charlotte, USA

We show that organic-inorganic hybrid perovskite CH₃NH₃PbI₃ (MAPbI₃) exhibits multiple stages of structure transformation occurring either spontaneously or under light illumination. In particular, we emphasize four stages along the transformation path from MAPbI₃ to PbI₂ with distinctly different Raman spectroscopy features. By performing spatially resolved Raman and photoluminescence spectroscopy studies with varying excitation wavelength, density, and data acquisition parameters, we have achieved a unified understanding towards the spectroscopy signatures of the material transforming from the pristine stage (MAPbI₃) to the fully degraded stage (i.e., PbI₂) for samples with varying crystalline domain size from mesoscopic scale (approximately 100 nm) to macroscopic size, synthesized by three different techniques. Additionally, characteristic features of partially degraded materials under the joint action of spontaneous and photo-induced degradation are given. This study offers reliable benchmark results for understanding the intrinsic material properties and structure transformation of this emerging material.

In collaboration with Qiong Chen and Henan Liu (UNCC), Hui-Seon Kim and Nam-Gyu Park (SKKU), Mengjin Yang and Kai Zhu (NREL), Yucheng Liu and Shengzhong (Frank) Liu (SNU), and Naili Yue and Gang (Gary) Ren (LBNL).

* yong.zhang@uncc.edu

Harvesting light through upconversion for photocatalysis applications

G. Ledoux¹, B. Mahler¹, Y. Chen^{2,3}, S. Mishra², E. Jeanneau⁴, M. Daniel², J. Zhang³, S. Daniele²

¹ Université Lyon1, Institut Lumière Matière UMR5306 CNRS, 10 rue Ada Byron, 69622

² Université Lyon1, IRCELyon UMR5256 CNRS, 2 Av. Albert Einstein, 69626 Villeurbanne

³ Key Laboratory for Advanced Materials and Institute of Fine Chemicals

East China University of Science and Technology 130 Meilong Road, Shanghai 200237

⁴ Centre de Diffractométrie Henri Longchambon, 5 rue de La Doua, 69100 Villeurbanne

Photocatalysis is an efficient and simple way to drive a chemical reaction but it is generally limited by the necessity to use ultraviolet or deep blue light. In the recent years there has been strong efforts to modify catalysts materials so that their band to band absorption comes more to the visible part of the electromagnetic spectrum for instance by synthesizing, so-called black titanium oxide.

An alternative option is to use infrared or visible light and through the use of upconverting materials to transfer the excitation to the photocatalytic material.

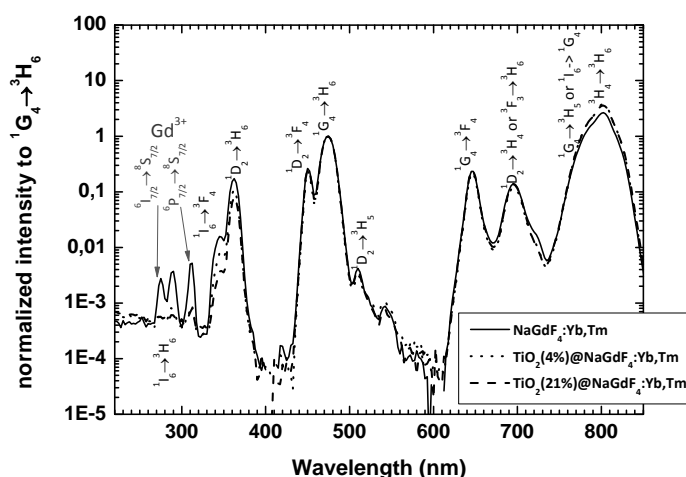
Recently, several groups have demonstrated that this solution could be viable [1-5] and in some cases allow an increase of more than 30% of the photocatalytic activity.

We have synthesized novel molecular precursors $\text{NaGd}(\text{TFA})_4(\text{diglyme})$ (TFA=trifluoroacetate) from which hexagonal phase NaGdF_4 nano-particles were formed. Doped with Yb^{3+} and Tm^{3+} ions they are excellent upconverters to generate UV photons. In a second step those particles have been used to form core-shell $\text{TiO}_2@ \text{NaGdF}_4: \text{Yb}^{3+}, \text{Tm}^{3+}$ structures.

Spectroscopic studies evidence the process of energy transfer from the upconverting phosphor to TiO_2 . In the figure for instance it appears clearly that for the transitions above the gap of TiO_2 the energy is transferred to titania while the other optical transitions are unchanged. This is accompanied by the appearance of photocatalytic activity when exciting with IR light

References:

- [1] Y. Chen, S. Mishra, G. Ledoux, E. Jeanneau, M. Daniel, J. Zhang, S. Daniele, Chemistry an asian journal. 9 (2014) 2415-2421.
- [2] W. Wang, M. Ding, C. Lu, Y. Ni, Z. Xu, Applied Catalysis. B 144, 379 (2014)
- [3] Y. Zhang, Z. Hong, Nanoscale 5, 8930 (2013)
- [4] Y. Tang, W. Di, X. Zhai, R. Yang, W. Qin, ACS Catalysis 3, 405 (2013)
- [5] W. Wang, W.J. Huang, Y.R. Ni, C.H. Lu, L.J. Tan, Z.G. Xu., Applied Surface Science 282, 832 (2013).



Upconversion spectra under 980nm excitation with a laser intensity of $100\text{W}/\text{cm}^2$ in the case of pure $\text{NaGdF}_4: \text{Yb}^{3+}, \text{Tm}^{3+}$ nanoparticles and the same particles with TiO_2 shell of different thicknesses.

Exciton dynamics in perovskite $\text{CH}_3\text{NH}_3\text{PbI}_3$ single crystals

Le Quang Phuong, Yumi Nakaïke, Atsushi Wakamiya, Yoshihiko Kanemitsu

Institute for Chemical Research, Kyoto University, Uji, Kyoto 611-0011, Japan

Hybrid organic-inorganic lead halide perovskites, in particular, methylammonium lead iodide $\text{CH}_3\text{NH}_3\text{PbI}_3$ (MAPbI_3), have attracted global attention in last five years due to their promising applications in photovoltaics and light-emitting devices [1]. Understanding of photophysics of excitations in MAPbI_3 , thus, is of importance for both fundamental researches and practical uses. The photophysics in high-temperature tetragonal-phase MAPbI_3 have been studied intensively, and it is widely considered that the dynamical optical properties in tetragonal-phase MAPbI_3 are governed primarily by free carriers [2]. On the other hand, there are a limited number of works so far devoted to examining the photophysics in low-temperature orthorhombic-phase MAPbI_3 [3]. The exciton binding energy in orthorhombic-phase MAPbI_3 is estimated to vary from 16 to 63 meV [4], which is fairly larger than the thermal energy at cryogenic temperatures. Therefore, it is anticipated that excitons determine optical responses of MAPbI_3 at low temperatures. However, a decisive evidence to discuss qualitatively the excitonic characteristics of orthorhombic-phase MAPbI_3 has not been obtained yet.

In this work, we investigate the photophysics of excitons in $\text{CH}_3\text{NH}_3\text{PbI}_3$ single crystals using time-resolved photoluminescence (PL) spectroscopy. At 15 K, we observe a sharp peak located at 1.633 eV. This emission band, denoted as X band, depends linearly on the excitation fluence and decays quickly within several hundreds of picoseconds. On the other hand, the low-energy-side broad band, denoted as D band, tends to be saturated under high excitation fluences and has a microsecond-scaled decay time. The D band is attenuated as the temperature increases, and disappears as the temperatures above 80 K. Thus, it is concluded that the D band is owed to recombination of excitons localized at the defects in MAPbI_3 . With increasing the temperature, the X band becomes broader, shifts to the high-energy side and no longer to be detected as the temperature is above ~160 K, where a phase transition from the orthorhombic phase to the tetragonal phase occurs. The blue-shift of the X band with the temperature is consistent with the temperature dependence of the band-gap energy of MAPbI_3 observed for thin-film samples [4]. Therefore, the X band is likely to be the free-exciton luminescence of orthorhombic-phase MAPbI_3 . At 15 K, a new emission band emerges at low-energy side of the X band under high excitation fluence. By utilizing one- and two-photon time-resolved PL measurements, we are also able to discuss the physical origin of this new emission band.

Part of this work was supported by JST CREST and JSPS KAKENHI.

References

- [1] S. D. Stranks, and H. J. Snaith, *Nat. Nanotechnol.* 10, 391 (2015).
- [2] Y. Yamada et al., *J. Am. Chem. Soc.* 136, 11610 (2014)
- [3] F. Fang et al., *Adv. Funct. Mater.* 25, 2378 (2015); R. L. Milot et al., *Adv. Funct. Mater.* 25, 6218 (2015) and references therein.
- [4] Y. Yamada et al., *IEEE J. Photovolt.* 5, 401 (2015); A. Miyata et al., *Nat. Phys.* 11, 582 (2015) and references therein.

Dynamics of the Photoexcited States in Octahedral Mo₆ Cluster Halides

Y. Wada^{1,2}, N. Saito^{1,2,3}, F. Grasset^{1,2,4}, S. Cordier⁵, K. Costuas⁵, and N. Ohashi^{1,2}

¹National Institute for Materials Science (NIMS),

1-1 Namiki, Tsukuba, Ibaraki 305-0044, Japan.

²NIMS-Saint-Gobain Center of Excellence for Advanced Materials, NIMS,

1-1 Namiki, Tsukuba, Ibaraki 305-0044, Japan.

³Department of Metallurgy and Ceramics Science, Tokyo Institute of Technology,

2-12-1 Ookayama, Meguro, Tokyo 152-8551, JAPAN

⁴Laboratory of Innovative Key Materials and Structures (LINK; UMI 3629), NIMS,

1-1 Namiki, Tsukuba, Ibaraki 305-0044, Japan.

⁵Institute des Sciences Chimiques de Rennes (ISCR; UMR 6226), University of Rennes 1,

General Leclerc, Rennes 35042, FRANCE.

Ultrafast dynamics of the photoexcited states in the single crystals of tetrabutylammonium (TBA) salts of octahedral Mo₆ cluster halides, (TBA)₂Mo₆X₁₄ (X=Cl, Br, I), (TBAMoX) have been investigated by the femtosecond transient absorption (TA) measurement.

When the lower lying singlet electronic states in TBAMoBr single crystals were generated by the laser light with the photon energy (E_{ex}) of 2.95eV, broad TA bands with a decay time of 80fs were observed. These TA bands are considered to be caused by the singlet-singlet transition of the photo-generated singlet states. Broad TA bands with longer decay times of 1.6ps, 5.5ps, 13ps, 35ps, and much longer than 400ps have been observed. These bands are considered to be caused by the triplet-triplet transitions. The rise time of these bands is 80fs. The singlet-triplet conversion by the intersystem crossing is considered to occur with a time constant of 80fs.

When the TBAMoBr single crystals were irradiated by the UV light (E_{ex} =3.82eV), decay time of the singlet-singlet absorption bands were 200fs. The time constant is considered to be that of the singlet-triplet conversion.

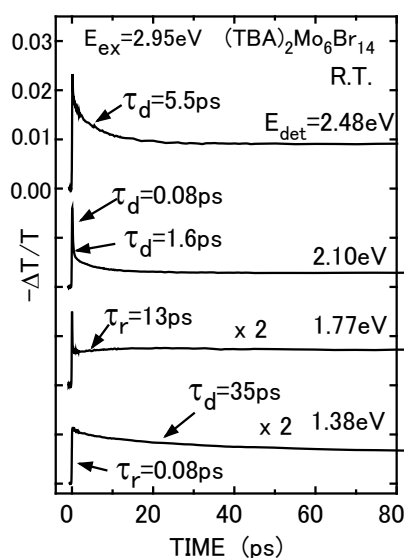


Fig.1 Time evolution of TA

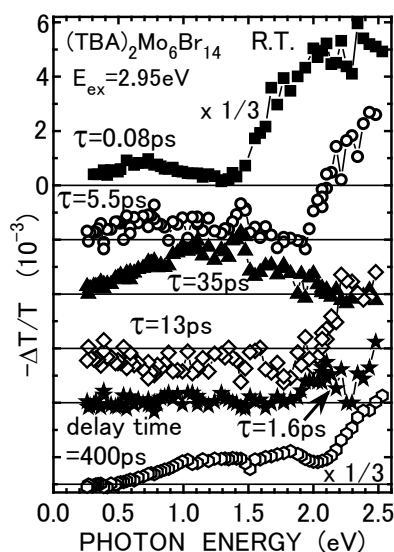


Fig.2 Spectra of the decay components

Chapter 4

**Wednesday 20th July 2016:
Presentations**

Photon conversion in the mid-infrared for gas sensing

A. Braud¹, A.L. Pelé¹, J.L. Doualan¹, R. Chahal², V. Nazabal², B. Bureau², R. Moncorgé¹, and P. Camy¹

1. Centre de Recherche sur les ions, les matériaux et la photonique (CIMAP), Caen, France

UMR 6252 CEA-CNRS-ENSICAEN, Université de Caen, 6 bd Maréchal Juin, 14050 Caen

2. Equipe EVC, UMR 6226, Institut Sciences Chimiques de Rennes, Rennes, France

Many radicals spectroscopic signatures associated to gases of interest are in the 2.5 – 15 μm spectral range (4000-350 cm^{-1}). This spectral range can be addressed by emissions from rare-earth ions embedded into chalcogenide glasses which are well-known for having low phonon energies. We will show results concerning the development of an all-optical sensor at 4.4 μm based on rare-earth doped chalcogenide glasses. The sensor schematic is presented in figure 1: a diode pumped Dy^{3+} doped chalcogenide fiber first produces the infrared signal, which is then sent to the gas cell to probe the gas absorption at 4.4 μm . The probe IR signal is then converted to 800nm by excited state absorption within an Er^{3+} doped chalcogenide fiber making possible to transport the probe signal through a silica optical fiber over large distances considerably increasing the scope of possible applications.

The optimization of the Dy^{3+} doped 2S2G fiber as the IR source, which will be presented, is based on a comparison between experimental data and the modeling of the luminescent fiber. The energy conversion mechanism from 4.4 μm to 800 nm presented in figure 2 has been recently successfully implemented in Er^{3+} doped GeGaSb(Se) chalcogenide fibers [1]. The IR probe signal is modulated while the pump is kept continuous. As a consequence, the 800 nm converted signal from the $^4\text{I}_{9/2}$ level is itself modulated at the IR signal frequency which allows the discrimination between the 800nm “gas” signal and parasitic 800nm luminescence due to upconversion mechanisms (T_{22} in Figure 2) by energy transfer among Er^{3+} ions. Like for the Dy^{3+} doped 2S2G fiber, the Er^{3+} doped 2S2G fiber was optimized to obtain the best signal to noise ratio and the maximum fluorescence at 800nm. Different energy conversion schemes and the corresponding dependence of the converted signal with the pump and probe wavelengths and with photon fluxes will be presented. We will also discuss, using experimental results and simulations, critical parameters for the energy conversion and the sensor itself such as the dopant concentrations, the fibers geometry or the impact of the pump upconversion parasitic signal on the converted signal to noise ratio.

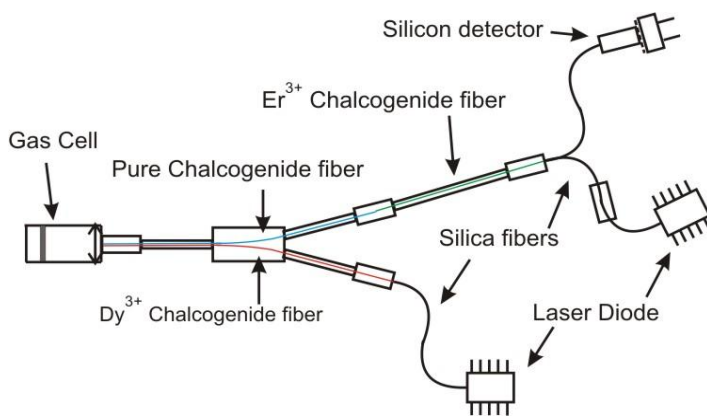


Fig. 1 All-optical sensor scheme

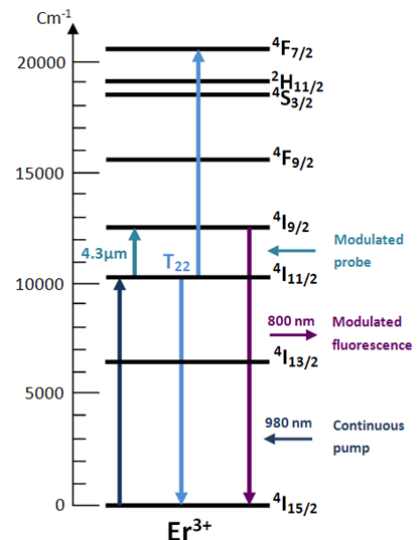


Fig. 2: 4.4 μm to 800 nm conversion in Er^{3+} ions

References

[1] AL. Pelé, A. Braud, J.L. Doualan, R.Chahal, V. Nazabal, B.Bureau, R. Moncorgé, and P. Camy, Optics Express, Vol. 23, Issue 4, pp. 4163-4172 (2015).

Investigation of Thermal Quenching for $\text{Y}_3\text{Al}_5\text{O}_{12}:\text{Ce}^{3+}$ by Thermoluminescence Excitation Spectroscopy

Jumpei Ueda[†], Pieter Dorenbos[§], Adrie J.J. Bos[§], Andries Meijerink[¶],
Setsuhisa Tanabe[†]

[†] Graduate School of Human and Environmental Studies, Kyoto University, Kyoto 606-8501, Japan

[§] Luminescence Materials Research Group, section FAME-RST, Faculty of Applied Sciences, Delft University of Technology, 2629 JB Delft, Netherlands

[¶] Debye Institute, Utrecht University, 3508 TA Utrecht, Netherlands

$\text{Y}_3\text{Al}_5\text{O}_{12}(\text{YAG}):\text{Ce}^{3+}$ is the most widely applied phosphor in white LEDs (w-LEDs) because of strong blue absorption and efficient yellow luminescence combined with a high stability and thermal quenching temperature, required for the extreme operating conditions in high power w-LEDs. The high luminescence quenching temperature (~600 K) has been well established, but surprisingly the mechanism for temperature quenching has not been elucidated yet. In this report we investigate the possibility of thermal ionization as a cause of this quenching process, by measuring thermoluminescence (TL) excitation spectra at various temperatures [1]. In the TL excitation (TLE) spectrum at room temperature, there is no $\text{Ce}^{3+}:5d_1$ band (the lowest excited $5d$ level) as shown in Figure 1. However, in the TLE spectrum at 573 K, which corresponds to the onset temperature of luminescence quenching, a TLE band due to the $\text{Ce}^{3+}:5d_1$ excitation was observed at around 450 nm. Based on our observations, we conclude that the luminescence quenching of $\text{YAG}:\text{Ce}^{3+}$ at high temperatures is caused by the thermal ionization and not by the thermally activated cross-over to the $4f$ ground state. The conclusion is confirmed by analysis of the positions of the $5d$ states of Ce^{3+} relative to the conduction band in the energy band diagram of $\text{YAG}:\text{Ce}^{3+}$.

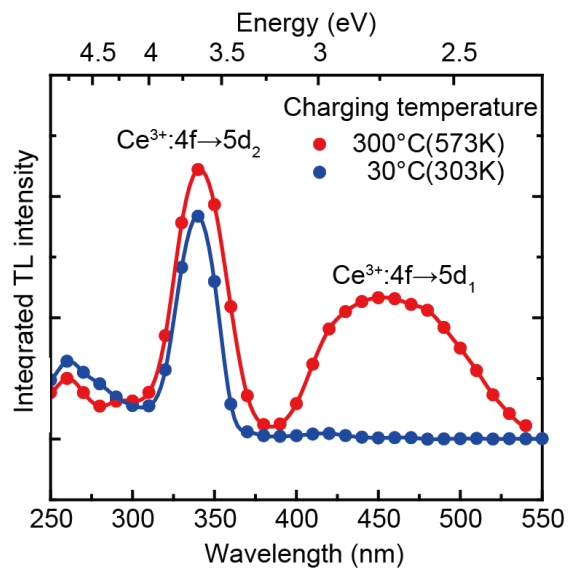


Figure 1. Thermoluminescence excitation (TLE) spectra at two charging temperatures: 303 K (30°C) and 573 K (300°C). The TLE spectra were recorded by measuring the integrated intensity for the high-temperature TL peak around 657 K for different excitation wavelengths between 250 and 550 nm.

References:

[1] Jumpei Ueda, Pieter Dorenbos, Adrie J.J. Bos, Andries Meijerink, Setsuhisa Tanabe, J. Phys. Chem. C **119**(44), 25003-25008.

Controlled Electron-Hole Trapping and Detrapping process in GdAlO₃ by Valence Band Engineering

H.Luo, * A.J.J. Bos, P. Dorenbos

Delft University of Technology, Faculty of Applied Sciences, Mekelweg 15, 2629JB Delft, The Netherlands

* Corresponding author: h.luo@tudelft.nl

Abstract

GdAlO₃:Ln³⁺,RE³⁺ (Ln=Sm, Eu and Yb, RE= Ce, Pr and Tb) were synthesized by solid-state reaction. Sm³⁺, Eu³⁺ and Yb³⁺ act as electron trapping and recombination centres, while Ce³⁺, Pr³⁺ and Tb³⁺ act as hole trapping centres. In this work we present evidence that recombination is by means of hole release from Pr³⁺ and Tb³⁺ instead of the more common electron release. The hole trap depth appears 1.33 eV for Pr³⁺ and 1.28 eV for Tb³⁺. The trapped holes are released from Pr⁴⁺ or Tb⁴⁺ and recombine with the trapped electrons on Sm²⁺, Eu²⁺ or Yb²⁺ to give characteristic trivalent emission from Sm³⁺, Eu³⁺ or Yb³⁺ with main emissions at ~600 nm, ~617 nm or ~980 nm, respectively. Lanthanum was introduced in Gd_{1-x}La_xAlO₃:Eu³⁺,Pr³⁺ and Gd_{1-x}La_xAlO₃:Eu³⁺,Tb³⁺ (x=0, 0.25, 0.5 and 1) to engineer the valence band energy and there with to change the hole trap depth. The vacuum referred binding energy (VRBE) diagram of Gd_{1-x}La_xAlO₃ (x=0, 0.25, 0.5 and 1) in Figure 1 has been constructed by combining low-temperature VUV spectroscopy and thermoluminescence results. The diagram shows that the valence band moves upwards and the trap depth related to Pr³⁺ or Tb³⁺ can be reduced to 0.65 eV or 0.56 eV with increasing the content of La from 0% to 100%. Spectroscopic data needed for construction of the VRBE diagram and TL spectra confirming the reducing of the hole trapping depth will be presented.

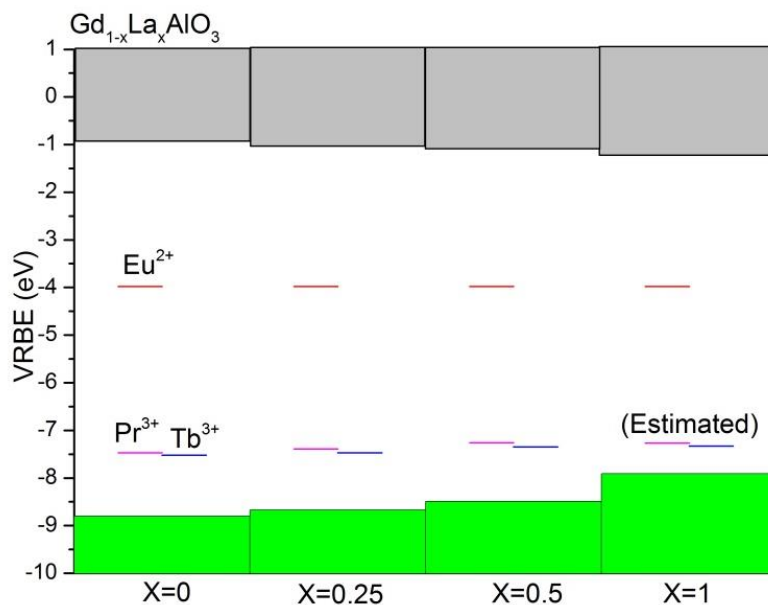


Figure 1. The VRBE diagram of Gd_{1-x}La_xAlO₃ (x=0, 0.25, 0.5 and 1) together with the location of the Pr³⁺, Tb³⁺, and Eu²⁺ ground state energy levels.

Red phosphors based on hexafluorides doped with Mn^{4+} . The new act of old game with $3d^3$ system.

M. Grinberg¹, S. Mahlik¹, T. Leśniewski¹, A. Lazarowska¹, Ye Jin^{2,3}, Ru-Shi Liu^{2,4}

¹ *Institute of Experimental Physics, University of Gdansk, Wita Stwosza 57, 80-952 Gdansk, Poland*

² *Department of Chemistry, National Taiwan University, Taipei 106, Taiwan*

³ *School of Optoelectronic Information, Chongqing University of Technology, Chongqing 400054, China*

⁴ *Department of Mechanical Engineering and Graduate Institute of Manufacturing Technology, National Taipei University of Technology, Taipei 106, Taiwan*

In the last years the Mn^{3+} has been successfully used as a dopant in the red-emitting phosphors based on fluoride matrices such as: AMF_6 ($A=Na, K, Cs, Ba, Rb$; $M=Si, Ti, Ge$), due to their red emission at around 630nm. The peculiarities of the Mn^{4+} emission are the consequence of the specific energetic structure related to three electrons occupying the $3d$ orbital that interacts with the crystal field of the lattice. One should notice that $3d^3$ ions are the most extensively investigated systems, specifically Cr^{3+} , since $Al_2O_3:Cr^{3+}$ (Ruby) has been used for laser generation. In this contribution the details of energetic structure and kinetics of radiative and non-radiative processes in the $3d^3$ system is discussed concerning the electron-lattice interaction and spin orbit-coupling. As an experimental tool which allows to investigate the fundamental aspects of the performance of phosphors doped with Mn^{4+} is the spectroscopy under high hydrostatic pressure applied in diamond anvil cell (DAC) is used. The high pressure spectroscopy has been found to be very effective since high pressure causes the increase of the energy of the excited quartet states 4T_2 and 4T_1 with respect to emitting 2E state and the ground state 4A_2 . Difference between the spectroscopic properties Cr^{3+} and Mn^{4+} ions in different lattices is analyzed in the framework of crystal field model. The diabatic approximation [1] developed for the Cr^{3+} is applied to describe differences in spectroscopic properties of $KNaSiF_6:Mn^{4+}$ and $K_2(Si_{1-x}Ge_x)F_6:Mn^{4+}$, especially the existence or absence of the zero-phonon line of the $^2E \rightarrow ^4A_2$ transition and dependence of the $^2E \rightarrow ^4A_2$ luminescence energy and lifetime on pressure. Analysis of pressure dependence of the luminescence excitation and emission spectra allowed to obtain the values of Racah parameters and crystal field strengths and their pressure dependence. Finally the nephelauxetic is discussed for Mn^{4+} in different lattices.

References

[1] M. Grinberg, A. Suchocki, J. Lumin. 125, 97-103 (2007)

Mn⁴⁺ doped aluminate phosphors for warm white LEDs

Mingying Peng*

*The China-Germany Research Center for Photonic Materials and Devices, State Key Laboratory of Luminescent Materials and Devices, School of Material Science and Engineering, South China University of Technology, Guangzhou 510640, China
pengmingying@scut.edu.cn*

For developing warm white light emitting diodes (WLEDs), it is essential to search for an efficient non-rare earth-based oxide red phosphor, particularly excitable by ultraviolet or blue rather than green lights [1-6]. It, when combined with either UV or Blue LED chips, can, therefore, absorb partially the excitation lights, and convert into red without reabsorbing the lights from the composite device, and eventually improve the device perception. Many efforts have been made on rare earth (e.g. Eu²⁺) doped nitride and oxynitride because of the outstanding performances such as high efficiency or tunable emission colors. Nevertheless, they absorb strongly in the visible (e.g. green) range, and, thus, cannot meet well the above requisition [1-3]. We, recently, found some Mn⁴⁺ doped aluminate red phosphors, e.g. Sr₄Al₁₄O₂₅: Mn⁴⁺, which show the potential as an alternative to Eu²⁺ doped (oxy)nitride [5-6]. In this talk, I will present our systematic works on it including how we found them as well as the fabrication of the proof-of-concept WLEDs.

Acknowledgement

This work was financially supported by National Natural Science Foundation of China (Grant No. 51322208), Guangdong Natural Science Foundation for Distinguished Young Scholars (Grant No. S20120011380), the Department of Education of Guangdong Province (Grant No. 2013gjhz0001) and Fundamental Research Funds for the Central Universities.

References:

1. R. J. Xie, N. Hirotsuki, K. Sakuma, and N. Kimura, J. Phys. D Appl. Phys. 41, 144013 (2008)
2. W. Chen, H. Sheu, R. Liu, J. Attfield, J. Am. Chem. Soc. 134 (19), 8022-802 (2012)
3. V. Bachmann, C. Ronda, O. Oeckler, W. Schnick, A. Meijerink, Chem. Mater. 21 (2), 316-325 (2009)
4. M. Shang, C. Li, J. Lin, Chem. Soc. Rev. 43, 1372-1386 (2014)
5. M. Peng, X. Yin, P. Tanner, C. Liang, P. Li, Q. Zhang, J. Qiu, J. Am. Ceram. Soc. 96, 2870-2876 (2013)
6. M. Peng, X. Yin, P. Tanner, M. Brik, P. Li, Chem. Mater. 27 (8), 2938-2945 (2015)

Degradation processes in the red emitting phosphors $\text{Na}_2\text{MF}_6\text{-Mn}^{4+}$ (M = Si, Ti) exposed to thermal and blue LED irradiation stresses

Anthony Barros^a, Philippe Boutinaud^b, Geneviève Chadeyron^b, Rachid Mahiou^c

*Université Clermont Auvergne, ^aUniversité Blaise Pascal / ^bSIGMA Clermont, Institut de Chimie de Clermont-Ferrand, BP 10448, F-63000 Clermont-Ferrand, France
^cCNRS, UMR 6296, ICCF-F-63178 Aubière, France*

Light sources based on a combination of blue LEDs and yellow + red emitting phosphors blends are nowadays confirmed as promising devices for the domestic market. The lifetime of these devices is one of their specific advantages compared to the other kinds of systems, although this property is still subject of improvements. In this connection, the degradation of the properties of the phosphors in the aged devices is one of the major issues that require appropriate remedies.

In this work, we have carried out a detailed investigation of the degradation processes occurring in the red phosphors $\text{Na}_2\text{MF}_6\text{-Mn}^{4+}$ (M = Si, Ti) that are relevant candidates in LED-based solid state lighting applications. A computer-controlled accelerated degradation setup has been designed for this purpose. The setup consists of a power-controlled blue emitting LED chip, a regulated heater, a moisture controller and a fibered spectrometer allowing the automatic collection of luminescence spectra over long periods of time.

This system allowed us the investigation of the action of moisture, of the incoming blue light power, of the thermal stress and of any combination of these stresses. Models accounting for the observed photoluminescence degradation kinetics are introduced and the physico-chemical processes involved in the phosphors degradation are discussed on the basis of diffuse reflectivity, ESR, NMR, XPS and magnetic susceptibility measurements.

Ionoluminescence as a Tool to Investigate the Dynamics of Electronic Excitations in Dielectrics: the Case of SiO₂

**Diana Bachiller-Perea^{1,2}, David Jiménez-Rey³, Ángel Muñoz-Martín¹,
Fernando Agulló-López¹**

¹*Centro de Micro-Análisis de Materiales, Universidad Autónoma de Madrid, Calle Faraday 3, E-28049, Spain*

²*Centre de Sciences Nucléaires et de Sciences de la Matière, Université Paris-Sud, Bât 108, 91405 Orsay, France.*

³*Laboratorio Nacional de Fusión, Ciemat, Madrid, Spain.*

SiO₂ is a dielectric compound with a wide band gap (around 8-10 eV) and presenting several crystalline and amorphous phases. Ion Beam Induced Luminescence or Ionoluminescence (IBIL or IL) is a useful technique relying on the light emission excited by ion-beam bombardment that has often been used to monitor the generation of point defects (microscopic damage) during irradiation. Recently, the ionoluminescence yield and kinetics at room temperature have been shown to provide useful information on the dynamics of electronic excitation. In particular, results on silica and quartz have been modelled in terms of the dynamics of self-trapped excitons (STEs) in the SiO₂ network: generation, migration by hopping and final recombination at color center sites (Non-Bridging Oxygen Hole Centers and Oxygen-Deficient Centers). A short overview of the model will be described including a mathematical simulation. By irradiating with different ions and energies one may modify the structure of the SiO₂ network and explore, *in situ*, the influence of such changes on the STE dynamics. In particular the transition from the crystalline (α -quartz) to the amorphous phase induces a marked decrease in the STE migration length. A significant decrease is observed in the amorphous phase due to the irradiation-induced compaction that can be correlated with the changes in the ω_4 vibrational frequency of the SiO₄ tetrahedra. Moreover, irradiation experiments at low temperature are also consistent with the model and reveal how the STE migration parameters change with temperature.

Qubits in diamond: solid state quantum registers and nanoscale sensors

Fedor Jelezko

Institute of quantum optics, Ulm University

Recently, atom-like impurities in diamond (colour centers) have emerged as an exceptional system for quantum physics in solid state. In this talk I will discuss recent developments transforming quantum control tools into quantum technologies based on single colour centers. Specially, realization of quantum optical interface between spins and photons and scalable quantum registers in diamond will be presented. New applications of diamond qubits involving nanoscale magnetic resonance and force measurements will be shown. I will discuss single spin NMR paving the way to ultrasensitive MRI and structure determination of single biomolecules. I will also highlight future directions of research including combination of quantum error correction and sensing protocols and quantum enabled sensing and imaging in living cells.

Lineshape in Spectra of XeCenter in Diamond: From Helium to Room Temperatures

Yury Deshko¹ and Anshel Gorokhovskiy²

¹Coriant Advanced Technology

²City University of New York / College of Staten Island and The Graduate Center

The ion implantation technique allows one to introduce into diamond different optical centers having emission lines in a broad spectral range, including the near-infrared region. Focused ion implantation and electron beam lithography enables nanoscale patterning of diamond, and may be used to fabricate single center optical emitters and optically active carbon nanostructures for quantum information processing. The Xe ion related center is of particular interest as it is one of a few centers (Ni, Si, Cr) in diamond having sharp zero phonon emission lines (ZPL) in the infrared spectral region, both in photo- and electroluminescence.

In this presentation we will focus on the mechanisms of ZPL shape and thermal broadening in the broad temperature range 1.8 – 300 K. At low temperatures the photoluminescence spectra feature a single narrow ZPL at 811.7 nm and a weak phonon sideband (the Debye-Waller factor is more than 0.9). The width of the ZPL at $T < 20$ K and low implantation doses could be less than 0.2 cm^{-1} - similar to lines of rare earth ions in good crystals. The lineshape investigation indicates inhomogeneous broadening due to 2D distribution of implanted ions [1]. At higher temperatures the interactions with phonons kick in: ZPL becomes broader and its shape develops a significant asymmetry. We attempt to describe the thermal changes, not just in the linewidth but also in the much more sensitive spectral shape of the ZPL, in terms of vibronic couplings without free parameters. The following topics will be discussed: low and high temperature luminescence spectra, manifestation of pseudolocal vibrational modes in the low-frequency Stokes and anti-Stokes phonon sidebands, mechanisms of optical dephasing and the lineshape due to quadratic vibronic coupling, fitting of the ZPL shape and width for the temperature range 30 - 200 K in the model of quadratic interaction with pseudolocal modes [2], fitting of the ZPL width for the temperature range 200 - 300 K taking into account Orbach processes in the excited electronic state.

References:

- [1] Y. Deshko, A. Gorokhovskiy, *Effects of planar geometry on the inhomogeneous broadening of zero phonon lines of optical centers in diamond*, Phys. Status Solidi B **250** (2013), 278-282.
- [2] V. Hizhnyakov, K. Seranski, U. Schurath, *Homogeneous lineshapes and shifts of the $b^1\Sigma^+ \leftarrow X^3\Sigma^-$ transition in matrix-isolated NH: comparison with quadratic coupling theory*, Chemical Physics **162** (1992), 249 – 256.

Implications of ultra-narrow linewidth stoichiometric rare earth crystals for quantum information

Rose Ahlefeldt¹, Michael Hush², Matthew Sellars¹

¹*Research School of Physics and Engineering, The Australian National University, Canberra 0200, Australia*

²*School of Engineering and Information Technology, University of New South Wales at the Australian Defence Force Academy, Canberra 2600, Australia*

Rare earth ions in crystals are an attractive system for quantum information applications because they have extremely long hyperfine coherence times, up to 6 hours [1]. To date, rare earth quantum information has focused on crystals in which the rare earth is a low concentration dopant, but there are a number of advantages offered by the opposite regime, crystals stoichiometric in the rare earth ion. First, the high concentration means that these materials can have extremely high optical depths, which is beneficial in particular for quantum memory applications. Second, stoichiometric crystals can have extremely low optical inhomogeneous linewidths, smaller than the hyperfine structure. In this limit, it is possible to optically pump the population of the crystal into a single spin state, which gives new possibilities for quantum information applications. For instance, the bandwidth of current spin wave storage memories can be improved, and off-resonant Raman memories[2], [3] are possible in solid state for the first time.

We have achieved an optical inhomogeneous linewidth of 25 MHz in a crystal of $\text{Eu}^{35}\text{Cl}_3 \cdot 6\text{H}_2\text{O}$ by isotopically purifying the crystal in ^{35}Cl . This is one of the narrowest linewidths in any material and is smaller than the hyperfine splitting of both Eu isotopes. As a result, over 95% of the ^{153}Eu ions in the crystal can be pumped into a single hyperfine ground state. We will discuss the use of this system to quantum memory applications.

The linewidth is also smaller than the static ion-ion interaction between Eu electronic levels. The system then closely resembles a Rydberg gas, and a variety of the effects predicted for Rydberg systems, such as excitation blockade, should be seen in these materials[4]. As we will describe, this opens new quantum information applications of these crystals, such as quantum many body studies, and new ensemble-based quantum computing protocols.

References:

- [1] M. Zhong, M. P. Hedges, R. L. Ahlefeldt, J. G. Bartholomew, S. E. Beavan, S. M. Wittig, J. J. Longdell, and M. J. Sellars, *Nature* 517 (2015) 177.
- [2] J. Nunn, I. A. Walmsley, M. G. Raymer, K. Surmacz, F. C. Waldermann, Z. Wang, and D. Jaksch, *Phys. Rev. A* 75 (2007) 011401.
- [3] A. V. Gorshkov, A. André, M. D. Lukin, and A. S. Sørensen, *Phys. Rev. A* 76 (2007) 033805.
- [4] M. Saffman, T. G. Walker, and K. Mølmer, *Rev. Mod. Phys.* 82 (2010) 2313.

Optical pumping in Neodymium-doped yttrium orthosilicate

Emmanuel Zambrini Cruzeiro¹, Imam Usmani², Alexey Tiranov¹, Cyril Laplane¹,
Jonathan Lavoie¹, Nicolas Gisin¹, Mikael Afzelius¹

1- Group of Applied Physics, University of Geneva, Switzerland

2- Laboratoire Charles Fabry, ParisTech, France

Many quantum information applications based on rare-earth ions require efficient optical pumping between ground state levels. In Kramers ions such as Nd³⁺ and Er³⁺, the ground state is doubly degenerated at zero magnetic field. This doublet can be described as a fictive spin $S=1/2$ system, with a Zeeman splitting proportional to an external magnetic field strength and the orientation of this field with respect to the crystal lattice. Those levels can be used for population storage [1-3]. For efficient optical pumping the Zeeman population lifetime (T_1^Z) must be much longer than the radiative lifetime T_1 of the optically excited state through which population is cycled. Zeeman population lifetimes have traditionally been studied in electron spin resonance (ESR) experiments. In the high magnetic-field conditions of ESR experiments T_1^Z is normally governed by spin lattice relaxation (SLR) between the spin states [4]. Extrapolating those lifetimes to lower fields predicts T_1^Z of several seconds for Nd³⁺ in Y₂SiO₅ [5].

We have measured the optical spectral hole lifetime using transient spectral hole burning techniques as a function of magnetic field, for several angles in the D1-D2 plane of the Y₂SiO₅ crystal host. We find a general trend where the lifetime is short at low field, then increases to a maximum value at around 0.5 Tesla, and then decays quickly for high fields up to 2 Tesla. We show that the high-field relaxation rate can be fitted to the direct phonon processes in the standard SLR theory, whereas the low-field regime requires a model not considered in conventional ESR experiments. We propose a model based on Nd³⁺ spin “flip-flops”, and show that this relaxation process is the main limitation to reach long T_1^Z . To test our hypothesis we studied three samples having different Nd³⁺ concentrations. We found that one can reach lifetimes of around 4 seconds at 3 K in a crystal with extremely weak Nd³⁺ concentration (around 1 ppm). The longest lifetime reported so far was 120 ms [6]. These results imply that the efficiency of optical pumping in Nd³⁺:Y₂SiO₅ can be greatly increased, which could lead to more efficient optical quantum memories based on such crystals [7].

[1] R. M. Macfarlane and J. C. Vial, Phys. Rev. B **36**, 3511 (1987)

[2] S. R. Hastings-Simon *et al.*, Phys. Rev. B **78**, 085410 (2008)

[3] M. Afzelius *et al.*, J. Lumin. **130**, 1566 (2010)

[4] G. H. Larson and C. D. Jeffries, Phys. Rev. **145**, 311 (1966)

[5] I. N. Kurkin and K. P. Chernov, Physica B **101**, 233 (1980)

[6] I. Usmani, M. Afzelius, H. de Riedmatten, and N. Gisin, Nature Comm. **1**, **12** (2010)

[7] M. Afzelius and H. de Riedmatten, in Engineering the Atom-Photon Interaction: Controlling Fundamental Processes with Photons, Atoms and Solids, Nano-Optics and Nanophotonics (Eds. A. Predojević and M. W. Mitchell) (2015)

High Resolution Spectroscopy of Single Erbium Sites in Silicon

Milos Rancic¹, Matthew Sellars¹, Chunming Yin², Gabrielle DeBoo², Qi Zhang², Sven Rogge², Sebastian Horvath³, Michael Reid³

¹ *Research School of Physical Sciences, Australian National University, Canberra, Australia*

² *Research School of Physics, University of New South Wales, Sydney, Australia*

³ *Department of Physics and Astronomy, University of Canterbury, Christchurch, New Zealand*

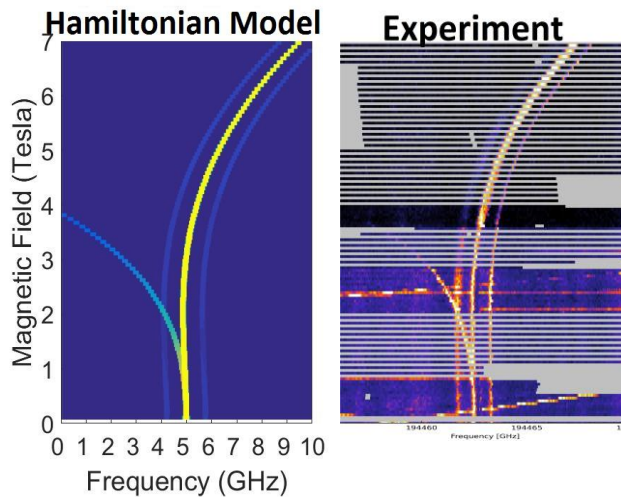
Trivalent erbium is well known for its optical transition at 1550 nm; corresponding to the telecoms fibre transmission window. For this reason, erbium is vital for classical data transmission in optical fibre networks. Many researchers in the quantum optics field are now investigating whether erbium can play a similar role in quantum networks, as an interface (and storage medium) of stationary and “flying” qubits. To this end, in 2013 we demonstrated resonant optical excitation and electronic readout of a single erbium dopant in a silicon based Single Electron Transistor (SET) [1].

The ultimate goal of our research is to develop an erbium based “optical bus” to interface phosphor in silicon (P:Si) based quantum computers [2] with a quantum network, by coupling phosphor and erbium qubits in a single silicon device.

This presentation will focus on our on-going investigation into these optical-electronic hybrid erbium doped devices. In particular, we are developing techniques to determine the crystal field structure of individual erbium sites. The characterisation techniques focus on the magnetic field dependence of the optical transitions of individual sites.

The purpose of characterising the crystal field of these erbium ions is to understand and determine whether any particular crystal field structure will have advantageous characteristics for an erbium based spin qubit.

In this presentation we report results on one particular erbium site, which has been determined to have approximately trigonal axial symmetry (C_{3v}).



The images to the left show the magnetic field dependence optical transitions for an axial trigonal erbium site. On the left is a complete crystal field Hamiltonian model, including the nuclear structure. On the right is the experimental data.

References:

- [1] Chunming Yin, Milos Rancic, et al. *Optical addressing of an individual erbium ion in silicon*. Nature **497**, 91–94, (02 May 2013)
- [2] M. Veldhorst, et al. *A two-qubit logic gate in silicon*, Nature, **526**, 410–414, (15 October 2015)

Smarter Modelling of Energy Levels of Rare-Earth Quantum-Information Candidates

M.F. Reid^{1,2,3*}, S.P. Horvath¹, J.S. Stewart¹, J.-P.R. Wells^{1,2}

¹*Department of Physics and Astronomy, University of Canterbury, Christchurch 8140, New Zealand*

²*The Dodd-Walls Centre for Quantum and Photonic Technologies*

³*MacDiarmid Institute for Advanced Materials and Nanotechnology*

**mike.reid@canterbury.ac.nz*

Advances in the use of rare-earth ions in quantum-information applications depend on extending storage times. Recent use of the ZEFOZ (Zero First Order Zeeman) technique has enabled coherence to be stored for up to six hours [1]. Searching for the ZEFOZ point requires a detailed knowledge of the spin Hamiltonian for the particular magnetic-hyperfine splitting of the electronic states of interest, which in turn entails exhaustive spectroscopic studies, and non-trivial parameter fitting. Consequently, this approach has so far only been applied to three rare-earth systems.

An alternative approach is to use crystal-field theory to calculate magnetic-hyperfine spin Hamiltonians [2]. Since the parameters in the crystal-field model vary predictably across the rare-earth series, parameter sets for a few ions may be extended to the whole series, thus enabling theoretical exploration of many candidate transitions and potentially saving considerable experimental effort.

The YSO system used in Ref. [1] has a very low symmetry, so the determination of crystal-field parameters has previously been an insoluble problem. However, a combination of ab-initio calculations [3], and parameter fitting that adds Zeeman and hyperfine data to the electronic energy-level data [2] makes this problem tractable. In this work we report on our progress in determining crystal-field parameters and spin Hamiltonians for rare-earth ions in YSO.

References:

- [1] M. Zhong, M.P. Hedges, R.L. Ahlefeldt, J.G. Bartholomew, S.E. Beavan, S.M. Wittig, J.J. Longdell, and M.J. Sellars. *Optically addressable nuclear spins in a solid with a six-hour coherence time*. Nature 517, 177 (2015).
- [2] S.P. Horvath, M.F. Reid, and J.P.R. Wells, M. Yamaga, *High precision wavefunctions for hyperfine states of low symmetry materials suitable for quantum information processing*. J. Luminescence 169,773 (2016).
- [3] J. Wen, C.K. Duan, L. Ning, Y. Huang, S. Zhan, J. Zhang, and M. Yin. *Spectroscopic Distinctions between Two Types of Ce³⁺ Ions in X₂-Y₂SiO₅: A Theoretical Investigation*. J. Phys. Chem. A 118, 4988 (2014).

Chapter 5

**Thursday 21st July 2016:
Presentations**

Spin dynamics of charged and neutral excitons in colloidal nanocrystals

D. R. Yakovlev

TU Dortmund University, 44221 Dortmund, Germany
Ioffe Institute, Russian Academy of Sciences, 194021 St. Petersburg, Russia

Colloidal semiconductor nanocrystals are attracting objects for basic research of the strongly confined systems as well as for applications for bio-sensors and photovoltaic. We have found that photo-excitation of core/shell CdSe/CdS nanocrystals (NCs), which shell thickness exceeds 4 nm, leads to a single electron charging of NCs [1,2]. This is consequence of the charge separation of photogenerated in NC an electron-hole pair: the hole is captured by a surface state and the long-lived electron is created in the CdSe core. Photogeneration of any consequent electron-hole pair in this singly-charged NC results in formation of the negatively charged exciton (trion), consisting of two electrons in the singlet state and a hole. We report on experimental and theoretical studies of the trion and exciton spin dynamics in core/thick shell CdSe/CdS NCs. Time-resolved photoluminescence measurements were performed at low temperatures and in high magnetic fields up to 15 Tesla. From the decay of the photoluminescence intensity the trion radiative time of 8 ns was measured. It is independent of the magnetic field reflecting the fact that the trion ground state is always optically bright (i.e. allowed in electric-dipole approximation). This is in strong contrast to the exciton states in NCs which dynamics is controlled by a competition of the bright and dark states.

Spin relaxation times were measured from dynamics of the magnetic-field-induced circular polarization degree, controlled by the trion or exciton thermalization on the Zeeman sublevels split by magnetic field. For excitons these times are shorter than a nanosecond, while for the trions very long spin relaxation time up to 60 ns was measured. Theoretical description of the polarization dynamics takes into account random orientation of NCs hexagonal axes to the magnetic field direction and the anisotropy of the heavy-hole g-factor. The longitudinal component of the hole g factor of -0.54 was received from the modeling of experimental data.

Linear and circular polarization is measured for dot-in-rod CdSe/CdS NCs and information on spin dynamics and rod orientations is received [3].

References:

- [1] C. Javaux, B. Mahler, B. Dubertret, A. Shabaev, A.V. Rodina, Al. L. Efros, D. R. Yakovlev, F. Liu, M. Bayer, G. Camps, L. Biadala, S. Buil, X. Quelin, and J.P. Hermier, *Nature Nanotechnology***8**, 206 (2013).
- [2] F. Liu, L. Biadala, A.V. Rodina, D.R. Yakovlev, D. Dunker, C. Javaux, J.P. Hermier, Al.L. Efros, B. Dubertret, and M. Bayer, *Phys. Rev. B***88**, 035302 (2013).
- [3] B. Siebers, L. Biadala, D. R. Yakovlev, A. V. Rodina, T. Aubert, Z. Hens, and M. Bayer, *Phys. Rev. B* **91**, 155304 (2015).

Local density of states and energy transfer in nanophotonics

Rémi Carminati

*Institut Langevin, ESPCI Paris, CNRS, 1 rue Jussieu, 75005 Paris
remi.carminati@espci.fr*

Measuring and engineering the electromagnetic local density of states (LDOS) at a subwavelength scale is a central issue nanophotonics. Indeed, the LDOS drives the dynamics of basic processes of light-matter interaction, such as spontaneous emission (fluorescence) or absorption [1]. Nanophotonics, including plasmonics, is at a stage where, on the one hand, fundamental studies of light-matter interaction are possible based on almost ideal experiments (e.g. a single emitter interacting with single shaped nano-objects), and on the other hand, the development of real devices is emerging.

We will describe recent developments towards the mapping and the characterization of the LDOS at the nanoscale. We will show that the radiative and non-radiative contributions to the LDOS can be identified and separated [2]. We will also report on a method to quantify the relative weights of the electric and magnetic components included in the local density of states [3]. These studies pave the way towards the full electric and magnetic characterization of nanostructures for the control of single emitter luminescence.

Beyond LDOS, the concept of cross density of states (CDOS) permits a description of the intrinsic spatial coherence sustained by the system itself, independently on the illumination or excitation conditions [4]. The CDOS essentially measures the spatial extent of the electromagnetic eigenmodes, which can be controlled, e.g., by using surface excitations (such as surface-plasmon polaritons). As a simple example, we will show that long-range energy transfer between fluorescent molecules can be achieved on a metal using surface plasmons [5].

[1] R. Carminati *et al.*, *Electromagnetic density of states in complex plasmonic systems*, Surf. Sci. Rep. **70**, 1 (2015).

[2] D. Cao *et al.*, *Mapping the radiative and the apparent non-radiative local density of states in the near field of a metallic nanoantenna*, ACS Photonics **2**, 189 (2015).

[3] L. Aigouy, A. Cazé, P. Gredin, M. Mortier and R. Carminati, *Mapping and quantifying electric and magnetic dipole luminescence at the nanoscale*, Phys. Rev. Lett. **113**, 076101 (2014).

[4] A. Cazé, R. Pierrat and R. Carminati, *Spatial coherence in complex photonic and plasmonic systems*, Phys. Rev. Lett. **110**, 063903 (2013).

[5] D. Bouchet, D. Cao, R. Carminati, Y. De Wilde, and V. Krachmalnicoff, *Long-Range Plasmon-Assisted Energy Transfer between Fluorescent Emitters*, Phys. Rev. Lett. **116**, 037401 (2016).

Modification of phonon processes in nano-structured rare-earth-ion-doped materials

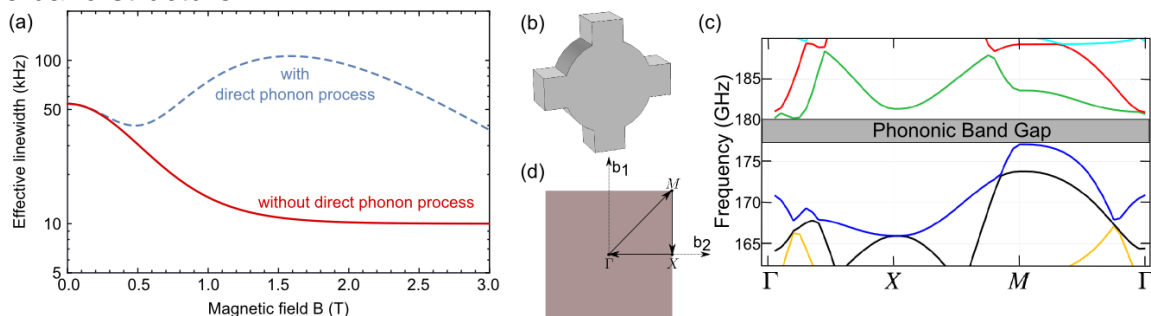
Thomas Lutz¹, Lucile Veissier¹, Charles W. Thiel², Philip J. T. Woodburn², Rufus L. Cone², Paul E. Barclay¹, Wolfgang Tittel¹

¹Institute for Quantum Science and Technology, Department of Physics & Astronomy, University of Calgary, Calgary, Alberta T2N 1N4, Canada

²Department of Physics, Montana State University, Bozeman, MT 59717 USA

Nano-structuring impurity-doped crystals affects the phonon density of states and thereby modifies the atomic dynamics induced by interaction with phonons. We propose the use of nanostructured materials in the form of powders or phononic bandgap crystals to enable or improve persistent spectral hole-burning and coherence for inhomogeneously broadened absorption lines in rare-earth-ion-doped crystals [1]. This is crucial for applications such as ultra-precise radio-frequency spectrum analyzers and optical quantum memories.

First, as an example, we present simulations for density of states of nano-sized powders and phononic crystals for the case of $\text{Er}^{3+}:\text{Y}_2\text{SiO}_5$, a widely-used material in current quantum memory research operating in the convenient telecommunication band. In the figure below, the effect of phonon restriction on the homogeneous linewidth (a) together with the geometry of the phononic crystal (b) and its bandstructure (c) are shown for a typical, erbium doped material. Panel (d) of the Figure shows the points of the reciprocal lattice of the phononic crystal traversed in the band structure.



Second, we will report on experimental investigation towards the realization of impurity-doped nanocrystals with good spectroscopic properties [2]. Crystal properties such as nuclear spin lifetime are strongly affected by mechanical treatment, and spectral hole-burning can serve as a sensitive method to characterize the quality of REI doped powders. Different methods for obtaining powders are compared and the influence of annealing on the spectroscopic quality of powders is investigated. We conclude that annealing can reverse some detrimental effects of powder fabrication and, in certain cases, the properties of the bulk material can be reached. Such nano-sized particles can be used to show the suppression of detrimental phonons.

References:

[1] T. Lutz, L. Veissier, C. W. Thiel, R. L. Cone, P. E. Barclay, W. Tittel, arxiv:1504:02471 (2015)

[2] T. Lutz, L. Veissier, C. W. Thiel, P. J. T. Woodburn, R. L. Cone, P. E. Barclay, W. Tittel, arxiv:1509:07862 (2015), accepted in *Sci. Technol. Adv. Mater.*

Spectroscopic properties of $\text{La}_{1-x}\text{Gd}_x\text{AlO}_3$ nanocrystals doped with Pr^{3+} ions

K. Lemański*, B. Bondzior, P.J. Dereń

*Institute of Low Temperature and Structure Research Polish Academy of Sciences,
ul. Okólna 2, 50-422 Wrocław, Poland*

**Corresponding author: K.Lemanski@int.pan.wroc.pl*

Perovskites crystals are one of the most important family of inorganic compounds. Because of their interesting structural, optical, magnetic, electrical and superconducting properties, they find numerous applications. Furthermore, the oxide perovskites are resistant to the UV radiation and other physicochemical factors, they are also chemically stable and non-toxic. Perovskites crystals are good matrices to examine for scientific and application purposes. Recently, these crystals have become even more interesting for the researchers, due to their huge potential applications in Solar Energy Systems.

The synthesis of the investigated $\text{La}_{1-x}\text{Gd}_x\text{AlO}_3$ perovskite powders were carried out by using the Pechini method. Crystal structures were confirmed with the X-ray diffraction diagrams (XRD) measured with a powder diffractometer. GdAlO_3 perovskite crystal possess a Pbnm orthorhombic space group [1]. LaAlO_3 is has a rhombohedral crystal structure with R-3c space group stable at 300 K and a cubic structure with space group Pm-3m at temperatures above 800 K [2].

The excitation, emission spectra, time decay profiles of the praseodymium(III) ions were measured and analyzed. The influence of luminescent properties depending on the annealing temperature and concentration of Pr^{3+} ions as well as the influence of the La / Gd ratio, were analysed and discussed.

References:

- [1] R. J. Angel, J. Zhao, and N. L. Ross, Phys. Rev. Lett. 95 (2005) 025503.
- [2] P. J. Dereń, R. Mahiou, Opt. Mater. 29 (2007) 766–772.

Hot intraband luminescence under different types of excitation

Sergey Omelkov, Vitali Nagirnyi and Marco Kirm

Institute of Physics, University of Tartu, W. Ostwaldi str. 1, 50411 Tartu, Estonia

Hot intraband luminescence (IBL) is a low yield ultrafast emission connected with the radiative transitions of hot electrons or hot holes between the sub-levels of the conduction or valence band of a crystal, respectively [1]. The continuous and structureless spectrum of IBL covers the whole transparency region of a material, with increase of the intensity in NIR [2]. The IBL decay time and yield are to a large extent defined by the competitive process of nonradiative transitions which are far more probable than the radiative ones. The decay time is expected to be below 1 ps, while the quantum yield has been reported as 10^{-4} photons per electron-hole pair for potassium iodide [1]. We estimated the value of its scintillation yield to 20 photons/MeV in CeF₃. Recently ultrafast emission processes have gained attention due to increasing demands for higher scintillation time resolution in medical and high-energy physics applications [3]. Despite its low yield, IBL can potentially improve scintillation time resolution by providing an almost instant time marker for the event.

However, there have been no reports on direct observation of IBL in the excitation conditions similar to single-photon scintillation counting. The primary excitation sources in the IBL studies have been pulsed electron guns, typically providing high peak current of 10–100 A/cm² and more [1]. We observed IBL under excitation by a low-energy (10 keV) and low-current (2 μ A/mm²) continuous electron beam, as well as by pulsed x-rays (8 and 17 keV). For the first time the IBL was monitored under low-power excitation, confirming the absence of a threshold of its mechanism. The data obtained allow the prediction that the IBL can be excited by single photons of 511-keV energy, which is required for enhancing scintillation time resolution in time-of-flight positron emission tomography (TOF-PET) [3].

Our observations of IBL reveal a substantial dependence of its yield on the energy of exciting particles in the range of 10–150 keV. The models of a non-proportional scintillator response, being actively developed recently, focus on the nonlinear quenching processes due to the interaction of both hot and thermalized quaziparticles [4]. As the mechanism of IBL concerns only hot charge carriers, the studies of its nonproportionality are potentially able to reveal the peculiarities of the quenching processes at the stages preceding thermalization. Our recent experimental results on the IBL properties, such as light yield, spectra and their dependencies on the type of excitation will be discussed.

References:

- [1] D. Vaisburd and S. Kharitonova, Russian Physics Journal 40 (1997) 1037
- [2] S. Omelkov, V. Nagirnyi, A.N. Vasil'ev and M. Kirm, submitted to J.Lumin. (2016)
- [3] P. Lecoq, M. Korzhik and A. Vasiliev, IEEE Trans. Nucl. Sci. 61 (2014) 229
- [4] X. Lu, Q. Li, G.A. Bizarri et al., Phys. Rev. B 92 (2015) 115207

Collective Higgs amplitude mode in superconductors studied by strong terahertz pulse

Ryusuke Matsunaga

Department of Physics, The University of Tokyo

Recently intense terahertz (THz) pulse generation technique on tabletop experiment has been remarkably progressed, which has offered novel opportunities to reveal ultrafast phenomena in a variety of materials strongly driven by low-frequency electromagnetic field [1]. By using the strong THz pump-THz probe spectroscopy, we have investigated nonequilibrium dynamics of s-wave superconductors $\text{Nb}_{1-x}\text{Ti}_x\text{N}$.

Phase transition from a normal metal to a superconductor is characterized by emergence of order parameter, a single macroscopic wavefunction representing the superfluid density. Order parameter in a conventional superconductor is observed as an energy gap in the single-particle excitation spectrum, typically of the order of meV, *i.e.*, in the THz frequency range (1 THz = 4.14 meV). Therefore the strong monocycle THz pulse can instantaneously excite high-density quasiparticles at the gap edge without excess energy, which realize *nonadiabatic* excitation to a superconducting state without heating the lattice subsystem, in contrast to the excitation by visible/near-infrared optical pulse. After the nonadiabatic excitation a transient oscillation of the order parameter was observed in the transmission of the THz probe pulse [2]. This result is attributed to the amplitude mode of the order parameter, namely the Higgs mode, a collective excitation mode originating from spontaneous symmetry breaking. Although the Higgs mode does not directly couple with electromagnetic field, we revealed that the Higgs mode is induced by shaking the superconducting ground state in a nonadiabatic way and can be observed in a time domain by ultrafast spectroscopy.

We also discovered that the Higgs mode can be resonantly excited by sub-gap narrow-band THz pulses in nonlinear response regime [3]. This resonance between the light and the Higgs mode results in an efficient third-order harmonics generation in the THz frequency. These results shed new light on the ultrafast control of macroscopic quantum condensates by optical means as well as THz nonlinear optics using superconductors. Recent experimental results for a two-gap superconductor MgB_2 will be also presented.

References:

- [1] T. Kampfrath, K. Tanaka, and K. A. Nelson, *Nature Photon.* 7 (2013) 680.
- [2] R. Matsunaga *et al.*, *Phys. Rev. Lett.* 111 (2013) 057002.
- [3] R. Matsunaga *et al.*, *Science* 345 (2014) 1145.

Nonlinear optical spectroscopy on exciton states in model semiconductors GaAs and ZnO

R.V. Pisarev

Ioffe Physical Technical Institute, Russian Academy of Sciences, St. Petersburg, Russia

Nonlinear optics of semiconductors is an important field of fundamental and applied research, but until recently the role of excitons in the coherent processes leading to harmonics generation has remained essentially unexplored. In this talk we will report some results of experimental and theoretical studies of the second (SHG) and third (THG) harmonic generation involving the exciton resonances in noncentrosymmetric semiconductors ZnO ($6mm$ symmetry) and GaAs ($-43m$ symmetry). External electric and magnetic fields are used to modify exciton states and their contributions to nonlinear optical properties. As an example, Fig. 1 shows the magnetic-field-induced SHG spectrum in ZnO for the incident and SHG light propagating along the sixfold optical axis. In this geometry, SHG is forbidden but becomes allowed in a magnetic field applied perpendicular to this axis [1]. The SHG signal arises due to mixing of the $2s$ and $2p$ exciton states in an applied magnetic field. Fig. 2 shows the electric-field-induced SHG in GaAs in the region of the $1s$ exciton [2]. Inset in this Figure shows SHG intensity as a function of positive and negative electric field.

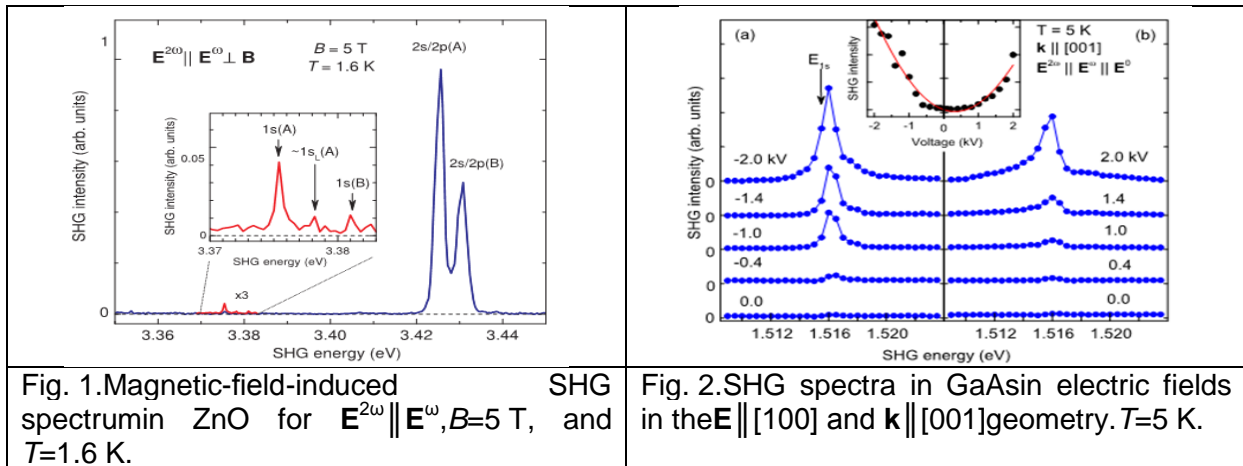


Fig. 1. Magnetic-field-induced SHG spectrum in ZnO for $E^{2\omega} \parallel E^{\omega}$, $B = 5$ T, and $T = 1.6$ K.

Fig. 2. SHG spectra in GaAs in electric fields in the $E \parallel [100]$ and $k \parallel [001]$ geometry. $T = 5$ K.

A microscopic theory of SHG and THG on excitons was developed [1,2] which showed that the nonlinear interaction of coherent light with excitons has to be considered beyond the electric-dipole approximation. Depending on the particular symmetry of the exciton states, SHG/THG can originate from the electric- and magnetic-field-induced perturbations of the excitons due to the Stark effect, the spin as well as orbital Zeeman effects, or the magneto-Stark effect. The observed mechanisms of optical nonlinearities due to harmonics generation open access to centrosymmetric and noncentrosymmetric semiconductors and dielectric materials. More details can be found in original papers and brief review papers [3,4].

This work is supported by the Project TRR144 and the RFBR Project 15-52-12015.

References:

- [1] M. Lafrentz, *et al.*, Phys. Rev. Lett. 110, 116402 (2013); Phys. Rev. B **88**, 235207 (2013).
- [2] D. Brunne, *et al.*, **93**, 085202 (2015).
- [3] D.R. Yakovlev *et al.*, Proc. SPIE 9503, Nonlinear Optics and Appl., **IX**, 950302 (2015).

[4] R.V. Pisarev *et al.*, Phys. Stat. Solidi B 247, 1498 (2010).

Exciton interband relaxation observed by time-resolved cyclotron resonance in diamond

Ikuko Akimoto and Nobuko Naka^A

Department of Material Science and Chemistry, Wakayama University

^A *Department of Physics, Kyoto University*

We have been investigating transport properties of optically generated carriers in semiconductors by the time-resolved cyclotron resonance (TRCR) method. For highly pure diamond crystals, we have thereby provided the effective masses, momentum relaxation times and mobilities of electrons and holes [1, 2]. The method is also capable of measuring sub-microsecond dynamics of carriers in cyclotron motion [3, 4], where the carriers are generated by two-body collisions of excitons under pulsed laser excitation. Here, we found that exciton interband relaxation before the collisions are reflected in the subsequent dynamics of carriers in diamond as observed by the TRCR.

Exciton bands in diamond with the energy minimum at the Δ point in the momentum space are split due to electron mass anisotropy and exchange interaction [5]. The bands of light hole (lh)- and heavy hole (hh)-excitons cross each other at points away from the Δ point (Fig.1a). When the excitation photon energy is higher than the crossing points, fast interband relaxation from the hh-exciton to the lh-exciton is expected, as indicated by the dashed arrow.

We performed TRCR measurements at 10 K with various excitation photon energies across the exciton bands. Fig.1 (b) shows the transients of microwave absorption due to CR of lh (black solid lines) and hh (red broken lines). Under the excitations below 5506 meV, lh and hh decayed similarly. In contrast, under the excitations above 5513 meV, hh decayed faster than lh. This implies that exciton relaxation pathway is memorized in the decay profiles of hole species, which were dissolved from excitons due to two-body collisions.

References:

- [1] N. Naka, K. Fukai, Y. Handa, and I. Akimoto, *Phys. Rev. B* **88** (2013) 035205.
- [2] I. Akimoto, Y. Handa, K. Fukai, and N. Naka, *Appl. Phys. Lett.* **105** (2014) 032102.
- [3] N. Naka, K. Fukai, Y. Handa, and I. Akimoto, *J. Lumin.* **152** (2014) 93.
- [4] I. Akimoto, N. Naka and N. Tokuda, *Diam. Relat. Mater.* **63** (2016) 38.
- [5] Y. Hazama, N. Naka, and H. Stolz, *Phys. Rev. B* **90** (2014) 045209.

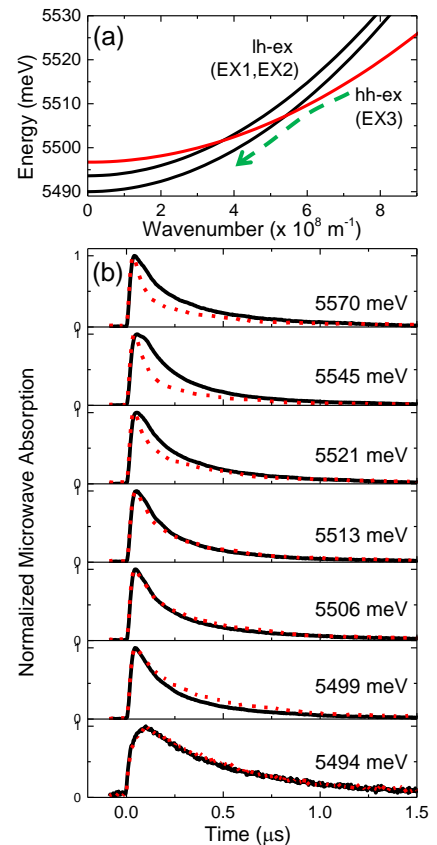


Fig.1 (a) Exciton bands near the Δ point in diamond, (b) Temporal profiles of microwave absorption due to CR of lh (black solid lines) and hh (red broken lines) at various excitation photon energies.

Exciton dynamics in solid ZnO: UV luminescence of ZnO crystal and nanoparticles excited by femtosecond IR, UV and VUV laser pulses

P. Martin¹, A. Belsky², M. Dumergue⁴, S. Petit¹, D. Descamps¹, A. Vasil'ev³

¹Centre Lasers Intenses et Applications (CELIA), UMR 5107, Université de Bordeaux-CNRS-CEA, 33405 Talence, France

²Institut Lumière Matière, UMR 5306, CNRS-Université Lyon 1, 69621 Villeurbanne, France

³Skobeltsyn Institute of Nuclear Physics, Lomonosov Moscow State University, Leninskie gory, 1(2), Moscow 119991, Russia

⁴ELI-HU, H-6728 Szeged, Tisza Lajos krt. 85-87

We present results on time resolved photo-luminescence induced by photons with different excitation conditions (photon energy, pulse duration, fluence) of ZnO ($E_g=3.4$ eV) single crystal (MC) and nanoparticles (NP). Samples were excited by femtosecond IR (1.55 eV and 1.2 eV), UV (4.65 eV and 3.61 eV - third harmonic) and VUV pulses (15-50 eV, high order harmonics generation and synchrotron radiation) of Ti-Sapphire and Ytterbium sources laser. The excitation fluence and the sample temperature in the range 13-300 K were controlled.

Under UV excitation at low temperatures the emission spectra show all emission bands originated from different states: free exciton Fx, bound exciton Dx, Dx phonon replica, TES state and Ax band.

Under IR excitation at all temperatures the emission spectra show that Fx emission is not detected, only emissions associated with Dx states (at low temperatures) and Ax band are observed.

This difference between UV and IR excitation can be explained by the supposition that Dx excitons can be created under IR excitation without preliminary formation of Fx state. One of the possibilities is the sequential creation of electrons and holes by ionizing of different defects with levels within the band gap of ZnO. Depending on the level position, a carrier creation process can be one- or two-photon process. However, we need three photons to produce sequentially an electron and a hole (one one-photon and one two-photons process). In this sequential process non-correlated electrons and holes are produced and then these carriers are captured by a defect with production of Dx state. On the contrary, UV photon creates a correlated electron-hole pair which form Fx state. Some of these free excitons decay radiatively with emission corresponding to Fx band, whereas other can be captured by defect with production of Dx state. Therefore Fx and Dx bands coexist under VUV excitation.

However, due to the whole bulk excitation volume in the IR excitation mode the role of the Urbach absorptions is also discussed.

The luminescence decay kinetics of the excitonic emissions (Dx, Fx, Ax and Dx phonon replica) were measured at different temperatures. The dynamics of Fx and Dx excitons are discussed depending on the excitation formation mode, energy, temperature and system size.

Excitation by VUV photons demonstrate also the effect of the electronic relaxation on decay kinetics.

Study of Exciton Dynamics in Multifunctional Oxides

F. A. Selim¹, P. Saadatkia¹, B. Wang², and D. C. Look²

¹*Center for Photochemical Sciences, Bowling Green State University, Bowling Green, OH 43403, USA*

²*Semiconductor Research Center, Wright State University, Dayton, OH 4543, USA*

Exciton dynamics is dominated by the presence of deep and shallow traps in the lattice. Deep traps capture charge carriers and excitons while shallow traps greatly affect their transport in the lattice, which have significant effects on the electrical and luminescence properties of semiconductors and dielectrics. In this work exciton dynamics is investigated in SrTiO₃ (STO), a multifunctional oxide that exhibits many interesting phenomena. The study is motivated by our recent observation of two orders of magnitude persistent photoconductivity in bulk annealed STO single crystals [1].

Thermally stimulated luminescence (TSL), thermally stimulated conductivity (TSC) and thermally stimulated depolarization current (TSDC) were applied to detect trapping centers and study exciton dynamics in as-grown and annealed STO single crystals. A special in-house spectrometer that simultaneously records the luminescence as a function of temperature and wavelength from 77 to 700 K was used for TSL measurements [2,3]. This allows one to resolve different recombination processes and reveal the interactions between traps and recombination centers. By combining TSL, TSC, and TSDC, we identified a number of deep and shallow traps that seem behind many interesting phenomena in STO. It was found that oxygen vacancy related form several trap levels and strongly alter the electrical conductivity and photo-conductivity of STO. Funding for this work was provided by the National Science Foundation (DMR1359523 grant, Charles Ying).

References:

- [1] M. C. Tarun, F. A. Selim, M. D. McCluskey, Physical review letters 111 (2013) 187403.
- [2] D. T. Mackay, C. R. Varney, J. Buscher and F. A. Selim, J. Appl. Phys. 112 (2012) 023522.
- [3] CR Varney, DT Mackay, A. Pratt, SM Reda and FA Selim, J. Appl. Phys. 111 (2012) 063505.

Optical quantum memory based on rare-earth-ion doped crystals

Mikael Afzelius, Group of Applied Physics, University of Geneva

Optical quantum memories are devices that can store and later retrieve quantum states encoded onto single photons. These are essential components of future quantum technologies such as quantum repeaters and quantum networks. However, it remains a major challenge to build an efficient and long-lived quantum memory, particularly using solid-state devices. Rare-earth-doped crystals are promising solid-state quantum memories, owing to their long optical and spin coherence times. They also have large inhomogeneous broadening in the optical domain, which can be used for time/frequency multiplexing, provided that the associated inhomogeneous dephasing can be controlled. In this talk I will discuss how a quantum memory can be implemented in a rare-earth-doped crystal, including control of both the optical and spin dephasing. I will show experimental data of storage of multiple qubits for up to 1 millisecond in a Europium-doped crystal. I will also discuss future challenges such as very long-lived memories and storage of quantum entanglement.

Spin-wave storage of heralded single photons in a crystal

A.Seri, D. Rieländer, A. Lenhard, M. Mazzera, H. de Riedmatten

*ICFO-Institut de Ciències Fotoniques, The Barcelona Institute of Science and Technology,
08860 Castelldefels (Barcelona), Spain*

Quantum memories are very important in quantum communication and information as they provide a quantum interface between photons, used for long distance, and matter, in which stationary qubits can be stored. Moreover they are fundamental building blocks in quantum repeaters. Rare-earth doped crystals (REDC) are promising candidates for the implementation of quantum memories because of their excellent coherence properties at cryogenic temperatures and because the solid state environment offers good prospect for scalability and integration. Until now the research on REDC quantum memories has been mostly focused on the mapping of light qubits to optical collective excitations using the atomic frequency comb (AFC) scheme [1], thus limiting to short and pre-determined storages.

For a real quantum memory, which would provide a storage with the possibility to read-out the photons on-demand, a lambda system with three hyperfine sublevels in the ground state is needed. In such a situation a full AFC scheme could be exploited by transferring the excitations to the spin-ground state before their re-phasing. Among REDC such energy level scheme is only exhibited by Eu^{3+} and Pr^{3+} where, in fact, spin-wave storage of weak coherent states at the single photon level has been already demonstrated [2,3]. Storage of quantum states of light though, has been only achieved in the excited state [4].

We report here on the preliminary results found on spin-wave storage of heralded single photons in a Pr^{3+} doped Y_2SiO_5 crystal. Widely non-degenerate narrow-band photon-pairs are produced by a cavity-enhanced SPDC source based on a PPLN crystal [5]. The idler photons, produced at telecom wavelength, are used as heralds for the signal ones, which are in resonance with the AFC created within the inhomogeneously broadened transition of Pr^{3+} (at 606nm). The main experimental challenges to implement spin-wave storage of single photons are to maximize the probability to find a single photon in front of the memory and to achieve sufficient signal to noise ratio in the storage and retrieval. We demonstrated storage and retrieval of heralded single photons with a signal to noise ratio around 2, limited by noise due to control pulses, efficiency of the memory and finite heralding efficiency of the source. Prospects to increase the efficiency and signal to noise ratio will be discussed.

References:

- [1] H. de Riedmatten, M. Afzelius, M. U. Staudt, C. Simon & N. Gisin, *Nature* 456 (2008) 773-777
- [2] M. Gündoğan, P. Ledingham, K. Kutluer, M. Mazzera & H. de Riedmatten, *Phys. Rev. Lett.* 114, (2015) 230501
- [3] C. Laplane, P. Jobez, J. Etesse, N. Timoney, N. Gisin & M. Afzelius, *New Journal of Physics* 18 (2016) 013006
- [4] D. Rieländer, K. Kutluer, P. Ledingham, M. Gündoğan, J. Fekete, M. Mazzera, & H. de Riedmatten, *Phys. Rev. Lett.* 112 (2014) 040504
- [5] J. Fekete, D. Rieländer, M. Cristiani & H. de Riedmatten, *Phys. Rev. Lett.* 110(2013) 220502

Rare-earth-activated Materials for Optical Frequency References

Charles W. Thiel,¹ Thomas Böttger,² Roger M. Macfarlane,¹ and Rufus L. Cone¹

¹ *Dept. of Physics, Montana State University, Bozeman, Montana, USA*

² *Dept. of Physics & Astronomy, University of San Francisco, San Francisco, California, USA*

Spectral hole burning (SHB) of optical transitions in crystals has enabled an impressive range of photonic applications that include signal processing, spectrum analysis, and solid-state quantum memories. Another emerging application for these materials is in ultrastable laser local oscillators for developing fieldable frequency reference systems with reduced environmental sensitivity compared to traditional approaches. The use of SHB crystals as optical frequency references was first demonstrated at Montana State University nearly two decades ago using Tm^{3+} and Er^{3+} ions in a number of different crystals [1,2]. These early efforts achieved fractional laser frequency stabilities as low as 10^{-14} with a very simple feedback control system and no passive isolation from environmental perturbations. More recently, groups at NIST [3] and the University of Düsseldorf [4] have demonstrated that SHB frequency references can provide stabilities of 10^{-17} over second or longer timescales, and work at NIST [3,5] has found that performance comparable to or greater than the best current frequency reference technologies are achievable. Furthermore, as other SHB applications such as signal processing and quantum information continue to mature, the capability for the SHB material itself to be used to stabilize the interrogation and preparation lasers provides unique advantages that enhance the potential performance of these systems.

Motivated by these applications, we will briefly review the current state of knowledge regarding SHB frequency reference technologies and describe new measurements and analysis of material properties that allow us to project even greater potential for improvement, with a specific focus on Tm^{3+} and Er^{3+} transitions that are accessible with commercial diode and fiber laser systems. In particular, we will describe our studies of mechanical and thermal perturbations on SHB frequency reference materials and the analysis of ultimate performance limits due to these effects. We will also discuss broader sample- and history-dependent variations in the transition frequencies and inhomogeneous linewidths of commonly employed SHB materials. Finally, we present results describing the unique capability for SHB to provide high-bandwidth dynamic optical filtering of laser phase noise, complementing traditional low-bandwidth opto-electronic frequency stabilization techniques.

References:

- [1] P.B. Sellin, N.M. Strickland, J.L. Carlsten, R.L. Cone, *Opt. Lett.* 24 (1999) 1038
- [2] N.M. Strickland, P.B. Sellin, Y. Sun, J.L. Carlsten, R.L. Cone, *Phys. Rev. B* 62 (2000) 1473
- [3] M.J. Thorpe, L. Rippe, T.M. Fortier, M.S. Kirchner, T. Rosenband, *Nature Photonics* 5 (2011) 688
- [4] Q.F. Chen, A. Troshyn, I. Ernsting, S. Kayser, S. Vasilyev, A. Nevsky, S. Schiller, *Phys. Rev. Lett.* 107 (2011) 223202
- [5] S. Cook, T. Rosenband, D.R. Leibbrandt, *Phys. Rev. Lett.* 114 (2015) 253902

Acousto-optic imaging using spectral holeburning in Tm^{3+} :YAG crystals

**Jean-Baptiste Laudereau¹, Anne Chauvet², Alban Ferrier³, Philippe Goldner³,
Thierry Chanelière² and François Ramaz¹**

¹ Institut Langevin - Ondes et Images, CNRS UMR 7587, ESPCI ParisTech, PSL Research University, UPMC, 1 rue Jussieu, 75005 Paris

² Laboratoire Aimé Cotton, CNRS UMR 9188, Université P-Sud, Bâtiment 505 Campus d'Orsay, 91405 Orsay

³ Institut de Recherche de Chimie Paris, CNRS UMR 8247, Chimie ParisTech, 11 rue Pierre et Marie Curie, 75005 Paris

Acousto-optic imaging is a light-ultrasound coupling technique based on the acousto-optic effect that allows accessing optical contrast deep inside scattering media (far beyond the transport mean free-path) with an ultrasonic resolution (millimetre or less). When an ultrasound (US) pulse propagates through an illuminated area, it shifts light frequency by US frequency. A proper detection scheme that can filter these frequency-shifted photons (the *tagged-photons*) allows recovering the local light irradiance within the turbid medium. The challenge here is to filter photons shifted by only few MHz, on very few photons – less than 0,1% of total flux. We recently developed a self-adapting holographic technique based on SPS ($\text{Sn}_2\text{P}_2\text{S}_6$) crystals [1] that showed first promising *ex vivo* results [2].

In order to converge toward clinical imaging, the next step is *in vivo* imaging. However, living tissues decorrelate the scattered light wavefront over characteristic times shorter than the typical response times of holographic systems. It has been shown that spectral holeburning within the inhomogeneously broadened transition $^3\text{H}_6 - ^3\text{H}_4$ (around 793 nm) in Tm^{3+} :YAG crystals can be used to obtain very narrow filters able to discriminate tagged-photons from untagged-photons [3]. This direct measurement of the flux of tagged-photons is insensitive to wavefront decorrelation so that spectral holeburning is a promising candidate for *in vivo* imaging. The major drawback of this technique is that the hole lifetime is limited to 10 ms so it is necessary to burn a new hole every few tens of ms. It results in a very low imaging rate. We propose a new filtering scheme based on spectral holeburning under a magnetic field. The advantage of such a setup is that the hole lifetime is increased up to few seconds. As direct consequences of this phenomenon, burning sequence repeating rate can be lower and deeper holes can be burnt. It results in increasing imaging rates and better filtering efficiency.

References:

- [1] Farahi *et al.*, Opt. Lett. 35, 11 (2010) 1798-1800
- [2] Laudereau *et al.*, J. Biophoton. 8, 5 (2014) 429–436
- [3] Li *et al.*, Appl. Phys. Lett. 93, 1 (2008) 011111

Towards quantum frequency conversion between atoms and light using rare earth ion dopants

Xavier Fernandez-Gonzalvo¹ Yu-Hui Chen¹, Chunming Yin², Sven Rogge² and Jevon J. Longdell¹

¹*The Dodd-Walls Centre for Photonic and Quantum Technologies & Department of Physics, University of Otago, Dunedin, New Zealand.*

²*Centre of Excellence for Quantum Computation and Communication Technology, School of Physics, University of New South Wales, Sydney, Australia*

Superconducting qubits have advanced significantly in recent years, but they have limitations. They can't be coupled directly to optical photons and so lack a mechanism for long distance quantum communication. And while the coherence times have improved greatly recently they are still much shorter than what has been achieved in optically addressed spin systems. Both of these limitations can be overcome with a device that can transfer quantum states encoded in microwave photons into those that are encoded in optical photons.

We have proposed (PRL 113,203601) implementing this quantum transducer using rare earth ion dopants that are simultaneously coupled to microwave and optical resonators, and are currently working towards the implementation. The approach can be considered as a resonator-enhanced version of the Raman-heterodyne spectroscopy, often used for characterising hyperfine structure in rare earth systems

I will present results showing low efficiency frequency conversion with a microwave resonator but single pass optics (PRA, **92**, 062313) , as well as more recent results using both a microwave and optical resonator. The microwave splitting in these experiments was achieved by splitting the Kramers degeneracy of the electronic ground state with a magnetic field. This magnetic field makes the use of 3D superconducting resonators problematic. An alternative is to use the hyperfine structure of Er-167 the one isotope of Er with nuclear spin. I will also show results of coupling a broadly tuneable, superconducting, 3D microwave resonator to Er-167 in YSO. The spectra we see at zero magnetic field is not well explained by the spin Hamiltonian parameters derived at higher magnetic fields, and we see a splitting in the peaks which we tentatively ascribe to super-hyperfine coupling. This suggests the possibility of transferring coherence from the erbium electron spin to a neighbouring yttrium nuclear spin.

Slow light based optical frequency shifter

Qian Li¹, Yupan Bao¹, Axel Thuresson², Adam N. Nilsson¹, Lars Rippe¹ and Stefan Kröll¹

¹Department of Physics, Lund University, Box 118, S-221 00 Lund, Sweden

²Theoretical Chemistry, Lund University, Box 124, SE-22100 Lund, Sweden

Qian.li@fysik.lth.se

Rare-earth-ion-doped crystals have been used to demonstrate highly narrowband filters where the pass-band of the filter can be shifted by applying an electric field [1]. In this work we demonstrate the frequency of a light pulse propagating in such a crystal can be shifted by shifting the resonance frequency of the ions using the linear Stark effect.

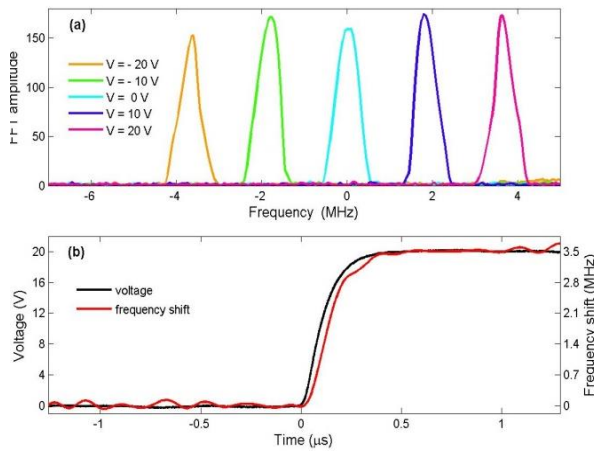


Figure 1. (a) The frequency distribution of the transmitted pulse for different applied voltages while the pulse is completely inside the crystal. (b) The instantaneous frequency of the transmitted pulse when the external voltage is applied.

A 1 MHz band-pass filter around ν_0 where all the ions in the surrounding 17MHz region have the same sign of their Stark coefficient is prepared in a $\text{Pr}^{3+}:\text{Y}_2\text{SiO}_5$ crystal. A 1 μs long pulse with centre frequency ν_0 entering the crystal will propagate with a group velocity of $c/200\,000$ and be compressed to a length of 1.5 mm inside the crystal. It is discussed in [3] that for a pulse propagating in an off resonance medium, the energy of the input pulse is distributed between the atomic polarization in the medium and the pure electromagnetic-field component. The more energy accumulated in the medium as off resonant polarization, the slower the group velocity. In the present

filter structure, more than 99.9% of the pulse energy is in the form of atomic polarization. If an electric field is applied while the pulse is inside the crystal, the ions undergo a linear Stark shift changing the resonance frequency by Δ , the light coming out of the crystal will then be shifted from ν_0 to $\nu_0 + \Delta$. The frequency shift is recorded by heterodyne detection. As shown in Figure 1 (a), the frequency component of the transmitted pulse changes as different external voltages are applied. Figure 1 (b) shows the instantaneous frequency of the pulse during the switch on of the external voltage, the frequency shift follows the external voltage applied.

Furthermore, it has been demonstrated in [2] that such a band-pass filter can be prepared throughout the entire crystal, so that it works for input light in any arbitrary spatial mode, including randomly scattered light. Therefore, the solid angle of acceptance for these filters can be close to 2π .

References:

- [1] Beavan, Goldschmidt and Sellers, J. Opt. Soc. Am. B 30 1173 (2013)
- [2] Zhang, Sabooni et al., Appl. Phys. Lett. 100, 131102 (2012)
- [3] Shakhmuratov, J. Modern Opt. 57 1355 (2010)

Energy Migration Upconversion in Spatially Separated Doping Nanostructures

Langping Tu,^{1,2} Fei Wu,^{1,2} Jing Zuo,^{1,2} Xiaomin Liu,² Xianggui Kong,² Hong Zhang¹

¹ Van't Hoff Institute for Molecular Sciences, University of Amsterdam, The Netherlands

² State Key Laboratory of Luminescence and Applications, Changchun Institute of Optics, Fine Mechanics and Physics, Chinese Academy of Sciences

The importance of energy migration upconversion (EMU) is protruded with the advance of nanotechnology. Near infrared antenna can now be well separated in space from the upconversion centers in nanostructures, which offers new possibilities in functional design of novel nanomaterials, e.g. tuning of excitation wavelength, optimization of excitation and emission, for solar energy utilization and biomedical imaging and image-guided therapy.^[1,2] This intriguing possibilities are, however, dimmed by the lack of a legible physical picture of energy migration dynamics due to the complex of the upconversion processes. We have in recent years explored the EMU by integrating theoretical modelling, various EMU nanostructures and advanced spectroscopic studies.

In this presentation we would like to introduce our recent study of EMU in most interesting spatially separated doping nanomaterials represented by (1) NaYF₄:Yb,Er @NaYF₄:Yb@NaYF₄:Nd,Yb and (2) NaYF₄:Yb,Er@NaYF₄:Yb heterogeneous nanostructures. From Monte Carlo simulation and steady-state and time-resolved spectroscopic results we have, for the first time, proposed and validated the 3-dimensional energy migration mechanism in these nanostructures and demonstrated the significant contribution of EMU to upconversion luminescence and the spectral tuning based on EMU, which may lead to a solution in lifting upconversion efficiency – the most important challenge on the way of commercialization of the upconversion nanomaterials.

References:

- [1] Langping Tu, Xiaomin Liu, Fei Wu, Hong Zhang, Chem. Soc. Rev. 44 (6) (2015) 1331
- [2] Feng Wang, Renren Deng, Juan Wang, Qingxiao Wang, Yu Han, Haomiao Zhu, Xueyuan Chen, Xiaogang Liu, Nat. Mater. 10 (2011) 968.

Controlling Photon Upconversion in Lanthanide-doped Nanocrystals

Xiaogang Liu

*Department of Chemistry, National University of Singapore, Singapore 117543 and Institute of Materials Research and Engineering, A*STAR, Singapore 117602*

E-mail: chmlx@nus.edu.sg

Abstract: Lanthanide-doped nanoparticles exhibit unique luminescent properties, including a large Stokes shift, a sharp bandwidth of emission, high resistance to optical blinking, and photobleaching. Uniquely, they can also convert long-wavelength stimulation into short-wavelength emission. These attributes offer the opportunity to develop alternative luminescent labels to organic fluorophores and quantum dots. In recent years, researchers have taken advantage of spectral-conversion nanocrystals in many important biological applications, such as highly sensitive molecular detection and autofluorescence-free cell imaging. With significant progress made over the past several years, we can now design and fabricate nanoparticles that display tailorable optical properties. In particular, we can generate a wealth of color output under single-wavelength excitation by rational control of different combinations of dopants and dopant concentration. By incorporating a set of lanthanide ions at defined concentrations into different layers of a core-shell structure, we have expanded the emission spectra of the particles to cover almost the entire visible region, a feat barely accessible by conventional bulk phosphors. In this talk, I will highlight recent advances in the broad utility of upconversion nanocrystals for multimodal imaging, bio-detection, display and photonics.

Modelling Blue to UV Upconversion in β -NaYF₄: 0.3% Tm³⁺

Pedro Villanueva-Delgado*¹, Karl W. Krämer¹, Rafael Valiente²

*pedro.villanueva@dcb.unibe.ch

¹Department of Chemistry and Biochemistry, University of Bern, 3012 Bern, Switzerland

²Departamento de Física Aplicada, Facultad de Ciencias, Universidad de Cantabria, 39005 Santander, Spain.

The decay curves of Tm³⁺-doped β -NaYF₄ contain sufficient information to determine the internal energy transfer steps responsible for the upconverted UV luminescence after blue excitation.

Although several models have been developed to analyse upconversion processes, none of them are able to both take into account all energy transfer interactions, including energy migration, and offer a microscopic picture of them.

A recently published model calculates all energy transfer interactions according to the distances between the ions in a lattice and assigns a rate equation system to each ion. The model outputs the decay curve of each relevant energy level.[1] These curves can be then compared to the experimental ones, and the energy transfer parameters can be determined from the fit.

In Figure 1, two energy transfer interactions cooperate to populate the Tm³⁺ ¹D₂ state in a β -NaYF₄: 0.3% Tm³⁺ sample. The model is able to reproduce the experimental data and determine the critical radius of the interactions.

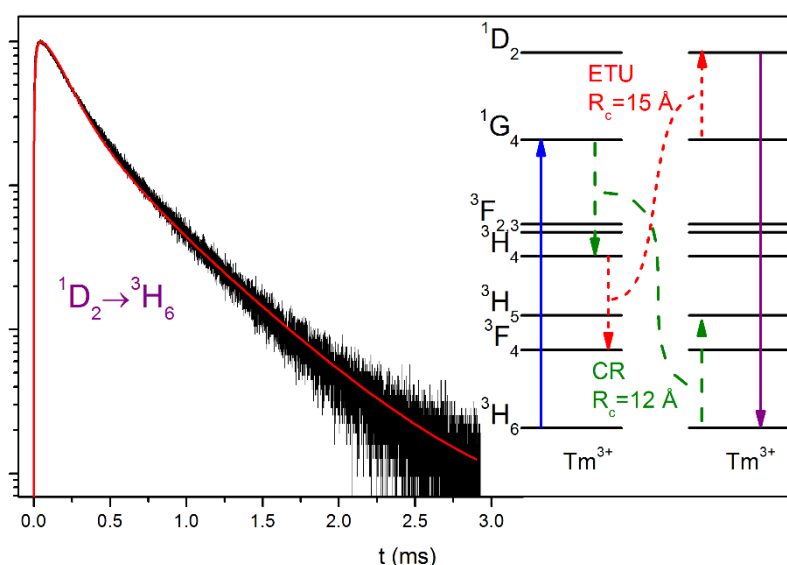


Figure 1: Experimental (black line) and simulated (red line) decay curve of the ${}^1D_2 \rightarrow {}^3H_6$ transition in β -NaYF₄: 0.3% Tm³⁺ and energy level scheme with interactions.

References:

[1] Villanueva-Delgado, P.; Krämer, K. W.; Valiente, R.; *J. Phys. Chem. C* 119 (2015) 23648.

Design rules for multiple d-f emission bands in lanthanides

Mathijs de Jong,¹ Daniel Biner,² Karl Krämer,² Zoila Barandiarán,³ Luis Seijo³ and Andries Meijerink¹

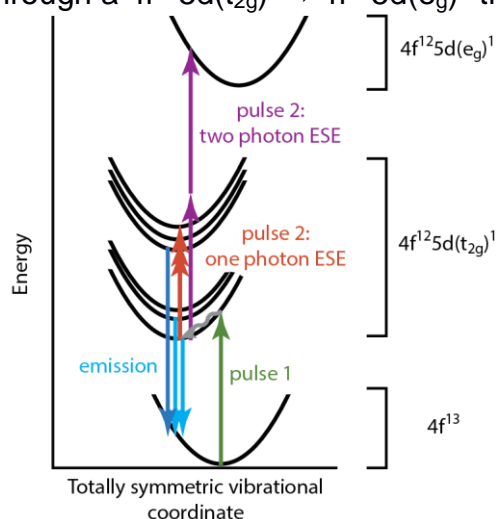
¹ Debye Institute for Nanomaterials Science, Utrecht University, The Netherlands

² Department of Chemistry and Biochemistry, University of Bern, Switzerland

³ Departamento de Química, Universidad Autónoma de Madrid, Spain

The lanthanide ions constitute the most important class of activators in inorganic luminescent materials. There have been extensive studies on the parity-forbidden $4f^n \rightarrow 4f^n$ transitions, resulting in a good understanding of these transitions. However, much remains to be understood about the parity-allowed $4f^n \rightarrow 4f^{n-1}5d^1$ transitions. In most luminescent materials, excitation of a high excited state results in rapid non-radiative relaxation to the lowest excited state, from which radiative decay can take place. The same is true for the manifold of $4f^{n-1}5d^1$ excited states in the lanthanides, with the notable exception of Tm^{2+} .¹

We use various methods to understand the behavior of the luminescence in Tm^{2+} -doped $CsCaBr_3$ and $CsCaCl_3$. We have performed a two-color two-photon excited state excitation (ESE) experiment, in which Tm^{2+} is brought with a first photon in the lowest $4f^{12}5d^1$ excited state (green line in Figure), from which higher excited states can be probed with a second photon of varying energy. We observed sharp lines in the excited state excitation spectrum, corresponding to transitions within the $4f^{12}$ core of the $4f^{12}5d^1$ excited state (red lines). Broad bands at higher energy are assigned to two-photon absorption through a $4f^{12}5d(t_{2g})^1 \rightarrow 4f^{12}5d(e_g)^1$ transition (purple lines).



Also, we present cutting-edge ab initio wavefunction-based embedded-cluster calculations. Both the experimental and theoretical approach confirm the presence of an energy gap within a group of $4f^{12}5d^1$ excited states that only differ in the state of their $4f^{12}$ core. Since the 4f-shell is well shielded from the environment, this results in the presence of parallel potential energy surfaces, in which non-radiative relaxation is very inefficient. Slow non-radiative relaxation allows for radiative transitions to take place from multiple $4f^{12}5d^1$ excited states.

References:

[1] J. Grimm, O.S. Wenger, K.W. Krämer, H.U. Güdel. *J. Lumin.* 126, **2007**, 590-596.

High pressure study of cooperative luminescence of $\text{CaAl}_4\text{O}_7:\text{Yb}^{3+}$

D. Jankowski¹, M. Puchalska², A. Bercha³, W. Trzeciakowski³, A. Suchocki^{1,4}

¹*Institute of Physics, Polish Academy of Sciences, Al. Lotników 32/46, Warsaw 02-668, Poland*

²*Faculty of Chemistry, University of Wrocław, 14.F.Joliot-Curie Street, 50-383 Wrocław, Poland*

³*Institute of High Pressure Physics "Unipress", Polish Academy of Sciences, ul. Sokołowska 29, Warsaw 01-142, Poland*

⁴*Institute of Physics, University of Bydgoszcz, Weyssenhoffa 11, Bydgoszcz 85-072, Poland*

Cooperative luminescence is a phenomenon of simultaneous de-excitation of a close pair of ions in solid resulting in anti-Stokes emission of doubled energy of separated emission centers and also doubled decay rate from the virtual energy level of pairs of ions. The process, although relatively weak, is often observed, especially for Yb^{3+} , when it produces a blue-green luminescence, not expected for separate ions due to the lack of real energy levels in this spectral region. Probability of the process should be strongly dependent on the separation, r , between the ions in the interacting pairs, at least as r^{-6} for the lowest dipole-dipole term in the interaction. Therefore application of high pressures, effectively reducing the distances between the ions should allow increasing strongly the effectiveness of the cooperative luminescence.

In this work we study the influence of high hydrostatic pressure on cooperative luminescence associated with pairs of Yb^{3+} ions in $\text{CaAl}_4\text{O}_7:\text{Yb}$ powders, where this effect was observed previously [1] at ambient pressure. Concentration of Yb ions was between 2% and 6%. The samples were inserted into a diamond anvil cell, and pressure up to 25 GPa was applied at room temperature. A tunable diode laser was used for excitation, assuring that the excitation is always tuned to the maximum of the excitation spectrum at a particular pressure.

Luminescence spectra and decay kinetics of luminescence were recorded both in the infrared and in the blue-green spectral regions. The red shift of the luminescence was observed in both regions together with an increase of the decay rate with increasing pressure. Interestingly, the observed decay rate of the blue-green luminescence is slightly smaller than expected at any pressure. In addition, we do not observe an increased intensity of the cooperative luminescence under pressure, although the application of pressure reduces lattice parameters of the crystallites. The results are discussed in the framework of the model of Goldner et al. [2]. Other mechanisms of the origin of the blue-green luminescence are also considered.

Acknowledgements: This work was partially supported by the project DEC 2012/07/B/ST5/02080 of the National Science Center, Poland.

References:

- [1] M. Puchalska, M. Sobczyk, J. Targowska, A. Watras, E. Zych, J. Lumin. 143 (2013) 503.
- [2] Ph. Goldner, F. Pelle, D. Meichenin, F. Auzel, J. Lumin. 71 (1997) 137.

Chapter 6

Friday 22nd July 2016: Presentations

Novel Optical Excited States of Nano-carbon and Atomically Thin Two-dimensional Materials

Kazunari Matsuda

*Institute of Advanced Energy, Kyoto University,
Gokasho, Uji, Kyoto 611-0011, Japan*

Since the discovery of graphene, the very thin materials with a few atomic layer thickness, such as nano-carbon and atomically thin two-dimensional (2D) materials, i.e. carbon nanotube, graphene and transition metal dichalcogenide, have attracted a great deal of attention and intensively studied from viewpoint of fundamental physics [1-8] and optical application.[9,10] These are emerging materials as new stages for studying the novel electronic and optical properties, because of characteristic band structures and enhanced Coulomb interaction between carriers. The enhanced Coulomb interaction in nano-carbon materials and atomically thin 2D materials leads to the formation of stable excitons and charged exciton (trion) with extremely large binding energies by optical excitation even at room temperature, as shown in Fig. 1. It is anticipated that the excitons and trions show various interesting optical phenomena.

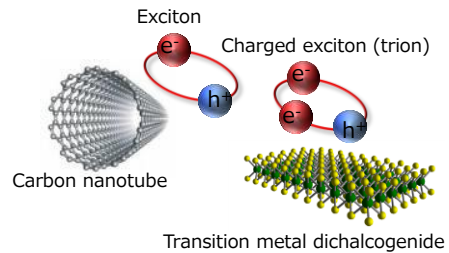


Fig. 1: Schematic of exciton and trion in nano-carbon and 2D materials.

We studied the novel optical properties and functionalities in carbon nanotube[1-3] and monolayer monolayer transition metal dichalcogenide (MX_2 ; M=Mo, W, X=Se, S, Te) by advanced laser spectroscopic techniques.[4-7] We revealed the drastic change of photoluminescence arising exciton and trion by chemical doping and exciton-exciton interactions in carbon nanotubes and monolayer MX_2 [7]. Moreover, the novel optically excited states and optical properties will be discussed.

References:

- [1] R. Matsunaga, K. Matsuda, *et al.*, *Phys. Rev. Lett.* **106**, 037404, (2011).
- [2] J. S. Park, N. Nakashima, K. Matsuda, *et al.*, *J. Am. Chem. Soc.* **134**, 14464, (2012).
- [3] Y. Miyauchi, K. Matsuda, *et al.*, *Nature Photonics* **7**, 715 (2013).
- [4] S. Mouri, Y. Miyauchi, and K. Matsuda, *Nano Lett.* **13**, 594 (2013).
- [5] S. Mouri, Y. Miyauchi, K. Matsuda *et al.*, *Phys. Rev. B* **90**, 155449 (2014).
- [6] D. Kozawa, K. Matsuda, G. Eda, *et al.*, *Nature Commun.* **5**, 4543 (2014).
- [7] S. Mouri, K. Matsuda *et al.*, *Phys. Rev. B* **90**, 155449 (2014).
- [8] N. Akizuki, K. Matsuda, Y. Miyauchi, *et al.*, *Nature Commun.* **6**, 8920 (2015).
- [9] F. Wang, K. Matsuda, *et al.*, *Nature Commun.* **6**, 6305 (2015).
- [10] Y. Tsuboi, K. Matsuda *et al.*, *Nanoscale* **7**, 14476 (2015).

Mid-infrared absorption imaging of a quantum degenerate exciton gas in cuprous oxide at 100 mK

Kosuke Yoshioka

Photon Science Center, School of Engineering, The University of Tokyo, JAPAN

An ensemble of electrons and holes is predicted to form a Bose-Einstein condensate (BEC) phase of excitons at low temperature and high density. The 1s exciton systems in Cu_2O have been the prime candidate for realizing ideal, three-dimensional BEC since the early days of experimental search for BEC: The long lifetimes enable the excitons ensembles to be in thermal equilibrium with the lattice. In addition, the large binding energies make the systems stable at high densities and against external perturbations. Biexcitons have never been observed, and the electron-hole liquid phase is unstable in Cu_2O crystals. However, the direct evidence for BEC has never been reported despite much experimental effort since 1980s.

In this talk, we will present our recent experimental results on BEC of 1s paraexcitons at sub-Kelvin temperatures. We have found that the effective lifetime of paraexcitons is reduced significantly due to the frequent two-body loss of excitons at superfluid temperatures and above [1]. The BEC is therefore expected to occur below 1 K. By using a helium-3 refrigerator, we found so-called the relaxation explosion process of paraexcitons in a strain-induced trap as an indirect evidence for the BEC transition at 800 mK [2]. The relaxation explosion process originates from the inelastic two-body collision process described above, and it prevents an exciton condensate from growing to a high condensate fraction. To stabilize the condensate, we need to reduce the density of the condensate by cooling the exciton gas further. We are now looking for the conclusive evidence for a stable BEC at 100 mK, using a dilution refrigerator [3]. By developing an absorption imaging technique using the hydrogen-like 1s-2p resonance [4], we are now able to visualize very cold and quantum degenerate excitons that cannot emit photons in their recombination process because of the momentum conservation principle.

References:

- [1] K. Yoshioka, T. Ideguchi, A. Mysyrowicz, and M. Kuwata-Gonokami, *Phys. Rev. B* 82 (2010) 041201(R).
- [2] K. Yoshioka, E. Chae, and M. Kuwata-Gonokami, *Nat. Commun.* 2 (2011) 328.
- [3] K. Yoshioka, Y. Morita, K. Fukuoka, and M. Kuwata-Gonokami, *Phys. Rev. B* 88 (2013) 041201.
- [4] K. Yoshioka and M. Kuwata-Gonokami, *Phys. Rev. B* 91 (2015) 195207.

Polariton-condensation effects on photoluminescence dynamics in a CuBr microcavity

Masaaki Nakayama, Katsuya Murakami, and Yoshiaki Furukawa

Department of Applied Physics, Osaka City University, Japan

Exciton polaritons in semiconductor microcavities, the so-called cavity polaritons, are bosonic quasiparticles resulting from strong coupling between excitons and cavity photons. The bosonic properties have attracted much attention in Bose-Einstein condensation and polariton lasing from polariton condensates [1]. In the present work, we have investigated the polariton-condensation effects on photoluminescence (PL) dynamics in a CuBr microcavity. The prominent characteristic of the CuBr microcavity is the giant Rabi splitting energy of the order of 100 meV [2], which is advantageous in polariton condensation because of high stability of the cavity polariton.

The sample used was a λ -thick CuBr microcavity with $\text{HfO}_2/\text{SiO}_2$ distributed Bragg reflectors (DBRs) prepared on a (0001) Al_2O_3 substrate. The DBRs were fabricated by rf magnetron sputtering, while the CuBr active layer was grown by vacuum deposition. In the PL measurements, the excitation light source was a mode-locked Ti:sapphire laser with a pulse duration of 110 fs. The excitation energy was 3.351 eV, much higher than the lower polariton branch (LPB): 2.911 eV at $k_{\parallel}=0$. We measured steady-state and time-resolved PL spectra at 10 K. The PL detection angle was normal to the sample surface; namely, the LPB-PL around $k_{\parallel}=0$ was detected. In addition, angle-resolved reflectance spectra were measured to characterize the cavity-polariton dispersions.

The excitation fluence dependences of the PL intensity, band width, and peak energy exhibit threshold-like changes at $6.0 \mu\text{J}/\text{cm}^2$ which is two orders lower than the Mott transition density. This demonstrates occurrence of the polariton condensation. Figure 1 shows the temporal LPB-PL profiles (circles) at excitation fluences of 4.0, 6.0, and $8.0 \mu\text{J}/\text{cm}^2$. The solid curves indicate the fitted results using convolution of the system response and a triple exponential function including the rise process. The prominent result is the fact that the rise and decay times are drastically shortened at 6.0 and $8.0 \mu\text{J}/\text{cm}^2$ above the threshold fluence in comparison with those at $4.0 \mu\text{J}/\text{cm}^2$ below the threshold. The very short rise time indicates that the relaxation process of the cavity polaritons in momentum space is considerably accelerated by the polariton condensation, which can be attributed to the bosonic final state stimulation [1]. In addition, the very short decay time of the fast component reflects the intrinsic cavity-polariton lifetime.

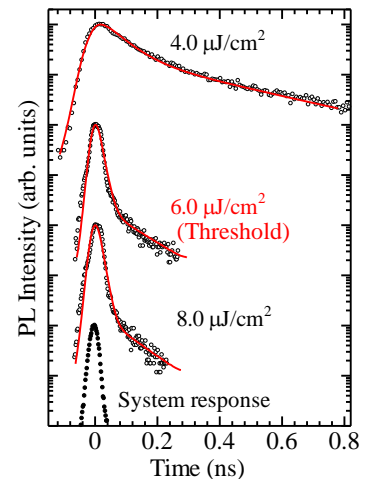


Fig. 1: Temporal profiles (circles) of the LPB-PL band at $k_{\parallel}=0$ at excitation fluences of 4.0, 6.0, and $8.0 \mu\text{J}/\text{cm}^2$, where the solid curves depict the fitted results.

References:

- [1] For a review, H. Deng *et al.*, Rev. Mod. Phys. **82** (2010) 1489.
- [2] M. Nakayama *et al.*, Phys. Rev. B **85** (2012) 205320.

Is there inter-valley Auger recombination in InGaAs/InP quantum wells?

Yu. A. Pusep¹, M. A. Tito¹, A. Gold², M. D. Teodoro³, G. E. Marques³, and R. R. LaPierre⁴

¹São Carlos Institute of Physics, University of São Paulo, 13560-970 São Carlos, SP, Brazil

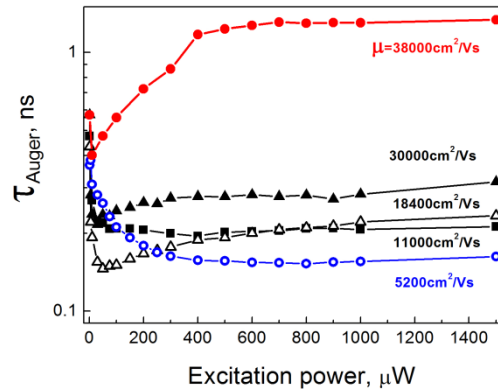
²Université de Toulouse (UPS), CEMES-CNRS, 118 Route de Narbonne, 31062 Toulouse, France

³ Universidade Federal de São Carlos, 13565-905, São Carlos, SP, Brazil

⁴Centre for Emerging Device Technologies, Department of Engineering Physics, McMaster University, Hamilton, Ontario L8S 4L7, Canada

Auger recombination is one of the most important non-radiative processes which affects the efficiency of optoelectronic devices particularly at high excitation power or high injection, when a high density of carriers is generated. In the presented work the electron transport and recombination processes of photoexcited electron-hole pairs were studied in InGaAs/InP single quantum wells. Comprehensive transport data analysis reveals asymmetric shape of the quantum well potential where the electron mobility was found to be dominated by interface-roughness scattering. The low-temperature time-resolved photoluminescence was employed to investigate recombination kinetics of photogenerated electrons. Remarkable modification of Auger recombination shown in Fig.1 was observed with variation of the electron mobility.

Fig.1. Auger recombination time measured as a function of the pump power at T=7 K in InGaAs/InP QWs with different electron mobility.



In high mobility quantum wells the increasing pump power resulted in a new and unexpected phenomenon: a considerably enhanced Auger non-radiative recombination time. We propose that the distribution of the photoexcited electrons over different conduction band valleys might account for this effect. Such phonon-assisted inter-valley Auger recombination process is important in direct band gap semiconductors when the difference between the energies of the Γ conduction band minimum and a lateral (X or L) conduction band minimum is close to the gap between the conduction band and valence band extrema. This condition favors transference of the energy of recombining electron-hole pair to a third electron excited into the lateral conduction band valley. In low mobility quantum wells, disorder-induced relaxation of the momentum conservation rule causes inter-valley transitions to be insignificant, resulting in decreasing of non-radiative recombination time with the increasing pump power. Thus, we propose that the disorder driven transition between two types of Auger processes (intra and inter-valley) was observed.

Emission properties of GaN/AlN multi-quantum-wells under high hydrostatic pressure – experimental and *ab-initio* comparative study

A. Kaminska^{1,2}, D. Jankowski¹, P. Strak³, K. P. Korona⁴, J. Borysiuk^{1,4}, E. Grzanka³, M. Beeler^{5,6}, K. Sakowski³, E. Monroy^{5,6}, and S. Krukowski³

¹*Institute of Physics, Polish Academy of Sciences, Al. Lotników 32/46, 01-142 Warsaw, Poland*

²*Cardinal Stefan Wyszyński University, College of Science, Department of Mathematics and Natural Sciences, Dewajtis 5, 01-815 Warsaw, Poland*

³*Institute of High Pressure Physics, Polish Academy of Sciences, Sokolowska 29/37, 01-142 Warsaw, Poland*

⁴*University of Warsaw, Faculty of Physics, Pasteura 5, 02-093 Warsaw, Poland*

⁵*Université Grenoble-Alpes, 38000 Grenoble, France*

⁶*CEA-Grenoble, INAC-PHELIQS, 17 av. des Martyrs, 38000, France*

In this work we report on the correlation of high-pressure photoluminescence (PL) studies of GaN/AlN multi-quantum-wells (MQWs) with *ab initio* calculations of their electronic and optical properties. The study was performed on GaN/AlN MQWs with various well thicknesses synthesized by plasma-assisted molecular-beam epitaxy on AlN-on-sapphire substrates. PL measurements as a function of the hydrostatic pressure were conducted in a diamond anvil cell. The optical properties of the MQWs were strongly affected by the quantum confined Stark effect stemming from the polarization-induced internal electric fields. Therefore, the ambient pressure PL peak energies decreased by over 1 eV with QWs thicknesses increasing from 1 nm up to 6 nm [1], and the respective PL decay times increased from about 1 ns up to 13 μ s, exhibiting characteristic changes of dynamics related to strong built-in electric field. The pressure coefficients of the PL energy were significantly reduced in the MQWs as compared to bulk AlN and GaN crystals, and they strongly depended on geometric factors such as the thickness of the wells and barriers.

The transition energies, their pressure dependencies and oscillator strengths were modelled for tetragonally strained structures of the same geometry using a full tensorial representation of the strain in the MQWs under external pressure. The same MQWs were also simulated directly using density functional theory calculations [2]. A good agreement between these two approaches and the experimental results indicates that the nonlinear effects induced by the tetragonal strain related to the lattice mismatch between the substrate and the MQWs are responsible for the drastic decrease of the pressure coefficients observed experimentally.

Acknowledgements: The authors acknowledge support of the Polish National Science Centre by grant No. DEC-2012/05/B/ST3/03113.

References:

- [1] A. Kaminska, P. Strak, J. Borysiuk, K. Sobczak, J. Z. Domagala, M. Beeler, E. Grzanka, K. Sakowski, S. Krukowski, E. Monroy, J. Appl. Phys. **119** (2016) 015703.
[2] P. Strak, K. Sakowski, A. Kaminska, S. Krukowski, J. Phys. Chem. Solids **93**(2016) 100.

Pressure induced mechano-chemistry in molecular solids

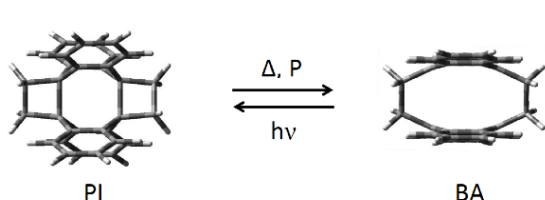
Eric L. Chronister, Andrew Rice, Sebastian Jezowski

Department of Chemistry, University of California at Riverside, Riverside, CA 92521

Spectroscopic studies under viable high-pressure conditions have yielded: pressure dependent dynamics in pure and mixed molecular crystals; mechanochemical studies of photochemical reactions; and kinetic studies of chemical and physical changes in a dynamic diamond anvil cell.

Pressure dependent homogeneous line-width studies under variable high-pressure and variable low-temperature conditions have allowed vibrational and electronic relaxation and dephasing to be studied as a function of intermolecular separation and pressure-induced crystalline phase changes [1][2]. High-resolution FTIR studies of pure molecular crystals and photon echo measurements of chromophores in host crystal lattices are demonstrated.

The ability to make impulsive pressure changes has also been used to study the kinetics of pressure-induced chemical changes. The ability of high pressure to affect forward and back reactions in a variety of photochemical systems is demonstrated (e.g. photodimerization of bis-anthracene and di-pentacene, and photoisomerization of 9-t-butyl anthracene) [3][4]. The mechanism by which pressure functions as a catalytic reactant is evaluated. The counter intuitive ability of compression to induced bond breaking reactions is demonstrated.



Optical excitation of bis-anthracene (BA) yields a photo-isomer (PI). The exothermic PI→BA reaction is accelerated with pressure, in contrast with dimerization in unlinked polyacenes.

The ability to make reversible and repetitive high-pressure changes (GPa) on a fast (microsecond) time scale in a dynamic diamond anvil cell permits studies of a variety of dynamic processes in condensed phases. These include: fast mechano-chemical changes; the kinetics of phase transitions, protein folding, and accelerated aging in polymers

References:

- [1] B.Schatschneider, E.L. Chronister, Chem. Phys.Lett.533 (2012) 30-34.
- [2] S. Jezowski, L. Zhu, Y. Wang, A. Rice, G. Scott, C. Bardeen, E.L. Chronister, J. Am. Chem. Soc.134 (2012) 7459-7466.
- [3] A. Rice, F. Tham, E.L. Chronister, J. Chem. Cryst.43 (2013) 14-25.
- [4] F. Tong, C. Cruz, S. Jezowski, X. Zhou, L. Zhu, R. Al-Kaysi, E.L. Chronister, C. Bardeen, J. Phys. Chem. 118 (2014) 5349-5354.

Excitation-induced processes in model molecular solid N₂

E.V. Savchenko¹, I.V. Khyzhniy¹, S.A. Uyutnov¹, M.A. Bludov¹, A.P. Barabashov¹,
G.B. Gumenchuk² and V.E. Bondybey²

¹*Institute for Low Temperature Physics & Engineering NASU, Kharkov 61103, Ukraine*

²*Lehrstuhl für Physikalische Chemie II TUM, Garching b. München 85747, Germany*

Excited states dynamics, energy storage and conversion in model solid N₂ attract much attention in diverse fields such as material and surface sciences, physics and chemistry of interstellar and solar systems, particle physics. Excitation-induced processes were discussed principally in terms of neutral species reactions. The role of the charge states in the relaxation of excitations is just beginning to be studied. Only recently the hole self-trapping – formation of N₄⁺, [1] and creation of N₃⁺ [2] in electron-bombarded solid N₂ were reported.

Here we present our recent findings on electronically induced processes in N₂ solids with a focus on relaxation channels involving charged centers. Low-energy electron beam was used for excitation to avoid knock-on sputtering. The samples were probed with depth by varying electron energy. Relaxation dynamics was monitored by cathodoluminescence (CL) and nonstationary luminescence (NsL), along with optical and current activation spectroscopy. We performed correlated in real time measurements of thermally stimulated luminescence (TSL) and exoelectron emission (TSEE) as well as optically stimulated luminescence (OSL) and exoelectron emission (OSEE). Desorption of excited particles was monitored spectroscopically. The total desorption yield was detected by pressure measuring above the sample.

Two kinds of desorption were detected – (i) desorption stimulated by an electron beam of subthreshold energy and (ii) desorption of particles from previously irradiated samples, which was named “post-desorption”. VUV photon emission from desorbing N atoms (the $^4P_{1/2-5/2} \rightarrow ^4S_{3/2}$ transitions) under irradiation by electrons was observed for the first time. Their distinctive feature is a coincidence with the gas phase lines within the experimental error. Relative intensities with respect to the bulk molecular emissions (the $a^1\Sigma_u^- \rightarrow X^1\Sigma_g^+$ and the $A^3\Sigma_u^+ \rightarrow X^1\Sigma_g^+$) significantly increased in thin films ($\ll 100$ nm) and with decreasing the penetration depth of the exciting electrons. These features are also characteristic of the excited N₂ (C³Π_u) molecule desorption [3]. The anomalously strong post-desorption (ii) was detected upon warm-up of pre-irradiated films at temperatures much lower than the characteristic sublimation temperature. The basis of the phenomena observed are thought to be charge recombination reactions: $N_3^+ + e^- \rightarrow N_2 + N^+ + \Delta E_1$ and $N_4^+ + e^- \rightarrow N_2 + N_2 + \Delta E_2$. Energy storage, conversion and transfer to desorbing particles are discussed.

References:

- [1] E.V. Savchenko, I.V. Khyzhniy, S.A. Uyutnov, A.P. Barabashov, G.B. Gumenchuk, M.K. Beyer, A.N. Ponomaryov, and V.E. Bondybey, *J. Phys. Chem. A* **119** (2015) 2475.
- [2] Y-J. Wu, H-F. Chen, S-J. Chuang, T-P. Huang, *Astrophys. J.* **768** (2013) 83.
- [3] E. Savchenko, I. Khyzhniy, S. Uyutnov, A. Barabashov, G. Gumenchuk, A. Ponomaryov, V. Bondybey, *Phys. Stat. Sol. C*, **12** (2015) 49.

Vibronic Spectra of Frenkel Excitons in a 2-Dimensional Polyacene Lattice

T. Hartmann¹, C. Warns¹, I. J. Lalov², and P. Reineker¹

¹*Institute of Quantum Optics, Ulm University, 89069 Ulm, Germany*

²*Faculty of Physics, Sofia University, Sofia 1164, Bulgaria*

We investigate the vibronic spectra of Frenkel excitons in a 2-dimensional lattice modelling the (a,b)-plane of real polyacene crystals. We take into account two different intramolecular, totally symmetric vibrational modes, one of which has no dispersion whereas the second one shows a slight dispersion. The absorption spectra are calculated on the basis of linear response theory using Green's functions at $T=0$ K. In the evaluation we use an approximation according Lalov and Zhelyazkov [1] and realistic model parameters. The calculations show that the linear electron-vibration coupling is strong enough to bind the exciton to a single phonon, but not to a larger number. A hypothetical quadratic coupling strengthens the binding. The dispersion of the phonons shows up only in those absorption spectra, in which the number of phonons with dispersion is larger than the number of phonons without. The quadratic exciton-phonon coupling weakens this effect.

References:

[1] I. J. Lalov, I. Zhelyazkov, Phys. Rev. B75, 245435 (2007)

Experimental Evidence for Enhancement of Optical Magnetization by Magnetic Torque

E. F. C. Dreyer¹, P. Anisimov², A. A. Fisher^{1,3}, and S. C. Rand^{1,3}

¹Center for Dynamic Magneto-optics, Univ. of Michigan, Ann Arbor, MI 48109-2099

²Los Alamos National Laboratory, Los Alamos, NM 87545 (LA-UR-16-21322)

³Division of Applied Physics, University of Michigan, Ann Arbor, MI 48109-1022

Abstract: Magnetic torque is investigated as an enhancement factor determining magnetic light scattering in molecular liquids and solids. Results in spherical top molecules, anisotropic organic molecular complexes and quartz are compared.

Experiments reveal induced high-frequency magnetism [1] as large as electric dipole polarization ($M = cP$) at intensities as low as 10^8 W/cm^2 , based on analyses of polarized and unpolarized components in electric (ED) and magnetic dipole (MD) light scattering. Spherical-top molecules show magnetization with a strong dependence on moment of inertia [2], while samples with internal dipoles respond via all-electric reorientation dynamics. Qualitative and quantitative agreement is obtained with quantum and classical models of librations stimulated by an EB -driven interaction and enhanced by magnetic torque.

Radiation patterns of cross-polarized light scattering were recorded for spherical top liquids CCl_4 , SiBr_4 , and SnCl_4 as well as organic liquids C_6H_6 , C_6D_6 , $\text{C}_2\text{H}_4(\text{OH})_2$, $\text{C}_6\text{H}_5\text{NH}_2$, $\text{C}_6\text{H}_5\text{CN}$ and fused quartz excited with ultrashort pulses. At modest intensities (Fig. 1), nonlinear magnetic components were as large as linear electric components. Enhancement was confirmed to be related to torque dynamics through a dependence on rotational resonant frequency.

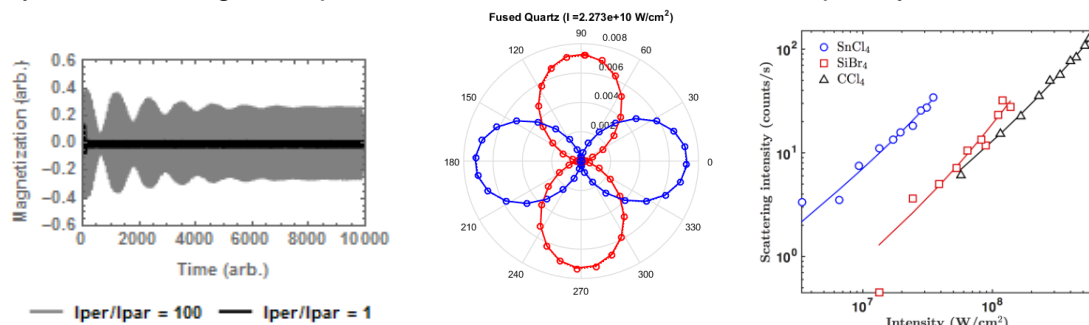


Fig. 1(a) Calculated magnetization versus time with (grey) and without (black) torque enhancement. (b) Polarized scattering components in fused quartz: Note that MD (blue) and ED (red) amplitudes are equal. Unpolarized backgrounds have been subtracted. (c) Unpolarized ED scattering in spherical top liquids with different moments of inertia.

References

- [1] A.A. Fisher, E.F. Cloos, W.M. Fisher, S.C. Rand, *Opt. Exp.* **22**, 202119 (2014).
- [2] A.A. Fisher, E.F.C. Dreyer, A. Chakrabarty and S.C. Rand (to be published).

Chapter 7

Poster Session I

Monday 18th July 17:15 – 19:15, Poster Session I

1. Tunable luminescence from silico-carnotite type double silicates doped with Tb³⁺ and Eu³⁺
Irene Carrasco, Fabio Piccinelli, Marco Bettinelli
2. Divalent bismuth doped deep red scintillating materials for X-ray detection
Liyi Li, Atul Sontakke, Mingying Peng, Bruno Viana
3. Photoluminescence properties and energy transfer via multi luminescent centers of Sr₂MgAl₂₂O₃₆:Ce³⁺ phosphor for near UV-pumped white LEDs
Haiming Zhang, Bingfu Lei, Haoran Zhang, Yingliang Liu
4. Spectroscopic properties of Ce³⁺ in the cuspidine-type oxide nitride compound Y₄Si_{2-x}Al_xO_{7+x}N_{2-x}
Agata Lazarowska, Sebastian Mahlik, Marek Grinberg, Ru-Shi Liu
5. Photoluminescence evolution with illumination time in CH₃NH₃PbI_{3-x}Cl_x thin films and MAPbI₃ crystals
Carmen Coya, Esteban Climent-Pascual, Emilio Juárez-Pérez, Alicia de Andres, Angel Luis Álvarez, Carmen Munuera
6. New phosphor MgCa₃Si₂O₈: Eu²⁺, energy level location of Ln³⁺ and Ln²⁺ in MgCa₃Si₂O₈
Dagmara Stefanska, Przemyslaw Deren
7. Cr³⁺-Nd³⁺ energy transfer in novel whitlockite phosphor Ca₉Cr(PO₄)₇: Nd³⁺ ions
Adam Watras, Natalia Miniajluk, Przemysław Dereń
8. Synthesis and spectroscopic characterization of Ca₉Al_{1-x}Cr_x(PO₄)₇ (x = 0, 1-1) powders
Natalia Miniajluk, Adam Watras, Przemysław Dereń
9. Meta-stability of silicate phosphors
Byungjoo Jeon, Wunho Lee, Taewook Kang, Gotaek Kim, Youngmin Cho, Youngwoo Jeong, Jaehyoung Park, Daehan Kim, Hyojun Kim, Kwangwon Park, Kim Jongsu, Heelack Choi, Taehoon Kim
10. Single crystal phosphors for high-power laser lighting
Taewook Kang, Gotaek Kim, Wunho Lee, Byungjoo Jeon, Hyojun Kim, Kwangwon Park, Kim Jongsu, Heelack Choi, Taehoon Kim
11. Strong blue absorption in heavy Mn-doped phosphors
Kwangwon Park, Jaehyoung Park, Hyojun Kim, Jongsu Kim, Byungjoo Jeon, Taewook Kang, Wunho Lee, Heelack Choi, Taehoon Kim
12. Temperature-dependent photoluminescence lifetimes of Cu-Doped Zn-In-S quantum dots
Jialong Zhao, Xi Yuan and Haibo Li
13. High density excitation with alpha particles
Weronika Wolszczak, Pieter Dorenbos
14. The vacuum referred binding energies of Bi³⁺ in wide band gap compounds
Roy Awater, Pieter Dorenbos
15. Luminescence of defective monoclinic zirconia prepared in a solar furnace
Ilmo Sildos, Laurits Puust, Claude Monty, Valter Kiisk
16. Luminescence investigations of ZnGa₂O₄: Mn²⁺ and ZnGa₂O₄: Mn²⁺, Eu³⁺ compounds with spinel structure
Oleg Kravets, Andriy Luchechko, Syvorotka Ihor
17. Dynamics of electron photoexcited states on the TiO₂ – xanthene dyes interface

- Niyazbek Ibrayev, Dmitriy Afanasyev, Evgeniya Seliverstova*
18. Luminescent properties of Eu³⁺ doped SrKB₅O₉
Bartosz Bondzior, Przemysław Dereń
 19. Optical spectroscopy and EPR studies of Mn²⁺ ions in YAlO₃
Yaroslav Zhydachevskii, Hanna Przybylińska, Agnieszka Wołoś, Michal Glowacki, Marek Berkowski, Andrzej Suchocki
 20. Optical and electron paramagnetic resonance spectroscopy of Yb³⁺:Y₂SiO₅
Sacha Welinski, Alban Ferrier, Mikael Afzelius, Philippe Goldner
 21. Mechanism of luminescence enhancement of SrSi₂O₂N₂:Eu phosphor via manganese addition
Justyna Barzowska, Tadeusz Lesniewski, Yaroslav Zhydachevskyy, Karol Szczodrowski, Daniel Michalik, Hanka Przybylińska, Małgorzata Sopicka-Lizer, Marek Grinberg, Andrzej Suchocki
 22. Eu(II) luminescence properties in hydrides and hydride fluorides
Nathalie Kunkel, Andries Meijerink, Holger Kohlmann
 23. The luminescence of electronic excitations in alkali halide crystals at lattice symmetry lowering
Kuanyshbek Shunkeyev, Saginbek Shunkeyev, Alexandra Barmina, Lyudmila Myasnikova, Nurgul Zhanturina, Daulet Sergeyev, Shynar Sagymbaeva, Zukhra Aimaganbetova
 24. Morphology control and upconversion luminescence properties of monoclinic Y₂WO₆:Yb³⁺/Er³⁺
Cuili Chen, Peiqing Cai, Sun Il Kim, Hyo Jin Seo
 25. Combustion synthesis and luminescence properties of Sr₃La₂(BO₃)₄:Eu³⁺ phosphors
Peiqing Ca, Cuili Chen, Sun Il Kim, Hyo Jin Seo
 26. Spectroscopic study of materials doped rare-earth ions
Adel Bitam, Saidi Khiari, Madjid Diaf
 27. Confined excitons in CdF₂-CaF₂ superlattices
Konstantin V. Ivanovskikh, Rosa B. Hughes Currie, Michael F. Reid, Jon-Paul R. Wells, Nikolay S. Sokolov, Roger J. Reeves
 28. High-pressure photoluminescence spectroscopy of codoped LiNbO₃:Cr³⁺; W⁴⁺ crystals.
Marco Sánchez-Alejo, Fernando Rodríguez, Antonio Barrera-Argüeso, Ignacio Camarillo, Cristina Flores, Héctor Murrieta, José Manuel Hernández, Francisco Jaque, Enrique Camarillo
 29. Luminescence properties of different Eu sites in Ba₂K(PO₃)₅ doped with Eu²⁺ and Eu³⁺
Anna Baran, Sebastian Mahlik, Marek Grinberg, Adam Watras, Robert Pażik, Przemysław Dereń
 30. Luminescence properties of silicate apatite phosphors M₂La₈Si₆O₂₆:Eu (M = Mg, Ca, Sr)
Nikolai Khaidukov, Marco Kirm, Eduard Feldbach, Henri Mägi, Vitali Nagirnyi, Eliko Töldsepp, Sebastian Vielhauer, Thomas Jüstel, Thomas Jansen, Vladimir Makhov
 31. Optically properties of K₂SO₄ doped by transition metal ions
Ainura Tussupbekova, Temirgaly Koketai, Askhat Baltabekov, Elizaveta Turmukhambetova, Elmira Mussenova
 32. Energy transfer and spectroscopic properties of UV active media Ce³⁺:LiCa_{1-x}Sr_xAlF₆

- Alexey Shavelev, Alexey Nizamutdinov, Mikhail Marisov, Vadim Semashko*
33. Theoretical study on photoinduced nucleation dynamics by injection of THz optical pulses
Kunio Ishida, Keiichiro Nasu
 34. Ultra-short pulse lasing from $\text{LiLu}_{0.7}\text{Y}_{0.3}\text{F}_4:\text{Ce}^{3+}$
Alexey Nizamutdinov, Ilnur Farukhshin, Vadim Semashko, Stella Korableva, Mikhail Marisov
 35. $\text{YAG}:\text{Ce}^{3+}$ nanoceramics: spectroscopy, dynamics and TSL
Q. Shi, A. Ishchenko, V. Osipov, V. Shitov, R. Maksimov, K. Lukyashin, V. Platonov, M. Sarychev, R. Abashev, B. Shulgin, A. Belsky, N. Fedorov, P. Martin, K. Ivanovskikh
 36. Radiative and nonradiative recombination in Si-doped InN thin films
Der-Jun Jang, Antaryami Mohanta, C.-F. Tseng, Li-Wei Tu
 37. Dynamics of changes in optical absorption induced by exposition to short- and long-wavelength radiation in the $\text{BTO}:\text{Al}$ crystal
Stanislav Shandarov, Valeriya Dyu, Marina Kisteneva, Elena Khudyakova, Yury Kargin
 38. Basic principles of ion beam induced luminescence and its application to the study of electronic excitation in insulators
Diana Bachiller-Perea, David Jiménez-Rey, Angel Muñoz-Martín, Fernando Agulló-López
 39. Theoretical modeling of transition metals tetroxanions adsorption on N(B)-doped single-walled carbon nanotubes and graphene
Yuriy Hizhnyi, Borysiuk Viktor, Sergii Nadilko, Andrii Shyichuk
 40. Luminescence and upconversion spectroscopy of $\text{Er}^{3+}/\text{Yb}^{3+}$ -doped $\text{Y}_3\text{Ga}_5\text{O}_{12}$ nano-garnets for optical nano-devices
Virginia Monteseuro, Vemula Venkatramu, Sergio Fabian León-Luis, Ulises Rodríguez-Mendoza, C. K. Jayasankar, Víctor Lavín
 41. Blue upconversion emission of Cu^{2+} ions sensitized by Yb^{3+} -trimers in CaF_2
Qin Weiping, Aidilibike Tuerxun
 42. Energy migration in doped crystals
Freddy Rabouw, Andries Meijerink
 43. Luminescent properties of Ce^{3+} -activated germanate scintillating glasses
Shan Qian, Lihui Huang, Kangying Shu, Shiqing Xu
 44. The influence of point defects on amplification and spectral characteristics of InGaAs-based laser diode arrays
Katsiaryna Platnitskaya, Volha Kabanava, Dzmitry Kabanau, Yahor Lebiadok
 45. The excited states of gallium and nitrogen vacancies in the GaN/AlN heterointerface and its relaxation
Yahor Lebiadok, Dzmitry Kabanau, Katsiaryna Platnitskaya
 46. Photonic effects on magnetic dipole transition probabilities
Z. J. Wang, A. Meijerink
 47. Carbon segregation phenomena on $\text{Fe}_{0.85}\text{Al}_{0.15}(110)$: a STM, LEED and XPS study
Z. Dai, P. Borghetti, G. Gabailh, J. Jupille, R. Laszari
 48. Quantum wells based structures tested by polarized photorefectance at room temperature
J. V. González-Fernández, J. Ortega-Gallegos, R. Díaz de León-Zapata, J.-P. Galaup, A. Lastras-Martínez and R. E. Balderas-Navarro
 49. Narrowing of excitation band in nanophosphors

- Hyojun Kim, Daehan Kim, Kwangwon Park, Jongsu Kim, Wunho Lee, Taewook Kang, Byungjoo Jeon, Heelack Choi*
50. Towards cavity-enhanced single rare earth ion detection
Bernardo Casabone, Franziska Beck, Thomas Hümmer, Alban Ferrier, Philippe Goldner, Theodor Hänsch, Hugues de Riedmatten, David Hunger
51. Towards bulk crystal coherence times in $\text{Eu}^{3+}:\text{Y}_2\text{O}_3$ nanocrystals
John Bartholomew, Karmel de Oliveira Lima, Alban Ferrier, Jenny Karlsson, Philippe Goldner
52. Persistent optical hole-burning spectroscopy of nano-confined dye molecules in liquid at room temperature: optical memory in liquid?
Hiroshi Murakami
53. Fluorescence microscopy of single organo-metal halide perovskite nanowires: effect of crystal-phase transition
Alexander Dobrovolsky, Eva Unger, Arkady Yartsev, Ivan Scheblykin
54. Optical properties of quantum dots coupled to cone-shaped nanoantennas
Kerstin Scherzinger K. Scherzinger,, R. Jäger, A. Bräuer, S. Jäger, J. Fulmes, S. zur Oven Krockhaus, D. A. Gollmer, D. P. Kern, M. Fleischer and A. J. Meixner
55. Polarized photoluminescence of carbon dots
Dmitrii Nelson, Anatolii Starukhin, Daniil Eurov, Dmitrii Kurdyukov, Ekaterina Stovpiaga, Valerii Golubev
56. Investigation of highly efficient energy transfer in porphyrin molecules/carbon nanotubes nanoassemblies
G. Delpont, F. Violla, S. Campidelli, C. Voisin and J. S. Lauret
57. Optical properties of graphene nanoribbons
Géraud Delpont, Shen Zhao, Loïc Rondin, Akimitsu Narita, Yunbin Hu, Xinlinag Feng, Klaus Müllen, Stéphane Campidelli, Jean-Sébastien Lauret
58. Lanthanide-ion-doped NaYF_4 upconversion nanophosphors: Optical spectroscopy of single particles
Yuri Vainer, Sergei Alyatkin, Andrei Nechaev, Evgeniy Khaydukov
59. Influence of plasmon silver films on photoinduced electronic processes in polymeric films of poly (3-hexylthiophene)
Dmitriy Afanasyev, Aslbek Zeinidenov, Niazbek Ibrayev
60. Anomalous exciton diffusion in disordered wire-like materials
Valentina Giorgis, Andrey Malyshev, Victor Malyshev
61. Photodynamic antimicrobial chemotherapy using zinc phthalocyanines in the treatment of bacterial infection
Zhuo Chen, Linsen Li, Yaxin Zhang, Jlnan Chen, Ping Hu, Mingdong Huang
62. Thermoelectric properties of disordered molecular wires with electron-vibron interaction
Elena Diaz, Francisco Dominguez-Adame, Rudolf Roemer
63. Mechanisms of protoporphyrin IX delayed fluorescence
Ivo Vinklársek, Marek Scholz, Roman Dědic, Jan Hála
64. Study of the thermal stability of the green fluorescent protein in the range 20-100°C
T. P. J. Han, L. M. Maestro, M. I. Marques, F. Jaque
65. Dephasing mechanisms in transparent ceramics with narrow optical linewidths
Nathalie Kunkel, John Bartholomew, Alban Ferrier, Akio Ikesue, Philippe Goldner

66. An infrared pump-probe measurement of the $6H7/2$ lifetime of Sm^{3+} in $LiYF_4$
Jon-Paul Wells, Sebastian Horvath, Alexander van der Meer, Michael Reid
67. Time evolution of softening of coherent phonon in antimony
Sho Nakayama, Masato Maruyama, Hideaki Kumagai, Tomobumi Mishina
68. Robust photon-echo generation in quantum dots using a pair of chirp pulses
Yoshitaka Sato, Naoto Aonuma, Kouichi Akahane, Ishi-Hayase Junko
69. Complex quantum beats of excitons in quantum dots observed using three-pulse photon echo
Arai Yuto, Kouichi Akahane, Kitazawa Sayaka, Ishi-Hayase Junko
70. Appearance of coherent LO phonons during the decay of LO-phonon–plasmon coupled mode in an undoped GaAs/n-type GaAs epitaxial structure
Takahiro Sumioka, Hideo Takeuchi, Masaaki Nakayama
71. Compact ultrafast X-ray and gamma-ray source driven by intense femtosecond laser pulses
Ruxin Li, Wentao Wang, Jiansheng Liu, Zhizhan Xu
72. Role of dynamical symmetry in an effective time-independent Hamiltonian for a laser-driven system
Jun-Ichi Inoue

Tunable luminescence from silico-carnotite type double silicates doped with Tb³⁺ and Eu³⁺

Irene Carrasco, Fabio Piccinelli, Marco Bettinelli

Luminescent Materials Laboratory, Dept. of Biotechnology, University of Verona,

Strada Le Grazie 15, 37134 Verona, Italy. Email marco.bettinelli@univr.it

Double silicates with the silico-carnotite orthorhombic structure and co-doped with Tb³⁺ and Eu³⁺, such as Ca₃Gd_{2-x-y}Tb_xEu_ySi₃O₁₂ and Ca₃Y_{2-x-y}Tb_xEu_ySi₃O₁₂, have been prepared by solid-state reaction. Room temperature luminescence spectra and decay kinetics have been measured and analysed. Upon UV excitation at 378 nm, the emission colour varies from red to pinkish, depending on the doping level. It has been shown that the resulting colour can be adjusted by controlling the Tb³⁺/Eu³⁺ concentration ratio. Tailoring of the doping leads to close-to-white emission in some of the analysed samples upon excitation in the wavelength region useful for LED lighting [1].

We would like to thank the European Commission for funding through the Marie Curie Initial Training network LUMINET, grant agreement No. 316906.

References:

[1] N. C. George, K. A. Denault, R. Seshadri, *Annu. Rev. Mater. Res.* 43 (2013) 481.

Divalent bismuth doped deep red scintillating materials for X-ray detection

Liyi Li,^{1,2} Atul Sontakke,¹ Mingying Peng,² Bruno Viana¹

¹PSL Research University, IRCP ChimieParisTech, 11 rue P. & M. Curie, 75231 Paris Cedex 05, France

²The China-Germany Research Center for Photonic Materials and Devices, The State Key Laboratory of Luminescent Materials and Devices, School of Materials Science and Engineering, SCUT, Guangzhou, China.

Scintillation materials have been used widely in either military or civil areas. These materials are used to convert high energy radiation into visible light, which should be detected by conventional photomultiplier tubes. But there are few candidates with an emission in the spectral range of 650 to 1200nm, which well correspond to the optimal sensitivity of some semiconductor detector such as silicon and furthermore lies in the more transparent region of human tissue. [1] There is a large number of possible redox states of the Bi-ion paired with the possibility of cluster formation. But recently, we have found that, bismuth stabilized in its divalent form, in the so-called Bi²⁺-doped phosphors exhibit deep red emission once exposed to X-ray. [2-4] Therefore, Bi²⁺-doped phosphors are considered as potential candidates for future applications in X-ray detection. Despite most of Bi²⁺-doped phosphors in powder form in our investigation show red radioluminescence in agreement with their photoluminescence properties when excited under the NUV-Blue light, some phosphors (such as Bi²⁺-doped borate) show different features (see Fig.1) and temperature effects under X-ray excitation. Their excited states dynamics will be presented at the conference.

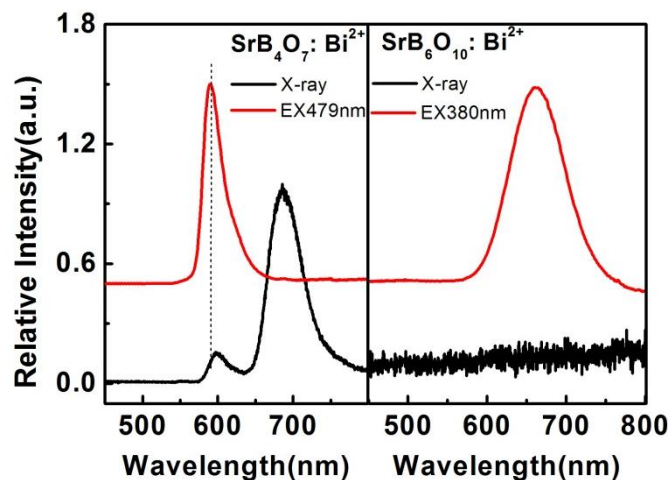


Fig.1 Photoluminescence and radioluminescence spectra of Bi²⁺-doped borate.

References:

- [1] H. A. Höpfe, *Angew. Chem. Int. Ed.*, 48 (2009), 3572.
- [2] M. Y. Peng and L. Wondraczek, *J. Am. Ceram. Soc.*, 94 (2010), 1437.
- [3] M. Y. Peng, B. Sprenger, M. A. Schmidt, H. G. L. Schwefel, and L. Wondraczek, *Opt. Express*, 18(2010), 12852.
- [4] M. Y. Peng and L. Wondraczek, *Opt. Lett.*, 34 (2009), 2885.

Photoluminescence properties and energy transfer via multi luminescent centers of $\text{Sr}_2\text{MgAl}_{22}\text{O}_{36}:\text{Ce}^{3+}$ phosphor for near UV-pumped white LEDs

Haiming Zhang, Bingfu Lei,* Haoran Zhang, Yingliang Liu

Guangdong Provincial Engineering Technology Research Center for Optical Agriculture, College of Materials and Energy, South China Agricultural University, Guangzhou 510642, China

* tleibf@scau.edu.cn

$\text{Sr}_2\text{MgAl}_{22}\text{O}_{36}:\text{Ce}^{3+}$ were prepared by using a high temperature solid-state reaction method. X-ray diffraction (XRD), photoluminescence (PL), decay curves properties of $\text{Sr}_2\text{MgAl}_{22}\text{O}_{36}:\text{Ce}^{3+}$ phosphors were investigated in detail. Under the excitation of 200 to 300 nm ultraviolet (UV), the PL spectra of phosphor exhibit emission bands centered at 325 nm. Under 310 nm excitation, $\text{Sr}_2\text{MgAl}_{22}\text{O}_{36}:\text{Ce}^{3+}$ presents a strong blue emission band at 421 nm which are assigned to 5d–4f transition of Ce^{3+} ion. Considering the result that different excitation wavelengths yield different emission spectra, we can deduce that two types of Ce^{3+} luminescent centers exist in the $\text{Sr}_2\text{MgAl}_{22}\text{O}_{36}$ host. According to PL spectra and decay curves of phosphors, the mechanism of energy transfer from Ce^{3+} (Ce(I), occupying the Sr(I) site) to Ce^{3+} (Ce(II), occupying the Sr(II) site) is proposed.

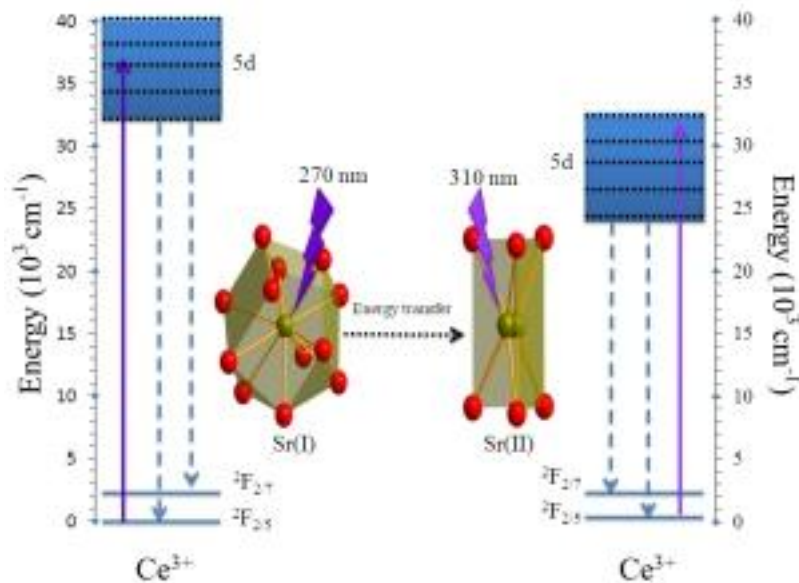


Fig.1 Schematic diagram of $\text{Ce}^{3+}(\text{I})$ - $\text{Ce}^{3+}(\text{II})$ energy transfer

References:

- [1] R. Yu, H. M. Noh, B. K. Moon, B. C. Choi, J. H. Jeong, K. Jang, H. S. Lee, and S. S. Yi, *Mater. Res. Bull.*, 51 (2014), 361.
- [2] R. P. Cao, M. Y. Peng, E. H. Song, and J. R. Qiu, *ECS J. Solid State Sci. Technol.*, 1 (2012), R123.
- [3] G. Li, C. C. Lin, W. T. Chen, M. S. Molokeev, V. V. Atuchin, C. Y. Chiang, W. Zhou, C. W. Wang, W. H. Li, H. S. Sheu, T. S. Chan, C. Ma, and R. S. Liu, *Chem. Mater.*, 26 (2014), 2991.

Spectroscopic properties of Ce³⁺ in the cuspidine-type oxide nitride compound Y₄Si_{2-x}Al_xO_{7+x}N_{2-x}

A.Lazarowska¹, S. Mahlik¹, M. Grinberg¹, R.-S.Liu²

¹ *Institute of Experimental Physics, University of Gdansk, WitaStwosza 57, 80-952 Gdańsk,*

Poland

² *Department of Chemistry, National Taiwan University, Taipei 106, Taiwan*

Ce³⁺ luminescence was studied in the Y_{3.98}Ce_{0.02}Al_xO_{7+x}N_{2-x} system with a weighted out x of 0, 0.2, 0.4, 0.6, 0.8 and 1. The XRD patterns of all samples matched well with the reported Y₄Si₂O₇N₂ phase, with the space group P2₂/c (cuspidine-type structure). The main XRD peaks show obvious shifts to the lower angle side between x=0 and 1, indicating an increasing substitution of Si-N by the larger Al-O pairs in the cuspidine-type structure. The luminescence spectra show typical Ce³⁺ luminescence with maximum near 510 nm which can be excited from 460 nm to the UV and. When part of Si-N in Y_{3.98}Ce_{0.02}Si₂O₇N₂ is replaced by Al-O, the position of the emission maximum shifts to higher energy. It is also observed that the emission intensity as well as decay time of luminescence strongly decrease. The luminescence quenching mechanism is explained as strongly related to the energy location between the lowest Ce³⁺ 5d₁ emitting state and the conduction band.

Photoluminescence evolution with illumination time in $\text{CH}_3\text{NH}_3\text{PbI}_{3-x}\text{Cl}_x$ thin films and MAPbI_3 crystals

C. Coya¹, E. Climent-Pascual², E. J. Juárez-Pérez³, A. de Andrés², C. Munuera², A. L. Álvarez¹

¹ Universidad Rey Juan Carlos, E.T.S.I Telecomunicación, Móstoles, 28933 Madrid, Spain.

² Instituto de Ciencia de Materiales de Madrid - CSIC, Cantoblanco, Madrid 28049, Spain.

³ Okinawa Institute of Science and Technology Graduate University (OIST), Energy Materials and Surface Sciences Unit, Okinawa, 904-0495 Japan.

Hybrid halide perovskites (PS) are among the “hottest” materials on photovoltaics by its certified power conversion efficiency (PCE) of 20.1% [1]. However, the properties of these materials are not yet well understood, namely, the dependence of the final performance on the morphology and chemistry of the MAPbI_3 layer within the different device architectures, or the influence of the ambient conditions. [2,3]

Here, we investigate the photoluminescence (PL) properties of $\text{CH}_3\text{NH}_3\text{PbI}_{3-x}\text{Cl}_x$ thin films deposited on different substrates: bare glass, commercial fluorine doped SnO_2 (FTO) on glass, or compact TiO_2 layer on glass/FTO substrates (FTO/ TiO_2), and $\text{CH}_3\text{NH}_3\text{PbI}_3$ crystals (tens of microns in size) for comparison. The laser (488 nm) was attenuated in order to avoid temperature effects (0.015 W/cm^2). PL evolves with illumination time for all samples in a clearly different way from crystals to thin films (Figure 1), being the more stable behavior for the $\text{CH}_3\text{NH}_3\text{PbI}_{3-x}\text{Cl}_x$ layer on TiO_2 . Besides, for this layer micro PL reveals greater emission intensity in the “bright” areas, and less quenched emission zones on average. It has been observed as well a directional enhancement of PL along c axis suggesting that the morphology of the PS layer affects the final performance. X-ray diffraction shows that the c-axis is exclusively parallel to the substrate for all films, except for the one with TiO_2 substrate.

Keywords: Hybrid halide perovskites, photoluminescence, X-Ray Diffraction, solar energy conversion.

References:

- [1] W. S. Yang, J. H. Noh, N. J. Jeon, Y. C. Kim, S. Ryu, J. Seo, S. I. Seok. *Science* 348, 1234–1237 (2015).
- [2] A. Listorti, Emilio J. Juárez-Pérez, C. Frontera, V. Rofailo, L. García-Andrade, Silvia Colella, A. Rizzo, P. Ortiz, I. Mora-Sero. *J. Phys. Chem. Lett.* 2015, 6, 1628–1637.
- [3] Yuxi Tian, Maximilian P., E. Unger, M. Abdellah, K. Zheng, Tõnu Pullerits, A. Yartsev, V. Sundström and I. G. Scheblykin. *Phys. Chem. Chem. Phys.*, 2015, 17, 24978–24987.

New phosphor $\text{MgCa}_3\text{Si}_2\text{O}_8$: Eu^{2+} , energy level location of Ln^{3+} and Ln^{2+} in $\text{MgCa}_3\text{Si}_2\text{O}_8$

D. Stefańska, P.J. Dereń

*Institute of Low Temperature and Structure Research, Polish Academy of Sciences, Okólna
Street 2, 50-422 Wrocław, Poland,
corresponding author. D.Stefanska@int.pan.wroc.pl*

$\text{MgCa}_3\text{Si}_2\text{O}_8$ doped with Eu^{2+} is a new phosphor which has been obtained by the solid state method. $\text{MgCa}_3\text{Si}_2\text{O}_8$ crystallizes in monoclinic space system in P 121/c1 unit cell. The stoichiometric amounts of MgO, CaCO_3 , SiO_2 and Eu_2O_3 were weighted and mixed. After that the samples were heated at different temperatures which ranged from 700 to 1300° C for a few hours. To reduce annealing temperature the small quantity of flux was added to the mixture. Subsequently, the samples were cooled down to room temperature and grounded to obtain a fine powder.

To characterize the structure of obtained materials the XRD analysis were performed. The excitation, emission spectra and luminescence decay profiles of the emitting level of Eu^{2+} have been measured. The influence of concentration of Eu^{2+} on luminescence properties has been analyzed as well as the thermal stability of the emission of Eu^{2+} in $\text{MgCa}_3\text{Si}_2\text{O}_8$.

The spectroscopy of 4f-5d excitation bands and CT-band of Ce^{3+} and Eu^{3+} , respectively have been also studied. A level scheme of divalent and trivalent lanthanides energy levels have been constructed. The knowledge about energy level location of Ln^{2+} and Ln^{3+} in $\text{MgCa}_3\text{Si}_2\text{O}_8$ is crucial to design new phosphors based on $\text{MgCa}_3\text{Si}_2\text{O}_8$.

Acknowledgements This works was financially supported National Science Center under Grant no. DEC- 2013/11/N/ST5/01986.

Cr³⁺-Nd³⁺ energy transfer in novel whitlockite phosphor Ca₉Cr(PO₄)₇: Nd³⁺ ions

A. Watras, N. Miniajluć, P. J. Dereń

Institute of Low Temperature and Structure Research, Polish Academy of Sciences, Okólna 2, 50-422 Wrocław, Poland

Phosphate are very wide family of materials, which can be doped with optically active ions. Among them there are still many new or barely known hosts. One of them is Ca₉Cr(PO₄)₇, which belongs to the whitlockite-type materials. Doping it with Nd³⁺ ions gives possibility for energy transfer between Cr³⁺ and Nd³⁺ ions, which is very useful for enhancing of solar cells efficiency.

In this work the series of Nd³⁺-doped (0.1 to 5%) Ca₉Cr(PO₄)₇ were prepared by wet chemistry method. The phase purity of all samples were confirmed by the XRD measurements.

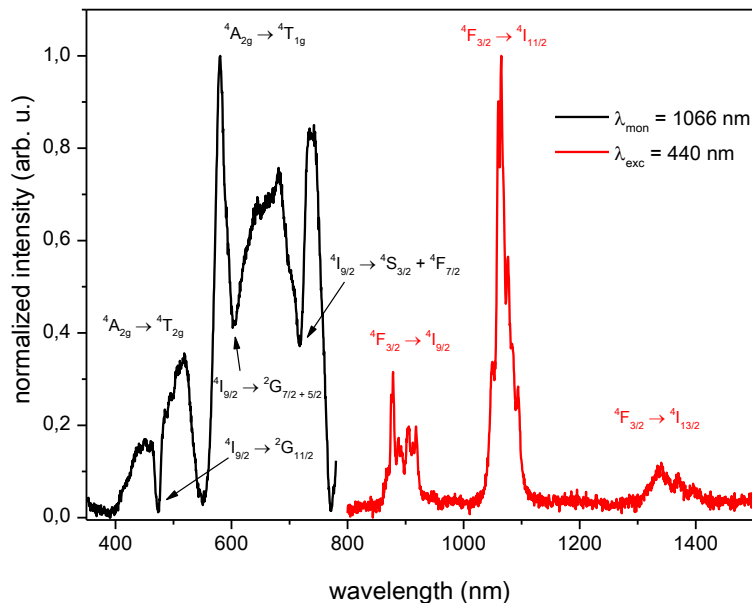


Fig. 1. The excitation (black) and emission (red) spectrum of Ca₉Cr(PO₄)₇: 5% Nd³⁺ measured at 300 K.

The excitation ($\lambda_{\text{mon}} = 1066 \text{ nm}$) and emission ($\lambda_{\text{exc}} = 440 \text{ nm}$) spectrum of Ca₉Cr(PO₄)₇: 5% Nd³⁺ ions is presented in Fig. 1. There are clearly visible absorption bands of Cr³⁺ ions assigned to the $^4A_{2g} \rightarrow ^4T_{2g}$ and $^4A_{2g} \rightarrow ^4T_{1g}$ transition, which have strong dips connected with reabsorption of Nd³⁺ ions. They are attributed to the $^4I_{9/2} \rightarrow ^2G_{11/2}$, $^4I_{9/2} \rightarrow ^2G_{7/2 + 5/2}$ and $^4I_{9/2} \rightarrow ^4S_{3/2} + ^4F_{7/2}$ transitions with maximum at 475, 605 and 715 nm, respectively. It confirms the energy transfer from the Cr³⁺ to the Nd³⁺ ions. The emission spectrum is characteristic for Nd³⁺ ions and consists bands lying in the IR region assigned to the $^4F_{3/2} \rightarrow ^4I_{9/2}$, $^4F_{3/2} \rightarrow ^4I_{11/2}$ and $^4F_{3/2} \rightarrow ^4I_{13/2}$ transitions.

Synthesis and spectroscopic characterization of $\text{Ca}_9\text{Al}_{1-x}\text{Cr}_x(\text{PO}_4)_7$ ($x = 0,1-1$) powders

Natalia Miniajluk, Adam Watras, Przemysław J. Dereń

Institute of Low Temperature and Structure Research, Polish Academy of Science, Okolna2, 50-422 Wrocław, Poland

Phosphors based on the mixed metal oxides are very attractive due to their thermal and chemical stability and excellent luminescence performances. The transition metal ion Cr^{3+} is widely applied as a dopant for many photonic applications including laser crystals. The aim of this paper was to synthesize and to determine the spectroscopic properties of $\text{Ca}_9\text{Al}_{1-x}\text{Cr}_x(\text{PO}_4)_7$ (where $x = 0,01-1$) powders.

Our samples were prepared by the citrate method and were characterized by X-ray diffraction (XRD) and spectroscopic measurement. Emission and excitation spectra as well as emission decay profiles were measured at 77 and 300 K.

All prepared powders have the structure of $\text{Ca}_9\text{Al}(\text{PO}_4)_7$ (JCPDS card no. 00-045-0345) without any additional phase. The luminescence band are broad and intense which is associated with the weak crystal field for which $Dq/B < 2.3$. The 300 K emission band, centered at 770 nm, and the R-line at 682 nm correspond to the ${}^4\text{T}_2 \rightarrow {}^4\text{A}_2$ and ${}^2\text{E}_g \rightarrow {}^4\text{A}_2$ transitions, respectively. It was found that the integrated intensity of the ${}^4\text{T}_2$ band increases with increasing of chromium concentration and even stoichiometric $\text{Ca}_9\text{Cr}(\text{PO}_4)_7$ sample exhibits an intense emission.

Excitation and absorption spectra present two characteristic broad and intense band, centered at 651 nm and 448 nm, which are associated with the ${}^4\text{A}_2 \rightarrow {}^4\text{T}_2$ and ${}^4\text{A}_2 \rightarrow {}^4\text{T}_1$ transitions, respectively. The lifetimes of Cr^{3+} ions emission measured at 77 K amounts to 113 μs for all samples.

References:

1. R. Pązik, K. Zawisza, A. Watras, K. Maleszka-Bagińska, P. Boutinaud, R. Mahiou, P.J. Dereń, *Materials Research Bulletin* 48 (2013) 337-342,
2. P.J. Dereń, A. Watras, A. Gańgor, R. Pązik, *Crystal Growth Design* 12 (2012) 4752-4757,
3. P.J. Dereń, M. Malinowski, W. Stręć, *Journal of Luminescence* 68 (1996) 91-103.

Meta-stability of silicate phosphors

**Byungjoo Jeon¹, Wunho Lee¹, Taewook Kang¹, Gotaek Kim¹, Youngmin Cho¹,
Youngwoo Jeong¹, Jaehyoung Park², Daehan Kim², Hyojun Kim², Kwangwon
Park², Jongsu Kim^{1, 2}, Heelack Choi^{1, 3}, Taehoon Kim⁴.**

¹Department of LED Convergence Engineering, Specialized Graduate School of Science and Technology Convergence, Pukyong National University, Busan 608-739, Republic of Korea.

²Department of Display Science and Engineering, Pukyong National University, Busan 608-737, Republic of Korea.

³Department of Materials Science and Engineering, Pukyong National University, Busan 608-739, Korea.

⁴LED-Marine Convergence Technology R&D Center, Pukyong National University, Busan 608-739, Korea.

Silicate phosphors have many polymorphic structures depending on the annealing conditions such as pressure, heating temperature and quenching time [1-4]. The rapid thermal quenching processes resulted in some metastable-structure phosphors with the different emission colors of the normal annealing processes. It indicates that the different emission colors of the metastable phosphors are attributed to the different crystal field of emission center from the different crystal structure of the reference. The metastability of the fast-quenched phosphors was demonstrated by their phase transformation to the stable-structure phase with changing emission colors by their normal reannealing processes. In this talk, we present some metastable phosphors; the orange $\text{Sr}_3\text{SiO}_5:\text{Eu}^{2+}$ was changed to the yellow $\text{Sr}_2\text{SiO}_4:\text{Eu}^{2+}$, the γ -phase yellow $\text{Ca}_2\text{SiO}_4:\text{Ce}^{3+}$ was changed to the β -phase blue one, the α -phase green $\text{Zn}_2\text{SiO}_4:\text{Mn}^{2+}$ was changed to the β -phase yellow one.

References:

- [1] Z. Mao, Z. Lu, J. Chen, B. D. Fahlman, and D. Wang, J. Mater. Chem. C, 3 (2015) 9454
- [2] T. Abe, and I. Sunagawa, Mineralogical Journal, 17 (1994) 257.
- [3] D. Turnbull, Mineralogical Transactions 12A (1981) 695.
- [4] J. Haines, J. M. Léger, F. Gorelli, and M. Hanfland, Phys. Rev. Lett., 87 (2001) 155503.

Acknowledgement

This work was supported by the Development of R&D Professional on LED Convergence Lighting for Shipbuilding/Marine Plant and Marine Environments (Project No: N0001363) funded by the Ministry of TRADE, INDUSTRY & ENERGY (MOTIE, Korea).

Single crystal phosphors for high-power laser lighting

**Taewook Kang¹, Gotaek Kim¹, Wunho Lee¹, Byungjoo Jeon¹, Hyojun Kim²,
Kwangwon Park², Jongsu Kim^{1,2}, Heelack Choi^{1,3}, Taehoon Kim⁴**

¹*Department of LED Convergence Engineering, Specialized Graduate School of Science and Technology Convergence, Pukyong National University, Busan 608-739, Republic of Korea.*

²*Department of Display Science and Engineering, Pukyong National University, Busan 608-737, Republic of Korea.*

³*Department of Materials Science and Engineering, Pukyong National University, Busan 608-739, Korea.*

⁴*LED-Marine Convergence Technology R&BD Center, Pukyong National University, Busan 608-739, Korea.*

Ce-doped garnet single crystals as a color conversion phosphor for high-power laser lighting were grown through a floating zone method in an image furnace. They showed excellent lumen maintenance, lower quantum efficiency, and broader photoluminescence excitation spectrum compared with the polycrystalline powder phosphor [1]. The higher lumen maintenance were explained by the less intrinsic defects and the less phonon generation at high temperature, confirmed by excitation spectra and temperature-dependent Raman spectra, respectively. To evaluate their feasibility for high-power laser lighting, they were applied to a 5 watt blue laser diode with a remote-phosphor structure, and thus they reached a lower equilibrium temperature after shorter operating time in comparison with the polycrystalline powder phosphor. Thus, the single crystal phosphors can achieve the extremely stable white-light emission without an efficiency loss under the high-power density of blue laser diode.

Reference:

[1] K. Park, S. Lim, G. Deressa, J. Kim, T. Kang, H. Choi, Y. Yu, Y. Kim, J. Ryu, S. Lee, and T. Kim, *J. Lumin.* 168 (2015)334.

Acknowledgement

This work was supported by the Development of R&D Professionals on LED Convergence Lighting for Shipbuilding/Marine Plant and Marine Environments (Project No: N0001363) funded by the Ministry of TRADE, INDUSTRY & ENERGY(MOTIE, Korea).

Strong blue absorption in heavy Mn-doped phosphors

Kwangwon Park¹, Jaehyoung Park¹, Hyojun Kim¹, Jongsu Kim^{1,2}, Byungjoo Jeon², Taewook Kang², Wunho Lee², Heelack Choi^{2,3}, Taehoon Kim⁴

¹Department of Display Science and Engineering, Pukyong National University, Busan 608-737, Republic of Korea.

²Department of LED Convergence Engineering, Specialized Graduate School of Science and Technology Convergence, Pukyong National University, Busan 608-739, Republic of Korea.

³Department of Materials Science and Engineering, Pukyong National University, Busan 608-739, Korea.

⁴LED-Marine Convergence Technology R&BD Center, Pukyong National University, Busan 608-739, Korea.

Heavily-Mn²⁺-doped phosphors showed an extremely enhanced photoluminescence excitation intensity from ${}^6A_1 \rightarrow {}^4A_1$ forbidden transition of Mn²⁺ ions, and an intensive emission from ${}^4T_1 \rightarrow {}^6A_1$ forbidden transitions with an excellent quantum efficiency and a lumen maintenance at high temperature.[1] The drastic enhancement of quantum efficiency under the blue light excitation was explained in terms of the relaxation of selection rule on the forbidden intra-transitions in higher concentrations of Mn²⁺ ions. It results from the spin-spin and the electron-phonon interactions, supported by electron spin resonance and Raman spectra, respectively. The optimized heavily-Mn-doped phosphors can be applied to blue-based white-light-emitting diode as a color conversion phosphors.

Reference:

[1] Kwangwon Park, Hyongseok Lim, Seongwoo Park, Gemechu Deressa and Jongsu Kim, Chem. Phys. Lett. 636 (2015)141.

Acknowledgement

This research was supported by a grant from the Advance Technology Center (ATC) program (no. 10042178) funded by the Ministry of Trade, Industry and Energy of Korea.

Temperature-Dependent Photoluminescence Lifetimes of Cu-Doped Zn-In-S Quantum Dots

Jialong Zhao, Xi Yuan and Haibo Li

Key Laboratory of Functional Materials Physics and Chemistry of the Ministry of Education, Jilin Normal University, Siping 136000, China

Colloidal semiconductor quantum dots (QDs) are very promising in applications of light-emitting diodes (LEDs) for the next generation display and solid-state lighting because of their size- and composition-tunable photoluminescence (PL) and high emission quantum efficiency. The working temperature of the LEDs is above room temperature, while their efficiency is temperature dependent. The significant high temperature PL quenching was observed in undoped QDs [1]. Recently almost no PL thermal quenching was observed in Mn:ZnS/ZnS QDs at 500 K, having high PL quantum yield of 50% [2]. In this work, the temperature-dependent PL spectra and decays of Cu:Zn-In-S QDs were studied by using steady-state and time-resolved PL spectra at temperature ranging from 80 to 400 K. The composition-tunable Cu:Zn-In-S/ZnS QDs with various emissions from deep red to green were synthesized. The effect of shell structure and host bandgap on PL lifetime of Cu dopant emissions with different emission wavelengths was compared to understand mechanisms and origins of PL emissions as well as thermal quenching. The PL in Cu:Zn-In-S/ZnS QDs with green and yellow emissions were suggested to mainly come from the recombination of the electron in the conduction band of host semiconductor and hole in Cu T_2 state. The origin of PL in red QDs is complex, which is probably not only from the recombination of the electron in the conduction band of host semiconductor and hole in Cu T_2 state but also from donor-acceptor pair.

References:

- [1] Y. Zhao, C. Riemersma, F. Pietra, R. Koole, C. de Mello Donegá and A. Meijerink, *ACS Nano*, **6**(2012)9058.
- [2] X. Yuan, J. Zheng, R. Zeng, P. Jing, W. Ji, J. Zhao, W. Yang and H. Li, *Nanoscale*, **6**(2014)300.

High density excitation with alpha particles

W. Wolszczak, P. Dorenbos

Delft University of Technology, Faculty of Applied Sciences, Department of Radiation Science and Technology, Luminescence Materials Research Group, 2629 JB Delft, Netherlands

Interest in improving performance of scintillators in industrial applications caused increased attention in high energy density excitation processes. While the luminescence processes are quite well studied, the non-radiative processes are still not fully understood. The latest theories on high energy density excitation explain observed losses by Auger and/or Förster quenching processes of excitons formed within a dense cloud of free charge carries. There is a lack of experimental data available on this topic, especially on how quenching is affected by the chemical composition of a material. To gain knowledge about these processes we studied the scintillation from alpha particles as a source of high density excitation. In this work we observed a correlation between the alpha particle induced light yield and the chemical composition of the material. We also studied the light yield due to low energy X-ray photons to determine the so-called alpha/beta ratio. It connects to the amount of non-proportional response of scintillators and is important for the intrinsic energy resolution of scintillators in nuclear spectroscopy application. We measured alpha/beta ratio for different Ce^{3+} concentrations in $\text{LaBr}_3:\text{Ce}$ and investigated the influence of co-dopants like strontium on the alpha particle light yield.

References:

[1] Xinfu Lu, Qi Li, G. A. Bizarri, Kan Yang, M. R. Mayhugh, P. R. Menge, and R. T. Williams
Phys. Rev. B 92 (2015) 115207

The Vacuum Referred Binding Energies of Bi³⁺ in wide band gap compounds

R. H. P. Awater and P. Dorenbos

Delft University of Technology, Faculty of Applied Sciences, Dept. RST/FAME, Mekelweg 15, 2629JB Delft, The Netherlands

Bi³⁺ has been extensively studied as activator and sensitizer in different luminescent materials. From spectroscopic data it is known that the Bi³⁺¹S₀→³P₁ (A-band) and ¹S₀→¹P₁ (C-band) transition energies in a compound decreases with increasing covalency and anion polarizability [1]. Such redshift is also observed for the transitions in the lanthanide ions and is known to follow the nephelauxetic sequence F⁻ < O²⁻ < Cl⁻ < N³⁻ < Br⁻ < I⁻ < S²⁻ < Se²⁻ [2]. Additional to the A- and C-band transition, spectroscopy of Bi³⁺-doped compounds show a metal-to-metal charge transfer (MMCT) transition, which is labelled as D-band. An empirical model was proposed by Boutinaud *et al.* to predict the MMCT energy of Bi³⁺ in closed shell d⁰ transition metal complex oxides [3]. However, this empirical model does not provide the absolute locations of the Bi³⁺ energy levels. From lanthanide spectroscopy it is known that using the Eu³⁺ charge transfer energies, the positions of the valance and conduction bands of the host compound relative to the vacuum level can be determined [4]. Since the D-band transition is defined as the energy required to transfer an electron from Bi³⁺ to the conduction band, the energy of the D-band can be used to position the Bi³⁺¹S₀ ground state relative to the conduction band. The A-band transition energy can then be used to position the ³P₁ excited state. Based on Bi³⁺ spectroscopy data available in the archival literature, the Bi³⁺ ground state was found to vary between -9 eV in fluorides and -4.5 eV in sulphides and selenides. The observed trends in MMCT energy upon changing the chemical environment surrounding the Bi³⁺ activator were consistent with literature [5]. The positions of the Bi³⁺ energy levels can be used to understand and predict the luminescent properties of Bi³⁺-activated luminescent materials.

References:

- [1] L. Wang, Q. Sun, Q. Liu and J. Shi, *J. Solid State Chem.* 191 (2012) 142 – 146
- [2] P. Dorenbos, *J. Lumin.* 136 (2013) 122 – 129
- [3] P. Boutinaud and E. Cavalli, *Chem. Phys. Lett.* 503 (2011) 239 - 243
- [4] P. Dorenbos, *Phys. Rev. B* 87 (2013) 035118
- [5] P. Boutinaud, *Inorg. Chem.* 52 (2013) 6028 – 6038

Luminescence of defective monoclinic zirconia prepared in a solar furnace

L. Puust¹, C. Monty², V. Kiisk¹ and I. Sildos¹

¹Institute of Physics, University of Tartu, W. Ostwaldi 1, 50411 Tartu, Estonia

²Procédés, Matériaux et Energie Solaire CNRS, Font-Romeu, France

Monoclinic zirconia (ZrO_2) nanocrystalline materials contain a complex system of intrinsic or extrinsic defects which are responsible for (a) the strong photoluminescence (PL) at 490 nm and (b) a number of traps at different depths leading to thermoluminescence (TL), optically stimulated luminescence (OSL) and a long afterglow of the PL [1]. The TL peaks within the temperature range from -100 to 300 °C were tentatively assigned to structural defects and surface states based on comparative studies of various sol-gel-derived or commercial ZrO_2 nanopowders. We propose that thermoluminescence and EPR study [2] can give supplementary information about defect origin of Zirconia.

Hereby zirconia nanopowders from Alfa Aesar was subjected to ceramic sintering in Heliotron reactor (PROMES CNRS, France) [3]. During this process the samples were heated up to 3000 °C in different ambient conditions and cooled down with different rate. It was found that the obtained zirconia samples were generally highly luminescent and at the same time the selection of preparation conditions allowed a pronounced engineering of the defect content responsible for the TL and PL afterglow (Fig. 1). Specifically, the traps responsible for the afterglow at RT were most efficiently produced when the sample was heated in air and slowly cooled. On the other hand, the deeper traps, which are more suitable for dosimetry, were more pronounced when the sample was heated in vacuum, which is in agreement with our previous results of sol-gel-derived zirconia annealed in reducing atmosphere [1]. Scanning and transmission electron microscopy of the materials is being studied and the nanostructure correlated to the TL peaks to identify the origin of the traps.

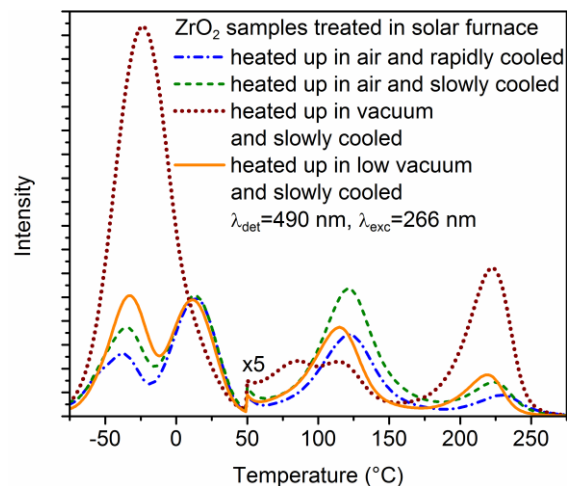


Figure 1. TL glow curves of various zirconia materials, obtained after charging the sample with 266 nm laser. Note that the PL thermal quenching is not yet accounted for.

References:

- [1] V. Kiisk et al., *Journal of Luminescence* 174 (2016) 49–55.
- [2] C. Gionco et al., *Chemistry of Materials* 25 (2013) 2243-2253.
- [3] K. Smits et al., *Optical Materials* 37 (2014) 251–256.

Luminescence investigations of $\text{ZnGa}_2\text{O}_4: \text{Mn}^{2+}$ and $\text{ZnGa}_2\text{O}_4: \text{Mn}^{2+}, \text{Eu}^{3+}$ compounds with spinel structure

¹A. Luchechko, ¹O. Kravets, ²I. I. Syvorotka

¹ Ivan Franko National University of Lviv, Faculty of Electronics,
Tarnavskogo str. 107, Lviv 79017, Ukraine

² SRC "Carat", Stryjska Str. 202, 79031, Lviv, Ukraine

Recently, the attention of researchers has been focused on the developing of different types of display technologies. Zinc gallate spinel compound is one of the promising materials with possible applications in vacuum fluorescent displays and field emission displays. ZnGa_2O_4 is transparent in near UV spectral region material with strong host luminescence and low-voltage cathodoluminescence [1]. Doped with Mn^{2+} and Eu^{3+} ions spinels show excellent luminescent properties in "green" and "orange-red" spectral regions, respectively [2].

In this work, $\text{ZnGa}_2\text{O}_4: 0,05 \text{ mol.}\% \text{ Mn}^{2+}$ and $\text{ZnGa}_2\text{O}_4: 0,05 \text{ mol.}\% \text{ Mn}^{2+}, X \text{ mol.}\% \text{ Eu}^{3+}$ ($X= 0-8 \text{ mol.}\%$) ceramic samples have been synthesized via high temperature solid-state reaction method at $\sim 1200^\circ\text{C}$ in air. X-ray diffraction measurements show single-phase nature with spinel structure of all samples. The luminescence properties were investigated under different excitation wavelengths at room temperature.

Excitation spectra of $\text{ZnGa}_2\text{O}_4: \text{Mn}$, $\text{ZnGa}_2\text{O}_4: \text{Mn}, \text{Eu}$ registered at 385, 440 and 505 nm show similar behavior in 230-380 nm spectral region. An intense excitation band was found in 230-270 nm region of spectrum at 385 and 440 nm registration. At 440 nm registration the gradual increase takes a maxima around 370 nm with further steep decrease. The excitation of Mn^{2+} ions was found in 230-280 nm intense band at 505 nm monitoring. A number of sharp lines were found in 320-550 nm spectral region which correspond to f-f transitions in Eu^{3+} ions. The charge transfer band from O^{2-} to Eu^{3+} ions with maximum around 270 nm was also found on the excitation spectra registered at 617 nm.

A broad emission band in 325-475 nm spectral region together with an intense band around 505 nm was found on luminescence spectra at 235 nm excitation for samples with Eu^{3+} ions content below 4 mol.%. The broad emission band with a maximum around 385 nm corresponds to luminescence of host defects and decreases with excitation wavelength increasing. The luminescence band with a maximum around 505 nm corresponds to Mn^{2+} ions emission that decreases with excitation wavelength increasing, as well as with increasing of Eu^{3+} ions concentration. Weak emission of Eu^{3+} ions takes place at 255 nm excitation and with further increase of excitation wavelength it becomes narrower and shapes into line spectra which corresponds to f-f transition in Eu^{3+} ions. The most intense line was found at 617 nm that appropriate to ${}^5\text{D}_0 \rightarrow {}^7\text{F}_2$ transitions. Concentration dependence shows that the optimal concentration of Eu^{3+} ions is around 3 mol.%. Possible energy transfer mechanisms between host, Eu^{3+} and Mn^{2+} ions is under discussion.

References:

- [1] Musa Mutlu Can et al., J. of Alloys and Compounds 549 (2013), 303-307.
- [2] A. Luchechko et al., Radiation measurements, 2015, Article in press.

Dynamics of electron photoexcited states on the TiO₂ – xanthene dyes interface

N. Ibrayev, D. Afanasyev, E. Seliverstova

Institute of Molecular Nanophotonics, E.A. Buketov Karaganda State University, Karaganda, Kazakhstan

A study of the dynamics of photo excited electrons at the interface of wide gap semiconductor – dye was performed. TiO₂ films doped by molecules of xanthene dyes - Rhodamine 6G (R6G), Rose bengal (BR), Eosin were used as objects of studying. To determine the contribution of process with charge transfer to the luminescence of the dye the comparison of the spectral-luminescent properties of TiO₂-dye films and dielectric SiO₂ –dye films was carried out. All studied dyes have LUMO orbitals above the edge of conducting band of semiconductor. For dye R6G quantum yield of the triplet state is very small (less than 0.01). Therefore, the main role in the process of charge transfer in the system of R6G-TiO₂ plays S₁ state of the dye. For BR and Eosin dyes quantum yield of the triplet state has a high value. In dye BR S₁ and T₁ states are located above the conduction band of the titanium dioxide. Therefore, electron transfer is possible both S₁ and T₁ states of the dye. For the Eosin molecules T₁ state is located lower than conducting band of semiconductor. Therefore electron transfer for Eosin is possible only from the S₁ state of the dye.

Sorption of dyes on the surface of TiO₂ films and wide porous silica (Silufol UV254) was performed from ethanol solutions with a concentration of dyes $C = 10^{-4}$ mol/L. Control of the number of adsorbed dye molecules is carried out by absorption and fluorescence spectroscopy. Titanium dioxide films were obtained by the standard method with using of anatase TiO₂ particles having an average particle radius of 21 nm [1]. Investigation of the effect of external magnetic field on the kinetics of fluorescence of the films was carried out by using of a pulsed spectrofluorometer with picosecond resolution (Becker & Hickl). For the formation of an external magnetic field a neodymium magnet was used. The magnetic field was measured by using of calibrated magnetic field sensor based on the Hall effect.

The data show that the intensity and the fluorescence lifetime of the dyes are quenched on the surface of the semiconductor film compared to the same parameters in solutions and on silica. Thus there is a bathochromic shift of the absorption spectra and fluorescence dyes was registered.

An external magnetic field effects on the kinetics of the luminescence of the dye in the dye-TiO₂ films in the nanosecond time range. There is a time dependence of the magnetic effect. The sign of the magnetic effect on the luminescence of R6G and Eosin dyes is distinguish from the sign of the magnetic effect that was observed for BR. Analysis of the obtained data of the magnetic effect shows the participation of triplet states of BR within the process of charge transfer from the dye to the TiO₂. The involving of molecular oxygen in the dynamics of photo-excited electrons at the interface between TiO₂-BR was found.

References:

[1] Ito S., Murakami T.N., Comte P., et al. Thin Solid Films 516 (2008) 4613-4619

Luminescent properties of Eu^{3+} doped SrKB_5O_9

B. Bondzior, P.J. Dereń

Institute of Low Temperature and Structure Research, Polish Academy of Sciences, ul. Okólna 2, P.O.Box 1410, 50-950 Wrocław, Poland

**Corresponding author: p.deren@int.pan.wroc.pl*

Although borates are mainly known for their non-linear properties, lately they have drawn attention also as luminescent materials. High transparency in UV, which determined their usefulness as non-linear laser materials, can also be an advantage in the field of phosphors. Along with other features like low-temperature synthesis and the high number of noncentrosymmetric structures among borate family[1] make borate materials interesting as host for phosphors.

Condensed borate polycrystalline powders with formula SrKB_5O_9 doped with Eu^{3+} ions in range 0.1 – 5% has been synthesised by citric route. The resulting samples are pure phase, which was confirmed by XRD measurements. Samples exhibit luminescent properties typical for Eu^{3+} ions, with emission ranging from 570 nm up to 850 nm with maximum at 617 nm. Intense excitation band attributed to charge transfer transition is at 264 nm. Luminescence intensity does not get quenched and increases along with dopant concentration up to 5 % of Eu^{3+} .

Luminescence decay curves measurements revealed that Eu^{3+} ions occupies two distinct sites in the crystal structure – most probably Sr^{2+} and K^+ sites due to the fact that they both have large coordination numbers (7 and 8 respectively)[2] and sizes larger than Eu^{3+} (Sr^{2+} - 140 pm, K^+ - 165 pm, Eu^{3+} - 120 pm).

Remarkable is also the fact, that luminescence decay lifetime seems to increase with Eu concentration of approximately with total difference between 0.1 and 5% Eu^{3+} of 800 μs , which suggests that the incorporation of dopant into the crystal structure may causing the contraction of the ions surrounding the Eu and resulting in site symmetry changes.

References:

- [1] P. Becker, "Borate Materials in Nonlinear Optics," *Adv. Mater.*, vol. 10, no. 13, pp. 979–992, 1998.
- [2] J. M. Tu and D. a. Keszler, " SrKB_5O_9 ," *Acta Crystallogr. Sect. C Cryst. Struct. Commun.*, vol. 51, no. 3, pp. 341–343, Mar. 1995.

Optical spectroscopy and EPR studies of Mn²⁺ ions in YAIO₃

Ya. Zhydachevskii^{1,2}, H. Przybylińska¹, A. Wołoś¹, M. Glowacki¹, M. Berkowski¹,
A. Suchocki^{1,3}

¹ *Institute of Physics, Polish Academy of Sciences, Al. Lotników 32/46, Warsaw 02-668, Poland*

² *Lviv Polytechnic National University, 12 Bandera, Lviv 79646, Ukraine*

³ *Institute of Physics, University of Bydgoszcz, Weyssenhoffa 11, Bydgoszcz 85-072, Poland*

Yttrium orthoaluminate (YAIO₃), called also yttrium aluminum perovskite (YAP), is widely known as a host material for solid-state lasers and scintillators. Mn-doped YAIO₃ became of particular interest after its application potential has been shown for holographic recording and optical data storage [1] as well as for thermoluminescent (TL) dosimetry of ionizing radiation [2-3].

Manganese in YAIO₃ can be present as Mn⁴⁺ ions (3d³ configuration) occupying octahedral Al³⁺ sites as well as Mn²⁺ ions (3d⁵) in strongly distorted dodecahedral Y³⁺ sites. In particular, the green emission near 530 nm from Mn²⁺ ions can be used for thermoluminescent dosimetry of ionizing radiation [2-3]. In order to get a better insight into the recharging and trapping processes involving Mn²⁺ ions, detailed optical spectroscopy and electron paramagnetic resonance (EPR) studies of YAIO₃:Mn²⁺ crystals have been performed.

The studied Mn²⁺-doped YAIO₃ crystals were grown by the Czochralski method in the Institute of Physics of the Polish Academy of Sciences. To obtain crystals with Mn mainly in the 2+ charge state, co-doping with Si⁴⁺ or Hf⁴⁺ ions was used. The samples for EPR studies were cut out from the as-grown crystal in the form of parallelepipeds in the directions parallel to the crystallographic axes *a*, *b*, and *c* in the in *Pbnm* setting.

Indeed, in the codoped crystals, only Mn²⁺ ions occupying the Y³⁺ sites were observed. This center has rhombic point symmetry with one of the principal axes coinciding with the crystal's *c*-axis and the other two lying in the *ab* plane. There are two magnetically inequivalent sites, which transform into each other by reflexion in the *ac* and *bc* planes, referred to as *A* and *B* sites. The EPR spectra were analyzed with a spin Hamiltonian appropriate for rhombic symmetry.

An effect of visible, UV and γ -rays irradiation on the intensity of EPR signal of Mn²⁺ ions has been analyzed and correlated with TL properties of the material. The obtained results are discussed and compared with the EPR and luminescence results reported previously for Mn-doped YAIO₃.

Acknowledgements: The work was partially supported by the EU within the European Regional Development Fund through the Innovative Economy grant (POIG.01.01.02-00-108/09), the Polish National Science Center (project DEC-2012/07/B/ST5/02080), and by the NATO SfP Project NUKR.SFPP 984649.

References:

- [1] G.B. Loutts et al., *Phys. Rev. B* 57 (1998) 3706-3709.
- [2] Ya. Zhydachevskii et al., *Nucl. Instr. Meth. Phys. Res. (B)* 227 (2005) 545-550.
- [3] Ya. Zhydachevskii et al., *Radiat. Meas.* 45 (2010) 516-518.

Optical and Electron Paramagnetic Resonance Spectroscopy of $\text{Yb}^{3+}:\text{Y}_2\text{SiO}_5$

S. Welinski¹, A Ferrier^{1,2}, Ph. Goldner¹

¹PSL Research University, Chimie ParisTech-CNRS, Institut de Recherche de Chimie Paris, 75005 Paris, France

²Sorbonne Universités, UPMC Université Paris 06, 75005, Paris, France

Crystals doped with paramagnetic rare earth (RE) ions are promising materials for quantum information processing because they can be coupled to microwave photons [1] or provide large bandwidth memories [2]. We also recently demonstrated that coherence transfer with high fidelity was possible between electron and nuclear spins in these materials, opening the way to long storage time capability [3].

In this paper, we report on the optical and paramagnetic spectroscopic properties of $\text{Yb}^{3+}:\text{Y}_2\text{SiO}_5$ at low concentration. In particular, we determined the ground state spin Hamiltonian (g and A tensors) for isotopes with $I=0$, $I=1/2$ and $I=5/2$ nuclear spins for ions in sites 1 and 2. As it has been done for $\text{Er}^{3+}:\text{Y}_2\text{SiO}_5$ [4], we also determined optically the g -tensor of the excited state $^2F_{5/2}$ of $\text{Yb}^{3+}:\text{Y}_2\text{SiO}_5$. This allows one to determine energy level structure of both the ground state ($^2F_{7/2}$) and the excited state ($^2F_{5/2}$) for an arbitrary magnetic field, which may be useful to minimize decoherence processes caused by Yb^{3+} - Yb^{3+} interactions [5].

References:

- [1] S. Probst, H. Rotzinger, S. Wünsch, P. Jung, M. Jerger, M. Siegel, A. V. Ustinov, and P. A. Bushev, "Anisotropic Rare-Earth Spin Ensemble Strongly Coupled to a Superconducting Resonator," 110, 157001 (2013).
- [2] F. Bussi eres, C. Clausen, A. Tiranov, B. Korzh, V. B. Verma, S. W. Nam, F. Marsili, A. Ferrier, P. Goldner, H. Herrmann, C. Silberhorn, W. Sohler, M. Afzelius, and N. Gisin, "Quantum teleportation from a telecom-wavelength photon to a solid-state quantum memory," Nat. Photonics 8, 775–778 (2014).
- [3] G. Wolfowicz, H. Maier-Flaig, R. Marino, A. Ferrier, H. Vezin, J. J. L. Morton, and P. Goldner, "Coherent Storage of Microwave Excitations in Rare-Earth Nuclear Spins," Phys. Rev. Lett. 114, 170503 (2015).
- [4] Y. Sun, T. B ottger, C. W. Thiel and R. L. Cone, "Magnetic g tensors for the $^4I_{15/2}$ and $^4I_{13/2}$ states of $\text{Er}^{3+}:\text{Y}_2\text{SiO}_5$," Phys. Rev. B 77, 085124 (2008).
- [5] T. B ottger, C. W. Thiel, R. L. Cone, and Y. Sun, "Effects of magnetic field orientation on optical decoherence in $\text{Er}^{3+}:\text{Y}_2\text{SiO}_5$," Phys. Rev. B 79, 115104 (2009).

Mechanism of luminescence enhancement of SrSi₂O₂N₂:Eu phosphor via manganese addition

J. Barzowska¹, T. Lesniewski¹, Y. Zhydachevskyy², K. Szczodrowski¹,
D. Michalik³, H. Przybylińska², M. Sopicka-Lizer³, M. Grinberg¹, A. Suchocki^{2,4}

¹*Institute of Experimental Physics, University of Gdansk, Wita Stwosza 57, 80-952 Gdańsk, Poland*

²*Institute of Physics, Polish Academy of Sciences, Al. Lotników 32/46, Warsaw 02-668, Poland*

³*Institute of Materials Science, Silesian University of Technology, Karasińskiego 8, 40-019 Katowice, Poland*

⁴*Institute of Physics, University of Bydgoszcz, Weysenhoffa 11, 85-072 Bydgoszcz, Poland*

SrSi₂O₂N₂ is an excellent host lattice for phosphors due to superior thermal and chemical stability as well as large energy band gap. When activated with europium, it exhibits an intense broadband luminescence with maximum at 540 nm, due to 4f⁶5d¹ → 4f⁷ transition in Eu²⁺, which can be effectively excited in the near UV to blue spectral region, appropriate to convert the emission from InGaN or GaN chips used in phosphor-converted white LEDs. Apart from the fact that SrSi₂O₂N₂:Eu²⁺ is an excellent conversion phosphor material for LED, it also exhibits persistent luminescence [1].

It had been shown that SrSi₂N₂O₂: Eu²⁺ luminescence can be improved by co-doping [2], inter alia it was reported that co-doping with Mn ions enhance luminescence [2, 3,4]. This phenomenon was explained in two contradictory ways: as the result of energy transfer from Mn²⁺ to Eu²⁺ ions [4] or as energy transfer from Eu²⁺ to Mn²⁺ ions [3]. The inconsistency has become a motivation for our investigations.

Series of europium doped SrSi₂O₂N₂ samples were prepared using the solid state synthesis method. In some of them MnO was added with intention of co-doping the material with Mn ions. Phase purity of all obtained phosphors was checked using standard XRD method and in all samples it was determined to be pure triclinic, independently of the MnO addition. Spectroscopic measurements confirmed that the addition of manganese in the synthesis cause enhancement of SrSi₂N₂O₂:Eu²⁺ luminescence, however it does not influence neither the shape of the excitation and emission spectra nor the emission decay time.

Moreover, samples synthesized with MnO addition reveal stronger persistent luminescence, lasting few tens of minutes, but the energy structure of traps relevant for the phenomenon of persistent luminescence (estimated from thermoluminescence experiment) is independent on the usage of manganese in the synthesis procedure.

Possible reasons for these effects are discussed in this contribution. Among them stoichiometry changes and defect creation induced by Mn are considered.

References:

- [1] J. Botterman, K. Van den Eeckhout, A. J.J. Bos, P. Dorenbos, P.F. Smet; Opt. Material Express 3 (2012) 345
- [2] Ru-Shi Liu, Yu –Huan Liu, Nitin C. Bagkar; Appl. Phys. Lett 91 (2007) 061119
- [3] Qin-Ni Fei Yan-HuaLiu, Tie-ChengGu Da-JianWang; J.Lumin. 131 (2011) 960
- [4] Xiufeng Song, Renli Fu, Simeon Agathopoulos, Hong He, Xinran Zhao, Jun Zeng; Mater. Sci. Eng. B 164 (2009) 12

Eu²⁺ luminescence properties in hydrides and hydride fluorides

Nathalie Kunkel^{1*}, Andries Meijerink², Holger Kohlmann³

¹ *Institut de Recherche de Chimie Paris –CNRS Chimie ParisTech, 75005 Paris, France
nathalie.kunkel@chimie-paristech.fr*

² *Debye Institute, Utrecht University, P.O. Box 80 000, 3508 TA Utrecht, The Netherlands
3Leipzig University, Inorganic Chemistry, Johannisallee 29, 04103 Leipzig, Germany*

Due to the often high emission intensities, Eu²⁺ 5d-4f emission is of great interest for lighting and similar applications. Since the 5d levels are relatively unshielded, the luminescence properties depend strongly on the host lattice [1].

We studied the Eu²⁺ emission in ionic hydride host lattices, as for instance in LiSrH₃ and LiBaH₃ [2] and observed a large red shift in comparison with corresponding fluorides, such as LiBaF₃ [3] that we attribute to the high polarizability of the hydride anion. Since ionic compounds of hydride and fluoride often show structural analogies [4], substitution of hydride and fluoride is consequently expected to allow for tailoring different polarizabilities and thus, also different Eu(II) emission energies.

In order to investigate the influence of hydride fluoride substitution, we studied luminescence in the solid solutions series EuH_xF_{2-x} for the fluoride rich side on which the compounds crystallize in the fluorite structure type [5]. Here, it could be shown that an increase of the hydride content leads to a red shift of the Eu(II) emission energies. This red shift is mainly explained by the high polarizability of the hydride anion that leads to a shift of the barycentre of the Eu(II) 5d levels to lower energies.

Furthermore, we studied the solid solution series LiSrH_{3-x}F_x, LiBaH_{3-x}F_x, KMgH_{3-x}F_x and EAH_{2-x}F_x (EA = Ca, Sr, Ba) by first principle calculations and also prepared selected samples in order to study their luminescence properties.

The present results show that the substitution of anions with different polarizabilities in solid solution series is a tool for tuning the emission colour of Eu²⁺.

References:

- [1] J. P. Dorenbos, *J. Lumin.* 104 (2003) 239.
- [2] N. Kunkel, A. Meijerink, H. Kohlmann, *Phys. Chem. Chem. Phys.* 16 (2014) 4807.
- [3] A. Meijerink, *J. Lumin.* 55 (1993) 125.
- [4] A. J. Maeland, W. D. Lahar, *Z. Phys. Chem.* 179 (1993) 181.
- [5] N. Kunkel, A. Meijerink, H. Kohlmann, *Inorg. Chem.* 53 (2014) 4800.
- [6] N. Kunkel, H. Kohlmann, *J. Phys. Chem C* (2016), in press, DOI 10.1021/acs.jpcc.6b00386.

The luminescence of electronic excitations in alkali halide crystals at lattice symmetry lowering

¹K. Shunkeyev, ¹S.Shunkeyev, ¹A.Barmina, ¹L.Myasnikova, ¹N.Zhanturina,
¹D.Sergeyev, ¹Sh.Sagymbaeva, ²Z.Aimaganbetova
¹Zhubanov Aktobe Regional State University
²Al-Farabi Kazakh National University

Currently alkali halide crystals (AHC) are widely used as scintillation detectors in standard and very urgent experiments, such the registration of the energy of dark matter particles [1]. The observed effect of the alkali halide crystals luminescence intensity enhancement by lattice symmetry lowering makes it possible to search for a generation of modern scintillators [2,3]. Low-temperature uniaxial deformation, which lowers the crystal symmetry was carried out in the direction of $\langle 100 \rangle$ and $\langle 110 \rangle$ in a special cryostat [4].

Radiation was detected directly in the compressed state of the crystal at 90K with irradiation by hard X-rays, which do not create radiation defects, distort the emission spectrum, in contrast to the characteristic X-ray radiation, i.e, excludes the effect of reabsorption of radiation-induced defects.

The effect of self-trapped excitons luminescence enhancement in the regular lattice sites and in the field of light cation was established. On example of KI-Tl crystal the value of reducing of the mean free path of free excitons before self-trapping in the regular lattice sites with the degree of low-temperature deformation was established. On example of KCl-Na the assembly of electron-hole pairs in the light cation Na field of the crystal was demonstrated, which radiative relaxation (2.8 eV) increases more than 30 times in the temperature range 80-300K, apparently due to an increase in the mean free path length of hot holes before self-trapping [5].

Thus, the increase in the luminescence of AHC was demonstrated by the impact on the mean free path of free excitons and holes by lowering the lattice symmetry.

Acknowledgments

This work was supported by the grant funding of Ministry of Education and Science of the Republic of Kazakhstan No 4903/GF4, 4904/GF4.

References

- [1] J.H. Davis, Phys. Rev. Lett. 113 (2014) 081302
- [2] K. Shunkeyev, V. Babin, A. Elango, A. Maaros, K. Kalder, E. Vasilchenko, S. Zazubovich, J. of Luminescence 81 (1999) 71
- [3] V. Babin, A. Bekeshev, A. Elango, A. Kalder, K. Shunkeyev, E. Vasilchenko, S. Zazubovich, J. of Physics: Condensed Matter 11 (1999) 2303
- [4] K. Shunkeyev, E. Sarmukhanov, A. Bekeshev, Sh. Sagymbaeva and K. Bizhanova, J. of Physics: Conference Series 400 (2012) 052032
- [5] Shunkeyev K.Sh., Zhanturina N.N., Sagymbaeva Sh.Zh., Shunkeyev S.K, Izvestia Vuzov Fizika T.57 №12/3 (2014) 76

Morphology Control and Upconversion Luminescence Properties of Monoclinic $Y_2WO_6:Yb^{3+}/Er^{3+}$

Cuili Chen, PeiqingCai, Sun Il Kim, Hyo Jin Seo

Department of physics and Interdisciplinary program of Biomedical, Mechanical & Electrical Engineering, Pukyong National University, Busan 608-737, Republic of Korea

An upconversion luminescence material of monoclinic $Y_2WO_6:Yb^{3+}/Er^{3+}$ with various Er^{3+} doping concentration was synthesized via both classical solid state and facile hydrothermal method. Therein, the sodium surfactant dodecyl benzene sulfonate (SDBS) was used to modify the sample to obtain the peculiar morphology during the hydrothermal synthesis process, and their crystal structure and morphology were characterized by X-ray diffraction(XRD) and scanning electron microscopy(SEM). Under the 980nm laser excitation, the emission bands of Er^{3+} are obtained which are respectively centred at 410nm($^2H_{9/2} \rightarrow ^4I_{15/2}$), 480nm($^4F_{7/2} \rightarrow ^4I_{15/2}$), 530nm($^2H_{11/2} \rightarrow ^4I_{15/2}$), 550nm($^4S_{3/2} \rightarrow ^4I_{15/2}$), 665nm($^4F_{9/2} \rightarrow ^4I_{15/2}$) and 867nm($^4I_{9/2} \rightarrow ^4I_{15/2}$)nm. It is found that the luminescence intensity ratio of green and red band gradually increased with the increase of excitation power. Based on the energy level structure of Er^{3+} and excitation power dependence, the dominant upconversion mechanism of the monoclinic $Y_2WO_6:Yb^{3+}/Er^{3+}$ phosphor is discussed.

Combustion Synthesis and Luminescence Properties of $\text{Sr}_3\text{La}_2(\text{BO}_3)_4:\text{Eu}^{3+}$ Phosphors

Peiqing Cai, Cuili Chen, Sun Il Kim, and Hyo Jin Seo

Department of physics and Interdisciplinary program of Biomedical, Mechanical & Electrical Engineering, Pukyong National University, Busan 608-737, Republic of Korea

A series of $\text{Sr}_3\text{La}_{2(1-x)}(\text{BO}_3)_4:x\text{Eu}^{3+}$ ($0.01 \leq x \leq 1.00$) nanocrystalline phosphors was prepared by a novel technique which is a slight variation of solution combustion synthesis. The XRD analysis confirmed the formation of the solid solution between $\text{Sr}_3\text{La}_2(\text{BO}_3)_4$ and $\text{Sr}_3\text{Eu}_2(\text{BO}_3)_4$. The morphology was determined with Scanning Electron Microscope (SEM). It was found that the size of nanocrystallites is around 50-60 nm. The excitation, emission spectra and decay curves are reported. The photoluminescence spectra show that the samples have intense and prevailing red emission at 612 nm corresponding to the $^5\text{D}_0 \rightarrow ^7\text{F}_2$ electric dipole transition. The Eu concentration and different annealing temperature have an effect significantly on the luminescence properties. In addition, the thermal stability of phosphor was also investigated. The results showed that the emission intensity of Eu^{3+} -activated phosphors decreases slightly no spectral shift is observed with increasing temperature.

Spectroscopic study of materials doped rare-earth ions

A.Bitam^{1,2}, S.Khiari², M. Diaf²

¹University Centre of Tamanrasset, Algeria,
adel.bitam@gmail.com

²Laboratory of Laser Physics, Optical Spectroscopy and Optoelectronics (LAPLASO),
University Badji Mokhtar, Annaba, Algeria,
diafma@yahoo.fr

The present work reported a Judd-Ofelt analysis of spectroscopic and lasers parameters of Er³⁺ [1] ions in crystal hosts. Rare earth-doped fluoride single crystals are considered to be an important class of optical device materials due, mainly, to their low phonon energies. They play a very significant role in the development of laser amplifiers for optical communications. Among the rare earth, trivalent erbium ions Er³⁺ have potential for laser applications due to a large number of available energy levels in the visible and near infrared domains.

We have studied the optical properties of Er³⁺ doped BaF₂ single crystals. Room temperature absorption spectra were recorded in order to investigate spectroscopic properties by using the Judd-Ofelt (JO) analysis [2,3]. The emission spectra, associated to ⁴S_{3/2}, ²H_{11/2} and ⁴F_{9/2} to ⁴I_{15/2} level, have been also registered between 530 and 700 nm. They have been calibrated in emission cross-sections using the usual Fuchtbauer-Ladenburg formula.

Keywords: Rare-earth, laser amplifier, Judd-Ofelt analysis, emission cross-section, fluorescence lifetime, absorption spectra.

References:

- [1] S.Djellab, M.Diaf, K.Labbaci and L.Guerbous, "Crystal growth and spectroscopic properties of Er³⁺ ions doped CdF₂ single crystals" *Physica Scripta*, vol.89, 2014, 045101 (7pp).
- [2] B. R. Judd, "Optical Absorption Intensities of Rare-Earth Ions," *Physical Review*, Vol. 127, No. 3, 1962, pp. 750- 761.
- [3] G. S. Ofelt, "Intensities of Crystal Spectra of Rare-Earth Ions," *Journal of Chemical Physics*, Vol.37, No. 3, 1962, pp. 511-520.

Confined Excitons in CdF₂-CaF₂ Superlattices

**Konstantin V. Ivanovskikh^{1,2}, Rosa B. Hughes-Currie², Michael F. Reid^{3,4},
Jon-Paul R. Wells⁴, Nikolay S. Sokolov⁵, Roger J. Reeves^{3,4}**

¹*Institute of Physics & Technology, Ural Federal University, Ekaterinburg, Russia*

²*Department of Physics & Astronomy, University of Canterbury, Christchurch, New Zealand*

³*MacDiarmid Institute for Advanced Materials & Nanotechnology, Wellington, New Zealand*

⁴*Dodd-Walls Centre for Quantum & Photonic Technologies and Department of Physics & Astronomy, University of Canterbury, Christchurch, New Zealand*

⁵*Ioffe Physical-Technical Institute, Russian Academy of Sciences, St. Petersburg, Russia*

Superlattices (SLs) are structures formed by a periodic combination of monolayers (MLs) of materials having different band gaps thereby representing a sequence of quantum wells and barriers with modified optical properties. This makes them useful for application in quantum devices such as resonant tunnelling diodes or quantum cascade lasers. In this work, we focused on spectroscopy and dynamics of relaxation of intrinsic electronic excitations in SLs grown using a molecular beam epitaxy (MBE) technique [1]. Time-resolved spectroscopic characterisation of emission properties was performed using UV-VUV and X-ray synchrotron radiation.

The SLs were composed periodically layered structures of 3 or 5 monolayers (MLs) of CdF₂ and CaF₂. It was shown that the luminescence spectroscopic properties of these materials are largely governed by the behaviour of the CdF₂ quantum well, due to its smaller band gap. Excitonic emission in CdF₂ MLs was detected at temperatures lower than 200 K (Fig. 1). Excitation spectra recorded monitoring excitonic emission revealed significant (up to 0.85 eV) blue shift of CdF₂ fundamental absorption in SLs relative to that observed for bulk CdF₂ crystals (Fig. 2). That was shown to be related to confinement of non-relaxed (high energy) excitons. In addition, for the both 3 and 5 ML superlattices confinement effects are well pronounced in emission spectra and luminescence decay transients.

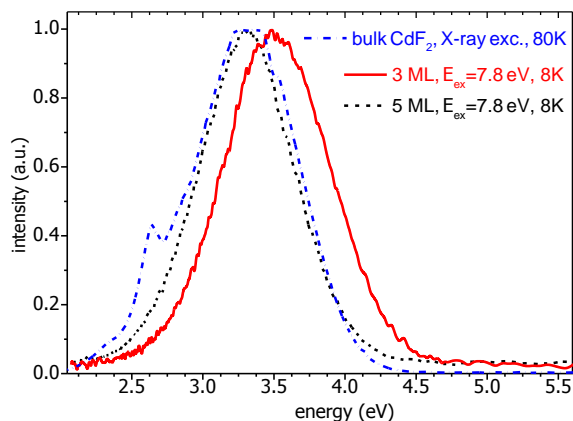


Fig. 1 Emission spectra of bulk CdF₂ crystal and SLs

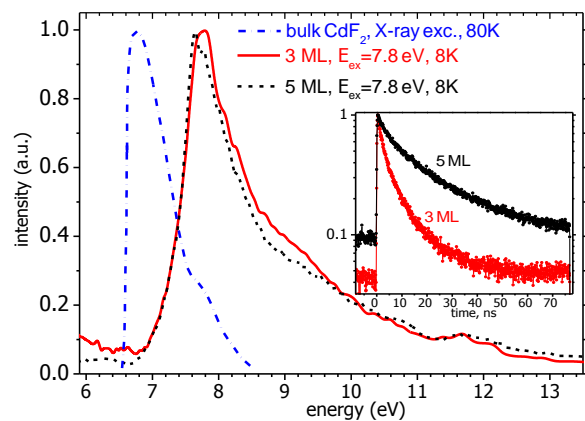


Fig. 2 Excitation spectra of bulk CdF₂ crystal (from [2]) and SLs. Insert shows decay curves for 3 and 5 ML SLs.

References:

- [1] N.S. Sokolov, S.M. Sutorin, Applied Surface Science, 175–176 (2001) 619-628.
[2] F. Fermi, C. Paracchini, N. Zema, J. Lumin. 31-32, (1984) 108.

High-pressure photoluminescence spectroscopy of codoped $\text{LiNbO}_3:\text{Cr}^{3+}; \text{W}^{4+}$ crystals.

M. A. Sánchez-Alejo¹, F. Rodríguez², J. A. Barreda-Argüeso², I. Camarillo³, C. Flores¹, H. Murrieta S.¹, J. M. Hernández¹, F. ⁴Jaque and E. Camarillo^{1*}.

¹*Instituto de Física-UNAM, Coyoacán, Cd. Mx., 04510, México. *E-mail: cgarcia@fisica.unam.mx*

²*MALTA ConsoliderTeam, DCITIMAC, Facultad de Ciencias, Universidad de Cantabria, 39005, Santander, Spain.*

³*Departamento de Física, UAM-Iztapalapa, Apdo. Post. 55-534, Cd. Mx., 09340, México.* ⁴*Facultad de Ciencias, Universidad Autónoma de Madrid, 28049, Madrid, Spain.*

In this work the photoluminescence properties of congruent codoped $\text{LiNbO}_3:\text{Cr}^{3+}; \text{W}^{4+}$ crystals have been systematically investigated by performing photoluminescence studies at room temperature in a wide range of hydrostatic pressures ranging from 1 bar to 280 kbar. In particular, our study has focused on the influence that hydrostatic pressure has on the ${}^2\text{E} \rightarrow {}^4\text{A}_2$ (R-lines) transitions. It has been observed that the pressure dependence of the spectral position of the R-lines associated with the two β and γ Cr^{3+} centres shows a bilinear behaviour with a change of slope near to 210 kbar. This has been related to the existence of a phase transition in the LiNbO_3 network. From the experimental results obtained, and considering the crystal field theory and the Murnaghan equation, the crystal field and hydrostatic pressure parameters have been calculated. Finally, considering the Sugano Tanabe theory, we propose an equation describing the pressure influence in the Racah values.

Luminescence properties of different Eu sites in $\text{Ba}_2\text{K}(\text{PO}_3)_5$ doped with Eu^{2+} and Eu^{3+}

A. Baran¹, S. Mahlik¹, M. Grinberg¹, A. Watras², R. Pązik², P. Dereń²

¹ *Institute of Experimental Physics, University of Gdansk, Wita Stwosza 57, 80-952 Gdansk, Poland*

² *Institute of Low Temperature and Structure Research, Polish Academy of Sciences, 2 Okólna Street, 50-422 Wrocław, Poland*

corresponding author: anna.baran@ug.edu.pl

Barium potassium phosphate ($\text{Ba}_2\text{K}(\text{PO}_3)_5$) doped with europium belongs to the hosts able to accommodate both Eu^{3+} and Eu^{2+} ions, which make it useful for white light emitting diodes (WLEDs) based on UV chip technology.

In this work effects of pressure and temperature on the luminescence of Eu^{2+} and Eu^{3+} -doped $\text{Ba}_2\text{K}(\text{PO}_3)_5$ are presented. The luminescence spectra and luminescence decays were measured as a function of temperature and pressure. Depending on the excitation wavelength phosphor shows different luminescence spectra. The emission color was bluish green, when only Eu^{2+} was excited, reddish orange when only Eu^{3+} was excited or white over simultaneous excitation of both ions. At room temperature under excitation with near UV light, the luminescence spectrum consists of broad emission band peaking at 480 nm due to the $4f^65d^1 \rightarrow 4f^7$ ($^8S_{7/2}$) transitions of Eu^{2+} and several sharp lines between 580 and 710 nm region, ascribed to the $^5D_0 \rightarrow ^7F_J$ ($J = 0, 1, 2, 3$ and 4) transitions in Eu^{3+} . At low temperatures, we observed three different bands related to the $4f^65d^1 \rightarrow 4f^7$ transitions in different Eu sites (at 415 nm (A), 450 nm (B) and 505 nm (C)): two Eu sites substituting for Ba^{2+} and one Eu site substituting for K^+ .

Under fixed excitation wavelength the effect of increasing of the intensity of Eu^{2+} emission with respect to Eu^{3+} emission was observed for temperature range 5 – 100 K. The nonradiative intersystem crossing was responsible for decreasing of the relative intensity of the Eu^{2+} luminescence for temperature range 150 – 500 K and causes decreasing of the Eu^{2+} to Eu^{3+} luminescence intensity ratio for temperature higher than 150 K. Luminescence decays were measured for selected temperatures and pressures. At 10 K the decays of Eu^{3+} luminescence were single-exponential, with time constant being 3.6 ms. When temperature increases all emissions decay faster and become multiexponential. Decay times slightly decreased with increasing pressure. In the range of 10 – 400 K the decays of $4f^65d \rightarrow 4f^7$ emission in the Eu^{2+} were single-exponential, with time constant being 0.65 μs , 0.62 μs and 0.35 μs for A, B and C emission bands, respectively, and did not depend on temperature. At higher temperatures (from 400 K to 500 K) the luminescence decays become shorter and non-exponential, as the result of thermal quenching. When pressure increases all emissions decay faster.

Luminescence Properties of Silicate Apatite Phosphors $M_2La_8Si_6O_{26}:Eu$ (M = Mg, Ca, Sr)

N. M. Khaidukov^a, M. Kirm^b, E. Feldbach^b, H. Mägi^b, V. Nagirnyi^b, E. Töldsepp^b,
 S. Vielhauer^b, T. Jüstel^c, T. Jansen^c, V. N. Makhov^d,

^aN. S. Kurnakov Institute of General and Inorganic Chemistry, 31 Leninskiy Prospekt, 119991 Moscow, Russia

^bInstitute of Physics, University of Tartu, 14c Ravila, 50411 Tartu, Estonia

^cMünster University of Applied Sciences, Stegerwaldstraße 39, 48565 Steinfurt, Germany

^dP. N. Lebedev Physical Institute, 53 Leninskiy Prospekt, 119991 Moscow, Russia

Silicate apatites are well-known hosts for high-efficiency and stable phosphors which are considered in particular as possible color converters for white light generation using LEDs (see, e.g. [1,2]). Within the crystal structure of silicate apatites ${}^{\text{IX}}\text{A}_{14}{}^{\text{VII}}\text{A}_2(\text{SiO}_4)_6\text{O}_2$ the alkaline earth (M^{2+}) and rare earth (Ln^{3+}) ions can occupy two crystallographic sites: a 9-coordinated tricapped trigonal prism site and a 7-coordinated distorted pentagonal bipyramid site. Owing to the presence of two sites, two types of emission centers for the dopants can be expected at least, which allows advanced materials engineering. Taking into account the features of the apatite structure [3] as well as the ionic radii of the ions involved one can expect that there are some differences in the luminescence properties of phosphors for Mg^{2+} -based and Sr^{2+} -based matrices. The Mg^{2+} ion having a small ionic radius tends to occupy preferably the A2-type sites in the matrix, which results in ${}^{\text{IX}}\text{La}_4{}^{\text{VII}}\text{La}_4{}^{\text{VII}}\text{Mg}_2(\text{SiO}_4)_6\text{O}_2$. Sr^{2+} ions having large ionic radii should occupy exclusively the A1-type sites, which corresponds to ${}^{\text{IX}}\text{Sr}_2{}^{\text{IX}}\text{La}_2{}^{\text{VII}}\text{La}_6(\text{SiO}_4)_6\text{O}_2$. However, Ca^{2+} -based phosphors are expected to show the features caused by the statistical distribution of the cations onto both crystallographic sites.

The ceramic phosphors, silicate apatites $M_2La_8(\text{SiO}_4)_6\text{O}_2$ (M = Mg, Ca or Sr) doped with ions of europium, were obtained by high-temperature solid-state reaction using the precursors synthesized under hydrothermal conditions. Some samples were annealed in H_2/Ar reducing atmosphere in order to convert Eu^{3+} into Eu^{2+} . The phosphors were characterized by XRD analysis and Raman spectroscopy. The photoluminescence under blue-to-VUV excitation as well as cathodoluminescence of these phosphors were studied for various concentrations of the doping ions.

Under excitation into the ($\text{O}^{2-} - \text{Eu}^{3+}$) charge transfer band (peaked near 275 nm) these phosphors show red luminescence due to the intraconfigurational 4f – 4f transitions of Eu^{3+} . The phosphors also exhibit a broad-band luminescence in the blue-to-yellow spectral region depending on the composition and treatment. The broad emission bands are assigned to interconfigurational 5d – 4f transitions of Eu^{2+} occupying different sites in the apatite matrix. The mechanisms of the $\text{Eu}^{3+}/\text{Eu}^{2+}$ luminescence excitation are discussed.

This research was performed within the ERA.Net RUS Plus Programme, project NANOLED # 361 (RFBR Grant 16-52-76028 ERA_a).

References:

- [1] Y. Shen, R. Chen, G. G. Gurzadyan, et. al., Opt. Mater. 34 (2012) 1155.
- [2] J. Sokolnicki, E. Zych, J. Lumin. 158 (2015) 65.
- [3] G. Blasse, J. Solid State Chem. 14 (1975) 181.

Optically Properties of K_2SO_4 Doped by Transition Metal Ions

Koketai T.A., Tussupbekova A.K., Baltabekov A.S., Turmukhambetova E.T., Mussenova E.K.

Ye.A. Buketov Karaganda State University, Karaganda, Kazakhstan

The absorption spectrum depending on the thickness of the crystal are measuring in this paper. Figure 1 shows the absorption spectrum of a single crystal $K_2SO_4-Ni^{2+}$ was measured at the room temperature.

There are three absorption bands in the spectrum (Fig. 1). The first absorption band starts at 5.17 eV and extends to the far ultraviolet region. The second absorption band has a maximum absorption near 4.13 eV. The third absorption band is observed only in crystals of a thickness exceeding 2.5 mm and has a maximum near 2.95 eV.

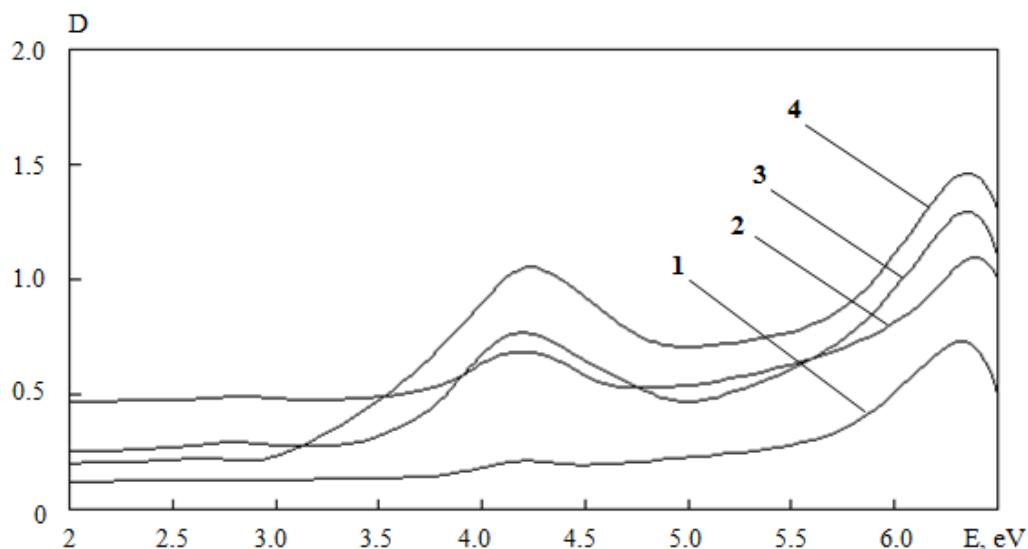


Figure 1. Absorption spectra of $K_2SO_4-Ni^{2+}$:

1 – $d=0.66$ mm; 2 – $d=1.74$ mm; 3 – $d=2.78$ mm; 4 – $d=3.59$ mm

Regardless of the concentration of nickel sulfate in the feed solution (0.2 mol% to 3.0 mol%) in the optical density of impurity absorption bands are linearly dependent on the sample thickness. Implementation of the Bouguer-Lambert-Beer law shows that the observed absorption is due to absorption centers, uniformly distributed in the bulk of the crystal. Consequently absorbing impurity centers uniformly distributed throughout the sample volume. By increasing the salt content of the impurity in the initial solution linearity is broken. Since the new absorption bands do not appear, the observed previously linearity due to the deficiency of the samples.

Energy transfer and Spectroscopic Properties of UV Active Media $\text{Ce}^{3+}:\text{LiCa}_{1-x}\text{Sr}_x\text{AlF}_6$

A A Shavelev, A S Nizamutdinov, V V Semashko, M A Marisov

Kazan Federal University, 420008, Kremlevskaja str., 18, Kazan, Russian Federation

Fluoride crystals of colquiriite structure LiCaAlF_6 and LiSrAlF_6 doped by Ce^{3+} are known as the most practically useful active media for generation and amplification of UV light despite low isomorphous capacity for Ce^{3+} ion and multicenter character of activation [1-3].

As it was shown earlier [4,5] changing the chemical content in mixture of homologous crystals give an opportunity to manage impurity ions segregation coefficient, optical properties and photochemical stability. Information on energy transfer between impurity centers of different symmetry in $\text{LiCa}_{1-x}\text{Sr}_x\text{AlF}_6$ and chemical content influence on this energy transfer could open the way to manage and improve lasing characteristics and optical properties of these crystals. Here we report on spectroscopic properties of series of mixed crystals $\text{Ce}^{3+}:\text{LiCa}_{1-x}\text{Sr}_x\text{AlF}_6$ grown by Bridgeman technique at room and low temperatures, energy transfer peculiarities between Ce^{3+} centers.

Optical absorption spectroscopy studies have shown that mixed crystals $\text{Ce}^{3+}:\text{LiCa}_{0.2}\text{Sr}_{0.8}\text{AlF}_6$ exhibit more than 3 times higher absorption coefficient compared to $\text{Ce}^{3+}:\text{LiCaAlF}_6$ sample and CeF_3 component content in the melt was the same for these two charges. We report time-resolved 5d-4f luminescence studies of Ce^{3+} in colquiriite type mixture crystals at temperatures in the range 300-5K.

Herewith mixture crystals exhibit higher relative intensity of luminescence for short wavelength centers, which appear to be active lasing centers mostly [3]. Our preliminary results are that redistribution of Ce^{3+} impurity centers appears in mixture crystals matrix in the favor of short wavelength emitting centers. And this leads benefits as higher gain coefficient at longer wavelengths and higher lasing efficiency due to lower energy transfer rates between centers in comparison to LiCaAlF_6 and LiSrAlF_6 matrices. Also we report on optical gain studies of 5d-4f transitions of Ce^{3+} ions in $\text{LiCa}_{1-x}\text{Sr}_x\text{AlF}_6$.

ACKNOWLEDGEMENTS

The work was performed under the framework and the financial support of Russian Scientific Foundation grant (project №15-12-10026).

REFERENCES:

- [1] M. Dubinskii, V. Semashko, A. Naumov, R. Abdulsabirov, S. Korableva, J. Modern Opt. 40 (1993) 1
- [2] T. Le, S. Schowalter, W. Rellergert, J. Jeet, G. Lin, N. Yu, E. Hudson, Optics Letters 37 (2012) 4961
- [3] V. Semashko, M. Dubinskii, R. Abdulsabirov, A. Naumov, S. Korableva, N. Scherbakova, Las. Phys., 5 (1995) 69
- [4] V. Castillo, G. Quarles, R. Chang, Proc. of SPIE 4970 (2003) 22-34.
- [5] Nizamutdinov, V. Semashko, A. Naumov, V. Efimov, S. Korableva, M. Marisov, JETP Letters 91 (2010) 21.

Theoretical study on photoinduced nucleation dynamics by injection of THz optical pulses

Kunio Ishida¹ and Keiichiro Nasu²

1. Corporate Research and Development Center, Toshiba Corporation, Kawasaki, Japan

2. Institute of Materials Structure Science, KEK, Tsukuba, Japan

Recent progress of intense optical pulse generation technology has made it possible to inject coherent phonons in a macroscopic scale[1], and the lattice deformation induced by such a process will cause electronic transitions in strongly coupled electron-phonon systems. Based on the analogy to the photoinduced phase transitions observed in various materials, we consider that cooperative interactions between electrons and coherent phonons will lead to the multiplication of excited electrons and/or growth of a transient phase, which is understood by bifurcation of quantum-mechanical wavepackets on adiabatic potential energy surfaces. Taking a model of localized electrons coupled with a quantized optical phonon mode, we have discussed the dynamics of the cooperative phenomena by THz pulse irradiation and, in particular, the role of the number and/or the initial distribution of phonons in the initial creation process of transient phases[2].

In this paper, we consider “double-pulse” experimental configurations in which intense THz pulses are irradiated to the system after pump pulses with shorter wavelength. In this case the THz pulses instantaneously generate multiple phonons during relaxation processes, and hence they affect the dynamics of photoinduced nucleation in strongly coupled electron-phonon systems.

In order to study the effect of the creation/annihilation of phonons during nucleation, we employ a model of electron-phonon systems in which each electron is localized in molecules arrayed on a square lattice. We have shown that this model is useful to reveal the nonadiabatic dynamics of photoinduced nucleation[2,3]. Applying a method of large deviation statistics[3], we calculated the power spectra regarding the distortion of the molecule at each site, and show that the resonance frequency of molecular vibration varies with the progress of nucleation. In particular, these frequencies are different between the molecules inside and outside of photoinduced nuclei. Hence, the relaxation dynamics of the system changes after creation/annihilation of phonons by THz optical pulses. These results show that it is possible to modulate the nucleation dynamics by choosing an appropriate frequency of THz pulses which is resonant to the vibration of molecules inside or outside of the nuclei.

References:

- [1] M. Hase et al. Nat. Photonics 6 (2012) 243.
- [2] K. Ishida and K. Nasu, J. Phys.: Conf. Ser. 633 (2015) 012061.
- [3] K. Ishida and K. Nasu, Phys. Rev. B 80 (2009) 140301.

Ultra-short Pulse Lasing from $\text{LiLu}_{0.7}\text{Y}_{0.3}\text{F}_4:\text{Ce}^{3+}$

A.S.Nizamutdinov, I.I.Farukhshin, V.V.Semashko, S.L.Korableva, M.A.MarISOV
Kazan Federal University, 420008, Kremlevskaja str., 18, Kazan, Russian Federation

Today new technologies express demands on lasers oscillating in ultraviolet (UV) spectral range and having short pulse duration [1]. One of perspective methods of obtaining UV lasing is using of fluoride crystals doped by Ce^{3+} ions as active media. Interconfigurational transitions of Ce^{3+} ions are characterized by large cross-sections and significant broadening thus providing short pulses with duration from several to tens of nanoseconds and even in subnanosecond time domain directly in UV [2]. But this also opens the complex picture of photodynamic processes in UV active medium resulting in formation of color centers [2]. This gives an opportunity to utilize the color center losses for arrangement the modulation of Q-factor of the cavity or even mode-locking. Thus formation of color centers turns the UV active medium into multifunctional material working as gain medium and modulator at the same time.

The aim of this work was obtaining UV laser oscillation in ultra-short pulse mode from $\text{LiLu}_{0.7}\text{Y}_{0.3}\text{F}_4:\text{Ce}^{3+}$ (Ce:LLYF) and modulation of dynamic processes via pumping radiation, additional irradiation and temperature.

As it was investigated earlier [3] level of losses due to color centers doesn't remain constant during experiment. It depends on bleaching factors i.e. amount of laser radiation inside the cavity, the external additional irradiation [4] and temperature [3,4]. We have obtained 400 ± 50 ps single short laser pulses in Ce:LiY_{0.3}Lu_{0.7}F₄ crystals at 311 nm with slope efficiency as high as 6 % for low Q-factor cavity under 6 ns pulses at 10 Hz pumping by Ce:LiCAF laser at 289 nm. Intracavity losses modulation alike Q-switching was demonstrated by laser color centers bleaching. Ce:LYLF single crystals can be operated as active media and Q-switching device at the same time. Thus measured contrast of losses level dependence on pump energy appeared to be 1.8. The results demonstrate a "saturated absorber" operation. Additional irradiation of active medium at 532 nm increases the slope efficiency up to 6.2 % and it is accompanied by a 600 ps second laser pulse generated 2.5 ns after the first one. Bleaching of color centers is accompanied by lowering the average losses in the cavity and increasing the slope efficiency.

By means of simulation fitted to experimental results some parameters of dynamic processes in our active medium were obtained. The significant probability of capture of an electron by defect from CB ($(7.1 \pm 0.9) \cdot 10^9 \text{ s}^{-1}$) speaks for high speed of saturated state vanishing, large color centers absorption cross section at lasing wavelength ($(4.0 \pm 1.2) \cdot 10^{-18} \text{ cm}^2$) provides significant contrast ratio of saturable absorber. This opens the way to manage the amount of color centers and saturable absorber contrast ratio and temporal distribution of laser pulses.

REFERENCES:

- [1] A. Saliminia, A. Proulx, R. Vallée, Optics Communications 333 (2014) 133
- [2] N. Sarukura, Z. Liu, Y. Segawa, V. Semashko, A. Naumov, S. Korableva, R. Abdulsabirov, M. Dubinskii, Opt. Lett. 20 (1995) 599
- [3] V.V. Semashko, M.A. Dubinskii, R.Yu. Abdulsabirov, S.L.Korableva, A.K. Naumov, A.S. Nizamutdinov, M.S. Zhuchkv, Proc. of SPIE 4766 (2002) 119
- [4] L. A. Nurtdinova, S. L. Korableva, Las. Phys. Lett. 11 (2014) 12580

YAG:Ce³⁺ nanoceramics: spectroscopy, dynamics and TSL

Q. Shi¹, A. Ishchenko¹, V. Osipov², V. Shitov², R. Maksimov^{1,2}, K. Lukyashin², V. Platonov², M. Sarychev¹, R. Abashev¹, B. Shulgin¹, A. Belsky³, N. Fedorov⁴, P. Martin⁴, and K. Ivanovskikh¹

¹Ural Federal University, Ekaterinburg, 620002, Russia

²Institute of Electrophysics UrB RAS, Ekaterinburg, 620016, Russia

³Institut Lumière Matière, UMR 5306, CNRS-Université Lyon 1, 69621 Villeurbanne, France

⁴CELIA, UMR 5107, Université de Bordeaux-CNRS-CEA, 33405 Talence, France

Ceramic technology offers design flexibility on a macro and micro level allowing development of cost effective large size scintillators and laser media as well as high-output microchip optics. An important issue arising along is related to the need for better understanding of defect structure and energy transfer peculiarities in the new kind of optical media. Herewith, we report on synthesis and characterisation of a series of highly transparent YAG:Ce³⁺ nanoceramic samples. The samples were prepared via solid-state reaction that is followed by a precalcining procedure [1]. The characterisation included T-dependent measurements of X-ray excited emission spectra, transmission spectra, thermally stimulated luminescence (TSL) glow curves and emission decay kinetics. The latter were taken upon excitation with synchrotron radiation in the range of 4-25 eV at SOLEIL facility (France).

As expected, exciton and defect emission showed quenching upon rising of temperature and Ce³⁺ concentration. Decay curves of YAG:Ce³⁺ revealed appearance of slow decay components and build-up upon excitation above fundamental absorption edge. Delayed host-to-Ce³⁺ energy transfer arises due to retrapping of electronic excitations on shallow traps of different nature. Excitonic energy transfer process was most effective for sample with 5% of Ce³⁺. The TSL measurements (Fig. 2) suggest that the shallow traps appeared below 100 K are reduced if compared to single crystals and other kinds of ceramics reported before [2].

Overall results indicate that the novel YAG:Ce³⁺ ceramics have improved structure in terms of distribution of defects and traps being of valuable potential for the development of bright and fast ceramic scintillators.

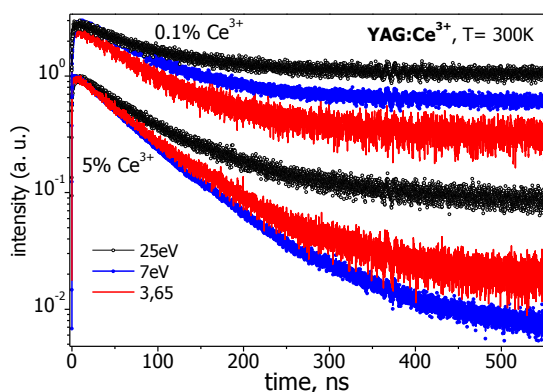


Fig. 1 Decay kinetics of YAG:Ce³⁺ at RT

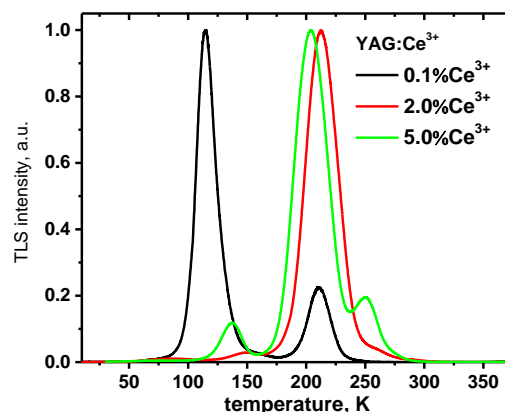


Fig. 2 X-ray excited TSL for YAG:Ce³⁺

References:

- [1] V.V. Osipov, K.E. Lukyashin, et al., Mater.Lett., 167 (2016) 81.
 [2] E. Mihóková, M. Nikl, J.A. Mareš, et al., J.Lumin.126 (2007) 77.

Radiative and nonradiative recombination in Si-doped InN thin films

Der-Jun Jang,*AntaryamiMohanta, C.-F. Tseng, and Li-WeiTu

Department of Physics, National Sun Yat-Sen University, Kaohsiung,80424, Taiwan, Republic of China.

The time-integrated and time-resolved photoluminescence were measured to study the radiative and nonradiative recombination in InN thin films grown by molecular beam epitaxy on sapphire substrates with GaN buffer layers. Using the van der Pauw Hall geometry, four different InN samples with mobilities of 757, 945, 832, and 115 cm²/Vs and background concentrations of 6.16×10¹⁸, 8.50×10¹⁸, 2.28×10¹⁹ and 1.27×10²⁰ cm⁻³ for the undoped sample I, Si-doped samples II, III, and VI, respectively, were obtained. Carrier concentration of 1.5×10¹⁹ cm⁻³ was photo-generated for all samples.

Radiative recombination in undoped and Si-doped InN thin films was found to be ineffective due to significant nonradiative recombination. The trap density and the Shockley-Read-Hall recombination rates were found to increase with increasing doping density. The SRH cross section were estimated to be 1.5~3.5× 10⁻¹⁶ cm. Auger recombination was found effective in these samples due to high background carrier density. We elucidate the discrepancies of the recombination rates determined from the Gourdon's model and those from the rate equation may due to the prominent nonradiative recombination by the Auger and Shockley-Read-Hall (SRH) recombination at high background concentrations.

Dynamics of changes in optical absorption induced by exposition to short- and long-wavelength radiation in the BTO:Al crystal

**S. Shandarov¹, V. Dyu¹, M. Kisteneva¹, E. Khudyakova¹, Yu. Kargin²,
T. Kornienko³, A. Tolstik³**

¹State University of Control System and Radioelectronics, Tomsk 634050, Russia

²A.A. Baikov Institute of Metallurgy and Materials Science RAS, Moscow 119991, Russia

³Belarusian State University, Minsk 220030, Belarus

Insistent behavior of the changes in the spectral dependences of optical absorption induced in the bismuth titanium oxide crystal doped by aluminum (BTO:Al) as a results of sequential exposition to cw laser radiation first with the wavelength $\lambda_d = 532$ nm and then with the longer wavelength λ_l has been recently discovered [1]. To account for observed dependence of an achievable bleaching of the BTO:Al crystal preliminary darkened by radiation with $\lambda_d = 532$ nm on the wavelength λ_l the model based on configuration coordinate diagram for deep-level defects characterized by large lattice relaxation is appropriate. We report here on the experimental study and the theoretical consideration of the dynamics of the changes in absorption induced by laser beams with the wavelengths $\lambda_d = 532$ nm and $\lambda_l = 655$ nm in the (100)-cut BTO:Al crystal with a thickness of 6.6 mm.

We study experimentally the absorption-coefficient dynamics in the BTO:Al crystal by using two techniques. First, the photoinduced absorption variations were caused by a strong light beam with the darkening wavelengths $\lambda_d = 532$ nm, while the changes in absorption were monitored by the sample transmission of weak radiation with another wavelength $\lambda_l = 655$ nm. Second, we measured the temporal behaviour of the changes for inherent absorption induced by a single laser beam with the wavelength $\lambda_d = 532$ nm or $\lambda_l = 655$ nm. In this case the enhanced transmittance of the crystal with monotonic time dependences were observed for $\lambda_l = 655$ nm, whereas for light with $\lambda_d = 532$ nm the crystal darkening was characterized by more complicated dynamics. In particular, we observed the time oscillations of the changes in light absorption for $\lambda_d = 532$ nm, which had been described previously [2] for Bi₁₂SiO₂₀:Al crystals in the absorption bands with $\lambda_{max} = 1590$ and 397 nm.

For a theoretical interpretation of experimental results we have considered the photoinduced electronic transitions between the ground and excited states of the deep-level defects characterized by large lattice relaxation in the frame of the model based on configuration coordinate diagram [3]. The changes in light absorption at these transitions result from different cross-sections of photoexcitation for such defects occupied the ground and excited states.

References:

- [1] V.G. Dyu, M.G. Kisteneva, S.M. Shandarov, E.S. Khudyakova, S.V. Smirnov, and Yu.F. Kargin, Physics Procedia 73 (2015) 131.
- [2] T.V. Panchenko, A.A. Dyachenko, and O.V. Khmelenko, Phys. Solid State 57 (2015) 771.
- [3] Y. Shinozuka, Jpn. J. Appl. Phys. 33 (1993) 4560.

Basic Principles of Ion Beam Induced Luminescence and its Application to the Study of Electronic Excitation in Insulators

Diana Bachiller-Perea^{1,2}, David Jiménez-Rey³, Ángel Muñoz-Martín¹,
Fernando Agulló-López¹

¹*Centro de Micro-Análisis de Materiales, Universidad Autónoma de Madrid, Calle Faraday 3, E-28049, Spain*

²*Centre de Sciences Nucléaires et de Sciences de la Matière, Université Paris-Sud, Bât 108, 91405 Orsay, France.*

³*Laboratorio Nacional de Fusión, Ciemat, Madrid, Spain.*

Luminescence is a very sensitive technique to identify and investigate optically-active point defects (color centers) in dielectric materials. As an example, for SiO₂ the correlation between optical absorption and photoluminescence has allowed to identify a number of relevant color centers [1]. On the other hand, luminescence during irradiation is a useful tool to investigate the generation of point defects by the irradiation and to reveal the operative mechanisms. An increasing number of papers is recently being devoted to understand the defects produced by irradiation with high-energy ion-beams on SiO₂ and their correlation with the associated luminescence processes (ionoluminescence)[2,3]. The light emission mechanisms are, indeed, of an electronic nature and so they may help to clarify the processes induced by the electronic excitation and stand out the differences with the elastic collision processes. One main intrinsic advantage of the ionoluminescence technique over other spectroscopic methods (optical absorption, Raman, Electronic Paramagnetic Resonance) is that spectra are obtained *in situ*, not requiring interruption of the irradiation and so avoiding the influence of possible recovery effects.

This poster presents the basic principles of the ionoluminescence technique as a support to the oral presentation: "Ionoluminescence as a Tool to Investigate the Dynamics of Electronic Excitations in Dielectrics: the Case of SiO₂". We present also some examples of how external factors (*e.g.*, temperature, stopping power of the incident ions, impurities in the sample) can affect the electronic processes and, therefore, the ionoluminescence signal.

References:

[1] A.N. Trukhin, J. Non-Cryst. Solids 357 (2011) 1931-1940.

[2] D. Bachiller-Perea, D. Jiménez-Rey, A. Muñoz-Martín and F. Agulló-López, J. Non-Cryst. Solids 428 (2015) 36-41.

[3] D. Bachiller-Perea, D. Jiménez-Rey, A. Muñoz-Martín and F. Agulló-López, J. Phys. D: Appl. Phys. 49 (2016) 085501.

Theoretical modeling of transition metals tetroxoanions adsorption on N(B)-doped single-walled carbon nanotubes and graphene

Hizhnyi Yu.¹, Borysiuk V.¹, Nedilko S.¹, Shyichuk A.²

¹Taras Shevchenko National University of Kyiv, 64/13 Volodymyrska st.,
01601 Kyiv, Ukraine

²Department of Rare Earth, Faculty of Chemistry, Adam Mickiewicz University, Umultowska
89b, 61-614 Poznań, Poland

Tetroxoanions XO_4^{2-} of hexavalent transition metals are toxic industrial pollutants and their removal from industrial wastes is a topical technological problem [1]. Carbon nano-structured materials, in particular carbon nanotubes (CNTs) and their assemblies are intensively studied at present as materials for efficient removal and storage of various toxic molecules. The XO_4^{2-} anions are characterized by well-distinguished bands of optical absorption, observed in particular when the anions exist in gaseous phase or are solved in aqueous solutions. The optical absorption bands of XO_4^{2-} anions can be independently predicted in the electronic structure-related computational modeling by calculations of the energies of their excited electronic states and corresponding transition probabilities. Such prediction can contribute to development of novel optical methods for monitoring the XO_4^{2-} anions adsorption on carbon nano-structured materials and this can be particularly important for the toxic waste remediation task.

In this work, adsorption of XO_4^{2-} molecular oxyanions on the surfaces of undoped, B(N)-doped carbon nanotubes is analyzed in computational studies. A geometry-optimized calculations of the electronic structure of undoped, B- or N-doped CNTs of (3,3) and (5,5) chiralities with adsorbed XO_4^{2-} oxyanions of various hexavalent transition metals are carried out within molecular cluster approach by Gaussian 03 program package [2]. Relaxed geometries, binding energies between the adsorbates and the nanotubes, charge states of the adsorbates, energies of excited states of adsorbed XO_4^{2-} anions are calculated and analyzed. The optical absorption spectra of XO_4^{2-} anions adsorbed on the CNTs surfaces are calculated and compared with corresponding experimental data. Obtained results are supplemented by calculations of adsorption of XO_4^{2-} oxyanions on B(N)-doped graphene sheets which are considered as model approximation for large-diameter CNTs.

Obtained results are analyzed together with existing experimental data on the optical and luminescence properties of carbon/oxide composites. The influence of the B(N) doping on the type of chemical bonding between XO_4^{2-} anions and CNTs is revealed. Possibilities for spectroscopic monitoring of the XO_4^{2-} anions removal from industrial wastes by carbon nano-structured materials are outlined.

References:

- [1] N. Tarutani, Ya. Tokudome, M. Fukui, et al. // RSC Adv. 5 (2015) 57187.
[2] M.J. Frisch, G.W. Trucks, H.B. Schlegel, et al. // Gaussian 03 (Gaussian, Inc., Wallingford, CT, 2003).

Luminescence and Upconversion spectroscopy of $\text{Er}^{3+}/\text{Yb}^{3+}$ -doped $\text{Y}_3\text{Ga}_5\text{O}_{12}$ nano-garnets for optical nano-devices

V. Monteseuro^{1,2}, V. Venkatramu³, S. F. León Luis², U. R. Rodríguez-Mendoza², C. K. Jayasankar⁴ and V. Lavín²

¹European Synchrotron Radiation Facility, BP 220, 38043 Grenoble, France.

²Departamento de Física and MALTA Consolider Team, Universidad de La Laguna. 38200 San Cristóbal de La Laguna, Santa Cruz de Tenerife, Spain.

³Department of Physics, Yogi Vemana University. Kadapa 516 003, India.

⁴Department of Physics, Sri Venkateswara University. Tirupati 517 502, India.

In the last decades, nano-structured garnets are being used in different applications in the field of the nano-technology since recent works have demonstrated that they conserve the great chemical and physical properties of their analogous bulk garnet crystals [1, 2]. Therefore, the combination of the great luminescence properties of rare earth (RE^{3+})-doped nano-garnets and the high optical transparency and mechanical and chemical stability of these nano-garnets make them extremely useful as solid-state lasers, scintillators and also as temperature and pressure NIR optical sensors. Moreover, there is considerable interest in upconversion emission from lanthanide (Ln^{3+})-doped nano-crystals because offers an attractive optical labeling technique in biological studies without many of the constraints associated with organic fluorophores and quantum dots. The Upconversion technique utilizes near infrared (NIR) excitation, thereby significantly minimizing background autofluorescence, photobleaching, and photodamage to biological specimens [3].

Concretely, our work is based in stokes and anti-stokes luminescence of the Er^{3+} -doped and $\text{Er}^{3+}, \text{Yb}^{3+}$ co-doped $\text{Y}_3\text{Ga}_5\text{O}_{12}$ nano-garnets for comparison. These nano-garnets have been synthesized by sol-gel method as nano-powders and they crystallize in the bcc structure (Ia-3d) and have 160 atoms in the unit cell. The garnet crystal structure can be described as a network of GaO_6 octahedra, GaO_4 tetrahedra and YO_8 dodecahedra. The Stark levels in luminescence spectra, with an intense green emission and weak emissions in the red and NIR regions, confirm that Er^{3+} and Yb^{3+} ions are incorporated to dodecahedra with D_2 symmetry of the garnet structure. When the Yb^{3+} ions are excited at 970 nm, a very bright green luminescence of the Er^{3+} ions is observed by the naked eyes, even for low laser power as 15 mW. The red upconverted emission increases compared to that found under direct excitation of the Er^{3+} ions. The power dependency and the dynamics of the infrared-to-visible upconverted luminescence show the existence of different two-photon ETU processes for the green and the red upconverted emission. These results make this nano-material interesting for its use as an upconversion phosphors, upconverted lasers and optical labels for biological studies in the green and red region under NIR excitation.

References:

[1] V. Monteseuro et al. Phys.Chem.Chem.Phys. 17 (2015) 9454.

- [2] V. Monteseuro et al. *J. Phys. Chem. C*, 118 (2014) 13177–13185.
[3] F. Wang and X. G. Liu. *Chem. Soc. Rev.* 38 (2009) 976-989.

Blue upconversion emission of Cu²⁺ ions sensitized by Yb³⁺-trimers in CaF₂

Weiping Qin* and Tuerxun-Aidilibike

State Key Laboratory on Integrated Optoelectronics, College of Electronic Science and Engineering, Jilin University, Changchun, Jilin 130012, China.

Under 978 nm near-infrared (NIR) excitation, blue upconversion (UC) emissions from CaF₂:Cu²⁺, Yb³⁺ was first observed at ~420 nm. It was ascribed to the 3d⁸4s¹ → 3d⁹ transition of Cu²⁺ ions. From transient measurements, the UC process was found to be dominated by the energy transfer process that three excited Yb³⁺ ions simultaneously transfer their energy to one Cu²⁺ ion. The influence of Cu²⁺ concentration and temperature on the UC emission as well as Jahn-Teller effect was also investigated.

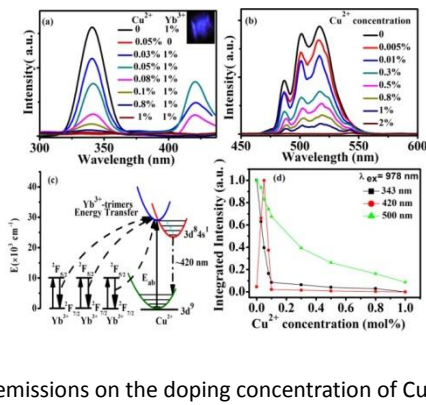


Fig.1. (a) Emission spectra (300-450 nm) of CaF₂: x%Yb³⁺, y%Cu²⁺ (x=0, 1; y=0.03, 0.05, 0.08, 0.1, 0.8, 1, 2) upon 978 nm excitation at room temperature. (b) Emission spectra (450-600 nm) of CaF₂:1%Yb³⁺, y%Cu²⁺ (y=0, 0.005, 0.01, 0.3, 0.5, 0.8, 1, 2) with various Cu²⁺ doping upon 978 nm excitation at room temperature. (c) Schematic energy level diagram of Yb³⁺ and Cu²⁺. The cooperative energy transfer from three excited Yb³⁺ ions to one Cu²⁺ ion is exhibited by using dash black arrows. (d) Integrated intensity dependences of 343 nm, 420 nm, and 500 nm UC emissions on the doping concentration of Cu²⁺.

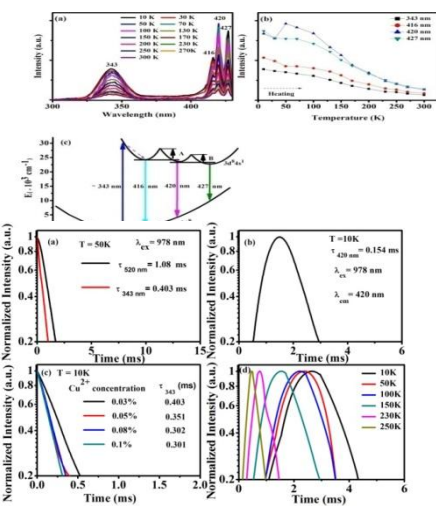


Fig.2. (a) Emission spectra of CaF₂:1% Yb³⁺, 0.05% Cu²⁺ powder taken at different temperature upon 978 nm excitation. (b) Integrated emission intensity of CaF₂:1%Yb³⁺, 0.05% Cu²⁺ at various temperatures during heating. (c) Schematic configurational coordinate diagram of Cu²⁺ ions.

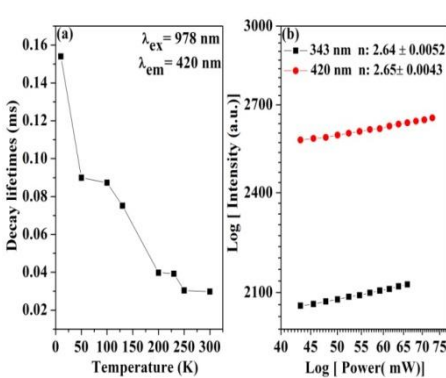


Fig.3. (a) Fluorescence decay curves of 520 nm and 343 nm CLs. (b) Fluorescence decay curve of the UC luminescence at 420 nm from Cu²⁺ ions upon 978 nm excitation (c) Fluorescence decay curves of 343 nm cooperative luminescence (CL) from Yb³⁺-trimers with different Cu²⁺ concentrations under 978 nm excitation in CaF₂: 1%Yb³⁺, y%Cu²⁺ (y=0.03, 0.05, 0.08, 0.1 mol%) at 10 K, respectively. (d) Decay curves of Cu²⁺ emission of CaF₂: 1% Yb³⁺, 0.05% Cu²⁺ at various temperatures (10-250 K).

Fig.4. (a) Life times of Cu²⁺ ions as a function of temperature (b) Double-logarithmic plots of the pump-power dependent UC emission intensity recorded under 978 nm excitation.

Reference

1. F. Auzel, "Upconversion and anti-stokes processes with f and d ions in solids," *Chem. Rev.* **104**, 139 (2004).
2. W. P. Qin, Z. Y. Liu, C. N. Sin, C. F. Wu, G. S. Qin, Z. Chen, and K. Z. Zheng, "Multi-ion cooperative processes in Yb³⁺ clusters," *Light: Sci. Appl.* **3**, e193 (2014).
3. W. P. Qin, S. Cholnam, Z. Y. Liu, G. S. Qin, and C. F. Wu, "Theory on cooperative quantum transitions of three identical lanthanide ions," *J. Opt. Soc. Am. B* **32**, 303 (2015).

*E-mail: wpgin@jlu.edu.cn

Energy migration in doped crystals

Freddy T. Rabouw & Andries Meijerink

¹ *Optical Materials Engineering Laboratory, Institute of Process Engineering, ETH Zürich, Switzerland*

² *Condensed Matter and Interfaces, Debye Institute for Nanomaterials Science, Universiteit Utrecht, The Netherlands*

Crystals doped with luminescent ions are widely used as phosphors in light emitting diodes, fluorescent tubes, displays, as gain medium in solid-state lasers, or as nanosize biolabels. The luminescent ions act as discrete optical centers that can absorb or emit photons. After the absorption of a photon, the energy is usually partially dissipated by internal relaxation on the absorber ion and/or by energy transfer to other types of dopant ions. Eventually, light with a lower photon energy is emitted. In some materials, upconversion is possible: the material can emit photons of higher energy than it absorbs, following energy transfer steps between dopant ions in which the absorption energy is collected on one type of ion.

In these materials, the active ions usually substitute non-luminescent cations of the host. One would naively expect that in order to make the emission brighter, the dopant concentration in the host must simply be increased because this enhances the absorption and emission rates. However, high dopant concentrations bring along the possibility that the absorbed energy migrates by hopping from dopant to dopant. This phenomenon is advantages for some applications if the energy reaches an intentional acceptor ion eventually [1]. On the other hand, it leads to “concentration quenching” if the energy reaches a quenching site [2].

We will present Monte Carlo simulations of energy migration, energy transfer and concentration quenching. The commonly employed diffusion model for energy migration by Yokota & Tanimoto [3; 651 citations] gives a very poor match to our Monte Carlo results. Energy migration affects the decay dynamics less strongly than predicted by the Yokota–Tanimoto model. The difference arises because the model neglects the discreteness of the crystal host and the randomness of dopant substitution. Our results imply that Yokota–Tanimoto fitting of photoluminescence decay curves cannot provide accurate estimates for energy diffusion constants and that Monte Carlo simulations are required to provide insight in the dynamics of energy migration and concentration quenching.

References:

- [1] F. Wang, R. Deng, J. Wang, Q. Wang, Y. Han, H. Zhu, X. Chen & X. Liu, *Nat. Mater.* **9** (2011), 968–973
- [2] R. Martín-Rodríguez, F. T. Rabouw, M. Trevisani, M. Bettinelli & A. Meijerink, *Adv. Opt. Mater.* **3** (2015), 558–567
- [3] M. Yokota & O. Tanimoto, *J. Phys. Soc. Jap.* **22** (1967), 779–784

Luminescent properties of Ce³⁺-doped germanate scintillating glasses

Shan Qian, Lihui Huang, Kangying Shu, Shiqing Xu

Hangzhou 310018, China

With respect to scintillating crystals, scintillating glasses have the advantages including low production cost, easy shaping of elements, possibility to incorporate activator ions at high concentrations and in the ease of manufacture in different sizes and shapes [1-4]. Scintillating glasses could have applications in high-energy physics, industrial and medical imaging fields. Compared to RE-doped silicate glasses, RE-doped germanate glasses exhibit lower phonon energy and consequently could have higher luminescence efficiency. Recently, RE-doped germanate glasses were developed successfully by melt-quenching method. In this paper, the luminescent properties of Ce³⁺-doped germanate glasses were investigated.

References:

- [1] S. Baccaro, A. Cevilia, A. Cemmi, G. Chen, E. Mihokova, N. Nikl, IEEE Trans. Nucl. Sci., 2001, NS-48, 360.
- [2] M. J. Weber, J. Lumin., 2002, 100, 35.
- [3] G. P. Pazzi, P. Fabeni, C. Susini, M. Nikl, E. Mihokova, N. Solovieva, K. Nitsch, M. Martini, A. Vedda, S. Baccaro, A. Cevilia, V. Babin, Nucl. Instrum. Methods B, 2002, 191, 366.
- [4] J. Fu, M. Kobayashi, J. M. Parker, J. Lumin., 2008, 128, 99.

The Influence of Point Defects on Amplification and Spectral Characteristics of InGaAs-based Laser Diode Arrays

**Katsiaryna A. Platnitskaya, Volha S. Kabanava, Dzmitry M. Kabanau,
Yahor V. Lebiadok**

*SSPA "Optics, Optoelectronics & Laser Technology", Minsk, Belarus
Belarussian State University, Minsk, Belarus*

The energy levels of gallium and arsenic vacancies as well as silicon impurities in the band gap of $\text{In}_x\text{Ga}_{1-x}\text{As}$ have been calculated as functions of the indium content. The calculation was conducted in the framework of density functional theory with the hybrid functionals B3LYP. The influence of defects on the lasing output power, spectral peculiarities and the optimal reflection coefficient of output mirrors of laser diode arrays (the lasing wavelength is about 940 nm) based on the $\text{In}_{0.11}\text{Ga}_{0.89}\text{As}/\text{AlGaAs}$ heterostructures has been estimated.

It has been shown that the lasing output power of laser diode arrays with active level containing defects with deep energy levels (charged and uncharged, excited and in the ground state) in the band gap is substantially lower (all other conditions being the same) than that of laser diode arrays with shallow level defects in their active layers. The influence of indium content in the InGaAs compound on the indium atoms clustering in the presence of point defects was estimated also.

The Exited States of Gallium and Nitrogen Vacancies in the GaN/AlN Heterointerface and Its Relaxation

Yahor V. Lebiadok, Dzmitry M. Kabanau, Katsiaryna A. Platnitskaya
SSPA "Optics, Optoelectronics & Laser Technology", Minsk, Belarus

The influence of gallium, nitrogen and aluminum vacancies on GaN/AlN heterointerface characteristics as well as its exited states were calculated. The density functional theory calculations with the hybrid functionals B3LYP [1] with Hay-Wadt effective core potentials [2] for all the heavy atoms in a combination with Hay-Wadt valence basis were used. All the calculations were performed using PC GAMESS-FireFly software [3]. The model cluster of GaN/AlN heterointerface with the mixing of gallium and aluminum atoms in the range of 0 - 100 % was under consideration.

The energy dependence of GaN/AlN clusters on different extent of gallium and aluminum atoms mixing in the interface was calculated. It was ascertain that the presence in the interface of nitrogen vacancy for cluster with 40% and more atom mixing facilitates the mixing of Ga and Al atoms in the AlN/GaN interface. It is known that the isolated nitrogen vacancies are formed in the GaN compounds under electron beam irradiation. So, the irradiation of GaN/AlN interface facilitates gallium and aluminum atoms mixing.

The exited states of complex defects such as gallium vacancy + interstitial gallium atom in the first and second coordinate sphere were calculated. The relaxation processes of the exited states relaxation are discussed in the report also.

References:

- [1] Hertwig R.H., Koch W., Chem. Phys. Lett., 268 (1997) 345
- [2] Hay P.J., Wadt W.R., J. Chem. Phys., 82 (1985) 299
- [3] <http://classic.chem.msu.su/gran/gamess/index.html>

Photonic Effects on Magnetic Dipole Transition Probabilities

Z. J. Wang, A. Meijerink*

Condensed Matter and Interfaces, Debye Institute for Nanomaterials Science, Utrecht University, Princetonplein 1, 3584 CC Utrecht, Netherlands.

*E-mail: A.Meijerink@uu.nl

Abstract:

The radiative transition probability, also known as spontaneously emission rate, is a fundamental property for an optical transition. In the past extensive research, both theoretical and experimental, has been conducted to establish the relation between the local density of states and electric dipole (ED) transition probabilities [1, 2]. Nanocrystals doped with luminescent ions are ideal as probes to test theoretical models. Recent work has established that the nanocrystal cavity model accurately describes the influence of the refractive index n of surrounding medium on ED transition rates for emitters in nanocrystals [2].

For magnetic dipole (MD) transitions theory predicts a simple n^3 dependence of the MD transition rate. However, experimental evidence is difficult to obtain [3]. In the present study, we use hydrophobic Eu^{3+} -doped core and core-shell nanocrystals (NC) (fluoride and tungstate NCs) suspended in apolar solvents with different refractive index n . As Eu^{3+} shows both pure ED and pure MD transitions, the influence of the refractive index on the ED and MD transition probabilities can be experimentally investigated. The ratio between the ED and MD transition rates and the total transition rate is in excellent agreement with the NC-cavity model for ED transitions and a n^3 dependence for MD transitions thus providing evidence for the theoretically predicted n^3 dependence.

Keywords:

Rare-earth, Magnetic Dipole transition, Electric Dipole transition, Refractive index

Acknowledgments:

This work was financially supported by the China Scholarship Council (No. 201506380101).

References:

- [1] T. Senden, F. T. Rabouw, A. Meijerink, *ACS Nano*, 9 (2015), 1801.
- [2] D. Topygin, *J. Fluoresc.*, 13 (2003), 201.
- [3] G. L. J. A. Rikken, Y. A. R. R. Kessener, *Phys. Rev. Lett.*, 74 (1995), 880.

Carbon segregation phenomena on $\text{Fe}_{0.85}\text{Al}_{0.15}$ (110) : a STM, LEED and XPS study

Surface structure of $\text{Fe}_{0.85}\text{Al}_{0.15}$ (110) single crystal in the ferritic phase is significantly influenced by carbon impurities inside the bulk. By combining Scanning Tunneling Microscopy (STM), Low Energy Electron Diffraction (LEED) and X-ray Photoelectron Spectroscopy (XPS), it was found that carbon impurities segregate on top of the reconstructed bare surface in the form of parallel stripes, spaced by approximately 8.6 nm. These stripes run along the [001] direction and have a temperature dependent coverage; terraces on surface are aligned in shape at higher temperatures, while the dominant step edges are parallel to the stripes at lower annealing temperatures. However, such kind of carbon segregation and self-organization phenomena along with regular terraces formation disappear after intensive sputtering/annealing cycles. The carbon free areas of the substrate show superstructure LEED diffraction spots which correspond to a local pseudo-hexagonal arrangement as imaged by STM (periodicity of 3 nm). This observation matches a FeAl_2 reconstruction model, which remains after disappearance of C segregation phenomena.

Authors: Z. Dai, P. Borghetti, G. Cabailh, J. Jupille, R. Lazzari.

Quantum wells based structures tested by polarized photoreflectance at room temperature

J. V. González-Fernández^a, J. Ortega-Gallegos^b, R. Díaz de León-Zapata^c,

J.-P. Galaup^a, A. Lastras-Martínez^b and R. E. Balderas-Navarro^b

^a *Laboratoire Aimé Cotton, CNRS UMR 9188, Université Paris-Sud, Bât. 505, 91405, Orsay cedex, France*

^b *Instituto de Investigación en Comunicación Óptica, Universidad Autónoma de San Luis Potosí, Av. Karakorum 1470, Lomas 4^a sección, C. P. 78210, San Luis Potosí, S. L. P., México.*

^c *Instituto Tecnológico de San Luis Potosí, Av. Tecnológico s/n Soledad de Graciano Sánchez, C. P. 78437, San Luis Potosí, S. L. P., México.*

Abstract

This work reports a visualization of interface optical anisotropies in III-V semiconductor based coupled double quantum wells (CDQWs) by extending the standard photoreflectance spectroscopy (PR) modulation technique through a contrast in polarization along [110] and [010] crystallographic directions.^[1]

By probing the in-plane interfacial optical anisotropies, we demonstrate that polarized PR spectroscopy (also termed photoreflectance anisotropy, PRA) has the capability to detect and distinguish buried layers with quantum dimensions at room temperature based on a linear electro-optic effect (LEO) through a piezoelectric shear strain. In this work, the observed quantum levels are associated to 11H and 22H transitions, both with a heavy hole character for each one analysed CDQWs structures. The notation *mnH* indicates transitions from the *m*th conduction to the *n*th valence subbands.^[2]

We propose to use photoreflectance anisotropy as a simple, fast, non-destructive and complementary tool for analysing anisotropic quantum structures with polarizable defects or anti-symmetries such as quantum dots, wells and wires; or even more complicated systems such as quantum cascade lasers or high electron mobility transistors.

References:

- [1] A. Lastras-Martínez, R. E. Balderas-Navarro, L. F. Lastras-Martínez and M. A. Vidal. *Phys. Rev. B* **59**, (1999) 10234.
- [2] J. V. González-Fernández, R. Herrera-Jasso, N. A. Ulloa-Castillo, J. Ortega-Gallegos, R. Castro-García, L. F. Lastras-Martínez, A. Lastras-Martínez, R. E. Balderas-Navarro, T. Mozume and S. Gozu. *Int. J. Mod. Phys. B* **29** (2015) 1550248.

Narrowing of excitation band in nanophosphors

**Hyojun Kim¹, Daehan Kim¹, Kwangwon Park¹, Jongsu Kim^{1, 2}, Wunho Lee²,
Taewook Kang², Byungjoo Jeon², Heelack Choi^{2, 3}**

¹*Department of Display Science and Engineering, Pukyong National University,
Busan 608-737, Republic of Korea.*

²*Department of LED Convergence Engineering, Specialized Graduate School of Science and
Technology Convergence, Pukyong National University, Busan 608-739, Republic of Korea.*

³*Department of Materials Science and Engineering, Pukyong National University,
Busan 608-739, Korea.*

Nanophosphors were prepared through a high-energy planetary milling of its bulk phosphor: $D_{50} < 200$ nm. They showed the drastic narrowing of photoluminescence excitation spectra [1] with slight blueshifting of emission bands [2], that is, smaller spectral overlap between the excitation and emission bands compared with the bulk phosphor. It leads to reducing the reabsorption rate. It results from significant quenching of all Raman scattering modes, implying the restriction of electron-phonon coupling. Finally the simulation of white LED based on the nanophosphors showed a higher luminous efficiency for their smaller concentrations.

References:

- [1] L. T. Su, A. I. Y. Tok, F. Y. C. Boey, X. H. Zhang, J. L. Woodhead, and C. J. Summers, *J. Appl. Phys.* 102 (2007) 083541.
- [2] Q. Li, L. Gao, and D. Yan, *Mater. Chem. Phys.* 64 (2000) 41.

Acknowledgement

This work was supported by the Development of R&D Professionals on LED Convergence Lighting for Shipbuilding/Marine Plant and Marine Environments (Project No: N0001363) funded by the Ministry of TRADE, INDUSTRY & ENERGY (MOTIE, Korea).

Towards cavity-enhanced single rare earth ion detection
**B. Casabone^{1,2}, F. Beck³, T. Hümmer^{1,3}, A. Ferrier⁴, P. Goldner⁴, T. W. Hänsch^{1,3},
H. de Riedmatten², D. Hunger^{1,3}**

¹*Max-Planck-Institut für Quantenoptik, Hans-Kopfermann-Straße 1, 85748 Garching, Germany*

²*ICFO-Institut de Ciències Fotoniques, Mediterranean Technology Park, 08860 Castelldefels(Barcelona), Spain*

³*Ludwig-Maximilians-Universität München, Fakultät für Physik, Schellingstraße 4, 80799 München, Germany*

⁴*Chimie ParisTech, Laboratoire de Chimie de la Matière Condensée de Paris, CNRS-UMR 7574, UPMC-Paris 06, 11 rue Pierre et Marie Curie 75005 Paris, France*

Rare earth ions doped into solids provide outstanding optical and spin coherence properties, which renders them as promising candidates for quantum optical applications ranging from quantum memories to quantum-nonlinear optics. However, due to the dipole-forbidden nature of the coherent transitions, they couple only weakly to optical fields. This limits most experiments to macroscopic ensembles, where inhomogeneous broadening complicates and limits quantum control.

Here, we first present an approach to get efficient access to individual ions or small ensembles by coupling them to a high-Finesse optical microcavity. We employ fiber-based Fabry-Perot cavities [1] with high finesse and a free-space mode volume as small as a few λ^3 to achieve substantial Purcell enhancement. This offers the potential to boost the spontaneous emission rate by several orders of magnitude (up to 10^4), thereby making the weak transitions bright. Finally, we present the current status of the experiment and we discuss further steps towards our goal.

References:

- [1] Hunger, Reichel et al., NJP 12, 065038 (2010)
- [2] Perrot, Ferrier et al., PRL 111, 203601 (2013)

Towards bulk crystal coherence times in $\text{Eu}^{3+}:\text{Y}_2\text{O}_3$ nanocrystals

John G. Bartholomew, Karmel de Oliveira Lima, Alban Ferrier, Jenny Karlsson and Philippe Goldner

PSL Research University, Chimie ParisTech - CNRS, Institut de Recherche de Chimie Paris, 75005, Paris

Rare-earth-ion-doped crystals have been extensively studied for quantum information applications because of their excellent coherence properties. Despite the very promising properties of the materials, development of quantum hardware is hindered by difficulties to access single ions and to couple several interacting units together, to create a scalable system in a bulk crystal.

Nanoparticles containing rare-earth ions open up opportunities for high contrast single-ion optical detection [1, 2], and optical coupling to ensembles through access to optical cavities with low mode volumes [3]. One key question is to what extent it is possible for the linewidths in nanocrystals to approach the sub-kHz linewidths achieved in bulk crystals.

Optical homogeneous linewidths of Eu^{3+} dopants in Y_2O_3 nanoparticles below 100 kHz have been previously reported for 60 nm crystallites [4,5], and we now present homogeneous linewidths below 50 kHz for 100 nm crystallites.

By performing hole burning and coherent spectroscopy on powdered nanoparticle samples we determine the broadening contributions of interactions between europium ions and dynamic disorder modes, phonons, and magnetic fluctuations within the host lattice. We explore the possibilities to extend the coherence times of sub-micron particles towards the bulk crystal values.

References:

- [1] T. Utikal, E. Eichhammer, L. Petersen, A. Renn, S. Götzinger, and V. Sandoghdar, *Nat. Commun.* 5, (2014) 3627
- [2] E. Eichhammer, T. Utikal, S. Götzinger, and V. Sandoghdar, *New J. Phys.* 17 (2015).
- [3] M. Mader, J. Reichel, T. W. Hänsch, and D. Hunger, *Nat. Commun.* 6, (2015) 7249
- [4] A. Perrot, P. Goldner, D. Giaume, M. Lovrić, C. Andriamiadamanana, R. R. Gonçalves, and A. Ferrier, *Phys. Rev. Lett.* 111, 203601 (2013).
- [5] K. de Oliveira Lima, R. Rocha Gonçalves, D. Giaume, A. Ferrier, and P. Goldner, *J. Lumin.* 168, 276–282 (2015).

Persistent optical hole-burning spectroscopy of nano-confined dye molecules in liquid at room temperature: optical memory in liquid?

Hiroshi Murakami

Kansai Photon Research Institute, Japan Atomic Energy Agency, Kyoto, Japan.

A reverse micelle is formed by self-assembly of surfactant molecules in a nonpolar solvent, and becomes a nanometer-scale spherical cage filled with water (Fig.1). Excellent properties of reverse micelles are that their size can be controlled experimentally, and that various molecules, such as proteins and DNA, can be dissolved in them. These properties allow us to study the confinement effect on the properties of water and molecules, under the condition similar to that in a cell [1]. Recently, we have found that the surrounding water of a dye molecule in AOT/isooctane reverse micelles with a radius of ~ 1 nm is glass-like, that is, shows no diffusional motions even at room temperature, and that the lattice relaxation energy is small owing to a small number of water molecules in the reverse micelle [2]. These properties are considered to be appropriate for persistent hole-burning spectroscopy of dye molecules in reverse micelles at room temperature. Further, nanometer-sized functional elements could be created using reverse micelles in liquids, because the efficiency will be enhanced owing to suppression of relaxation processes. In the present study, we explore the properties of persistent hole-burning spectra of dye molecules in reverse micelles, and compare the results with those in bulk.

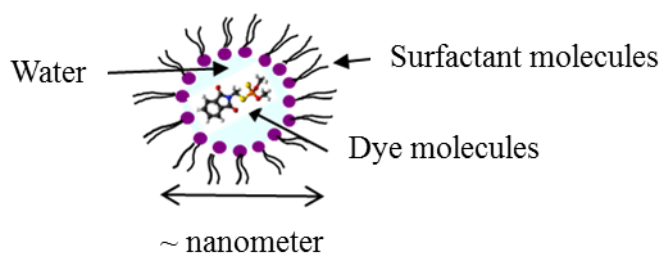


Fig.1. Schematic cross-section diagrams of dye-molecule-containing reverse micelles

References:

- [1] H. Murakami, T. Nishi, and Y. Toyota, *J. Phys. Chem. B* **115**, (2011)p.5877, references therein.
- [2] H. Murakami, T. Sada, M. Yamada, and M. Harada, *Phys. Rev. E* **88**, (2013)p.052304.
- [3] W. E. Moerner (Ed.), *Persistent Spectral Hole-Burning: Science and Applications*, Springer-Verlag, Berlin Heidelberg (1988).

Fluorescence microscopy of single organo-metal halide perovskite nanowires: effect of crystal-phase transition

A. Dobrovolsky^{*}, E.Unger, A. Yartsev, I. G. Scheblykin

Department of Chemical Physics, Lund University, SE 22100 Lund, Sweden

**e-mail: alexander.dobrovolsky@chemphys.lu.se*

Organic-inorganic lead halide perovskites $\text{CH}_3\text{NH}_3\text{PbI}_3$ have attracted much attention in last several years as very promising materials for solar cells, light-emitting diodes and laser devices. Organo-metal halide perovskites possess properties of traditional inorganic semiconductors, combined with the great advantage of low-cost solution processing. Their exceptional solar energy conversion and emission performance are driven by long carrier lifetimes, high carrier mobility, strong broadband optical absorption and high fluorescence quantum yield with possibility to tune the emission wavelength. Recent structural and photophysical studies concluded that $\text{CH}_3\text{NH}_3\text{PbI}_3$ has two accessible crystal forms below room temperature: a tetragonal phase from 160 K to room temperature and an orthorhombic phase for temperatures T below 160 K. The purpose of this work is to investigate effect of crystal-phase transition on luminescence properties of $\text{CH}_3\text{NH}_3\text{PbI}_3$ perovskites using optical microscopy techniques.

We studied $\text{CH}_3\text{NH}_3\text{PbI}_3$ nanowires (NWs) grown by a surface-initiated solution fabrication method. Scanning electron microscopy has shown that resulting NWs had length up to 4 μm and diameter varying from 100 to 500 nm with flat rectangular end facets indicating high-quality single crystal structure. Temperature-dependent steady-state and time-dependent micro-photoluminescence measurements on the individual NWs were performed in temperature range of 77 – 295 K. Photoluminescence microscopy combined with spectroscopy allows us to study the local variations of photophysical properties in a single NW with high spatial resolution.

Fluorescence microscopy of single $\text{CH}_3\text{NH}_3\text{PbI}_3$ NWs at different temperatures reveals the coexistence of the tetragonal and orthorhombic phases in $120 \text{ K} < T < 160 \text{ K}$. For the first time, temperature-dependent luminescence intensity variation along NW axis induced by crystal phase transition was observed. Emergence of bright areas characterized by the red-shifted luminescence spectra at the temperature region of the phase transition may be attributed to small inclusions of domains of the room-temperature phase with the narrower band gap, in which a large fraction of photoexcited carriers agglomerate. Processes of carrier migration between domains of different phases and spatial carrier localization are discussed.

This effect can be potentially beneficial for optoelectronic device applications for emission enhancement in LEDs and decrease of the gain threshold in lasers.

Optical properties of quantum dots coupled to cone-shaped nanoantennas

K. Scherzinger^{*a}, R. Jäger^a, A. Bräuer^b, S. Jäger^a, J. Fulmes^b, S. zur Oven Krockhaus^a, D. A. Gollmer^b, D. P. Kern^b, M. Fleischer^b and A. J. Meixner^a

^a *Institute of Physical and Theoretical Chemistry and Center LISA⁺, University of Tübingen, Auf der Morgenstelle 18, 72076 Tübingen, Germany*

^b *Institute for Applied Physics and Center LISA⁺, University of Tübingen, Auf der Morgenstelle 10, 72076 Tübingen, Germany*

**e-mail: kerstin.scherzinger@uni-tuebingen.de*

Metal nanoparticles are able to enhance the luminescence of nearby emitters such as single molecules or quantum dots (QDs). This is why these nanoparticles are also often referred to as optical nanoantennas. While the ability of the enhancement is already known [1], the mechanisms behind this effect however are still partially unclear. In order to gain more understanding of this effect, we placed single QDs on the tips of gold nanocones using a self-aligned technique similar to the one we recently described in literature [2]. To obtain efficient coupling, the resonance of the nanocones was adjusted to coincide with the emission maximum of the QDs. To compare the results obtained from coupled QDs, we investigated single QDs on glass as well.

We observed a distinct enhancement in spectral intensity of a single QD in a hybrid structure along with a red-shift of the emission as well as a dramatic reduction in lifetime compared to the QDs on glass. Intensity trajectories were also recorded, which are shown in Figure 1. They clearly demonstrate that the QD on the cone apex (right) shows longer on-times with significantly higher intensities than the quantum dot on glass (left) [3].

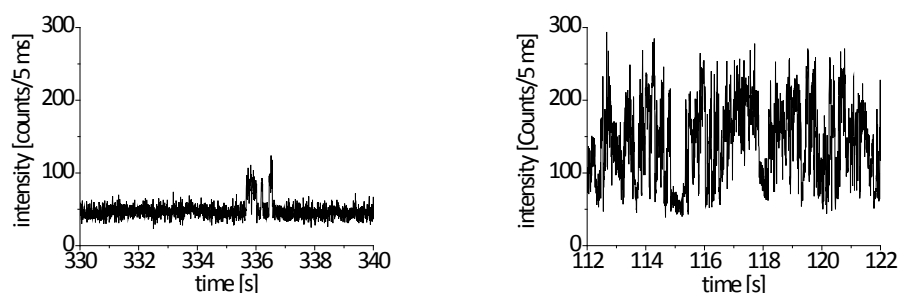


Figure 1: Left: Intensity trajectory of a single QD on glass. Right: QD on a gold cone

References:

- [1] Kern, A.M., et al., Enhanced single-molecule spectroscopy in highly confined optical fields: from $\lambda/2$ -Fabry-Perot resonators to plasmonic nano-antennas. *Chemical Society Reviews*, 2014. 43(4): p. 1263-1286.
- [2] Fulmes, J., et al., Self-aligned placement and detection of quantum dots on the tips of individual conical plasmonic nanostructures. *Nanoscale*, 2015. 7(35): p. 14691-14696.
- [3] Meixner, A.J., et al., Coupling single quantum dots to plasmonic nanocones: optical properties. *Faraday Discussions*, 2015. 184(0): p. 321-337.

Polarized photoluminescence of carbon dots

**D.K. Nelson, A.N. Starukhin, D.A. Eurov, D.A. Kurdyukov, E.Yu. Stovpiaga,
V.G. Golubev**

*Ioffe Physical-Technical Institute, Russian Academy of Sciences,
194021, St. Petersburg, Russia*

In recent years carbon nanodots (CDs) have attracted a great attention due to their remarkable fluorescent properties. CDs photoluminescence covers all visible region of the spectrum, the spectral position of the emission band being easily controlled via the excitation wavelength. CDs could compete with semiconductor quantum dots in many applications, especially in biological and medical ones having the advantage of their low toxicity, biocompatibility, low cost and chemical inertness. The effective use of CDs in the applications invites detailed investigations of their optical properties and finding out feasible mechanisms of the photoluminescence. Despite of a number of papers devoted to the study of photophysical properties of CDs these mechanisms still remain unclear [1]. In this connection a study of CDs fluorescence anisotropy could be a powerful tool in investigating processes of electron energy relaxation and light emission in this material [2].

The carbon dots under study were prepared in mesoporous silica particles whose pores were used as nanoreactors [3]. A number of organic materials, such as paraffin and APTES, were used as precursors. By etching the silica matrix in HF a transparent colloid solution of the carbon dots could be obtained. In our experiments both types of samples were used – carbon dots in mesoporous silica particles and carbon dots colloid solution. In the latter case an essential CDs fluorescence anisotropy was revealed: upon excitation with polarized light the CDs emission was also polarized. The origin of the anisotropy is the existence of transition moments for absorption and emission that lie along specific directions within the CDs. The polarized photoluminescence of the carbon dots was investigated under different excitation conditions and over a wide temperature region – from room to liquid helium temperatures. It was found that the degree of the CDs fluorescence polarization depends on the excitation and emission wavelengths, on the type of precursor used for synthesis, on the sample temperature, and on the type of matrix in which CDs were embedded.

The influence of different factors (angular displacement between the absorption and emission moments, CDs rotations, various mechanisms of energy transfer in an ensemble of the CDs) on the polarization characteristics of the CDs emission are discussed.

The authors are grateful to the RFBR for the financial support (gr. 16-03-00472).

References:

- [1] S.Y. Lim, W. Shen, Z.Q. Gao, Chem. Soc. Rev., 44 (2015) 362.
- [2] M.O. Dekaliuk, O. Viagin, Yu.V. Malyukin, A.P. Demchenko, Phys. Chem. Chem. Phys. 16 (2014) 16075.
- [3] J. Zong, Y.H. Zhu, X.L. Yang, J.H. Shen, C.Z. Li, Chem. Commun. 47 (2011) 764.

Investigation of highly efficient energy transfer in porphyrin molecules/ carbon nanotubes nanoassemblies.

G. Delport¹, F. Vialla², S. Campidelli³, C. Voisin² and J.S. Lauret¹

¹ Laboratoire Aimé Cotton, CNRS, Univ. Paris-Sud, ENS Cachan, Université Paris-Saclay, 91405 Orsay Cedex, France

² Laboratoire Pierre Aigrain, Ecole Normale Supérieure, CNRS, UPMC, Université Paris Diderot, Paris, France.

³ CEA Saclay, IRAMIS, LICSEN, Gif sur Yvette, France.

e-mail: geraud.delport@ens-cachan.fr

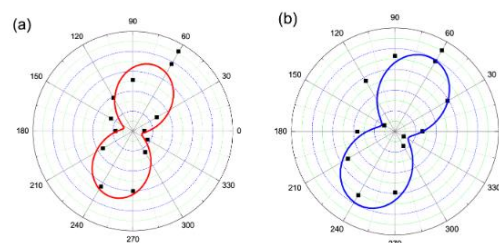
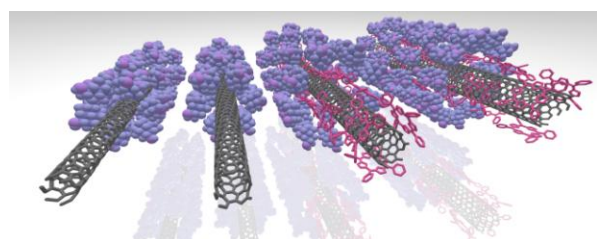
Semiconducting single wall carbon nanotubes (Swcnts) are promising nanoobjects in particular for optoelectronics applications. Thanks to surfactant molecules, they can be easily dispersed in water phase while preserving their excitonic luminescence properties. Moreover, due to their carbon sp² surface, Swcnts can be easily coupled to organic molecules. In this context, we designed a nondestructive functionalization method to couple porphyrin molecules to nanotubes while preserving the nanotubes optical properties.

We evidenced that such porphyrins interact strongly with nanotubes, creating stable nano-assemblies with remarkable optical properties. Their spectroscopic properties change dramatically with a 200 meV red shift in absorption, 100 % quenching of their fluorescence, leading to a 100% efficient ultrafast energy transfer from the molecule to the nanotube [1-3].

Finally, we have also investigated the adsorption mechanism of the molecules onto the wall of the nanotube. In particular, we unveil a cooperative adsorption thermodynamical behavior that matches with a classical adsorption Hill model. We extract the Gibbs energy of this reaction and monitor its evolution with nanotube diameter. On 16 nanotube chiral species [4] we show that such energy increases with diameter in good agreement with recent DFT calculations.

In this poster, we will focus on the influence of the cylindrical shape of the nanotube on the angular dependence of the energy transfer by means of anisotropy measurements both on ensemble and at the single compound level. The main feature is that the energy transfer is driven by the anisotropy of the nanotube [5]. Finally, the influence of the geometry of the molecule on the anisotropy of the energy transfer has been investigated.

Figure : (left) “in micelle” stacking reaction in progress, (right) “anisotropic transfer resonance”



References :

- [1] C. Roquelet, et al, ChemPhysChem **2010**, 11, 1667
- [2] G. Clave, G. Delport et al, Chem. Mat. **2013**, 25, 2700
- [3] C. Roquelet, et al, Appl. Phys. Lett. **2010**, 97,141918
- [4] F. Vialla, G. Delport et al, Nanoscale, **accepted**
- [5] C. Roquelet et al. ACS nano 6.10 (**2012**): 8796-8802

Optical Properties of Graphene Nanoribbons

G. Delpo¹, S. Zhao¹, L. Rondin¹, A. Narita², Y. Hu², X. Feng², K. Müllen²,
S. Campidelli³ and JS Lauret¹

¹Laboratoire Aimé Cotton, CNRS, Univ. Paris-Sud, ENS Cachan, Université Paris-Saclay,
91405 Orsay Cedex, France

²Max Planck Institute for polymer research Ackermannweg 10, 55128 Mainz, Germany

³LICSEN, IRAMIS, CEA Saclay

In the last decade, research on graphene has been extensively developed. It is now well established that graphene shows unique physical properties such as high carriers' mobility, which promises a wealth of applications in nanoelectronics. However, graphene is a zero-bandgap semiconductor. Different possibilities are explored to obtain semiconducting graphene-like structures such as the use of transition-metal dichalcogenides. Here we explore an original route consisting in opening a gap directly in graphene. This is achieved through quantum confinement by reducing the size of graphene. The reduction of one dimension of graphene leads to graphene nanoribbons (GNRs) and nanotubes (CNTs) while the reduction of the two dimensions leads to graphene quantum dots (GQDs).

The easiest way to obtain GNRs and GQDs is to use top-down physical synthesis methods. For instance, GQDs can be obtained by oxidation cutting of commercial carbon fibers. It leads to small pieces of graphene of ~3 nm [1]. Nevertheless, this fabrication technique does not allow to control accurately neither the lateral size nor the number of layers. Moreover, the edges of these objects are not controlled at all [1]. The consequence is that their electronic and optical properties are dominated by defective states located on these edges [2]. Concerning the fabrication of GNRs, an historical route is the unzipping of carbon nanotubes [3]. Once again, the very nature of the edges is poorly controlled. Fortunately, a new approach for the building of nanographenes is emerging. 'Bottom-up' synthesis of GQDs and GNRs has been recently reported [4, 5]. Depending on the nature of the chemical precursor, one can in principle control the shape, the width, the length and the nature of the edges of the graphene nano pieces.

In this poster, we will present our recent work on the optical properties on GNRs synthesized by the bottom-up approach. In particular, we report on the emission properties of GNRs in solution by means of photoluminescence and time-resolved photoluminescence experiments. Finally, the influence of inter-chain interactions on the luminescence spectrum of GNRs has been investigated [6].

References:

- [1] J. Peng et al Nano Letters 12, (2012) 844 (2012)
- [2] Q. Xu et al, ACS Nano 7, (2013) 10654
- [3] X. Li et al Science 319, (2008) 5867
- [4] X. Liang et al, Nano Lett. 10, (2010) 2454
- [5] A. Narita et al, Nature Chemistry 6, (2014) 126
- [6] G. Delpo et al, in preparation

New inorganic nanoprobles, upconversion nanoparticles (UCNPs) based on fluoride matrices doped by lanthanide ions, have attracted a great attention due to unique features. They absorb light in the near infrared region and exhibit anti-Stokes luminescence in the visible and UV region. It enables evading high tissue absorption and high-contrast optical biomedical imaging by suppressing the background of biological tissue autofluorescence. In comparison with organic dye molecules and quantum dots UCNPs have additional advantages such as an excellent photostability, no blinking and bleaching, a large anti-Stokes shift etc. The crucial advantage of UCNPs is long enough lifetimes (in submillisecond region) for the most levels and rich energy structure. It enables upconversion of NIR emission of CW diode laser of modest power with wavelength about 980 nm into visible and even UV light. It is important that an excitation light and a shifted red emission are coincided with the window of transparency for the most biological tissues (the so-called therapeutic window). It makes UCNPs very promising for “transfer” visible and UV light into biological tissue by introducing them in subsurface tissue layer and is a basis for a high-contrast optical biological imaging (by suppressing the crowded background of biological tissue autofluorescence) and for photodynamic therapy.

The nonlinear dependence of the UCNPs luminescence on the excitation intensity and small volumes of these particles results in dramatic reduction of observed signals and difficulties with a detection. One more problem in detection and imaging of single UCNPs is how to distinguish single and aggregated particles.

Here, we report the results of our experimental spectral studies of single nanoparticles based on hexagonal-phase NaYF_4 crystalline matrix codoped with trivalent Yb^{3+} , Tm^{3+} and Er^{3+} ions. Results of our studies have shown that spectra of single and aggregated UCNPs under study differ markedly. The observed difference can be used to answer one of the basic questions: is the observed object single nanoparticle or cluster consisted of two or more particles?

Acknowledgements

Financial support from the Russian Foundation for Basic Research (1,2) - Projects No 14-02-00834, No 14-29-07132 and No 14-29-07241- is gratefully acknowledged.

Influence of plasmon silver films on photoinduced electronic processes in polymeric films of poly (3-hexylthiophene)

D. Afanasyev, A. Zeinidenov, N. Ibrayev

Institute of Molecular Nanophotonics, E.A. Buketov Karaganda State University, Karaganda, Kazakhstan

Poly(3-hexylthiophene) (P3HT) is a model semiconducting conjugated polymer. P3HT is used for producing of organic solar cells with bulk heterojunction. This interest is conditioned by the fact that P3HT possess high hole conductivity and high absorption capability in the visible spectrum.

Spectral and luminescent properties of semiconductor polymer films of P3HT on the surface of Ag island films were studied. Films were deposited onto quartz substrates with thermal evaporation of metal silver in vacuum chamber at residual pressure equal to $P=5 \cdot 10^{-4}$ mm Hg. Further films were annealed in muffle furnace at temperatures between 60 °C and 240 °C. The growth of temperature leads to decreasing of size and increasing in number of Ag islands. The size of island ranges from 40 up to 90 nm. Absorption spectra of silver films shows that at thermal treatments short-wavelength shift of maximum plasmon resonance band, significant decreasing of half-bandwidth and increasing of intensity of absorption band occurs with increasing in annealing temperature from 60 °C up to 240 °C.

P3HT polymer films were prepared by spin-coating. Increasing in optical density P3HT takes place in the polymer film deposited onto Ag films. Maximum increasing in optical density of P3HT film (in ~ 4 times) was observed on silver film that was annealed at 240 °C.

Fluorescence spectrum of P3HT polymer is a broad band with a maximum at wavelengths at 572, 642 and 708 nm [1]. Change in the spectrum shape and redistribution intensity of fluorescence peaks is observed in the P3HT films on the surface of Ag film. The fluorescence intensity at 572 nm increases and the intensity of other peaks is significantly reduced. Increasing of absorption and fluorescence intensity of P3HT is associated with increased rate of intramolecular electronic transitions in the polymer under the influence of the local electromagnetic field near the surface of the Ag nanoparticles.

Fluorescence decay kinetics of P3HT polymer films was measured at pulsed spectrofluorimeter with picosecond resolution and registration with time-correlated photon counting mode. The lifetime of the excited state of P3HT is equal 0.33 ns. It was calculated from the luminescence decay curve at a wavelength of 572 nm. Luminescence duration of polymer is reduced for P3HT films on the Ag island films.

As has showed by spectral-luminescent properties of P3HT films the formation of disordered polymer film takes place on the surface of the Ag films. The increase in temperature annealing of Ag films leads to an increase in the degree of disorder of P3HT films. Influence of molecular resonance of P3HT polymer to the intensity of the surface plasmon resonance of Ag island films was found.

References:

[1] Ou J., et al. *Synthetic Metals* 195 (2014) 9-15

Anomalous exciton diffusion in disordered wire-like materials

Valentina Giorgis¹, Andrey V. Malyshev^{2,3} and Victor A. Malyshev⁴

¹Université Catholique, ISEN, Lille, France

¹GISC, Departamento de Física de Materiales, Universidad Complutense, Madrid, Spain

²On leave from: Ioffe Phisico-Technical Institute, St. Petersburg, Russia

³Zernike Institute for Advanced Materials, University of Groningen, Groningen, Netherlands

Excitons are elementary excitations of solids responsible for the charge-less energy transport. Low-dimensional objects, such as molecular aggregates (light harvesters), conjugated polymers (solar cell units) and many others hold a prominent role among these excitonic systems.

Disorder is an attributive feature of solids, leading to the appearance of a tail in the density of states (DOS) below the bare exciton band edge, the so-called Lifshits tail [1]. The states of the tail are well localized and have a (hidden) energy structure [2,3]. This part of the DOS is responsible for the exciton transport at temperatures smaller than the characteristic tail extension. The states above the bare exciton band edge are more extended and become crucial in accelerating the exciton migration at higher temperatures [4].

We investigate theoretically the random walk in underlined materials and uncover different regimes of exciton motion depending on the temperature: diffusive and super-diffusive. The exciton migration is considered as incoherent hoppings between localized states due to a weak coupling of excitons to vibrations of the host into which the system is embedded. We argue that the extension of the Lifshits tail, which depends on the disorder strength, provides the characteristic energy scale ΔE for the exciton transport. At temperatures $T < \Delta E$, the exciton transport is of a diffusive nature, involving only the states of the Lifshits tail of the DOS, with a characteristic length given by the typical tail state localization length N^* . Contrary to that, the motion at $T > \Delta E$ is determined by hops via higher-energy band states of the system whose typical extension depends on the energy. The distribution function of the localization length of these states has a heavy tail so, when they are involved into play, the exciton transport turns into a super-diffusive regime, known as Lévy flights [5]. Our findings can be relevant for the adequate interpretation of the energy transfer in wire-like materials.

References:

- [1] I. M. Lifshits, Zh. Exp. Teor. Fiz. **53** (1967) 743 [Sov. Phys. JETP **26** (1968) 462].
- [2] V. Malyshev and P. Moreno, Phys. Rev. B **51** (1995) 14587.
- [3] A. V. Malyshev and V. A. Malyshev, Phys. Rev. B **63** (2001) 195111.
- [4] A. V. Malyshev, V. A. Malyshev, and F. Domínguez-Adame. Chem. Phys. Lett. **371** (2003) 417; J. Phys. Chem. B **107** (2003) 4418.
- [5] P. Barthelemy, J. Bertolotti, and D. S. Wiersma, Nature **453** (2008) 495.

Photodynamic antimicrobial chemotherapy using zinc phthalocyanines in the treatment of bacterial infection

Zhuo Chen, linsen Li, Yaxin Zhang, Jincan Chen, Ping Hu, Mingdong Huang

State Key Laboratory of Structural Chemistry and Danish-Chinese Centre for Proteases and Cancer, Fujian Institute of Research on the Structure of Matter, Chinese Academy of Sciences, Fuzhou, Fujian 350002, China

Photodynamic antimicrobial chemotherapy (PACT) is one of the promising technique to address the prevalent challenge of antibiotic resistance. It is based on an initial photosensitization of the infected area, followed by irradiation with visible light, producing singlet oxygen which is cytotoxic to bacteria. Here, we conjugated mono-substituted ZnPc-COOH with a series of oligolysine moiety with different number of lysine residues (ZnPc-(Lys)_n(n=1, 3, 5, 7, 9)) to improve the water solubility of the ZnPc conjugates. We measured the photosensitizing efficacies and the cellular uptakes of this series of conjugates on several different types of bacteria. Our results showed that ZnPc-(Lys)₅ has the highest photodynamic efficacy compared to the other conjugates investigated.

References:

[1] Zhuo Chen,* Yaxin Zhang, Dong Wang, Linsen Li, Shanyong Zhou, Joy H. Huang, Jincan Chen, Ping Hu, Mingdong Huang*, **Journal of Biomedical Optics**, 21(2016), 18001.

[2]Zhuo Chen*, Shanyong Zhou, Jincan Chen, Linsen Li, Ping Hu, Song Chen, Mingdong Huang*,**Journal of Luminescence**, 152 (2014), 103-107.

Thermoelectric properties of disordered molecular wires with electron-vibron interaction

E. Díaz¹, F. Domínguez-Adame^{1,2} and R. A. Römer²

¹Departamento de Física de Materiales, Universidad Complutense, Madrid, Spain

²Department of Physics and Centre for Scientific Computing, University of Warwick, UK

Since the advent of nanotechnology, many discoveries have demonstrated that nanometer-sized objects exhibit physical properties not shared by bulk materials. In particular, theoretical predictions and experiments pointed out that thermoelectric properties at the nanoscale are strongly enhanced. Efficient thermoelectric bulk materials display values of the figure of merit ZT lower than unity. However, Venkatasubramanian *et al.* reported $ZT = 2.4$ in thin-film superlattices at room temperature [1]. Similarly, Harman *et al.* studied a quantum dot superlattice and found $ZT = 1.6$ [2]. Therefore, nanostructures pave the way to achieve large ZT and consequently more efficient thermoelectric devices as refrigerators and generators.

In this work we report on the non-equilibrium electron transport through a molecular wire with N molecules, each one coupled to a vibronic degree of freedom. We assume that each vibron has a different temperature, leading to a temperature gradient in the system. In addition, disorder in the chain is modelled by an Anderson Hamiltonian. The lattice is tunnel coupled to two leads, as shown schematically in figure 1.

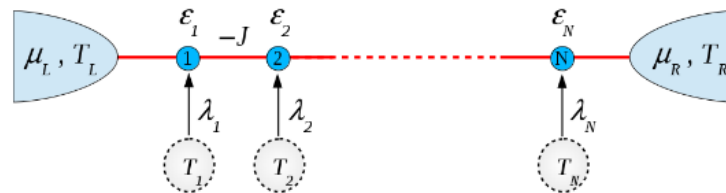


Figure 1. Schematic diagram of the molecular wire with N molecules coupled to vibronic degrees of freedom. The temperature of each molecule T_i is different and presents a linear profile along the wire. The electron-vibron coupling is assumed to be Holstein-type.

Using the Keldysh non-equilibrium Green's function formalism [3], we compute the electric current and energy flux through the molecular wire for a number of disorder realisations. We find that the thermopower and the figure of merit ZT are greatly affected by the disorder.

References:

- [1] R. Venkatasubramanian, E. Siivola, T. Colpitts, and B. O'Quinn, *Nature* **413** (2001) 597.
- [2] T. C. Harman, P. J. Taylor, M. P. Walsh, and B. E. LaForge, *Science* **297** (2002) 2229.
- [3] H. Haug and A. P. Jauho, *Quantum Kinetics in Transport and Optics of Semiconductors* (Springer, Berlin, 2008).

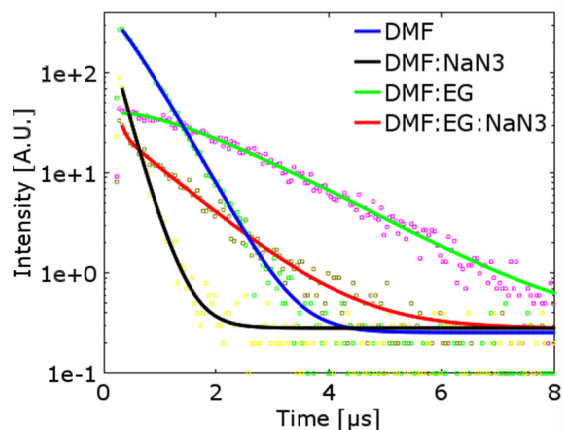
Mechanisms of Protoporphyrin IX Delayed Fluorescence

Vinklárík I., Scholz M., Dědic R., Hála J.

Charles University in Prague, Faculty of Mathematics and Physics,
Department of Chemical Physics and Optics, Prague, Czech Republic
vinklarekivo@gmail.com

Protoporphyrin IX (PpIX) is a naturally occurring precursor in heme biosynthesis pathway in all cells. It is also a potent singlet oxygen ($^1\text{O}_2$) photosensitizer, which is used under elevated concentrations of PpIX in photodynamic therapy (PDT) of cancer and other serious chronic diseases. PpIX exhibits delayed fluorescence (DF), which can be utilized as a probe in monitoring of PDT [1] and as a measure of mitochondrial oxygen tension *in vivo* [2]. However, these studies considered only the thermal mechanism of DF. We have demonstrated that singlet-oxygen sensitized DF (SOSDF) mechanism, where triplet state of PpIX is excited to the first singlet state by energy transfer from $^1\text{O}_2$, is the major contributor to DF kinetics in the case of wide range of hydrophilic photosensitizers in solutions and in living cells [3]. Therefore, we investigated kinetics of PpIX DF in mixtures of dimethylformamide and ethylene glycol of different viscosities to evaluate contributions of various DF mechanisms.

Simultaneous detection of time-resolved kinetics of $^1\text{O}_2$ phosphorescence (around 1275 nm) and DF of PpIX (100 μM) at 632 nm was used for this purpose. Concave biexponential decays of DF suggest a presence of SOSDF mechanism. Sodium azide (NaN_3) is a well-known quencher of $^1\text{O}_2$. Its addition (10mM) changes the concave character of the kinetics to a convex one and leads to a dramatic decrease of DF intensity accompanied by shortening of the lifetimes (see the Figure). It further supports



the presence of SOSDF mechanism. A possibility of quenching of PpIX triplets by NaN_3 was excluded by triplet-triplet transient absorption experiments. Another way to probe the role of oxygen was a gradual removal of dissolved oxygen by nitrogen purging. The decreasing oxygen concentration was reflected in a substantial increase of DF kinetics lifetimes while the distinct concave shape of kinetics was preserved initially. Finally, the kinetics converged to convex biexponential decays. The gradual formation of PpIX photoproduct during the experiments was shown to cause a decrease of DF decay intensity but no change in its shape and lifetimes.

All these experiments point out to the significant role of SOSDF mechanism of PpIX. The results have to be considered when developing diagnostic tools based on DF of PpIX in PDT and other clinical applications.

References:

- [1] PIFFARETTI, F. *et al.* J Biomed Opt. 17 (2012) 115007
- [2] MIK, E. G. *et al.* Anesth. Analg. 117 (2013) 834
- [3] SCHOLZ, M., R. DĚDIC. Chapter 28 in NONELL, S. Singlet Oxygen: Applications in Biosciences and Nanosciences, Royal Society of Chemistry (2016)

Study of the thermal stability of the GFP in the range 20-100°C

T. P.J. Han¹, L. M. Maestro², M. I. Marqués^{2,3}, F. Jaque²

¹ *Department of Physics, University of Strathclyde, Glasgow, Scotland, UK.*

² *Departamento de Física de Materiales, Universidad Autónoma de Madrid, Madrid, Spain.*

³ *Condensed Matter Physics Center (IFIMAC) and Instituto Nicolás Cabrera, Universidad Autónoma de Madrid, Madrid, Spain*

The temperature dependence luminescence of green fluorescent protein (GFP) in pure liquid water is studied in the temperature range 0-100 °C. The luminescence intensity measured, by the total area of the emission spectrum, presents three different stages, growth in the range 20-40 °C, followed by a linear decrease until ~70 °C and then a marked drop above this temperature. This quenching of the luminescence above 70 °C is irreversible even when the samples are returned to 20 °C.

Similar behaviour has also been reported in the thermal stability study of lysozyme protein in pure liquid water using NMR technique [1] and has described the three temperature ranges as native (0-40 °C), reversible (40-70 °C) and irreversible (≥ 70 °C). The high temperature region is related with the protein denaturation due to its dehydration processes.. These results are discussed in consideration of the anomaly in the dielectric constant about 60 °C recently reported and associated with the existence of two phases in pure liquid water with different dipole moments [2].

[1]. F. Mallamace, C. Corsaro, D. Mallamace, S. Vasi, H. E. Stanley *J. Chem. Phys.* 141 (2014) 18C504.

[2]. J. C. del Valle, C. Camarillo, L. M. Maestro, J. A. Gonzalo, C. Arago, M: I. Marqués, D. Jaque, G. Lifante, J. G. Solé, K. Santacruz-Gomez, R. C. Carrillo-Torres, F. Jaque. *Phil. Mag.* 95, 7 (2015) 683-690.

Dephasing mechanisms in transparent ceramics with narrow optical linewidths

Nathalie Kunkel^{1*}, John Bartholomew¹, Alban Ferrier^{1,2}, Akio Ikesue², Philippe Goldner¹

¹*Institut de Recherche de Chimie Paris –CNRS ChimieParisTech, 75005 Paris, France
nathalie.kunkel@chimie-paristech.fr*

²*Sorbonnes Universités, UPMC Univ Paris06, 75005 Paris, France;*

³*World Laboratory, Mutsuno, Atsuta-ku, Nagoya 456-0023, Japan*

Rare earth doped materials are of great interest for applications in quantum information technology [1] or highly stable laser locking[2], because optical transitions of trivalent rare earth ions can exhibit very narrow linewidths. In the past mostly single crystals were used and thus, applications have been limited. Only recently, coherence properties in transparent ceramics were studied [3] and homogeneous linewidths below 10 kHz were found in Eu^{3+} doped Y_2O_3 ceramics [4]. In the present work we investigate the coherence properties of $\text{Eu}^{3+}:\text{Y}_2\text{O}_3$ transparent ceramics with 2- and 3-pulse photon echo techniques and spectral hole burning, also in high magnetic fields up to 3 Tesla. In some samples homogeneous linewidths of below 3 kHz can be found, which is in the range of high quality single crystals [5]. In order to shed light on the dephasing mechanisms in such systems, we also relate the coherence properties with the materials properties that may be influenced by different processing and annealing procedures and are investigated using for instance EPR, XRD, luminescence and thermoluminescence as well as vibrational spectroscopy. Consequently, these studies will lead to a better understanding and therefore the possibility to improve the preparation of rare earth doped ceramic samples with regard to obtaining extremely narrow optical linewidths.

References:

- [1] W. Tittel, T. Chanelière, R. L. Cone, S. Kröll, S. A. Moitseev, M. J. Sellars *Laser & Photon.Rev.* 4 (2010) 244.
- [2] M. J. Thorpe, L. Rippe, T. Fortier, M. S. Kirchner and T. Rosenband, *Nat. Photonics* 44 (2011) 699.
- [3] A. Ferrier, C. W. Thiel, B. Tumino, M. O. Ramirez, L. E. Bausá, R. L. Cone, A. Ikesue, and Ph. Goldner *Phys. Rev. B* 49 (2013) 5821.
- [4] N. Kunkel, A. Ferrier, C. W. Thiel, M. O. Ramirez, L. E. Bausá, R. L. Cone, A. Ikesue, Ph. Goldner, *Appl. Phys. Lett. Mat.* 3 (2015) 096103.
- [5] G. P. Flinn, K. W. Jang, J. Ganem, M. L. Jones, R. S. Meltzer, R. M. Macfarlane, *Phys. Rev. B: Condens. Matter Mat.* 49 (1994) 5821.

An Infrared Pump-Probe Measurement of the ${}^6\text{H}_{7/2}$ Lifetime of Sm^{3+} in LiYF_4

J.-P.R. Wells^{1,2*}, S.P. Horvath¹, A.F.G. van der Meer³, M.F. Reid^{1,2,4}

¹*Department of Physics and Astronomy, University of Canterbury, Christchurch 8140, New Zealand.*

²*The Dodd-Walls Centre for Quantum and Photonic Technologies.*

³*Radboud University Nijmegen, Institute for Molecules and Materials, FELIX Facility, 6525 ED Nijmegen, The Netherlands.*

⁴*MacDiarmid Institute for Advanced Materials and Nanotechnology.*

**jon-paul.wells@canterbury.ac.nz*

We have used a short pulsed, infrared free electron laser (FEL) to perform a three beam, balanced pump-probe experiment on Sm^{3+} ions doped into LiYF_4 . For resonant excitation of the $Z_1(\gamma_6) \rightarrow Y_2(\gamma_7)$ transition at 1079 cm^{-1} [1], a weak pump-probe transient is observed due to absorption saturation by the sub-picosecond FEL pulses having a $\Delta T/T$ of approximately 10^{-3} for pump pulse energies of $1 \mu\text{J}$.

From a rate equation analysis, we infer lifetimes as long as 9 picoseconds for samples cooled to 10 K in a cold finger cryostat. These lifetimes are substantially faster than would be predicted by the commonly used exponential energy gap law.

References:

[1] J.-P.R. Wells, M. Yamaga, T.P.J. Han, H.G. Gallagher and M. Honda. *Polarized Laser Excitation, Electron Paramagnetic Resonance and Crystal-Field Analyses of Sm^{3+} - Doped LiYF_4* Phys. Rev. B. **60**, 3849 (1999).

Time Evolution of Softening of Coherent Phonon in Antimony

Sho Nakayama, Masato Maruyama, Hideaki Kumagai, Tomobumi Mishina

Department of Physics, Faculty of Science, Hokkaido University, Sapporo 060-0810, Japan

Up to now coherent phonon have been studied by using a femtosecond pump-probe technique in various materials, including semiconductor and semi-metal. Under the high excitation, an obvious reduction of the frequency of coherent phonon, so to called softening of coherent phonon have been observed. So far, softening mechanism have been discussed and not been resolved.

On the other hand, from the experimental results of the time-resolved electron diffraction and X-ray diffraction [1], lattice contracts when the solid surface is strongly excited by the laser pulse. Also it is known that strain due to lattice contraction is propagated into the crystal interior as a wave (Strain pulse) [2]. Such a lattice contraction would be expected even in the case of coherent phonon. The frequency will be changed depending on the contraction of the lattice. Therefore, we simulate the time evolution of the coherent phonon by considering the modulation effect due to strain.

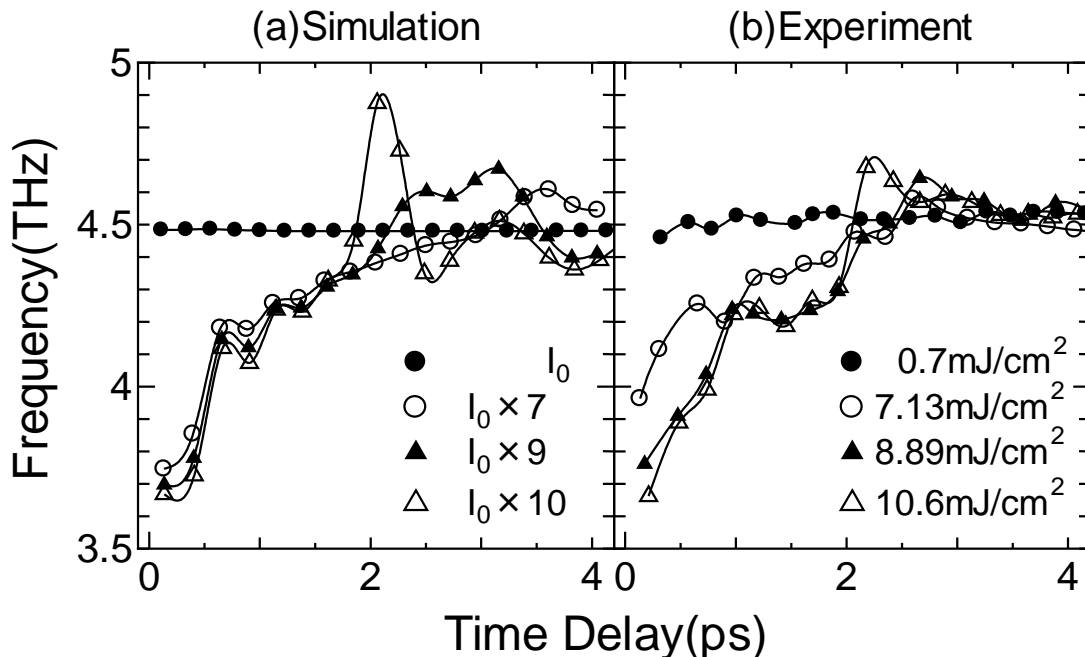


Fig.1. Time evolution of frequency of coherent phonon (a) simulation result (b) experimental result, measured by changing the fluence.

Figure.1 shows the simulation and experimental result. From the simulation result, the time evolution of frequency of coherent phonon clearly shows irregular time evolution. On the other hand, analysing the experimental result in the same way, similar time evolution can be seen.

We will report the detailed simulation of the time evolution of coherent phonon.

References:

- [1] F. Carbone et al., PRL 100, 035501 (2008)
- [2] J. J. Baumberg et al., PRL 78, 3358 (1997)

Robust photon-echo generation in quantum dots using a pair of chirp pulses

Y. Sato¹, N. Aonuma¹, K. Akahane², and J. Ishi-Hayase^{1,*}

¹*School of Fundamental Science and Technology, Keio University, Yokohama, Kanagawa 223-8522, Japan*

²*National Institute of Information and Communications Technology (NICT), Tokyo 184-8795, Japan*

**hayase@appi.keio.ac.jp*

Excitons in a quantum dot (QD) ensemble in conjunction with photon echo (PE) technique is one of the candidates for broadband (~10 THz) light-matter quantum interface. However, this protocol is not suitable for transferring single photons, because the intense rephrasing pulse causes the large population inversion resulting in the degradation of the single photon state due to the amplification of PE signal [1]. Although, PE-based quantum interface using controlled reversible inhomogeneous broadening (CRIB) can overcome this problem, the acceptable bandwidth is limited. Alternatively, PE-based quantum interface via adiabatic rapid passage (ARP) using a pair of frequency-chirped controlled pulses was proposed to generate PE signal without residual population inversion [2]. This also enables us to generate PE robustly against inhomogeneity of pulse area and detuning inherent to QDs. In this study, we theoretically and experimentally demonstrate and evaluate PE generation in QDs using a pair of chirp pulses.

We calculated time evolution of polarization and population in the two-level under excitation by first incident pulse (data pulse) and following a pair of chirp pulses (read pulses). The calculations were done by solving von-Neumann equation in the semi-classical region taking into account inhomogeneity of pulse area and detuning. In the calculation, we used the material parameters for InAs QDs fabricated by strain compensation [3]. Figure 1 shows an example of calculated results under excitation by 1.3-ps data pulse and a pair of chirped pulses. As a result, we confirm PE generation at the expected time without any degeneration of temporal profile of data pulse. The ratio of pulse area of data pulse to PE is 0.8. This result is much different from the result for conventional two-pulse PE using transform limited rephrasing pulse. We also found that most population can transfer to ground state after irradiating a pair of chirped pulse. This means that amplification of PE by population inversion can be significantly suppressed by using a pair of chirped pulses.

This work was partially supported by MEXT KAKENHI Grand Number (15H05868), Advanced Photon Science Alliance (APSA), JSPS core-to-core Program, and Photonic Device Laboratory at NICT.

References:

- [1] J. Ruggiero *et al.*, Phys. Rev. **A 79**, 053851 (2009).
- [2] M.F.Pascual *et al.*, New. J. Phys. **15**, 21 (2013).
- [3] K.Akahane *et al.*, J.Crystal Growth **245**, 31 (2002).

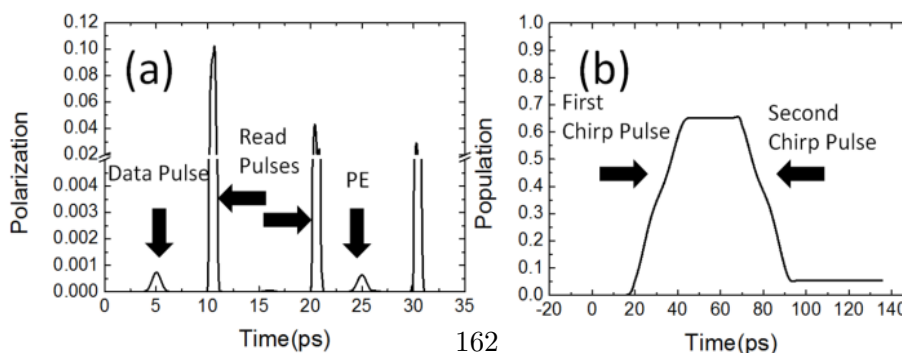


Fig.1. Time evolution of (a) polarization and (b) population in an inhomogeneous two-level system.

Complex Quantum Beats of Excitons in Quantum Dots observed using Three-Pulse Photon Echo

Y. Arai¹, K. Akahane², S. Kitazawa¹, and J. Ishi-Hayase^{1,*}

¹School of Fundamental Science and Technology, Keio University, Yokohama, Kanagawa 223-8522, Japan

²National Institute of Information and Communications Technology (NICT), Tokyo 184-8795, Japan

*hayase@appi.keio.ac.jp

Excitons in semiconductor quantum dots (QDs) have been subjects for ultrafast coherent control and quantum information processing, since they exhibit long coherence times and large dipole moment. Recently, our group observed complex, previously unreported quantum beats of excitons in InAs QDs using three-pulse photon echo (3PE) technique^[1]. In this presentation, we show that three different inhomogeneities of physical quantities play important roles in determining behaviour of excitonic quantum beats in QDs.

The QD used in this study was 150-layer-stacked InAs QDs on InP(311) substrate fabricated using strain compensation^[2]. Because of the antisymmetric shape and/or strain of QDs, exciton ground states split into two orthogonal linearly polarized states with the fine-structure splitting. In a 3PE experiment, we used 1.1-ps optical pulses whose wavelength was tuned to the resonant wavelength of exciton ground states (1530 nm). The 3PE signals with the wavevector $-\mathbf{k}_1 + \mathbf{k}_2 + \mathbf{k}_3$ was measured using optical heterodyne technique for three incident pulses with the wavevectors $\mathbf{k}_1, \mathbf{k}_2, \mathbf{k}_3$ at the temperature of 5 K (Fig. 1(a)).

Figure 1(c) shows time delay τ dependence of 3PE signal amplitude by varying the polarization angles φ of the excitation pulses $\mathbf{k}_1, \mathbf{k}_2$ with respect to the crystal axis (Fig. 1(b)). By varying φ , we observe exciton fine-structure quantum beats whose visibilities are complexly modulated depending on τ and φ . The complex behaviors of quantum beats can be explained by analytical calculation using the density matrix semi-classical theory taking into account three inhomogeneities of QDs, i.e., inhomogeneous distribution of exciton energy, exciton fine-structure energy, and directions of quantized axes (Fig. 1(d)). We found that these inhomogeneities cause the large differences of dephasing rate of 2-level and 3-level processes attributed to 3PE signals, which results in complex behaviors of quantum beats.

This work was partially supported by MEXT KAKENHI Grant Number (15H05868), Advanced Photon Science Alliance (APSA), JSPS core-to-core Program, and Photonic Device Laboratory at NICT.

References:

[1] W. Langbein, *et al.*, Phys. Rev., (2004) **B 69**, 161301. [2] K. Akahane, *et al.*, J. Crystal Growth, (2002) **245**, 31.

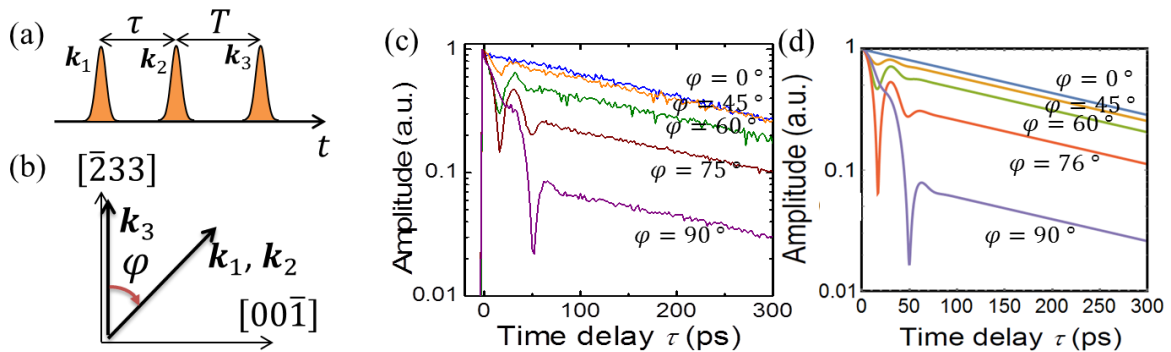


Fig.1 (a) Pulse sequence and (b) polarization directions of excitation pulses used in 3PE. (c) Experimental results and (d) analytical calculations of time delay τ dependence of amplitude of 3PE signals for various polarization directions of excitation pulses $\mathbf{k}_1, \mathbf{k}_2$.

Appearance of coherent LO phonons during the decay of LO-phonon–plasmon coupled mode in an undoped GaAs/n-type GaAs epitaxial structure

Takahiro Sumioka, Hideo Takeuchi, and Masaaki Nakayama

Department of Applied Physics, Graduate School of Engineering, Osaka City University, Japan

In polar semiconductors, It is well known that the longitudinal optical (LO) phonon couples with plasmon, which results in formation of LO-phonon–plasmon coupled (LOPC) modes with lower and upper branches (L- and L+). In our previous work, we demonstrated that the coherent LOPC modes emit frequency-tunable terahertz (THz) electromagnetic waves in undoped GaAs/n-type GaAs (*i*-GaAs/*n*-GaAs) epitaxial structures [1]. In the *i*-GaAs/*n*-GaAs structure, surface Fermi-level pinning produces a considerable built-in electric field in the *i*-GaAs layer [1]. The built-in electric field enhances the polarization of the coherent LO phonon and the surge current of photogenerated carriers. Thus, the *i*-GaAs/*n*-GaAs structure is advantageous in the generation of the THz electromagnetic waves from the coherent LOPC modes. In this work, we have investigated the dynamical properties of the coherent LOPC modes using short time Fourier transform (STFT) analysis of time-domain THz signals to reveal the characteristics of the decay process.

The sample of the *i*-GaAs/*n*-GaAs epitaxial structure was grown on an *n*-type (001) GaAs substrate by metalorganic vapor phase epitaxy. The thickness of the *i*-GaAs (*n*-GaAs) layer was 200 nm (3.0 μm), and the doping concentration in the *n*-GaAs layer was $3.0 \times 10^{18} \text{ cm}^{-3}$. The built-in electric field in the *i*-GaAs layer was estimated to be 28 kV/cm. The surface of the sample was covered with an aluminium thin film having an optical window with a diameter of 50 μm , which results in spatially homogeneous excitation and THz radiation. The excitation light source was a mode-locked Ti:sapphire laser with a pulse duration of 50 fs and center wavelength of 800 nm. Time-domain THz signals were detected at room temperature using an optical gating method with a photoconductive dipole antenna.

We confirmed that the frequencies of the L- and L+ modes observed at various excitation powers can be fitted by the electron-type LOPC-mode dispersions as a function of photogenerated carrier density. Figure 1 shows the time-frequency image map of STFT spectra at an excitation power of 30 mW. Here, we used the Gaussian function as a time window with a time resolution of 0.18 ps and frequency resolution of 0.45 THz in the STFT analysis. The sharp (broad) THz band originates from the coherent LO phonon (L- mode). The prominent result is that the coherent LO phonon appears during the decay process of the L- mode. This fact suggests that the disappearance of the LOPC mode regenerates the coherent LO phonon.

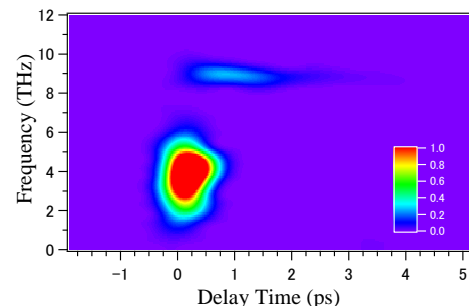


Fig. 1: Time-frequency image map of STFT spectra at 30 mW, where the sharp (broad) THz band corresponds to the coherent LO phonon (L- mode).

References:

- [1] H. Takeuchi *et al.*, J. Appl. Phys. **110** (2011) 013515.

Compact ultrafast X-ray and gamma-ray sources driven by intense femtosecond laser pulses

Ruxin Li, Wentao Wang, Jiansheng Liu, and Zhizhan Xu

State Key Laboratory of High Field Laser Physics, Shanghai Institute of Optics and Fine Mechanics, Chinese Academy of Sciences (SIOM, CAS)

Compact ultrafast X-ray and gamma-ray sources are very useful in the detection of dynamics of material under extreme conditions. The short-pulse gamma-ray source driven by intense femtosecond laser pulses based on Compton scattering is a promising approach towards compact ultrafast high brightness gamma-ray sources [1]. We will report the generation of compact gamma-ray sources based on the laser wake-field electron accelerators driven by a 5Hz 200TW laser facility. We have demonstrated a MeV gamma-ray source of high brightness (10^{22} photons/s·mm²·mrad² per 0.1% bandwidth), based on the Compton scattering of laser accelerated high quality quasi-mono-energetic electron beams with intense femtosecond laser pulses. Meanwhile, a compact XUV-free electron laser (FEL) at 30nm based on a 0.5GeV level laser wake-field electron accelerator is at the final stage of experiments.

References:

- [1] Ta Phuoc, K. *et al.* All-optical Compton gamma-ray source. *Nat. Photonics* **6**, 308-311 (2012)
- [2] Changhai Yu *et al.*, submitted.

Role of dynamical symmetry in an effective time-independent Hamiltonian for a laser-driven system

Jun-ichi Inoue

National Institute for Materials Science, Tsukuba, Japan 305-0044

Symmetries lie at the heart of physics and materials science. In static cases, point- and space-group symmetries govern physical properties of molecular and solid-state systems. When a problem is time-dependent, other types of symmetries would manifest themselves in many forms. One of those symmetries is a dynamical symmetry, which works in conjunction with an operation along time axis. Dynamical process in solid states is an ideal platform to study effects of the dynamical symmetry. Here, one of them is discussed.

Time reversal symmetry is recognized as, even in static systems, a crucial element, and constraint imposed by that can be seen in, for instance, an energy band structure of solids as, to name a few, Kramers degeneracies and band sticking together[1]. In particular, the former has tight link with novel phenomena expected in topological insulators. Once driven by a laser field, the solid system is considered to lose conventional time reversal symmetry[2], and thus, Kramers degeneracies are lifted by the dynamical stimulus. However, the band sticking together in an energy band is found to be robust against the broken time reversal symmetry. In this sense, this feature of band structures falls into a class of symmetry-protected states, which are nowadays highlighted in topological condensed matter physics.

To demonstrate this, we consider a two-dimensional lattice system driven by circularly polarized light. Dynamical symmetry in the time-dependent problem was addressed in [3]. In this work, albeit inspired by this work, we take another route: we rely on a scheme [4] to construct an effective time-independent Hamiltonian from a time-periodic one. By examining energy band structures of the newly obtained Hamiltonian, we found that band sticking together remains unchanged even though an electron hopping with complex amplitude has been induced, and identified origin of the degeneracies along the Brillouin-zone boundaries with a dynamical symmetry inherent to the system.

References:

- [1] V. Heine, *Group Theory in Quantum Mechanics*, (Dover, 1993).
- [2] F. Haake, *Quantum signatures of chaos*, (Springer, 2010).
- [3] O. E. Alon, *Phys. Rev. A* 66, (2002)013414.
- [4] N. Goldman and J. Dalibard, *Phys. Rev. X* 4, (2014)031027.

Chapter 8

Poster Session II

Tuesday 19th July 18:15 – 20:15 , Poster Session II

1. Pulse photoconductivity and light-induced absorption in undoped photorefractive Bi₁₂SiO₂₀ and Bi₁₂TiO₂₀ crystals
Tatiana Kornienko, Marina Kisteneva, Stanislav Shandarov, Alexei Tolstik
2. Spectroscopic properties of Eu³⁺:GdBO₃ nanopowders obtained by the sol-gel method
Mourad Seraiche, Guerbous Lakhdar, Kechouane Mohamed, Audrey Potdevin, Geneviève Chadeyron, Rachid Mahiou
3. Energy relaxation processes in Zn_xMg_{1-x}WO₄ mixed crystals
Nataliya Krutyak, Irina Kamenskikh, S. Ivanov, Dmitry Spassky, Vitaly Nagirnyi
4. Spectroscopy of Er³⁺ ions in Li₅La₃Nb₂O₁₂ garnets.
A. Egaña, M. Tardío, C. de la Torre Gamarra, A. Várez, E. Cantelar, F. Cussó, V. Lavín and J. E. Muñoz Santiuste
5. Photoluminescence properties of nanoporous anodic alumina alloyed with manganese ions
I. V. Gasenkova, N. I. Mukhurov, S. P. Zhvavyi, E. E. Kolesnik, A. P. Stupak
6. Influence of crystal field on optical properties of KNaSiF₆:Mn⁴⁺ phosphor at ambient and high hydrostatic pressure
Tadeusz Lesniewski, Sebastian Mahlik, Marek Grinberg, Ye Jin, Ru-Shi Liu
7. Influence of the compensation defects on the luminescence of Sr₂SiO₄:Eu³⁺ and Sr₂SiO₄:Eu²⁺
Karol Szczodrowski, Justyna Barzowska, Natalia Górecka, Marek Grinberg
8. Investigating the thermal stability of luminescence from some w-LED phosphors
Suchinder Sharma, Irene Carrasco, Yuan-Chih Lin, Marco Bettinelli, Maths Karlsson
9. Up-conversion luminescence – a new property in tenebrescent Hackmanites
Isabella Norrbo, Mika Lastusaari
10. Research the centers of electron capture in K₂SO₄
Ainura Tussupbekova, Temirgaly Koketai, Askhat Baltabekov, Aizhan Salkeyeva
11. Green emitting Ca₃SiO₄Cl₂: Eu²⁺ phosphor for blue converted white LEDs
Rupesh Talewar, Pooja Yadav, Charusheela Joshi and S. V. Moharil
12. Scintillation properties of alkaline metal doped LiCaAlF₆
Takayuki Yanagida, Masanori Koshimizu, Yutaka Fujimoto, Kentaro Fukuda, Go Okada
13. ZnGa₂O₄:Cr and ZnGa₂O₄:Cr,Bi as new temperature sensing phosphors
Estelle Glais, Morgane Pellerin, Corinne Chanéac, Bruno Viana
14. Defect luminescence and relaxation kinetics in amorphous yttrium-alumino-borate (a-YAB) phosphors
Atul Sontakke, Vinicius Guimarães, Lauro Maia, Pauline Burner, Mathieu Salaun, Isabelle Gautier-Luneau, Alban Ferrier, Bruno Viana, Alain Ibanez
15. Dynamics of sensitization in (Cr,Nd,Yb):YAG ceramics
Voicu Lupei, Aurelia Lupei, Cristina Gheorghe, Stefania Hau, Akio Ikesue
16. Electron-phonon interaction of Pr³⁺ and Sm³⁺ in YAG
Aurelia Lupei, Voicu Lupei, Stefania Hau, Cristina Gheorghe, Akio Ikesue
17. Effects of Si codoping on optical properties of Ce-doped Ca₆BaP₄O₁₇ from

- first-principles calculations
Lixin Ning, Huang Xiaoxiao, Zhiguo Xia
18. Ponderomotive forces mediate UV solid-state laser operation
Vadim Semashko, Oleg Akhtyamov, Alexey Nizamutdinov, Evangelia Sarantopoulou, Alciviadis-Constantinos Cefalas
 19. Propagating, confined and interface acoustic phonon modes in GaN/AlN quantum wells
Yuhai Zan, Qu Yuan, Shiliang Ban
 20. Luminescence properties of organic-inorganic layered perovskite-type compounds under vacuum ultraviolet irradiation
Naoki Kawano, Masanori Koshimizu, Yutaka Fujimoto, Keisuke Asai
 21. Cyclical changes in optical properties of SrTiO₃ structure
Vitaliy Gorbenko, Galina Gorbenko
 22. Polariton-like propagation of photoluminescence from exciton-exciton scattering in a GaAs/AlAs multiple-quantum-well structure
Yoshiaki Furukawa, Masaaki Nakayama
 23. X-ray excited luminescence of Ba₂MgSi₂O₇:Eu²⁺
Hongbin Liang, Jing Yan, Chunmeng Liu, Jianbang Zhou, Pieter Dorenbos, Bingbing Zhang, Yan Huang, Ye Tao
 24. Ce³⁺ to Tb³⁺ energy transfer in Ce₂(SO₄)
Aarti Iyer Muley, S. Moharil
 25. Luminescence study of SrB₄O₇: Sm²⁺ as multimode temperature sensor with high sensitivity
Zhongmin Cao, Yonghu Chen, Xiantao Wei, Changkui Duan, Min Yin
 26. Pathways of relaxation of excited states of Pr³⁺ in Y₂Si₂O₇: Pr³⁺, Yb³⁺
Karina Grzeszkiewicz, Wiesław Stręk, Dariusz Hreniak
 27. Chromium pairs in combustion synthesized alpha-alumina
John Krebs, Sarah Robitaille, Ned Dixon, Linda Fritz
 28. Energy transfer between different transitions within rare-earth ions
Jiuping Zhong, Hongbin Liang, Qiang Su
 29. Peculiarities of Er³⁺ ↔ Yb³⁺ energy transfer in CaSc₂O₄:Er:Yb
Angela Stefan, Serban Georgescu, Octavian Toma
 30. Initial process of photoluminescence dynamics in a β-Ga₂O₃ single crystal
Suguru Yamaoka, Yoshiaki Furukawa, Masaaki Nakayama
 31. Luminescence of Ce³⁺ ion activated potassium gadolinium pyrosilicates phosphor under vacuum ultraviolet and X-Rays excitation
Ni Haiyong, Liang Hongbin
 32. Near-infrared spectroscopy of lattice defects in anion-defective sapphire at 4-300 K
Zhayloo Mamytbekov, Igor Milman, Maksim Sarychev, Aleksandr Syurdo, Rinat Abashev, Viktor Voinov
 33. Influence of synthesis parameters on the spectroscopic properties of Ca₉Y(PO₄)₇ doped with Eu³⁺, Eu²⁺
Natalia Gorecka, Karol Szczodrowski, Justyna Barzowska, Marek Grinberg
 34. Photoemission calculations using projection operator method for metals and semiconductors.
Zoliana Bawitlung, Ram Thapa
 35. Luminescence properties and energy transfer of GdBO₃:Ce³⁺, Tb³⁺ phosphor
Qihong Zhang, Haiyong Ni, Lingli Wang, Fangming Xiao

36. MREI-model calculation of two-mode property of bulk transverse optical phonons and its influence on electronic mobility in Al_xGa_{1-x}N/GaN quantum well
Gu Zhuo, Ban Shiliang, Qu Yuan
37. Anomalous polaritonic luminescence from rare-gas solids
Alexander Ogurtsov, Nikolaj Kleshchev, Olga Bliznjuk
38. Nonlinear composition dependent optical spectroscopy of Ba₂xSr_{2-2x}V₂O₇
Hongwei Fang, Yonghu Chen, Chang-Kui Duan, Min Yin
39. The environmental factor model: a tool for the design of Eu²⁺-doped orthophosphate phosphors?
Mariam Amer, Philippe Boutinaud
40. Relaxation through conical intersection: quantum friction of pseudorotation and Slonczewski resonances
Kaja Pae and Vladimir Hizhnyakov
41. Electroluminescence of PLZT relaxor ceramics at fast-rising electric fields
Suleyman Kallae, Sadyk Sadykov
42. Green emission of U⁶⁺ activated lithium based tungstates
Swapnil Pote
43. Tunable and white-light emission nitride phosphors Ca₂Si₅N₈:Ce³⁺,Na⁺, Eu²⁺
Huan Jiao, Chao Li, ShiJie Qiu, Kun Li
44. TDDFT study of thiocarbonyl compounds in RAFT polymerization
Nadia Ouddai, Salima Zekri and Nadja Latelli
45. Thermoluminescence of novel lanthanum oxide obtained by a glycine-based solution combustion method
Victor Orante-Barrón, Bakang Mothudi, Catalina Cruz-Vázquez, Rodolfo Bernal
46. Thermoluminescence of novel zinc oxide nanophosphors obtained by glycine-based solution combustion synthesis
Victor Orante-Barrón, Flor Escobar-Ochoa, Catalina Cruz-Vázquez, Rodolfo Bernal
47. Plasmon-assisted upconversion energy-transfer in Er³⁺,Yb³⁺:LiNbO₃
David Hernandez-Pinilla, Pablo Molina, José L. Plaza, Mariola Ramirez, Luisa Bausá
48. Investigation on emission and topological phase transition of individual NaREF₄ nanoparticle
Chun-Hua Yan, Wei Feng, Ling-Dong Sun
49. Photon avalanche upconversion in rare-earth doped nanoparticles
Thomas Kornher, Roman Kolesov, Kangwei Xia, Rolf Reuter Rolf, Jörg Wrachtrup
50. Towards better understanding of the persistent luminescent properties of Cr-doped and Cr, Bi-doped ZnGa₂O₄ nanoparticles
Morgane Pellerin, Cristina Coelho-Diego, Christian Bonhomme, Nadia Touati, Laurent Binet, Corinne Chanéac, Bruno Viana
51. Influence of optical phonons on the electronic mobility in Al₂O₃/AlGa_n/Ga_n double heterojunctions
Zhou Xiaojuan, Qu Yuan, Gu Zhuo, Zan Yuhai, Ban Shiliang, Wang Zhiping, Xiaojuan Zhou
52. Optical properties of CdTe quantum dot superlattices self-organized with electrostatic interaction

- Taichi Watanabe, Yong-Sin Lee, Kohji Takahashi, DaeGwi Kim*
53. Single donor-acceptor pair attached to a protein molecule as a tool for studying folding/unfolding fluctuations in the protein
Igor Osad'ko
 54. Synthesis and spectroscopic properties of cage-like SrAl₂O₄:Eu²⁺ microspheres via a sol-gel method
J. Wan, Y. Zhang, Y. Wu, X. Qiao, F. Wang, X. Fan
 55. Au islands enhanced luminescence of Er³⁺/Yb³⁺ co-doped Gd₂(MoO₄)₃ thin films and application in temperature sensing
Haoyue Hao, Yuxiao Wang, Xueru Zhang
 56. Enhance the sensitivity of optical thermometer based on non-thermally coupled levels of Tm³⁺
Hongyu Lu, Yuxiao Wang, Xueru Zhang
 57. Metal transition ion implantation on Ga₂O₃ nanowires
Alicia Gonzalo, Emilio Nogales, Bianchi Mendez, Javier Piqueras, Katharina Lorenz
 58. Formation of chelated rare earth clusters in porous sol-gel silicate materials
Ann Silversmith, Nathan Arndt, Daniel Boye
 59. Transport and recombination of photo-injected electrons in dye-sensitized solar cells based ZnO nanostructures
Baurzhan Ilyassov, Niyazbek Ibrayev
 60. Study of surface effect on photoassisted field emission from Ta(112) and Ti(0001) by using the Transfer Hamiltonian method
Rosangliana Chawngthu and R. K. Thapa
 61. Light induced toxicity of rare earth doped trifluoride crystalline nanoparticles
Maksim Pudovkin, Alina Krashennicova, Vadim Semashko, Alexey Nizamutdinov, Pavel Zelenihin, Egor Alakshin, Vitaliy Pavlov, Angelo Ferraro, Stella Korableva
 62. Optical thermometry of Er³⁺-doped transparent NaYb₂F₇ glass-ceramics
Fangfang Hu, Xiantao Wei, Xinyue Li, Jiajia Cai, Yanguang Qin, Zeng Peng, Yonghu Chen, Chang-Kui Duan, Min Yin
 63. Enhanced near-infrared response of c-Si solar cell using YVO₄: Bi³⁺, Ln³⁺ (Ln = Yb and Nd) phosphors
R.A. Talewar, Charusheela Joshi, S. V. Moharil
 64. Photo-physical properties of spin-coated lead halide perovskite thin films
Kien Wen Sun
 65. Frequency selective transient and permanent spectral hole burning processes in Ce:YSO at liquid helium temperatures
Jenny Karlsson, Adam Nilsson, Diana Serrano, Andreas Walther, Lars Rippe, Stefan Kröll, Alban Ferrier, Philippe Goldner
 66. Intersubband optical absorption between multi energy levels in InGaN/GaN spherical core-shell quantum dots
Wen-Hao Liu, Yuan Qu, Shi-Liang Ban
 67. Directionally solidified Ce:LaBr₃/CaBr₂ eutectic scintillator for radiation imaging applications
Kei Kamada, Hiroyuki Chiba, Shunsuke Kurosawa, Yasuhiro Shoji, Yuji Ohashi, Yuui Yokota, Akira Yoshikawa
 68. Electronic structure of optical properties of host material (Gd₂O₂S, Gd₂O₃ and Gd₂O_{3-x}S_x) for upconversion phosphor computational modeling
Wang Fei, Xiumin Chen, Bin Yang, Dachun Liu, Qingchun Yu

69. Giant negative magnetoresistance in oxygen-deficient Mn-substituted ZnO
X. L. Wang, Q. Shao, R. Lortz, J. N. Wang, Antonio Ruotolo,
70. Epitaxial seeded growth of rare earth nanocrystals with efficient 800 nm near-infrared to 1525 nm short-wavelength infrared downconversion photoluminescence for in vivo bioimaging
Rui Wang, Xiaomin Li, Lei Zhou, Fan Zhang
71. Single-band upconversion nanoprobles for multiplexed simultaneous in situ molecular mapping of cancer biomarkers
Zhou Lei, Zhang Fan
72. A many-particle quantum-kinetic formalism for describing emission properties of single quantum objects in frozen environments
Maxim G. Gladush, Andrei V. Naumov

Pulse photoconductivity and light-induced absorption in undoped photorefractive $\text{Bi}_{12}\text{SiO}_{20}$ and $\text{Bi}_{12}\text{TiO}_{20}$ crystals

T. Kornienko*, M. Kisteneva, S. Shandarov**, A. Tolstik***

**Belarusian State University, Minsk, Belarus*

***Tomsk State University of Control Systems and Radioelectronics, Tomsk, Russia*

The important characteristic for practical use such sillenite photorefractive crystals as bismuth silicon $\text{Bi}_{12}\text{SiO}_{20}$ (BSO) and bismuth titanium $\text{Bi}_{12}\text{TiO}_{20}$ (BTO) oxide crystals is obtaining stable characteristics of optical switches, which are mostly determined by the structure of impurity and defect centers. Therefore, it is actual to develop a unified theoretical model able to describe and range the basic processes of charge transfer between the various defect centers characterizing by energy levels in the band gap.

The paper presents the theoretical analysis of photoconductivity and light-induced absorption variation kinetics induced in mentioned photorefractive crystals by nanosecond laser exposure. The model of charge transfer describing the kinetics of photoconductivity and light-induced absorption is presented.

The attempts to describe the experimental data of photoconductivity and light-absorption variation kinetics in photorefractive BSO and BTO crystals by the previously reviewed models [1, 2] haven't led to satisfactory results. The main contradiction in the behaviour of compared experimental and numerical calculated dependencies is a strong relaxation time difference of mentioned kinetics. To wit relaxation kinetics of the crystals are characterized by complex exponential and hyperbolic functions. Typical lifetimes of trapping levels can be dozens and hundreds of nanoseconds and dozens of microseconds (for photoconductivity kinetics) and dozens of microseconds and milliseconds (for kinetics of light-absorption variations).

Two-level model of charge transfer have been used as the basis. Its model have been become more complex by addition shallow defect center located near the bottom of the conduction band, and each of two basic model levels present pairs of donor and acceptor deep centers describing temperature dependences of optical absorption and light-induced changes by variation of tunneling probability between centers [2]. In our model electrons are thermally generated from mentioned shallow trap to conduction band and are captured from conduction band to this center with different probability. Thermal transitions between conduction band and the donor and acceptor levels are impossible because above pairs of levels characterize deep-lying centers.

Thus the numerical analysis has shown the ability to describe the experimental kinetics of photoconductivity and light-induced absorption by the theoretical model which takes into account five centers to the complex structure of the energy levels in the band gap of the real photorefractive crystal: shallow trap and two pairs of deep donor and deep acceptor centers.

References:

- [1] A. Matusevich, A. Tolstik, M. Kisteneva, S. Shandarov, V. Matusevich, A. Kiessling, R. Kowarschik, Applied Physics B, 96 (2009), pp.119–125.
- [2] S.M. Shandarov, A.E. Mandel, M.G. Kisteneva, V.I. Itkin, A.S. Vishnev, High Energy Chemistry, 42, 7 (2008), p. 49–51.

Spectroscopic properties of $\text{Eu}^{3+}:\text{GdBO}_3$ nanopowders obtained by the sol-gel method

M. Seraiche^{a, b, c*}, L. Guerbous^a, M. Kechouane^b

^a Laser Department, Nuclear Techniques Division, Algiers Nuclear Research Center (CRNA), 02, bd Frantz Fanon, BP 399, Algiers 16000, Algeria.

^b Department of Materials and Components, Faculty of Physics, USTHB, BP 32 El alia, Bab Ezzouar 16111, Algiers, Algeria.

A. Potdevin^c, G. Chadeyron^c, R. Mahiou^c

^c Université Clermont Auvergne, Institut de Chimie de Clermont-Ferrand, UMR 6296 CNRS / UBP / ENSCCF - 63171 Aubière

*Corresponding author: seraiche28@hotmail.fr

Abstract

Vaterite $\text{Eu}:\text{GdBO}_3$ nanopowders were successfully synthesized using a sol-gel method, followed by subsequent annealing at different temperatures, between 600 °C and 1200 °C. The powders were characterized by X-ray diffraction (XRD), field emission scanning electron microscopy (FE-SEM) and photoluminescence (PL) spectroscopy. Effects of annealing treatment on structural, morphological and photoluminescence properties of Eu^{3+} doped GdBO_3 are studied and discussed. The VUV-PL properties of the prepared phosphors with different concentrations of Eu^{3+} showed that the optimum luminescence output was obtained at a doping rate of 10 at.% and pH=10. The emission spectra, characteristics of the Eu^{3+} : ${}^5\text{D}_0 \rightarrow {}^7\text{F}_J$ ($J=0-4$) radiative de-excitation, are dominated by the ${}^5\text{D}_0 \rightarrow {}^7\text{F}_1$ DM- transition. Fine analysis of the spectral repartition of this DM-transition shows clearly that the Eu^{3+} ions lie on more than one crystallographic site. The energy transfer mechanisms are studied at room temperature ($T = 300$ K) using a laser excitation source. The decay curve shapes of ${}^5\text{D}_0:\text{Eu}^{3+}$ emissions confirm the energy transfer between Gd^{3+} to Eu^{3+} . The non-exponential character of the decay curves of the ${}^5\text{D}_0$ emissions are discussed and analyzed considering the possible mixing of two crystallographic forms (vaterite and calcite) and possible energy transfer between the Eu^{3+} ions in the framework of Inokuti-Hirayama model.

Keywords:

$\text{GdBO}_3:\text{Eu}^{3+}$; Sol-gel; Annealing; Luminescence; Energy transfer; laser excitation

Energy relaxation processes in $Zn_xMg_{1-x}WO_4$ mixed crystals

**N. Krutyak¹, I. Kamenskikh¹, S. Ivanov¹, D. Spassky², V. Nagirnyi³, M. Buryi⁴,
I. Tupitsyna⁵, A. Dubovik⁵, P. Maksimchuk⁵**

¹Physics Department, Moscow State University, Leninskie Gory 1, 119991, Moscow, Russia

²Skobeltsyn Institute of Nuclear Physics, Moscow State University, 119991, Moscow, Russia

³Institute of Physics, University of Tartu, Ravila 14 c, 50411, Tartu, Estonia

⁴Institute of Physics AS CR, Cukrovarnicka 10, 162 00, Prague, Czech Republic

⁵Institute for Scintillation Materials, NAS of Ukraine, Lenin ave. 60, 61001, Kharkiv, Ukraine

The enhancement of the light output in $Zn_xMg_{1-x}WO_4$ mixed crystals for intermediate values of x (with the maximum at $x = 0.5$) allows to consider these crystals as new and promising scintillating materials [1]. The modification of structural and optical properties demonstrates a linear dependence on x [2], while the efficiency of energy transfer is the highest at the intermediate values of x . Here we present new data on the modification of the energy relaxation processes in $Zn_xMg_{1-x}WO_4$ mixed crystals. The studies were performed using optical and luminescence spectroscopy as well as EPR method.

The set of $Zn_xMg_{1-x}WO_4$ ($x = 0.3, 0.4, 0.5, 0.6, 0.7, 0.8, 0.9, 1$) single crystals were grown by Czochralski technique from platinum crucibles using high-frequency heating. $MgWO_4$ single crystal was grown from the melted flux solution by pulling on a rotating seed from the platinum crucible. All the grown crystals belong to the wolframite structural type. Luminescence excitation spectra were measured in the UV-VUV region at a VUV setup (Institute of Physics, UT) in the 3-8 eV energy region and the LOCUS station at RRC "Kurchatov Institute" in the 4-18 eV energy region. Absorption spectra were measured using a Perkin Elmer Lambda 950 Spectrophotometer. EPR measurements were performed on a Bruker X-/Q-band E580 FT/CW ELEXSYS spectrometer at X-band with the microwave frequencies 9.3-9.5 GHz within the 10-296 K temperature range. The TSL glow curves were obtained using an ARS DE-204AE cryostat with a LakeShore 335 temperature controller by linear heating from 10 K to 270 K after X-ray irradiation for 15 minutes. The emission of samples was detected by an R9110 Hamamatsu photomultiplier tube.

Absorption spectra demonstrated a gradual shift of the optical bandgap to higher energies with the decrease of x . The presence of defects was revealed as well by the presence of an absorption band below the bandgap. However, the defect-related luminescence was not detected and we observed a single emission band related to self-trapped excitons. The excitation spectra were measured in a wide energy region from the fundamental absorption edge up to photon multiplication region, which allowed to study the processes controlling the efficiency of self-trapped exciton creation from separated electrons and holes. The modification of energy relaxation processes with temperature, in particular the self-trapping of holes, was analysed using the data of TSL and EPR.

References:

[1] D. Spassky, S. Omelkov, H. Mägi, et al, Optical Materials 36 (2014) 1660.

[2] N. Krutyak, V. Nagirnyi, D. Spassky, I. Tupitsyna, A. Dubovik, A. Belsky, Rad. Meas., 2016, DOI [10.1016/j.radmeas.2016.01.007](https://doi.org/10.1016/j.radmeas.2016.01.007)

Spectroscopy of Er³⁺ ions in Li₅La₃Nb₂O₁₂ garnets.

A. Egaña^(a), M. Tardío^(a), C. de la Torre Gamarra^(b), A. Várez^(b), E. Cantelar^(c),
F. Cussó^(c), V. Lavín^{(d),(e)} and J.E. Muñoz Santiuste^{(a),(e)}

^(a)Departamento de Física, Escuela Politécnica Superior, Universidad Carlos III de Madrid, Avda. de la Universidad, 30, 28911 Leganés (Madrid), Spain.

^(b)Departamento de Ciencia de Materiales, Escuela Politécnica Superior, Universidad Carlos III de Madrid. Avda. de la Universidad, 30, 28911 Leganés (Madrid), Spain.

^(c)Departamento de Física de Materiales C-IV, Universidad Autónoma de Madrid, Cantoblanco 28045, Madrid, Spain.

^(d)Departamento de Física, Universidad de La Laguna. E-38200 San Cristóbal de La Laguna, Santa Cruz de Tenerife, Spain

^(e)MALTA Consolider Team

Solid-state lithium ion conductors have recently drawn much attention due to their potential application in solid-state rechargeable batteries and other solid-state electrochemical devices. The garnet-type ceramic Li₅La₃Nb₂O₁₂ shows potential application in this field that can be improved by doping with low levels of In, V and K to increase density and Li ion conductivity and storage[1-2]

On the other hand, compounds with ideal garnet-type structure exhibit technologically related physical and chemical properties, which make them ideal materials for magnetic and optical devices. The presence of La ions in the Li₅La₃Nb₂O₁₂ structure allows their substitution by other rare-earth ions. Erbium ions can be introduced in Li₅La₃Nb₂O₁₂ garnet-type system, and can be used in both directions, to characterize the material in energy storage applications and also to explore the capabilities of the compound as optical active media. Due to its unique electronic properties, erbium is an interesting probe for a large variety of physical effects. In particular, using Er³⁺ as active ions it is possible to obtain efficient (up-converted) emission under infrared pumping suitable for different applications [3-4]

The optical spectroscopy of this new Er³⁺ activated garnet-type system is presented. The absorption and photoluminescence spectra have been obtained both at room and low temperatures. In addition, life time measurements have been made in order to investigate the several luminescence resulting channels.

References:

- [1] V. Thangadurai, S. Narayanan and D. Pinzaru, Chem. Soc. Rev., 43 (2014) 4714
- [2] V. Thangadurai, W. Weppner, J of Solid State Chemistry 179 (2006) 974
- [3] M. Haase, H. Schäfer, Angew. Chem. 50 (2011) 5808
- [4] J. Zhou, Z. Liu, F. Li, Chem. Soc. Rev. 41 (2012) 1323

Photoluminescence properties of nanoporous anodic alumina alloyed with manganese ions

I.V. Gasenkova¹, N.I. Mukhurov¹, S.P. Zhvavyi¹, E.E. Kolesnik¹, A.P. Stupak²

¹State Research and Production Association "Optic, Optoelectronic and Laser technique",

²B.I. Stepanov Institute of Physics of National Academy of Sciences of Belarus,
68 Nezavisimosti Ave., Minsk, Belarus 220072

The results are presented of a comparative study of photoluminescence (PL) properties of unalloyed and alloyed anodic alumina (AA) subjected to annealing at temperatures in the range of $T_a=200\text{--}1300\text{ }^\circ\text{C}$. AA specimens were formed in oxalic acid-based electrolytes with the addition of alloying element into the electrolyte, namely, manganese in the form of potassium permanganate KMnO_4 (0.8g/l). Luminescence spectra were measured by means of an SDL-2 automated spectrofluorometer. It is found that luminescence spectra taken from original specimens and unalloyed and alloyed specimens annealed at up to $600\text{ }^\circ\text{C}$ are characterized by the presence of broad bands in the wavelength range of $350\text{--}650\text{ nm}$ with a maximum at $450\text{--}500\text{ nm}$ which are determined by oxygen vacancies (F- and F_2 -type centers) in various charge states. With the spectra being generally similar, the PL intensity rise with increasing T_a for unalloyed specimens is significantly higher due to a large number of oxygen vacancies formed during annealing as a result of dehydration and dehydroxylation. For $T_a \geq 800\text{ }^\circ\text{C}$, a dissimilarity in the PL spectra is observed which occurs due to changing of amorphous AA structure to the crystalline one: for annealing at 900 and $1000\text{ }^\circ\text{C}$ it is a mixture of γ - and δ -phases, for $T_a=1300\text{ }^\circ\text{C}$ it is α -phase. The luminescence spectra of α -phases are characterized by bands at 677 nm and 694 nm , which are attributable to impurity ions Mn^{4+} and Cr^{3+} (${}^2\text{E} \rightarrow {}^4\text{A}_2$) located in the octahedral sites. The spectra obtained are similar to those taken from corundum crystals, proving that Mn^{4+} and Cr^{3+} ions are embedded in the AA lattice. The occurrence of these bands was unexpected and is due to the presence of the above impurities in the original aluminum and contamination of specimens in the process of formation. The alloyed AA specimens have a high intensity of Mn^{4+} R-line. The observed decrease in the PL intensity under a prolonged UV radiation exposure is well described by a two-component exponential decay. The decline in intensity of the R-line of Mn^{4+} ions is due to a decrease in the concentration of F-type centers in complex defects. This is the result of variation of the valence state of manganese ions and the charge states of oxygen vacancies due to charge transfer in the process of UV radiation absorption, for example, according to the scheme $\text{Mn}^{3+} - \text{F}^+ - \text{Mn}^{4+} \rightarrow \text{Mn}^{2+} - \text{V}_0 - \text{Mn}^{4+}$, as well as due to decreased concentration of F^+ -centers (480 nm) that excite Mn^{4+} ions in the absorption band at 470 nm . A decrease in intensity of the R-line of Cr^{3+} ions under prolonged (up to 20 min) UV irradiation and the constant intensity value in case of excitation at $\lambda_{\text{ex}}=405\text{ nm}$ is explained by decreased concentration of F-(415 nm), F_2^+ -(380 nm) and F_2^{2+} -(560 nm) centers whose radiations excite Cr^{3+} ions in the absorption bands at 410 nm and 560 nm . For the first time ever it is established that metastable phases (annealed at 900 and $1000\text{ }^\circ\text{C}$) have different spectral properties. In contrast to α -phase, chromium bands occur only under direct excitation of Cr^{3+} ions at $\lambda_{\text{ex}}=405\text{ nm}$ and the bands of manganese ions are not observed. R-lines are not separated and two new lines occur at 666 nm and 707 nm . These bands cannot be caused by interaction of the neighboring chromium atoms that form paired centers. The 666 nm band corresponds to unseparated R'-lines while 707 nm to vibrational replicas of R-line.

Influence of crystal field on optical properties of $\text{KNaSiF}_6:\text{Mn}^{4+}$ phosphor at ambient and high hydrostatic pressure

T. Lesniewski¹, S. Mahlik¹, M. Grinberg¹, Ye Jin^{2,3}, Ru-Shi Liu^{2,4}

¹ Institute of Experimental Physics, University of Gdansk, Wita Stwosza 57, 80-952 Gdansk, Poland

² Department of Chemistry, National Taiwan University, Taipei 106, Taiwan

³ School of Optoelectronic Information, Chongqing University of Technology, Chongqing 400054, China

⁴ Department of Mechanical Engineering and Graduate Institute of Manufacturing Technology, National Taipei University of Technology, Taipei 106, Taiwan

In this work we present the influence of pressure on optical properties of $\text{KNaSiF}_6:\text{Mn}^{4+}$ which is an efficient red phosphor emitting in 600 – 650 nm spectral range. KNaSiF_6 host has orthorhombic crystal structure ($Pnma$ space group) where Mn^{4+} replaces Si^{4+} forming distorted MnF_6^{2-} octahedra. High pressure spectroscopy allows to examine the impact of crystal field strength and symmetry distortion on Mn^{4+} emission allowing to fine tune the material for use in warm white LED lighting.

Photoluminescence excitation (PLE) and emission (PL) spectra as well as luminescence decay profiles have been measured at ambient conditions and high pressure up to 30 GPa. Ambient pressure PLE spectra consist of two broad bands centred at 460 and 355 nm ascribed to ${}^4\text{A}_{2g} \rightarrow {}^4\text{T}_{2g}$ and ${}^4\text{A}_{2g} \rightarrow {}^4\text{T}_{1g}$ transitions, respectively. Luminescence spectra consist of several lines attributed to ${}^2\text{E}_g \rightarrow {}^4\text{A}_{2g}$ zero phonon line (620 nm) and phonon assisted ${}^2\text{E}_g \rightarrow {}^4\text{A}_{2g}$ transitions. Under influence of pressure ${}^4\text{A}_{2g} \rightarrow {}^4\text{T}_{2g}$ and ${}^4\text{A}_{2g} \rightarrow {}^4\text{T}_{1g}$ excitation bands shift towards shorter wavelengths reaching 406 and 320 nm at 30 GPa, respectively. ${}^2\text{E}_g \rightarrow {}^4\text{A}_{2g}$ emission band shifts towards longer wavelengths reaching 640 nm at 30 GPa. Energies of the ${}^2\text{E}_g$, ${}^4\text{T}_{2g}$ and ${}^4\text{T}_{1g}$ states obtained from PLE and PL spectra allowed to calculate the Racah parameters B , C and crystal field strength parameter Dq as well as their dependence on pressure. Obtained values and their pressure rates are: $Dq = 1925 \text{ cm}^{-1}$, $dDq/dp = 9.4 \text{ cm}^{-1}/\text{GPa}$, $B = 646 \text{ cm}^{-1}$, $dB/dp = -0.8 \text{ cm}^{-1}/\text{GPa}$, $C = 4065 \text{ cm}^{-1}$, $dC/dp = -7.1 \text{ cm}^{-1}/\text{GPa}$.

Luminescence related to ${}^2\text{E}_g \rightarrow {}^4\text{A}_{2g}$ decays exponentially with the lifetime which increases with pressure (from 6.2 ms at ambient pressure to 12.5 ms at 27 GPa.) Perturbation theory has been used to analyze the pressure dependence of ${}^2\text{E}_g \rightarrow {}^4\text{A}_{2g}$ decay probability by considering the admixture of ${}^4\text{T}_{2g}$ quartet state into ${}^2\text{E}_g$ due to spin-orbit interaction. Calculated formula for radiative decay probability of the mixed state gives approximately quadratic dependence of ${}^2\text{E}_g \rightarrow {}^4\text{A}_{2g}$ decay time on energy difference $\Delta = E({}^4\text{T}_2) - E({}^2\text{E}_g)$. Fitting the experimental data yielded the ratio between spin orbit coupling constant $|V_{s-o}|^2$ and ${}^4\text{T}_{2g} \rightarrow {}^4\text{A}_{2g}$ decay time τ_T : $\frac{1}{\tau_T} |V_{s-o}|^2 = 1.91 \cdot 10^{-7} \text{ cm}^{-2} \text{ s}^{-1}$.

Influence of the compensation defects on the luminescence of $\text{Sr}_2\text{SiO}_4:\text{Eu}^{3+}$ and $\text{Sr}_2\text{SiO}_4:\text{Eu}^{2+}$

Karol Szczodrowski*, Justyna Barzowska, Natalia Górecka, Marek Grinberg
Institute of Experimental Physics, University of Gdańsk, Wita Stwosza 57, 80-952 Gdańsk, Poland

In this contribution the influence of Na^+ , Li^+ , Al^{3+} , B^{3+} co-dopants on the luminescence of $\text{Sr}_2\text{SiO}_4:\text{Eu}^{3+}$ and $\text{Sr}_2\text{SiO}_4:\text{Eu}^{2+}$ is studied. The samples were synthesized *via* solid state method using neutral and reductive atmosphere. During the calcination process realized under H_2/N_2 the Eu^{3+} introduced into the Sr_2SiO_4 can be easily reduced to form of Eu^{2+} doped phosphor. Due to the presence of the two different Sr^{2+} sites available for the europium substitution the emission spectrum of $\text{Sr}_2\text{SiO}_4:\text{Eu}^{2+}$ consists of two strong and board emission bands attributed to the d-f transitions located at blue-green (max. 490 nm) and yellow-orange (max. 570 nm) region of spectra. The relative intensities of the bands can be easily controlled by the excitation wavelength.

In the case of the materials co-doped with Na^+ , Li^+ , Al^{3+} and obtained under neutral atmosphere the emission intensity of Eu^{3+} increases with increasing concentration of co-dopants. This phenomenon is usually explained by the charge compensation effect. The emission spectra of Al^{3+} and B^{3+} co-doped materials obtained after reduction process, excited at 325 nm show, besides of typical broad band with maximum at 490 nm, also the narrow bands attributed to the f-f transitions in Eu^{3+} . The emission intensity of Eu^{3+} increases with increasing of co-dopants concentration to compare with emission intensity of Eu^{2+} . It means that Al^{3+} and B^{3+} co-dopant acts as a stabilizer of Eu^{3+} under reduction process applied. This situation is not observed in the case of Na^+ , Li^+ co-doped samples.

The concentration ratio of europium ions incorporated into the inorganic matrix in both oxidation states can be easily controlled by the changing of the Al^{3+} and B^{3+} concentration. Taking into account that in a typical synthesis of materials doped with lanthanide ions introduced in both oxidation states the only parameter influencing on the concentration ratio of lanthanide ions on the appropriate oxidation state is a heating time of the material under a suitable atmosphere, the control of the concentration ratio by co-doping is much more effective. The precision of the control of the $[\text{Ln}^{2+}]/[\text{Ln}^{3+}]$ ratio *via* co-doping is incomparable better. The observed stabilization process is perspective from point of view of phosphors designing that can be used in White-LEDs.

The work has been partially supported by the National Science Centre, Poland, agreement number: UMO-2014/13/D/ST3/04032 and POIG.01.01.02-02-006/09 project co-funded by European Regional Development Fund within the Innovative Economy Program. Priority I, Activity 1.1. Sub-activity 1.1.2.

Investigating the thermal stability of luminescence from some w-LED phosphors

Suchinder K. Sharma¹, Irene Carrasco², Yuan-Chih Lin¹, Marco Bettinelli², Maths Karlsson¹

¹*Department of Applied Physics, Chalmers University of Technology, Gothenburg, Sweden*

²*Laboratorio Materiali Luminescenti, DB, Università di Verona and INSTM, UdR Verona, Strada Le Grazie 15, 37134 Verona, Italy*

White light generation using solid state devices can be achieved *via* three different techniques namely, (a) UV LED chip with combination of red, green and blue emitting phosphors; (b) multiple LED chips emitting at different wavelengths in a single device, and (c) a blue LED chip with yellow emitting phosphor, where, the emission from blue and yellow combines to form white light. Ce doped hosts (especially YAG) has found wide applicability for solid state lighting application due to their high quantum efficiency despite it has low colour rendering index (<80) and high colour coordinate temperature (>4500 K). YAG can be easily coated on 450nm emitting InGaN chips to produce white light. The scientific community has been continuously searching for new phosphors to overcome such issues.

Various parameters which can affect the performance of phosphor converted LEDs are physical parameters like particle size, geometry, concentration, thickness and uniformity; and the optical parameters like luminous flux, colour temperature, colour uniformity and the thermal stability of emission (intensity & lifetime). In the present work, we thoroughly investigate the thermal stability of different Ce doped phosphors possessing cubic structure (for example- $Y_3Al_5O_{12}$, $Ca_3Sc_2Si_3O_{12}$ and $Sr_3Y_2Si_3O_{12}$). Suggestions are made to develop new phosphors suitable for coating InGaN chips (which emits in blue) to overcome the present drawbacks of w-LEDs.

Up-conversion luminescence – a new property in tenebrescent Hackmanites

Isabella Norrbo^a, Mika Lastusaari^a

a) University of Turku, Department of Chemistry, FI-20014 Turku, Finland

Hackmanites ($\text{Na}_8\text{Al}_6\text{Si}_6\text{O}_{24}(\text{Cl},\text{S})_2$) are minerals that belong to the sodalite group. They have many optical properties including tenebrescence, luminescence and persistent luminescence [1]. In the present work we doped Hackmanites with ytterbium and erbium to obtain up-conversion luminescence. In up-conversion luminescence, the sensitizer ion (here Yb^{3+}) is first excited. Then the energy is transferred to the activator ion (here Er^{3+}) which then emits the output photon (Figure 1a). [2]

Hackmanite consists of AlO_4 and SiO_4 tetrahedra that construct a three dimensional network of cages [3]. Normally in Hackmanite the cages are filled with four Na^+ cations and one anion (Cl^- or $\text{S}_2/\text{S}_2^{2-}$). When Hackmanites are doped with ytterbium and erbium they are expected to replace some of the Na^+ in the caves, because the trivalent Al^{3+} site is too small for them. Occupying the Na^+ site requires charge compensation, which limits the amount of Yb^{3+} and Er^{3+} that can be doped.

The up-conversion emission spectra show that green up-conversion emission was obtained (Figure 1 b). By adding up-conversion luminescence into Hackmanites multiple optical properties we have produced a material with four different optical properties that can be excited with different wavelengths. This material can find potential uses in optical multiplexing. However, additional work is still needed to intensify the up-conversion luminescence intensity.

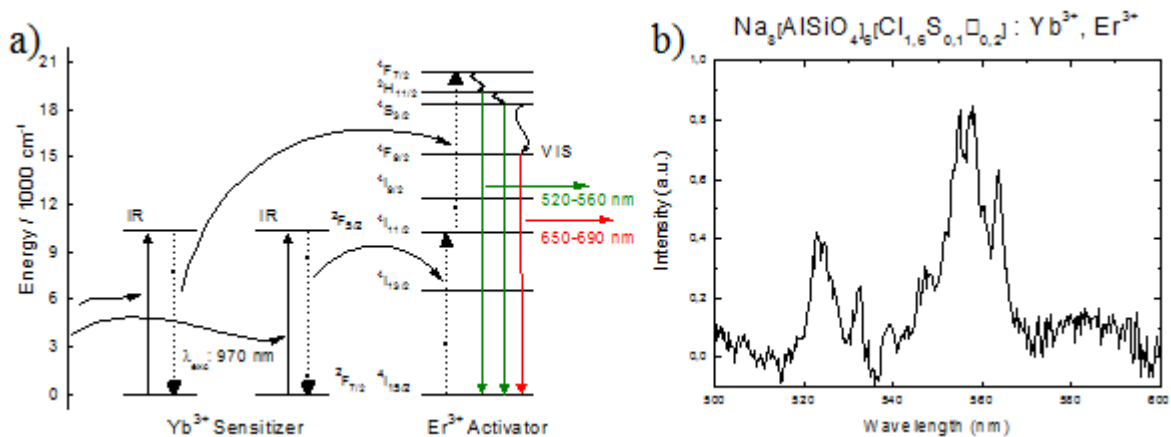


Figure 1 Up-conversion luminescence in Hackmanites. a) Simple mechanism for up-conversion luminescence in Hackmanites doped with ytterbium and erbium. b) Green up-conversion luminescence in Hackmanites doped with ytterbium and erbium. Laser excitation with 976 nm.

References:

- [1] I. Norrbo, P. Gluchowski, P. Paturi, J. Sinkkonen and M. Lastusaari, *Inorg. Chem.* 54, (2015), 7717-7724.
- [2] F. Auzel, *Chem. Rev.* 104, (2004), 139-173.
- [3] E. Williams, A. Simmonds, Armstrong J. and Weller M., *J. Mater. Chem.* 20, (2010), 10883-10887.

Research the centers of electron capture in K_2SO_4

Koketai T.A., Tussupbekova A.K., Baltabekov A.S., Salkeyeva A.K.

Ye.A. Buketov Karaganda State University, Karaganda, Kazakhstan

The influence of ions Co^{2+} , Ni^{2+} and Mn^{2+} on radiation and stimulated processes in crystal K_2SO_4 is similar. It can be proved by means of dependence curves of speeds of accumulation lightsum on the radiation dose in TSL peak at the temperature 190 K (Fig. 1). From Fig. 1. it is clear that the impurity ions Co^{2+} , Ni^{2+} and Mn^{2+} increase the speed of lightsum accumulation in the TSL peak. Therefore, the impurity ions Co^{2+} , Ni^{2+} and Mn^{2+} in crystals of potassium sulphate are the efficient centers of capture for electrons.

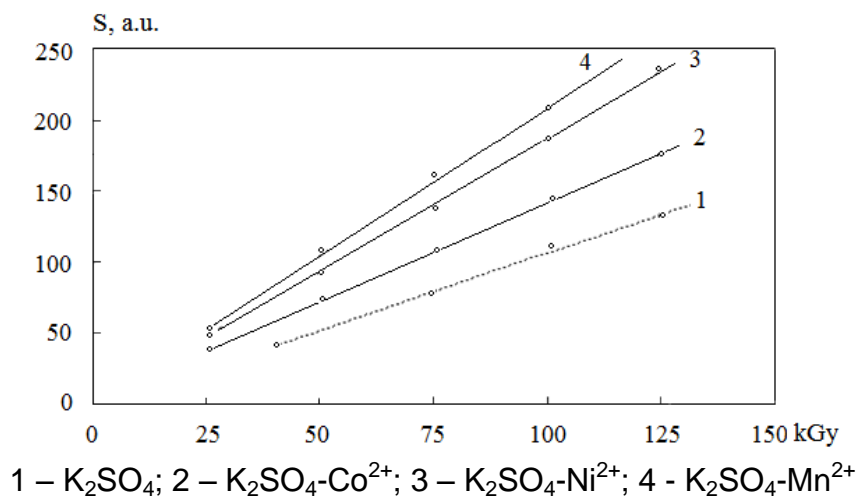


Fig. 1. The dependence curves of speeds of accumulation lightsum on the radiation dose in TSL peak at the temperature 190 K

The emergence of absorption bands in the crystals of potassium sulphate activated by Co^{2+} , Ni^{2+} and Mn^{2+} in the field of the matrix transparency according to [1] can be connected to the individual impurity centers. Exaltation of exemplars in these strips does not lead to emergence of photoluminescence. The activated Co^{2+} , $K_2SO_4-Ni^{2+}$ and $K_2SO_4-Mn^{2+}$ the absorption spectra (Figures 1, 3, 5) measured at ambient temperature are qualitatively similar.

Thus, the impurity ions of the transitional metals Me^{2+} (Co, Ni, Mn) are the centers of electron capture in K_2SO_4 . These impurity ions influence emergence of padding cationic vacancies in a crystal. The impurity anions (SO_4^{2-} and NO_3^-) in potassium sulphate are also traps for electrons.

References:

[1] Baltabekov A.S., Koketaitegi T.A., Kim L.M. Eurasian Physical Technical Journal. V. 7 (2010). - p.12-17.

Green Emitting $\text{Ca}_3\text{SiO}_4\text{Cl}_2: \text{Eu}^{2+}$ Phosphor for Blue Converted White LEDs

Rupesh Talewar[#], Pooja Yadav[#], Charusheela Joshi[#] and S.V. Moharil^{\$}

[#]Physics Department, Shri Ramdeobaba College of Engineering and Management, Nagpur, India 440013

^{\$} Physics Department, RTM Nagpur University, Nagpur, India 440010

The first commercially available white LED based phosphor combines a blue light-emitting (In,Ga)N with a yellow $(\text{Y}_{1-x}\text{Gd}_x)_3(\text{Al}_{1-y}\text{Ga}_y)_5\text{O}_{12}:\text{Ce}^{3+}$ [1]. However, this type of white light has a poor color-rendering index (CRI), because of the color deficiency in the red region.

To solve this problem, green and red phosphors in combination with a blue LED and red, green, and blue phosphors with a UV LED were introduced [2]. Both these methods need efficient green phosphors. Several phosphors such as $\text{SrGa}_2\text{S}_4:\text{Eu}^{2+}$, $(\text{Sr},\text{Ba})\text{SiO}_4:\text{Eu}^{2+}$ have been suggested in the past as green components. However, there are issues of sensitivity and stability of such phosphors. Here, we describe synthesis of europium doped $\text{Ca}_3\text{SiO}_4\text{Cl}_2$ phosphor as a green emitter and fabrication of white LED using blue chip coated with this as green and $\text{SrS}:\text{Eu}$ as red phosphors[3,4].

Green emitting $\text{Ca}_3\text{SiO}_4\text{Cl}_2: \text{Eu}^{2+}$ phosphor was prepared by solid state reaction. $\text{Ca}_3\text{SiO}_4\text{Cl}_2: \text{Eu}^{2+}$ was characterized by XRD and excellent match was found with standard JCPDS file no. 24-0032. Photoluminescence excitation and emission spectra recorded on Hitachi F-7000 spectrophotometer show broad excitation extending from 250 nm to 480 nm and intense emission at 505 nm. Eu^{2+} concentration in $\text{Ca}_3\text{SiO}_4\text{Cl}_2$ was optimized to be at 1 mol%.

The phosphor in desired quantity was then dispersed in a transparent silicone resin (Wells Electronic Materials Company, 5012-2A and 5012-2B), and LED was then fabricated by coating the blue LED chip (CREE 450nm, 300 mm) with the epoxy resin. The electroluminescence (EL) spectra, colour temperature, CIE chromaticity coordinates, CRI and lumen output at room temperature were measured using a 300 mm integrating sphere and lumen meter (Hangzhou Zhongwei Photoelectricity Company ZVision ZW 3900).

White LEDs were fabricated by coating mixtures of $\text{Ca}_3\text{SiO}_4\text{Cl}_2: \text{Eu}^{2+}$ and $\text{SrS}:\text{Eu}$ phosphors on blue chip. All the phosphors can be excited by blue light. The phosphor combination along with blue chip provides all three emissions viz. blue, green, and red. Colour coordinates obtained were (0.3593, 0.2901) and CRI 75 for optimized phosphor concentration. These coordinates lie close to centre of the colour triangle. Thus $\text{Ca}_3\text{SiO}_4\text{Cl}_2: \text{Eu}^{2+}$ is a suitable phosphor for blue converted white LED.

References:

- [1] S. Nakamura and G. Fasol, The Blue Laser Diode: GaN Based Light Emitters and Lasers (Springer, Berlin) 1997, 216.
- [2] Y. Xu, L. Chen, Y. Li, G. Song, Y. Wang, W. Zhuang, Z. Long, Appl. Phys. Lett. 92 (2008) 021129
- [3] T. Yamashita, N Nada, H Onishi, S Kitamura, Health Phys. 21 (1971) 295.
- [4] R.P. Rao, J. Mater. Sci. 21 (1986) 4117

Scintillation properties of alkaline metal doped LiCaAlF₆

**Takayuki Yanagida¹, Masanori Koshimizu², Yutaka Fujimoto², Kentaro Fukuda³,
Go Okada¹**

¹*Nara Institute of Science and Technology*

²*Department of Applied Chemistry, Graduate School of Engineering, Tohoku University*

³*Tokuyama Corp.*

Scintillator is one of the luminescent materials which typically emit 1-6 eV photons when they are excited by ionizing radiations [1-2]. Many industries utilize scintillators, and most common applications are medical imaging and border security inspections. Recently, due to the internationally decreasing supply of ³He gas, development of alternative scintillator materials for thermal neutron detectors is of increasing demand. For this purpose, we have developed rare earth and transitional metal doped LiCaAlF₆ crystalline scintillators and scintillation detectors using LiCaAlF₆ (e.g., [3]). Among developed scintillators, Eu-doped LiCaAlF₆ showed the best performance and became a commercial product [4]. In order to improve the scintillation properties, we have carried out many experiments mainly in optimizing chemical compositions and synthesis processes. Throughout the course of R&D, we discovered Na co-doping improved the scintillation light yield [5]. Following this discovery, we found that alkaline metal co-doping improves scintillation light yield of Eu-doped LiCaAlF₆ and LiSrAlF₆ (e.g., [6]). However, the mechanism of the improvement is still unclear. In order to understand this phenomenon more deeply, in this work, we synthesized only alkaline earth elements (Na, K, Rb, Cs) doped LiCaAlF₆ crystals and investigated their optical and scintillation properties.

The sample crystals were synthesized by the μ -PD method in Tokuyama Corp. X-ray induced scintillation spectra and decay time profiles were compared with the nondoped LiCaAlF₆ sample. Then, emission/excitation spectra and decay time under vacuum ultra violet (VUV) photon irradiation at a synchrotron facility (UVSOR, Japan) were observed.

The synthesized crystals were in a typical size of 2 × 7 × 1 mm³. Scintillation was observed from 300 to 500 nm with a broad band in all the samples. In K and Cs doped LiCaAlF₆, very fast scintillation decay of a few ns was observed while we did not observe such fast signal in the other samples. Under VUV excitation using synchrotron radiation, alkaline earth doped LiCaAlF₆ showed a new band around 80-100 nm in addition to those in the nondoped LiCaAlF₆. Further, very fast luminescence similar with X-ray excitation was observed under VUV excitation. Therefore we propose one hypothesis that a new stable band is created by alkaline earth co-doping and energy migration efficiency at excitation processes may be improved. In the conference, further results will be presented and discussed in more detail.

References:

- [1] T. Yanagida, J. Lumin., 169 544 (2016).
- [2] T. Yanagida, Opt. Mater., 35 1987 (2013).
- [3] K. Watanabe, T. Yanagida, K. Fukuda, et al., Sens.Mater., 27 269 (2015).
- [4] T. Yanagida, N. Kawaguchi, Y. Fujimoto, et al., Opt. Mater., 33 1243 (2011).
- [5] T. Yanagida, A. Yamaji, N. Kawaguchi, et al., Appl. Phys. Exp. 4 106401 (2011).
- [6] S. Wakahara, T. Yanagida, Y. Yokota, et al., phys. status solidi (c) 9 2235 (2012).

ZnGa₂O₄:Cr and ZnGa₂O₄:Cr,Bi as new temperature sensing phosphors

Estelle Glais^{a,b}, Morgane Pellerin^{a,b}, Corinne Chanéac^a, Bruno Viana^b

^a*Sorbonne Universités, UPMC Univ Paris 06, CNRS, Collège de France, Laboratoire de Chimie de la Matière Condensée de Paris, 4 Place Jussieu, 75005 Paris, France
estelle.glais@etu.upmc.fr, corinne.chaneac@upmc.fr*

^b*PSL Research University, Chimie ParisTech – CNRS, Institut de Recherche de Chimie Paris, 11 Rue Pierre et Marie Curie, 75005 Paris, France
bruno.viana@chimie-paristech.fr*

Chromium (III) doped nanomaterials are investigated as new thermographic phosphors.^[1] ZnGa₂O₄: Cr³⁺ (ZGO:Cr) are synthesized by a new microwave way in aqueous medium and characterized by X-ray diffraction, transmission electron microscopy, scanning electron microscopy and optical spectroscopy.

The obtained 10 nm diameter nanoparticles synthesized by a soft chemistry method crystallize with normal spinel structure. They exhibit, after annealing at 1000°C, a high brightness persistent luminescence centered at 695 nm when doped with Cr³⁺ ions.

In this work the fluorescence emission decay is studied in a large temperature range (10 K-700 K), in order to investigate the ability of the host to be a wide temperature sensor. ZGO:Cr exhibits a high sensitivity versus temperature between 200 K and 500 K since the decay lifetime dramatically decreases with the temperature increase in that temperature range.^[2-4] Persistent luminescence decay is also studied, showing a significant change of the profile by varying the temperature.

Finally, comparison with co-doped chromium (III) and bismuth (III) zinc gallate oxide nanoparticles presenting enhanced persistent luminescent properties^[5] is presented. The obtained results could be used to determine the optimal design parameters for “nanothermometer” development. This kind of nanoprobe could allow a local temperature measurement for various applications in medicine (hyperthermia), marine, aeronautic or in the understanding of catalysis mechanisms.

References:

- [1] Jaque D. and Vetrone F. *Nanoscale*, 4 (2012) 4301-4326
- [2] Sharma S. et al. *Proceedings SPIE*, 9749 (2016) 974922
- [3] Chen D. et al. *Journal of the European Ceramic Society*, 35, (2015) 4211-4216
- [4] Venturini, F. et al. *Sensors and Actuators a-Physical*, 233, (2015) 324-329
- [5] Zhuang, Y. et al. *Journal of Materials Chemistry C* 1 47, (2013) 7849-7855

Defect luminescence and relaxation kinetics in amorphous yttrium-alumino-borate (a-YAB) phosphors

Atul D. Sontakke¹, Vinicius F. Guimarães², Pauline Burner², M. Salaun², Isabelle Gautier-Luneau², Lauro Maia³, Alban Ferrier¹, Bruno Viana¹, and Alain Ibanez²

¹PSL Research University, Chimie-ParisTech, CNRS, IRCP, 75005 Paris, France

²Inst NEEL, CNRS & UGA, F-38042 Grenoble, France

³Instituto de Física, Universidade Federal de Goiás, Goiânia/GO, Brazil

Phosphor converted white LEDs (pc-wLEDs) are considered as promising systems for overall lighting applications.¹ A dominant majority of wLED devices are based on the blue LED encapsulated with a yellow emitting YAG:Ce phosphor, giving rise to the white light output. YAG:Ce, due to its high luminescence quantum yield, strong absorption coefficient in blue region and high thermal stability is highly favourable phosphor for wLEDs. However, the low color rendering index (CRI ~ 81) of YAG:Ce based wLEDs limits their wide scale use in specific applications requiring high color rendering lighting. Several efforts are being made to improve the wLED properties, such as the use of mixed phosphors (YAG:Ce + K₂SiF₆:Mn⁴⁺), multiple LEDs (blue + green + red), broadband phosphors, etc.¹

Recently, we observed that the amorphous yttrium-alumino-borate (g-YAB) phosphors synthesized by the polymeric precursor (Pechini) method exhibit intense broadband emission from 400 nm to 750 nm generated by paramagnetic centers.² The luminescence covers whole visible spectrum with favorable CIE color coordinates for white light, exhibits high luminescence quantum yield (*i*-QY ~ 90%), excellent CRI (~ 94) and good stability over temperature and time under continuous excitation, which is ideal for the wLED phosphors. We further investigated the luminescence relaxation kinetics of the g-YAB phosphors. It has been observed that the broadband luminescence exhibits a fast nanosecond decay with decay lifetime $\tau < 10$ ns, as well as a slow persistence decay lasting for few seconds. Moreover, the time resolved spectroscopy revealed that the blue region emission exhibits relatively faster relaxation than the green-red region emission for both fast (ns) as well as slow persistence (s) decay kinetics. A systematic analysis suggests that the fast nanosecond component may be due to the intrinsic fluorescence decay of luminescent centers, whereas the slow persistence emission may be a result of thermal relaxation of trapped electrons at ambient temperature, as evidenced from the thermo-luminescence spectroscopy revealing the presence of a wide trap distribution in g-YAB phosphors.

References:

- [1] J. McKittrick, and L. E. Shea-Rohwer, *J. Am. Ceram. Soc.*, 97, 132, 2014.
 [2] V. F. Guimarães, L. J. Q. Maia, I. Gautier-Luneau, C. Bouchard, A. C. Hernandez, F. Thomas, A. Ferrier, B. Viana, and A. Ibanez, *J. Mater. Chem. C*, 3, 5795, 2015.

Dynamics of Sensitization in (Cr,Nd,Yb):YAG Ceramics

V. Lupei¹, A. Lupei¹, C. Gheorghe¹, S. Hau¹, A. Ikesue²

¹National Institute for Laser, Plasma and Radiation Physics, 077125, Bucharest Romania

²World Lab Co, Ltd., Nagoya

Sensitization of emission of the weakly absorbing Nd³⁺ laser ion with strongly absorbing 3d ions such as Cr³⁺ is currently considered of prospect for improvement of the laser performances under broad-band (lamp or solar radiation) pumping [1, 2]. Essential conditions for the efficient sensitization are good absorption of pump by sensitizer and highly efficient energy transfer ET to the active ion. Relevant information on the ET is provided by investigation of dependence of the emission decay of sensitizer and of temporal evolution of the acceptor excited population under excitation in sensitizer for different Cr and Nd concentrations C_{Cr} and C_{Nd} . Investigation and utilization of these processes in single crystals is restricted by the difficulties to control the doping due to the large differences between the segregation coefficients of these ions; however, the compositional versatility of the transparent ceramic materials [3] would enable tailoring of composition to grant the relevant information and maximum of performance. This paper extends the investigation [4] of ET in (x at.% Cr, y at.% Nd):YAG ceramics (x = 1, 2, y = 0, 1, 3) produced by solid-state synthesis. High-resolution decay of Cr³⁺ emission at 300K after 10 ns 445 nm pulse excitation in the ⁴T₁ band of Cr³⁺ evidences, besides the known non-exponential decay determined by electric dipole interaction with Nd³⁺ a very fast initial drop proportional to C_{Nd} , which can be attributed to superexchange coupling dominating ET to the n.n. and n.n.n. Nd³⁺ ions. These characteristics are confirmed by the evolution of Nd emission after excitation in Cr³⁺, which shows a sudden initial jump, consistent with the dominance of superexchange inside the near Cr-Nd pairs. Calculation of ET efficiency indicates increase from 52% for 1 at.% Nd to 77% for 2 at.% Nd. Modeling of CW laser emission under solar pumping evidences the positive role of sensitization; at the same time it indicates enhancement of heat generation compared with the materials without sensitization, caused by the larger quantum defect. It is found that the higher ET efficiency when increasing C_{Nd} within certain limits would be beneficial in improving the laser parameters (threshold, slope efficiency) but this will be accompanied by enhanced heat generation caused both by the increased contribution of the quantum defect between the Cr³⁺ luminescence and the Nd³⁺ emission and due to the self-quenching of Nd³⁺ emission. The possibility to avoid this last effect by subsequent energy transfer from Nd³⁺ to Yb³⁺ is considered and the characteristics of this process by co-doping the (Cr, Nd):YAG ceramics with Yb are reported; contribution of direct ET from Cr³⁺ to Yb³⁺ is also evidenced.

References:

- [1] Z. J. Kiss, R. C. Duncan, Appl. Phys. Lett. 5 (1964) 2000.
- [2] H. Yagi, T. Yanagitani, M. Nakatsuka, K. Ueda, Opt. Las. Technol. 39 (2007) 1295.
- [3] A. Ikesue, Y. L. Aung, V. Lupei, "Ceramic Lasers", Cambridge Univ. Press (2013).

[4] V. Lupei, A. Lupei, C. Gheorghe, A. Ikesue, J. Lumin. 170 (2016) 594.

Electron-phonon interaction of Pr³⁺ and Sm³⁺ in YAG

A.Lupei, V. Lupei, S. Hau, C. Gheorghe, A. Ikesue

¹*National Institute for Laser, Plasma and Radiation Physics, 077125, Bucharest
Romania*

²*World Lab. Co., Ltd, Nagoya, Japan*

The advent of RE³⁺-doped transparent ceramics and the comparative investigation of these materials with single crystals enables deepening the knowledge of their properties and applicative potential. This paper investigates comparatively the optical spectral characteristics of several less investigated RE³⁺ ions (Pr³⁺, Sm³⁺) in YAG, Czochralski crystals or ceramics, in the to attempt to elucidate the electron-phonon interactions effects in these systems. Common features in the spectra of crystals and ceramics can be associated to main centers - RE³⁺ in Y³⁺ dodecahedral sites, vibronic satellites or RE-RE pairs (with quadratic dependence on RE content). Similar to the previous studies on Nd:YAG [1], for a major difference is the small intensity in ceramics of the satellites connected to the perturbing effects of nearby nonstoichiometric defects – Y³⁺ in Al³⁺ octahedral sites. The new data of this work enable clarification of many aspects reported but, not explained in previous papers on Pr:YAG crystals or ceramics (for references see [2]).

Possible electron -phonon coupling effects in some transitions of Pr³⁺ [3] or Sm³⁺ [4] spectra of YAG crystals have been invoked previously, especially in connection with the elucidation of main centers electronic structure, but no analysis has been reported, due to interferences with multicenter structure. This work reports new spectral features associated to vibronic sidebands in Pr³⁺ ³H₄→¹D₂ 10 K absorption or Pr³⁺ ³P₀→³H₄, ¹D₂ →³H₄ emission spectra of YAG crystals and ceramics, and different mechanisms determining these spectral characteristics, involving especially intense IR sharp peaks of phonon spectra, are discussed [5, 6]. Several lines in the Sm:YAG ⁴G_{5/2}→⁴H_{5/2,7/2,9/2} emission spectra at 10K in ceramics show doublet structure similar to crystals [4]. A modeling in terms of quasi-resonant electron-phonon interaction between a vibronic and a pure electronic state [5] is presented. From the shapes of the lines and degree of resonance with peaks in Raman spectra, an estimation of the electron-phonon coupling strengths and the shifts of the electronic lines are done.

References

- [1]. V. Lupei et al, Phys. Rev. B **64**, 092102 (2001)
- [2]. O.K. Moune et al, Eur. Phys. J. D **19**, (2002) 275–291
- [3]. P. Caro, J. Less Common Metals, **126** (1986) 239
- [4]. S. B. Stevens, et al J. Appl. Phys. **70** (1991) 948-953.
- [5]. O.L. Malta, J. Phys. Chem. Solids **56** (1995) 1053.
- [6]. A. F.Campos et al, J. Phys. Chem. Sol. **61**, 1489 (2000)

Effects of Si Codoping on Optical Properties of Ce-doped $\text{Ca}_6\text{BaP}_4\text{O}_{17}$ from First-Principles Calculations

Lixin Ning,[†] Xiaoxiao Huang,[†] Zhiguo Xia,[‡]

[†] Center for Nano Science and Technology, Department of Physics, Anhui Normal University, Wuhu, Anhui 241000, China

[‡] School of Materials Sciences and Engineering, University of Science and Technology of Beijing, Beijing 100083, China

It was recently reported that Ce-doped $\text{Ca}_6\text{BaP}_4\text{O}_{17}$ displayed blue-green emission under excitation in the near-ultraviolet (UV) region and luminescence intensities can be greatly improved by codoping with Si. Here, a combination of hybrid density functional theory (DFT) and wave function-based CASSCF/CASPT2 calculations at the spin-orbit level has been performed on geometric and electronic structures of the material to gain insights into effects of Si codoping on its optical properties. It is found that the observed luminescence arises from 4f–5d transitions of Ce^{3+} occupying the two crystallographically distinct Ca1 and Ca2 sites of the host compound with comparable probabilities, with the energy of the lowest 4f → 5d transition of Ce_{Ca1} being slightly higher than that of Ce_{Ca2} . The codopant Si prefers to substitute for the nearest-neighbor (NN) P1 atom over the NN P2 atom around Ce^{3+} , and this preference induces a blueshift of the lowest-energy 4f → 5d transition, consistent with experimental observations. The blueshift originates from a reduction in 5d crystal field splitting of Ce^{3+} associated mainly with electronic effects of the NN Si_{P1} substitution, while the contribution from the change in 5d centroid energy is negligible. On the basis of calculated results, the energy-level diagram for the 4f ground states and the lowest 5d states of all trivalent and divalent lanthanide ions on the Ca^{2+} sites of $\text{Ca}_6\text{BaP}_4\text{O}_{17}$ is constructed and discussed in connection with experimental findings.

References:

[1] L. Ning, X. Huang, J. Sun, et al. J. Phys. Chem. C, 120 (2016), pp 3999–4006.

Ponderomotive forces mediate UV solid-state laser operation

**V.V. Semashko¹, O.R. Akhtyamov¹, A.S. Nizamutdinov¹, E.Sarantopoulou^{1,2} and
A.C.Cefalas^{1,2}**

¹*Kazan Federal University, 18 Kremlin str., Kazan, 420008, Russia*

²*National Hellenic Research Foundation, Theoretical and Physical Chemistry Institute, 48
Vassileos Constantinou Avenue, Athens 11635, Greece*

The effects of ponderomotive forces [1] following interaction of light with optical materials and interfaces are now best exploited in a wide range of scientific and technological applications such as atomic optics, nanotechnologies, isotope separation and laser cooling of atoms and molecules [2-4]. However, nowadays, there is a limited number of data demonstrating either solid-state surface modification from both enhanced bulk diffusion and surface adsorption of ambient atoms and molecules via ponderomotive forces [5], or mediated optical responses of nonlinear optical elements.

In this study, the impact of ponderomotive forces on the efficiency of UV solid-state lasers based on Ce:LiCaAlF₆ and Ce:LiLuF₄ single crystals are presented and discussed.

It is found that high power UV laser pumping accelerates diffusion of environmental molecules, dust or impurities, leading to molecular adsorption on the laser optical surfaces, causing thus inevitable degradation of laser performance. In contrast, the all the way transmitted optical pumping radiation through the laser active medium, cleans the exit aperture of the pumping radiation.

This work was performed under the financial assistance from the Russian Scientific Foundation grant (project №15-12-10026) and the Competitive Growth of Kazan Federal University among World's Leading Academic Centers.

References:

- [1] P.N. Lebedev Collected works. - Moskow: USSR Acad. Of Sci., 1963
- [2] A. Ashkin, Phys. Rev. Lett. 24 (1970) 156
- [3] V.I. Balikin, Vestnik RAN 81 (2011) 291
- [4] S.D. Zakharov, M.A. Kazaryan, N.P. Korotkov, JETP Letters 60 (1994) 322
- [5] E. Sarantopoulou, et al., Applied Surface Science 254 (2007) 804

Propagating, Confined and Interface Acoustic Phonon Modes in GaN/AlN Quantum Wells

Y. H. Zan, Q. Yuan and S. L. Ban

*School of Physical Science and Technology, Inner Mongolia University, Hohhot 010021,
China*

Dispersion relations and phonon modes of propagating, confined and interface acoustic phonons have been solved theoretically for symmetric AlN/GaN quantum wells (QWs). Contrary to the previous conclusion in an early year for a real QW structure^[1], some regular patterns for the existence of interface acoustic phonons are revealed. Numerical computation is performed for a AlN/GaN/AlN (25nm/20nm/25nm) QW, all the dispersion relations and phonon modes are obtained by using an elastic continuum model^[2]. The transition conditions between different phonon modes and the existence conditions of the three kinds of phonons especially for the interface phonon modes are discussed. With increase of wave vector, the dispersion relations split into four sections. Phonons in section one and three, from bottom to top, are confined in the GaN layer, and in section two and four are confined in AlN layers. Furthermore, the tangent of the dispersion relation at bottom of these sections approaches to the velocities of longitudinal and transverse acoustic phonons propagating in bulk materials in turns.

This work is supported by the National Natural Science Foundation of China (Grant No. 61274098).

References:

- [1] L. Wendler, V. G. Grigoryan, Surf. Sci. **206** (1988) 203
- [2] A. Balandin, K. L. Wang, Phys. Rev. B **58** (1998) 1544

Luminescence Properties of Organic-Inorganic Layered Perovskite-Type Compounds under Vacuum Ultraviolet Irradiation

Naoki Kawano, Masanori Koshimizu, Yutaka Fujimoto, and Keisuke Asai
*Department of Applied Chemistry, Graduate School of Engineering, Tohoku University,
 Sendai 980-8579, Japan*

Quantum confinement in semiconductors has been a subject of great interest from the viewpoint of the applications for optical devices as well as basic science. Among various materials having low-dimensional quantum confinement structure, Pb-based organic-inorganic perovskite-type compounds have attracted much attention due to their unique optical properties. We have been developing scintillation materials using these compounds. In recent years, the demand for fast scintillation materials has increased owing to their application in radiation detectors with excellent timing property and their ability to operate at a high counting rate. The large binding energy and oscillator strength of the exciton enables us to fabricate scintillation materials with an excellent timing response [1]. During the course of development, we found that the scintillation properties largely depend on the amine molecules used in the organic layer, in which no luminescence occurs. In order to reveal the origin of this dependence, the luminescence decay characteristics should be obtained under excitation (1) only in the inorganic layers and (2) both in the inorganic and the organic layers. In this report, we show that the excitation in the organic layers has little influence on the luminescence behavior.

The chemical formula of the sample compound is $(C_6H_5C_2H_4NH_3)_2PbBr_4$. Single crystals of the compound were grown by the solvent diffusion technique. The photoluminescence spectra and time profiles were measured using vacuum ultraviolet (VUV) light as an excitation source at UVSOR BL7B operated in single bunch mode.

Figure 1 shows the photoluminescence time profiles at 410 nm with excitation at 300 nm and 180 nm. In the case of the excitation at 180 nm, both the inorganic and the organic layers were excited. The decay characteristics were quite similar. Hence, these results indicate that the excitation in the organic layer has little influence on the luminescence and scintillation behavior.

References:

[1] K. Shibuya, et al., *Appl. Phys. Lett.* 84 (2004) 4370; K. Shibuya, et al., *Jpn. J. Appl. Phys.* 43 (2004) L1333; S. Kishimoto, et al., *Appl. Phys. Lett.*, 93 (2008) 261901.

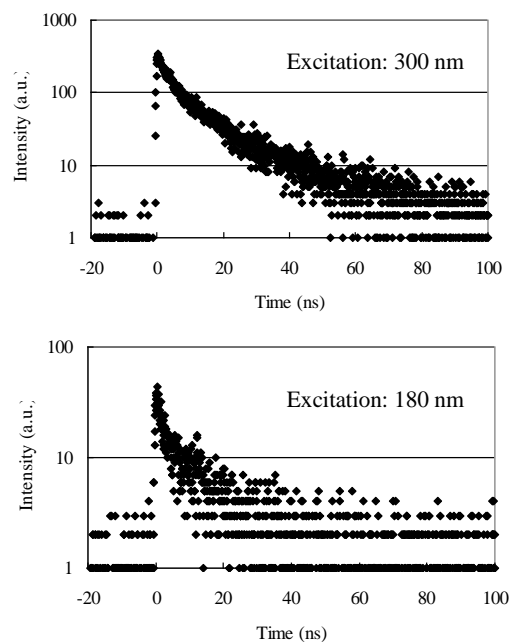


Fig. 2 Luminescence time profiles at 410 nm.

Cyclical Changes in Optical Properties of SrTiO₃ Structure

V.Gorbenko¹, G.Gorbenko²

¹Zaporizhe National University, Ukraine

²Classical Private University, Ukraine

Such process conditions as high temperature, pressure and pulsed laser acting are the causes of defects forming in the SrTiO₃ crystal structure one of which is oxygen vacancy. It has been good established the high concentration of oxygen vacancies can to change both optical and dielectric properties of samples. The Vis/UV spectroscopy and high vacuum system has been used for study of absorption spectrum changes that caused by cyclic consecution of annealing treatments under vacuum and oxygen enriched environment. Additionally the PCGAMESS [1] has been used for ab-initio calculations of Vis/UV absorption specters both ideal perovskite structure SrTiO₃ and oxygen vacancies with.

It has been established that the annealing of strontium titanate samples under vacuum leads to the appearing of new spectrum lines at 400-600 nm (fig.1). The lines intensity has been controlled by both the duration and the temperature of the annealing process. After the annealing of the samples in oxygen-enriched environment the strength of new lines were decreasing. The ab-initio calculations by Hartree-Fock (HF) and time dependent density functional theory methods (TDDFT) has shown the essential changes of crystal structure caused by the forming of oxygen vacancy. It has been obtained from the simulation the both oxygen vacancies and the changes of crystal structure are influencing on the Vis/UV spectrum and the appearing of lines at 300-600 nm range (fig.2).

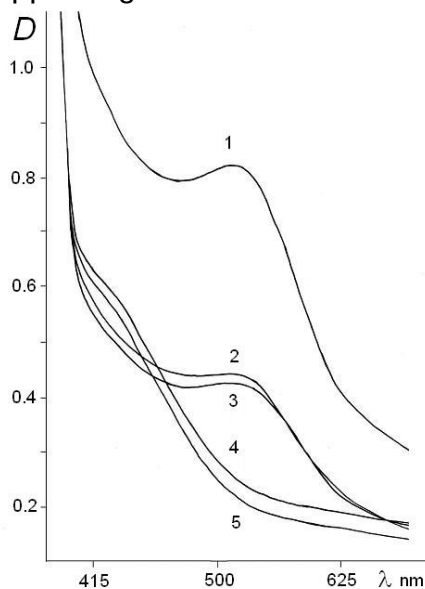


Fig.1 Experimental spectrum

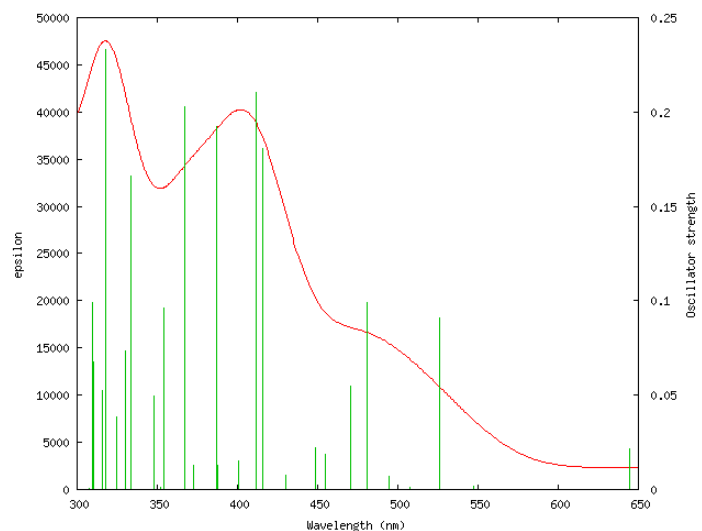


Fig.2 Spectrum obtained by ab-initio simulation

References:

[1] A.V.Nemukhin, B.L.Grigorenko, A.A.Granovsky, Moscow University Chemistry Bulletin, 2004, vol.45, No.2, P.75.

Polariton-like propagation of photoluminescence from exciton-exciton scattering in a GaAs/AlAs multiple-quantum-well structure

Yoshiaki Furukawa and Masaaki Nakayama

Department of Applied Physics, Graduate School of Engineering, Osaka City University, Japan

Exciton-exciton scattering is one of the prominent phenomena in optical properties of semiconductors under intense excitation condition [1]. The exciton-exciton scattering has mainly observed in wide band-gap semiconductors such as CdS, GaN, ZnO, and copper halides because the large exciton binding energies lead to the high stability of excitons. The exciton-exciton scattering in a GaAs bulk crystal, the exciton binding energy of which is 4 meV, has not been reported. Nakayama *et al.*, reported occurrence of the exciton-exciton scattering resulting from enhancement of the exciton binding energy by the quantum size effect in GaAs/AlAs multiple-quantum-well structures (MQWs) from an aspect of steady-state photoluminescence (PL) spectra [2]. In the present work, we have focused on the polariton-like PL dynamics of the exciton-exciton scattering in a GaAs/AlAs MQW.

The sample used was a GaAs (10 nm)/AlAs (10 nm) MQW grown on a (001) GaAs substrate by molecular beam epitaxy. For PL measurements, the excitation light source was a mode-locked Ti:sapphire laser with a pulse duration of 110 fs and a repetition rate of 76 MHz. The excitation energy was fixed at 1.640 eV. A streak-camera system with a time resolution of 15 ps was used for the detection of time-resolved PL spectra. All the optical measurements were performed at 10 K.

We confirmed from steady-state PL measurements that the exciton-exciton scattering appears with a threshold-like nature at an excitation fluence of $0.3P_0$, where the maximum excitation fluence P_0 is 0.10 mJ/cm^2 . Figure 1 shows the energy dependence of the decay rate of the exciton-exciton scattering at various excitation fluences. The decay rate was estimated from line-shape analysis of PL decay profiles using convolution of the system response and double exponential function. The decay rate of the exciton-exciton scattering systematically decreases with an increase in photon energy. In addition, the decay rate hardly depends on excitation fluence. This fact suggests that the decay rate is dominated by the final state of the exciton-exciton scattering process, which corresponds to the photon-like polariton in the lower polariton branch (LPB). The solid curve indicates the scaled group velocity of the photon-like polariton in the LPB calculated using a polariton equation. The energy dependence of the decay rate is consistently scaled by the polariton group velocity. This fact demonstrates that the exciton-exciton scattering reflects the polariton characteristics.

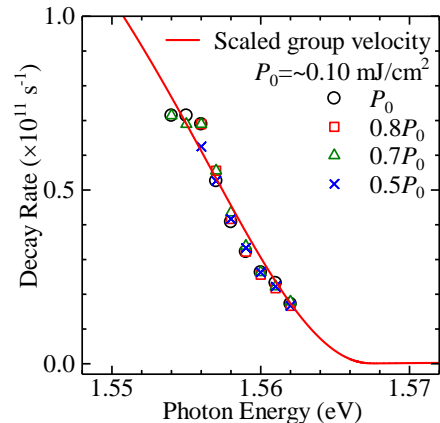


Fig. 1 : Energy dependence of the decay rate of the exciton-exciton scattering at various excitation fluences, where the solid curve depicts the scaled group velocity of the photon-like polariton.

References:

- [1] For a review, see C. Klingshirn and H. Haug, *Phys. Rep.* **70** (1981) 315.
 [2] M. Nakayama, T. Hirao, and T. Hasegawa, *J. Appl. Phys.* **105** (2009) 123525.

X-ray excited luminescence of $\text{Ba}_2\text{MgSi}_2\text{O}_7:\text{Eu}^{2+}$

Jing Yan^a, Chunmeng Liu^a, Jianbang Zhou^a, Pieter Dorenbos^b, Bingbing Zhang^c, Yan Huang^c, Ye Tao^c, Hongbin Liang^{a,*}

^a MOE Laboratory of Bioinorganic and Synthetic Chemistry, KLGHEI of Environment and Energy Chemistry, State Key Laboratory of Optoelectronic Materials and Technologies, School of Chemistry and Chemical Engineering, Sun Yat-sen University, Guangzhou 510275, China

^b Faculty of Applied Sciences, Delft University of Technology, Mekelweg 15, 2629 JB Delft, The Netherlands

^c Beijing Synchrotron Radiation Facility, Institute of High Energy Physics, Chinese Academy of Sciences, Beijing 100039, China

Eu^{2+} shows 5d-4f emission in a specific host when the energy of the relaxed lowest 5d state is below that of the $4f^7 \text{}^6\text{P}_J$ states. Its fluorescence decay constant is usually in the range of 0.2–2.0 μs and the emission band is tunable in the entire visible range, depending on the type of host. On the basis of these features, a variety of Eu^{2+} -activated luminescent materials have been investigated widely as phosphors in LED lighting and 3D displays as well as scintillators in detection devices [1-3]. $\text{Ba}_2\text{MgSi}_2\text{O}_7$ is an important host compound for luminescence of lanthanides and transition metal ions [2, 4]. In this paper, $\text{Ba}_2\text{MgSi}_2\text{O}_7$ phosphors activated with Eu^{2+} ions were prepared by a solid state reaction technique at high temperature. The excitation spectra in VUV–UV range, the emission spectra in UV–vis range, the decay time spectra and the temperature-dependent luminescence under X-ray and 370 nm UV light excitation together with the thermoluminescence spectra were investigated and discussed. The results demonstrated that the light yield of the optimal $\text{Ba}_{1.93}\text{Eu}_{0.07}\text{MgSi}_2\text{O}_7$ sample under X-ray excitation is more than three times higher in comparison with that of commercial BaF_2 , showing that a further optimized sample $\text{Ba}_{1.93}\text{Eu}_{0.07}\text{MgSi}_2\text{O}_7$ could be a potential scintillation material for X-ray detecting [5, 6].

References:

- [1] Chunmeng Liu, Zeming Qi, Chong-Geng Ma, Pieter Dorenbos, Dejian Hou, Su Zhang, Xiaojun Kuang, Jianhui Zhang, Hongbin Liang, *Chem. Mater.* 26 (2014) 3709.
- [2] Jing Yan, Lixin Ning, Yucheng Huang, Chunmeng Liu, Dejian Hou, Bingbing Zhang, Yan Huang, Ye Tao, Hongbin Liang, *J. Mater. Chem. C* 2 (2014) 8328.
- [3] Chunmeng Liu, Su Zhang, Zhiyu Liu, Hongbin Liang, Shuaishuai Sun, Ye Tao, *J. Mater. Chem. C* 1 (2013) 1305.
- [4] Jing Yan, Mikhail G. Brik, Chunmeng Liu, Dejian Hou, Weijie Zhou, Bingbing Zhang, Yan Huang, Ye Tao, Hongbin Liang, *Opt. Mater.* 43 (2015) 59.
- [5] Weijie Zhou, Dejian Hou, Fengjuan Pan, Bingbing Zhang, Pieter Dorenbos, Yan Huang, Ye Tao, Hongbin Liang, *J. Mater. Chem. C* 3 (2015) 9161.
- [6] Dejian Hou, Weijie Zhou, Cen Wu, Pieter Dorenbos, Hongbin Liang, Tsun-Kong Sham, Bingbing Zhang, Yan Huang, Ye Tao, *Phys. Chem. Chem. Phys.* 17 (2015) 22035.

Ce³⁺ to Tb³⁺ Energy Transfer in Ce₂(SO₄)

Aarti Iyer Muley, S.V. Moharil

*SIES College of Arts, Science and Commerce, Sion (West), Mumbai-22, India
Department of Physics, RTM Nagpur University, Nagpur, India*

Abstract: Energy transfer from Ce³⁺ to Tb³⁺ is observed in several luminescent materials and studied extensively during the last decades. The main interest is in the development of new and high efficient green energy phosphor used as a green component in the low pressure mercury vapor lamps. Lanthanum phosphate finds the application of Ce³⁺ to Tb³⁺ energy transfer and use as a commercial phosphor. The nano particles of cerium phosphate have also prepared and find intense green emission due to transfer of energy in Ce³⁺ to Tb³⁺. The stoichiometric compound Ce₂(SO₄) shows intense luminescence. It has been observed that when the Ce₂(SO₄) has synthesized by controlled precipitation method the emission changes from double humped spectra which has been observed at 335nm and the shoulder around 324nm to single emission at 344nm. The shift is due to the change of phase. However negligible energy transfer is observed for this compound. Also It is observed that doping of PO₄ during the synthesis process gives the efficient energy transfer from Ce³⁺ to Tb³⁺. The synthesis process to achieve this and the systematic study of Ce³⁺ to Tb³⁺ energy transfer is described in this paper.

References:

- [1] Gangyan Hong, Youmo Li, Lumin. Display Devices 5 (1984) 1-11.
- [2] G. Blasse, Chem. Mater. Chem. Phys. 16 (1989) 294-301.
- [3] J.L. Sommerdijk, J.A.W. Van Der Dose De Bye, P.H.J.M. Verberene. J. Luminescence 14 (1976) 9.
- [4] Thomal Justel, Jean-Claude Krupa, Detlef U. Wiechert J. Luminescence 93 (2001) 179-189.
- [5] Y.C. Kang, I.W. Lenggoro, S.B. Park, K. Okuyama Appl. Phys A 72 (2001) 1, 103-105.
- [6] Jianlin Shi Appl. Phys Lett 85 (2004) 4307-4309.

Luminescence Study of $\text{SrB}_4\text{O}_7: \text{Sm}^{2+}$ as Multimode Temperature Sensor with High Sensitivity

Zhongmin Cao, Yonghu Chen, Xiantao Wei, Changkui Duan*, Min Yin*

Department of Physics, University of Science and Technology of China, Hefei, Anhui

230026, P.R. China

Abstract

Sm^{2+} doped SrB_4O_7 was synthesized for the exploring high thermometry sensitivity. Highly thermal sensitive fluorescence intensity ratio and fluorescence lifetime were achieved in a wide range of temperatures. At 500 K, the relative sensitivities of temperature sensing are determined to be as high as $2.33\% \text{ K}^{-1}$ for fluorescence intensity ratio and $3.36\% \text{ K}^{-1}$ for fluorescence lifetime. Furthermore, the fluorescence color turns dramatically from deep red at room temperature to green at 700 K. Based on this color appearance, a visible temperature field was realized on a quartz glass covered with our sample, which could make thermal conduction and distribution visible with human eyes. These outstanding properties combined with the high thermal and chemical stability of the borate host make $\text{SrB}_4\text{O}_7: \text{Sm}^{2+}$ a promising material for high sensitive thermometry applications.

*Corresponding authors: ckduan@ustc.edu.cn (C.K. Duan) and yinmin@ustc.edu.cn (M. Yin).

Pathways of relaxation excited states of Pr^{3+} in $\text{Y}_2\text{Si}_2\text{O}_7: \text{Pr}^{3+}, \text{Yb}^{3+}$

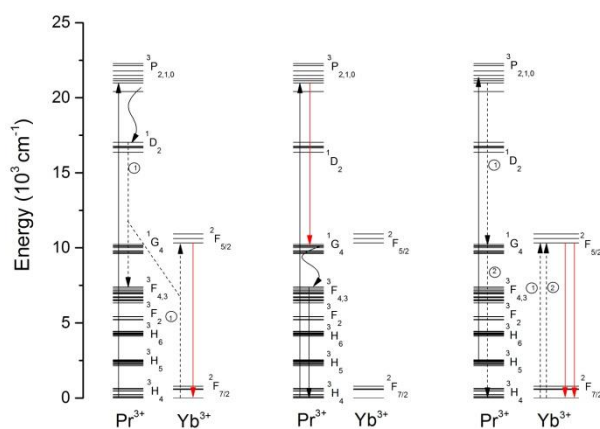
K. Grzeszkiewicz, W. Stręk, D. Hreniak

Institute of Low Temperature and Structure Research, Department of Spectroscopy of Excited States, Polish Academy of Sciences, Wrocław, Poland

corresponding author: k.grzeszkiewicz@int.pan.wroc.pl

A growing number of materials doped with rare-earth ions is extensively studied for quantum computation due to long coherence times of their optical and hyperfine transitions and the strong electric dipole–dipole coupling [1]. One of them is praseodymium doped yttrium orthosilicate ($\text{Y}_2\text{SiO}_5:\text{Pr}^{3+}$) which hyperfine interaction for the ground $^3\text{H}_4$ and excited $^1\text{D}_2$ states has been characterized in [2]. The impact of energy transfer on quantum computing schemes has been presented for $\text{Pr}^{3+}\text{-Ce}^{3+}$ pair in the same lattice by Serrano et.al. [3]. All these studies indicate the importance for the understanding of the course of energy transfer processes as well as the paths of depopulation of excited states of RE ions, especially in applications as a qubit and readout ions for quantum computing.

In this work yttrium disilicate co-doped with praseodymium and ytterbium ions ($\text{Y}_2\text{Si}_2\text{O}_7: \text{Pr}^{3+}, \text{Yb}^{3+}$) has been investigated due to characterization of energy transfer



pathways occurred in the system. Based on the spectroscopic techniques such as excitation and emission spectra measurements and on obtained luminescence decay times, a model of relaxation of $^3\text{P}_j$ and $^1\text{D}_2$ excited states of Pr^{3+} after Vis excitation has been proposed and verified. This work is a direct extension of research on downconversion mechanism in this material.

Fig.1 Pathways of relaxation of $^3\text{P}_0$ excited state of Pr^{3+} .

References:

- [1] R. Ahlefeldt, W. Hutchison, M. Sellars, J Lumin 130 (2010) 1594
- [2] J.J. Longdell, M.J. Sellars, N.B. Manson, Phys Rev B 66 (2002) 035101
- [3] D. Serrano, Y. Yan, J. Karlsson, L. Rippe, A. Walther, S. Kröll, A. Ferrier, P. Goldner, J Lumin 151(2014) 93

Chromium Pairs in Combustion Synthesized α -Alumina

Sarah Robitaille, J.K. Krebs, N. Dixon, and L. Fritz

Department of Physics and Astronomy, Franklin & Marshall College, Lancaster, PA 17603

High surface area alumina has gained much attention as a support structure for a number of possible biological and biomedical applications [1]. Combustion synthesis provides a simple route to produce large quantities of nano-crystalline alumina with optically active impurities after liquid phase mixing [2]. In this report, we present results on chromium ion separation in combustion-synthesized highly-doped ruby. The liquid phase mixing is achieved by dissolving stoichiometric ratios of aluminium and chromium nitrates in water/urea solutions. The solutions are then heated above 550 degrees, at which point they undergo a self-propagating combustion reaction converting them to high surface area solids. The structure is confirmed by X-ray diffraction to be that of single phase α -alumina. Optically excited fluorescence (excited at 473 nm) spectra were used to measure the ratio of the fourth nearest neighbour emission peak to that of the single ion peak [3] to quantify impurity clustering as a function of chromium concentration. Whereas the clustering in melt-grown single crystal ruby is observed to increase super linearly [4], the impurity clustering in the combustion synthesized materials is observed to increase linearly over a concentration range up to four atomic percent. The observed reduction in exchange coupling of ions is discussed in the context of the increased porosity of the high surface area materials.

References:

- [1] C. Toccafondi, S. Dante, A.P. Reverberi, M. Salemo, *Current Nanoscience* 11 (2015) 572-580
- [2] J.J. Kingsley and K.C. Patil, *Materials Letters* 6 (1988) 427-432
- [3] S.A. Basun, R.S. Meltzer, G.F. Imbusch, *Jour. of Luminescence* 125 (2007) 31-39
- [4] A.L. Schawlow, D.L. Wood, A.M. Clogston, *Phys. Rev. Lett.* 3 (1959) 271

Energy Transfer between Different Transitions within Rare-earth Ions

Jiuping ZHONG,^{1,2,*}Hongbin LIANG,¹Qiang SU¹

¹MOE Laboratory of Bioinorganic and Synthetic Chemistry, State Key Laboratory of Optoelectronic Materials and Technologies, School of Chemistry and Chemical Engineering, Sun Yat-sen University, Guangzhou 510275, China

²Center for Rare-earth Optoelectronic Materials, School of Metallurgy and Chemical Engineering, Jiangxi University of Science and Technology, Ganzhou 341000, China

Energy transfer between donor and acceptor is a common physical phenomenon, and the luminescence performance of optical materials is influenced directly by the energy transfer efficiency. In this work, the luminescence decay curves of energy transfer from f-f transition to d-f transition, from f-f transition to f-f transition, and from f-d transition to f-f transition within rare-earth ions were determined. And the luminescence dynamical formulas of the above energy transfer processes were provided according to the experimental results. In order to improve the luminescence performance of rare-earth phosphors using energy transfer mechanism between rare-earth ions, the competitive absorption of rare-earth activators codoped in one host were also investigated. It was found that the energy transfer efficiency is relative to the overlap of acceptor's absorption with the donor's emission.

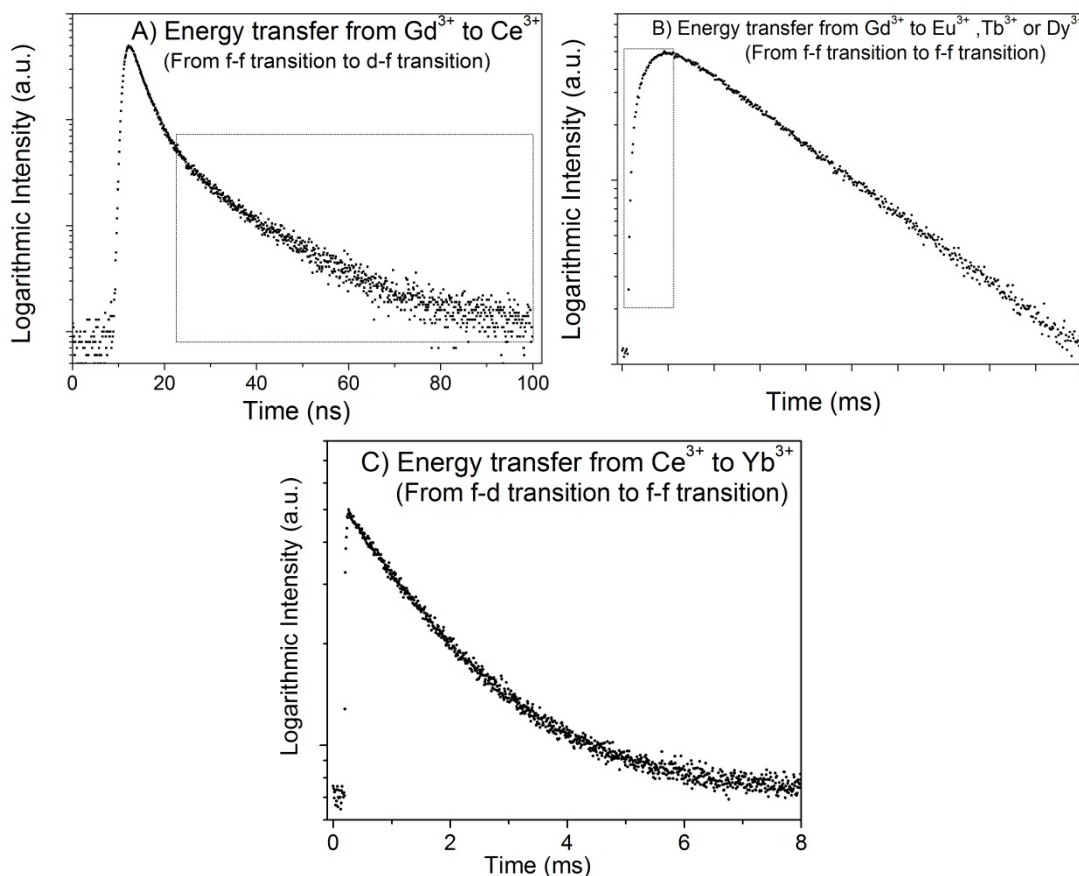


Figure 1 The Luminescence decay curves of energy transfer between different transitions within rare-earth ions.

* To whom correspondence should be addressed: zhongjp@mail.sysu.edu.cn
Tel: +86 20 8411 1037; fax: +86 20 8411 1038

Peculiarities of $\text{Er}^{3+} \leftrightarrow \text{Yb}^{3+}$ energy transfer in $\text{CaSc}_2\text{O}_4:\text{Er}:\text{Yb}$

A. Stefan^{1,2}, S. Georgescu¹, O. Toma¹

¹ National Institute for Laser, Plasma and Radiation Physics, Magurele, Jud. Ilfov, 077125, Romania,

² University of Bucharest, Faculty of Physics, Magurele, Jud. Ilfov, 077125, Romania

The calcium scandate ceramic samples doped with Er^{3+} and Yb^{3+} were synthesized by the solid state reaction method (at 1500°C for 4 h) from stoichiometric quantities of high purity oxides (Sc_2O_3 , Er_2O_3 , Yb_2O_3) and CaCO_3 .

The calcium scandate (CaSc_2O_4) is a new and promising host for efficient upconversion [1] due to low energy phonons (540 cm^{-1}), short distances between positions that can be occupied by the dopants (yielding an efficient energy-transfer) and high solubility of ytterbium ions. The room-temperature luminescence spectra were excited at 488 nm and 980 nm and recorded in the wavelength domain 500–1700 nm. $\text{Yb}^{3+} \rightarrow \text{Er}^{3+}$ energy transfer processes of the emitting levels of Er^{3+} are discussed and the back-transfer $\text{Er}^{3+} \rightarrow \text{Yb}^{3+}$ was evidenced. The decay curves of metastable levels (${}^2\text{H}_{11/2}$, ${}^4\text{S}_{3/2}$), ${}^4\text{F}_{9/2}$ of Er^{3+} and ${}^2\text{F}_{5/2}$ of Yb^{3+} were analyzed and the lifetimes of the metastable levels were measured. The upconversion luminescence is analyzed using luminescence spectra, power dependence of the emission intensity, and lifetime measurements.

Concentration-optimized $\text{CaSc}_2\text{O}_4:\text{Er}^{3+}/\text{Yb}^{3+}$ phosphor presents efficient $\text{Yb}^{3+} \rightarrow \text{Er}^{3+}$ energy transfer and strong green ($({}^2\text{H}_{11/2}, {}^4\text{S}_{3/2})(\text{Er}^{3+}) \rightarrow {}^4\text{I}_{15/2}(\text{Er}^{3+})$) and red ($({}^4\text{F}_{9/2})(\text{Er}^{3+}) \rightarrow {}^4\text{I}_{15/2}(\text{Er}^{3+})$) luminescence. The red/green intensity ratio is found to be mainly influenced by the energy back-transfer process ($({}^2\text{H}_{11/2}, {}^4\text{S}_{3/2})(\text{Er}^{3+}), {}^2\text{F}_{7/2}(\text{Yb}^{3+}) \rightarrow ({}^4\text{I}_{13/2}(\text{Er}^{3+}), {}^2\text{F}_{5/2}(\text{Yb}^{3+}))$).

Acknowledgment: This work was supported by (UEFISCDI), in the frame of the Project IDEI 82/06.10.2011

References:

[1] J. Li, J. Zhang, Z. Hao, X. Zhang, J. Zhao, Y. Luo, J. Appl. Phys. 113 (2013) p. 223507.

Initial process of photoluminescence dynamics in a β -Ga₂O₃ single crystal

Suguru Yamaoka, Yoshiaki Furukawa, and Masaaki Nakayama

Department of Applied Physics, Graduate School of Engineering, Osaka City University, Japan

Recently, one of wide-gap group-III oxides, β -Ga₂O₃, has attracted much attentions in applications for high-power field effect transistors and optical functional materials in a deep ultraviolet region. In the previous work, we demonstrate that self-trapped excitons (STEs) in a β -Ga₂O₃ single crystal are stable states relative to free excitons and the broad UV photoluminescence (PL) band is attributed to the STE emission [1]. In this work, we have investigated the initial process of the PL dynamics in a β -Ga₂O₃ single crystal from the viewpoint of the transformation process from free excitons to STEs.

The sample used was a (010)-oriented undoped β -Ga₂O₃ single crystal with a thickness of 0.60 mm. In the PL measurements, the excitation light source was a mode-locked Ti:sapphire laser with a pulse duration of 110 fs and a repetition rate of 4.8 MHz. The central energy of the fundamental laser light was doubled for two-photon excitation at 2.87 eV. A streak-camera system with a time resolution of 18 ps was used to detect time-resolved PL spectra.

Figure 1(a) shows the temporal PL profiles (circles) of the STE emission at temperatures from 10 to 250 K. The solid curves indicate the fitted results using convolution of system response and two exponential functions consisting of the PL rise and decay components. From the fitted results, the PL rise time at each temperature is almost constant and its value is obtained to be 23 ± 1 ps. Figure 1(b) shows the schematic diagram of the exciton and STE energy states. The PL rise time is mainly determined by the rate of tunnelling or thermal activation from the free exciton state to the STE state [2]. The result that there is no temperature dependence of the PL rise time indicates that the STEs in β -Ga₂O₃ are dominantly formed by the tunnelling process. Furthermore, it is expected that the barrier height E_b between the exciton state and self-trapped state is sufficiently higher than thermal energy at room temperature. This estimation is consistent with the theoretical value of $E_b = 0.10$ eV [3].

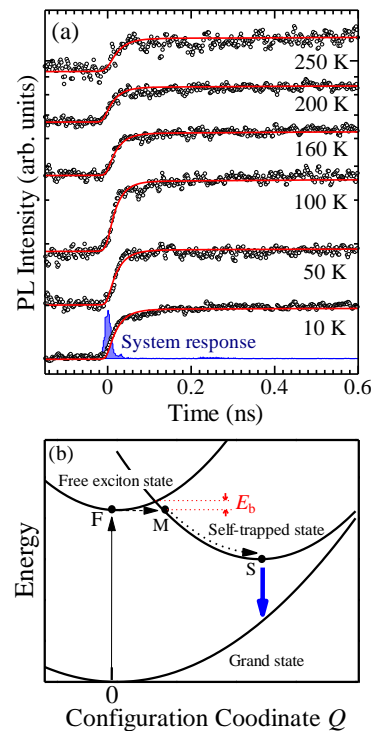


Fig. 1: (a) Temporal profiles (circles) of the STE emission at temperatures from 10 to 250 K, where the solid curves depict the fitted result. (b) Schematic diagram of the free exciton and STE energy states.

References:

- [1] S. Yamaoka and M. Nakayama, *Phys. Status Solidi C* **13** (2016) 93.
- [2] K. Nasu and Y. Toyozawa, *J. Phys. Soc. Jpn.* **50** (1981) 235.
- [3] J. B. Varley, *et al.*, *Phys. Rev. B* **85** (2012) 081109(R).

Luminescence of Ce³⁺ ion Activated Potassium Gadolinium Pyrosilicates Phosphor under Vacuum Ultraviolet and X-Rays Excitation

Haiyong NI^{1,2} Hongbin LIANG³ Lingli WANG^{1,2} Qihong ZHANG^{1,2}

¹(Guangdong Province Key Laboratory of Rare Earth Development and Application, GuangZhou, China, 510650)

²(The Institute of Rare Metals, GuangZhou Research Institute of Nonferrous Metals GuangZhou, China, 510650)

³(School of Chemistry and Chemical Engineering, Sun Yat-sen University, Guangzhou 510275, P. R. China)

Abstract: The phosphors, Ce³⁺ doped with Potassium gadolinium pyrosilicates K₃Gd_{1-x}Ce_xSi₂O₇ were prepared through a high-temperature solid-state reaction technique. The excitation and emission spectra in range of vacuum-ultraviolet-vis at 55 k, fluorescent decays and X-rays excitation luminescence (XEL) of Ce³⁺ in two sites both 6-fold octahedron coordination (trigonal antiprism tap) (Gd(1)³⁺) and 6-fold trigonal prism coordination (tp) (Gd(2)³⁺) were investigated, and the 5d centroid ϵ_c were calculated in view of crystal structure and an improved ligand polarization model. The results show that the emission spectra of phosphors K₃Gd_{1-x}Ce_xSi₂O₇ are composed of broad band with the strongest intensity at ~518 nm and color coordination (x=0.318, y=0.473), fluorescent lifetime $\tau_{1/e}$ and light yields are 98.1 ns and 3760 ph/MeV when Ce³⁺ concentration is 0.04 (mol/mol), respectively.

Keywords: Rare earth; Vacuum Ultraviolet; XEL; Potassium gadolinium pyrosilicates; phosphor;

References:

- [1] Alexander B., Kristin A. D., Nathan C. G., et al. Chem. Mater., 2012, 24, 1198–1204.
- [2] Li X.J., Jiao H., Wang X.M., J. Rare Earth, 2010, 28(4): 504 -508.
- [3] Yang P. P., Quan Z.W., Li C.X. et al. J. Solid State Chem., 2009, 182(5): 1045–1054.
- [4] Men D., Patel M.K., Usov I.O. et al. J. Am. Ceramic Soc., 2013, 96(10): 3325-3332.
- [5] Ingole D K , Joshi C P , Moharil S V , et al. Lumin. 2012, 27:24-27.
- [6] Shah K S, Cirignano L, Grazioso R, et al., IEEE Trans. Nuclear Sci., 2002, 49:1655-1660

Near-infrared Spectroscopy of Lattice Defects in Anion-defective Sapphire at 4-300K

Zh.K.Mamytbekov^{1,3*}, I.I. Milman¹, M.N. Sarychev¹, A.I. Syurdo²,
R.M. Abashev^{1,2}, V.S. Voinov¹

¹Ural Federal University, Russia

²Institute of Industrial Ecology UrB RAS, Russia

³Institute of Physical and Technical Problems and Material Science NAS KR, Kyrgyzstan

*zzhayloo@gmail.com

Due to its unique properties, corundum ($\alpha\text{-Al}_2\text{O}_3$) is widely investigated with different methods but many questions concerning its own color centers (F-type defects, interstitial Al atoms and their agglomeration) are still opened. Luminescence of corundum in the near infrared region does not have an adequately comprehensive description yet. In literature different methods are reported to induce complex defects in corundum by stoichiometric crystals, as for example high fluence irradiation, fast neutrons or high-energy electrons [1].

Here we present an optical spectroscopy investigation (200 - 2200 nm) as a function of temperature (4-300 K) on the effects induced by thermo-optical treatment (TOT) at 920 K on the color centers of anion-defective corundum. The complex color centers were created by irradiation of anion-defective corundum ($\alpha\text{-Al}_2\text{O}_{3,\delta}$) by using a mercury lamp at high temperatures [2]. Photoluminescence band

centered at 1,01eV has been detected only for anion-defective samples; the zero-phonon line at ~ 1.154 eV and phonon repetitions were observed in its excitation spectrum at temperatures below 200 K. This features were not seen in the stoichiometric and neutrons irradiated samples [3]. Moreover, TOT at 920 K or annealing to 1250 K did not have a noticeable effect on this band. All these findings indicate that the emission band of ~ 1 eV is related to color centers due to oxygen deficiency in the lattice different from F-type defects.

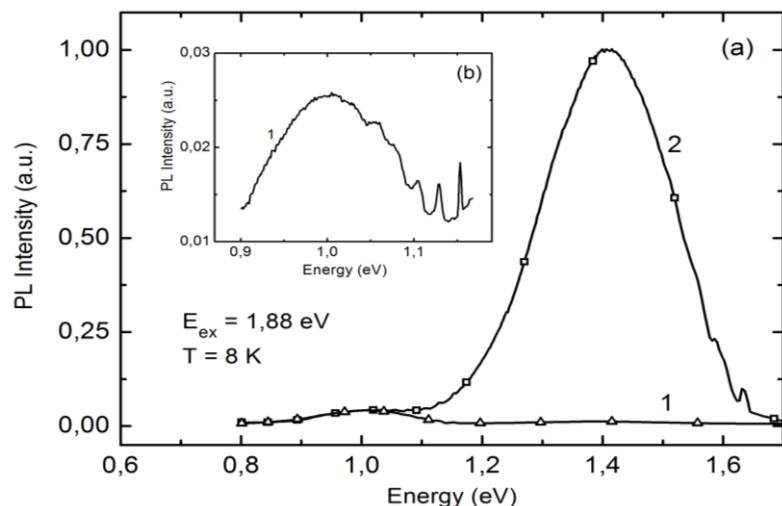


Fig 1. IR photoluminescence anion - defective corundum before TOT (1) and after (2). On (b) shows a fine structure before TOT.

References:

- [1] A.Z.M.S. Rahman et. al. Phys. Stat Sol A, **211**, 1535 (2014).
- [2] S.V.Solovyev et al. Solid-state physics, **54**, 683(2012).
- [3] B. D. Evans. Journal of Nuclear Materials, **219**, 2029 (1995).

Influence of synthesis parameters on the spectroscopic properties of $\text{Ca}_9\text{Y}(\text{PO}_4)_7$ doped with $\text{Eu}^{3+}, \text{Eu}^{2+}$

N. Gorecka, K. Szczodrowski, J. Barzowska, M. Grinberg

Institute of Experimental Physics, University of Gdansk, Wita Stwosza 57, 80-952 Gdansk, Poland, natalia.gorecka@ug.edu.pl

The main goal of the research was to investigate the spectral properties of the europium doped phosphate ($\text{Ca}_9\text{Y}(\text{PO}_4)_7$) which belongs to whitlockite-like family of phosphate minerals. Due to the presence of two different cations in the studied matrix (Ca^{2+} and Y^{3+}) that are available for europium substitution [2] the synthesis parameters were selected for incorporation of europium ions into the calcium sites (Sample 1), yttrium sites (sample 2) and equally (50/50) into the calcium and yttrium sites (sample 3).

The single phase phosphors were obtained using Pechini synthesis method. The method is based on a mixing of positive ions in a solution, controlled transformation of the solution into a polymer gel, removal of the polymer matrix and calcination of an oxide precursor with a high degree of homogeneity. A two-step strategy of synthesis was applied. This strategy involved an initial annealing of mixture of reagents under inert gas atmosphere and then, after cooling and grinding the product, the reduction - under hydrogen/nitrogen atmosphere. The phase composition analysis as well as spectroscopic measurements of products, were performed to characterize the obtained phosphors. The XRD patterns show, that we obtained the 100% pure $\text{Ca}_9\text{Y}(\text{PO}_4)_7$ in all cases. Emission spectra of materials obtained after first step of the synthesis consist of narrow bands, which are characteristic for $^5\text{D}_0 \rightarrow ^7\text{F}_J$ transitions in Eu^{3+} ion. However in 450 nm-550 nm spectral range we can also see a broad band originating from europium ion on +2 oxidation states. The emission spectra of materials, which were obtained after reduction process, are characterized by the intensive, broad band attributed to the d-f transitions in Eu^{2+} and slight line at 619 nm attribute for the europium 3+ ion [1,3]. The time resolved emission spectrum measurement were carried out to confirm the transition nature.

Reference to a journal publication:

- [1] O.Liu, Y.Liu, Z.Yang, X.Li, Y.Han, Spectrochimica Acta Part A 87 (2012) 190-193
- [2] Y.Lu, C.H.Huang, T.M.Chen, J.H.Lin, Y.R.Ma, J.L.Chen, C.C.Hsu, C.L.Chen, C.L.Dong, T.S. Chan, Chemical Physics Letters 515 (2011) 245-248
- [3] B.Wang, Y.Lin, H.Ju, Journal of Alloys and Compounds 584 (2014) 167-170

Photoemission Calculations using Projection Operator Method for Metals and Semiconductors.

B.Zoliana^{*1} and R.K.Thapa²

¹ Department of Physics, Govt. Zirtiri Residential Science College, Aizawl, Mizoram, India

² Department of Physics, Mizoram University, Aizawl, Mizoram, India.

*Corresponding author: bzoliana@gmail.com, Phone: +919436140347.

Key words: photocurrent, Kronig-Penney model, projection operator method of group theory, initial state wavefunction, surface state.

Photoemission spectroscopy has been used as an investigative method for the conceptual understanding of the behaviour of electrons in the surface and bulk of a solid. Theoretically photocurrent is calculated by evaluating the matrix element $\langle \Psi_f | H | \Psi_i \rangle$ involved in the photocurrent density formula as given by Fermi golden rule. Due to the presence of the surface, the calculations of electronic states $|\Psi_i\rangle$ is a complicated problem. A model wave function Ψ_i has been developed for calculation of photocurrent from Cu (110) surface where surface states were found to be existing in the band gap L_2-L_1 and in our calculations we have considered the surface state at symmetry point L_2 . A projection operator method of group theory has been used in deriving the initial wavefunction Ψ_i and the wavefunction was deduced for a periodic crystal potential which was defined by Kronig -Penney δ - function type. The final state wavefunction Ψ_f is the scattering state of step potential which is encountered by the electron. This model derivation of Ψ_i is further applied to semiconductors and the photocurrent data showed interesting features conforming to experimentally measured results for semiconductor as well.

Reference:

- [1]. E Bertel, Phys. Rev. B50, (1995) 4925
- [2]. J.F.Cornwell, Group Theory and Electronic Energy Bands in Solids, Amsterdam-London (North Holland,1969), p.54
- [3]. S. L. Weng, T. Gustaffson and E. W. Plummer, Phys. Rev. B18, (1978) 1718
- [4]. B.Zoliana, Ph.D. thesis- Theoretical Formulation of Initial State wavefunction using Projection Operator Method of Group Theory, North Eastern Hill University, Shillong, India (2004).

Luminescence properties and energy transfer of $\text{GdBO}_3:\text{Ce}^{3+},\text{Tb}^{3+}$ phosphor

QiuHong Zhang, Haiyong Ni, Lingli Wang, Fangming Xiao

Guangdong Province Key Laboratory of Rare earth development and Application, Guangdong Research Institute of Rare Metals, Guangzhou 510650, China

Abstract: Ce^{3+} and Tb^{3+} singly doped and co-doped GdBO_3 phosphors were synthesized by solid state reaction. The crystal structure, luminescent properties, the lifetimes and the temperature-dependent luminescence characteristic of the phosphors were investigated. Through an effective energy transfer, the emission spectra of $\text{GdBO}_3:\text{Ce}^{3+},\text{Tb}^{3+}$ phosphor contains both a broad band in the range of 340-450 nm originated from Ce^{3+} ions and a series of sharp peaks at 487, 542, 587 and 625 nm due to Tb^{3+} ions. The energy transfer mechanism from Ce^{3+} to Tb^{3+} in GdBO_3 host is also investigated. Based on the principle of energy transfer, the emission intensity ratio of Ce^{3+} and Tb^{3+} could be appropriately tuned by adjusting the contents of activators.

References:

- [1] C.F. Guo, X.Ding, H.J. Seo, Z.Y. Ren, J.T. Bai, Opt. Laser Technol. 43 (2011) 1351–1354.
- [2] G. Zhu, Y.H. Wang, Z.P. Ci, B.T. Liu, Y.R. Shi, S.Y. Xin, J.Lumin. 132 (2012) 531–536.
- [3] Q.H. Zhang, H.Y. Ni, L.L. Wang, F.M. Xiao, Ceram. Int. 42 (2016) 6115-6120.

MREI-model Calculation of Two-mode Property of Bulk Transverse Optical Phonons and Its Influence on Electronic Mobility in $\text{Al}_x\text{Ga}_{1-x}\text{N}/\text{GaN}$ Quantum Well

Z. Gu, Y. Qu, and S. L. Ban

School of Physical Science and Technology, Inner Mongolia University, Hohhot 010021, China

Two-mode property of bulk transverse optical phonons (TO_1, TO_2) has been calculated using modified random element isodisplacement (MREI) model in ternary mixed crystals of wurtzite $\text{Al}_x\text{Ga}_{1-x}\text{N}$. The influence of the two-mode property on the interface (IF) phonon modes and confined (CO) phonon modes in $\text{Al}_x\text{Ga}_{1-x}\text{N}/\text{GaN}$ quantum wells (QWs) is considered by a method of probability. Based on the dielectric continuous model, uniaxial model and Lei-Ding balance equation^[1], electrostatic potentials of IF modes and CO modes and their influence on electronic mobility in QWs are discussed. The results show that the total electron mobility decreases with increase of Al component and symmetric IF modes plays a major role on electronic mobility. Electronic scattering of IF and CO phonons influenced by TO_1 of $\text{Al}_x\text{Ga}_{1-x}\text{N}$ becomes stronger than that influenced by TO_2 with increase of Al component in a $\text{Al}_x\text{Ga}_{1-x}\text{N}/\text{GaN}$ QW. As a comparison, the electron mobility is calculated for a $\text{Al}_{0.58}\text{Ga}_{0.42}\text{N}/\text{GaN}$ QW at room temperature and our result is $1222.3\text{cm}^2/\text{Vs}$ which is 1.4 times of the experimental value^[2]. Our result is expected since the difference between our theory and the experiment is mainly due to the neglect of interface roughness and other secondary scattering mechanism. Furthermore, a comparison with the previous approximation of bulk transverse optical phonons is given to show the reasonability of our model.

This work is supported by the National Natural Science Foundation of China (Grant No. 61274098).

References:

- [1] X. L. Lei, C. S. Ting, Phys. Rev. B **30**(1984) 4809
- [2] K. Hoshino, T. Someya, Y. Arakawa, Phys. Stat. Sol. (a) **188**(2001) 877

Anomalous Polaritonic Luminescence from Rare-Gas Solids

A. N. Ogurtsov, N. F. Kleshchev, O. N. Bliznjuk

National Technical University "KhPI", Frunse Str. 21, Kharkov, 61002, Ukraine

Polaritonic phenomena interconnected with excitonic spatial dispersion were extensively explored theoretically and experimentally. The exciton-photon interaction leads to the formation of polaritonic states energetically positioned at both sides of the initial exciton. In a large ideal crystal of cubic symmetry, where the interval of the longitudinal-transverse splitting does not contain excitonic levels, the polaritonic dispersion branches lie beyond this interval at both sides of its boundaries. On the contrary, in a crystalline grain comparable or less in size than the wavelength in the substance, the interval of the longitudinal-transverse splitting is filled in continuously by excitonic states intercepting a significant part of the oscillator strength of the excitonic transition. In the previous experiments with polycrystalline samples of solid Kr and Xe the formation of the lower polaritonic state was traced by the red shift of the luminescence spectrum relative to the bottom E_1 of the lowest excitonic band ($E_1^{\text{Kr}}=10.14$ eV; $E_1^{\text{Xe}}=8.36$ eV).

In the present report we explore the new crystal growing technique, which allowed to obtain the solid Kr and Xe samples with essentially improved crystallographic properties and to resolve the internal structure of the luminescence bands at the edge of exciton absorption. The photoluminescence experiments were carried out at the SUPERLUMI experimental station at HASYLAB, DESY, Hamburg. Unlike previous works, where the observed red polaritonic shift was small commensurably with a weak inelastic polariton-photon scattering, a large polaritonic shift of luminescence is not due to energy dissipation, the energy conservation law being met due to equal probabilities for opposite-sign energy shifts. Such effect is possible if the crystalline grains are comparable in size with light wavelength, which provides the filling in the interval of the longitudinal-transverse splitting by excitons with sufficient oscillator strength. And the sample structure must be perfect enough to lowering the exciton scattering rate with respect to the rate of the polariton formation through exciton-photon coupling.

For the first time the excitation spectra of free-exciton luminescence band were recorded simultaneously below E_1 and within the interval of the longitudinal-transverse splitting. The luminescence of non-equilibrium polaritons was observed both within the longitudinal-transverse splitting interval and at photoexcitation below the bottom of the excitonic band. The excitation spectrum below E_1 is determined by competition of two processes. The first one is the creation of excitons by photons with energy E_1 at the Lorenz tail of excitonic absorption. The second process is a competing absorption related to the direct formation of two-site excitonic polarons (self-trapped excitons). Both excitation spectra of polaritonic luminescence below E_1 and within the longitudinal-transverse splitting interval show high sensitivity to crystal quality of the samples.

Nonlinear composition dependent optical spectroscopy of $\text{Ba}_{2x}\text{Sr}_{2-2x}\text{V}_2\text{O}_7$

Hongwei Fang, Yonghu Chen, Changkui Duan & Min Yin

Department of Physics, University of Science and Technology of China, Hefei 230026, China

Abstract:

In general, changing the composition of fluorescent materials is an effective way to adjust luminescent properties such as emission peak's shift. In most solid-solutions, this shift is usually linearly dependent on the material composition, which is referred to as Vegard's Law. However, we found extraordinary variations in our samples $\text{Ba}_{2x}\text{Sr}_{2-2x}\text{V}_2\text{O}_7$ (BSVO), i.e., both the excitation and the emission peaks show nonlinear dependence on the composition x , and the same are true for the spectral bandwidths. The nonlinearities are not due to structural anomaly as all the samples are confirmed to be solid-solutions by XRD measurements. To explain this phenomenon, we proposed a model by considering the disorder of Ba^{2+} and Sr^{2+} distributions in solid-solutions and the changes of configurations between the ground and excited electronic states. This novel phenomenon could be applied in color-tunable photoluminescence, and may be further exploited for new fluorescent materials.

Reference:

1. Kim, T. W., Yuan P., Galli, G. A. & Choi K. S. Simultaneous enhancements in photon absorption and charge transport of bismuth vanadate photoanodes for solar water splitting. *Nat. Commun.* **6**, 8769 (2015)
2. Semih, A., Frank, K., Christian, M., Andreas, B. & Reinhard, N. New high capacity cathode materials for rechargeable Li-ion batteries: Vanadate-borate glasses. *Sci. Rep.* **4**, 7113 (2014)

The environmental factor model: a tool for the design of Eu^{2+} -doped orthophosphate phosphors?

Mariam Amer^a, Philippe Boutinaud^b

Université Clermont Auvergne, ^aUBP / ^bSIGMA Clermont, Institut de Chimie de Clermont-Ferrand, BP 10448, F-63000 Clermont-Ferrand

Developed in the late 60's, the dielectric theory of chemical bonding has been successfully applied in a wide variety of physical problems before being extended to phosphors as a possible predictive tool¹⁻³. One aspect of interest is the use of this semi-empirical model to evaluate relationships between the host environment and the crystal field splitting (CFS) or the centroid energy (E_c) of the $4f^{n-1}5d^1$ electron configuration of ions like Eu^{2+} ^{1,2}. Following the model, it is assumed (1) that E_c is determined mostly by the fractional covalence of the chemical bonds between the central ion and the nearby anions, the effective charge Q of the neighboring anions and the chemical bond volume polarizability and (2) that the magnitude of the CFS is determined mostly by the homopolar part of the average energy gap, the coordination number of the central ion, the fractional bond ionicity between the central ion and the nearby anions and Q . The above parameters are combined in the calculation of "environmental factors". They can be obtained from the knowledge of the crystal structure of the host lattice. The first motivation of this work is to evaluate the relevancy of this model on the case of the phosphates $\text{ABPO}_4:\text{Eu}^{2+}$ with $A = \text{Li}^+$, Na^+ , K^+ and $B = \text{Mg}^{2+}$, Ca^{2+} , Sr^{2+} , Ba^{2+} . These lattices are known to show interesting luminescence properties upon blue and near-UV excitations but they present many possible crystal structures and a variety of possible sites for Eu^{2+} which makes the rationalization of the situation rather difficult. A good illustration of this issue is the member $\text{NaMgPO}_4:\text{Eu}^{2+}$ that shows either blue or red emission depending on the preparation method^{4,5}. The second motivation of this paper is to evaluate the relevancy of the environmental factor model to be used as a tool for the design of orthophosphate lattices doped with Eu^{2+} .

References

- [1] J. S. Shi, Z. J. Wu, S. H. Zhou, S. Y. Zhang, Chem. Phys. Lett. 380 (2003) 245
- [2] J. S. Shi, S. Y. Zhang, J. Phys. Chem. B 108 (2004) 18845
- [3] Q. Su, J. Wang, J. S. Shi, J. Solid State Chem. 183 (2010) 1174
- [4] W. Tang, Y. Zheng, Luminescence 25 (2010) 364
- [5] S. W. Kim, T. Hasegawa, T. Ishigaki, K. Uematsu, K. Toda, M. Sato, ECS Solid State Letters 2 (2013) R49

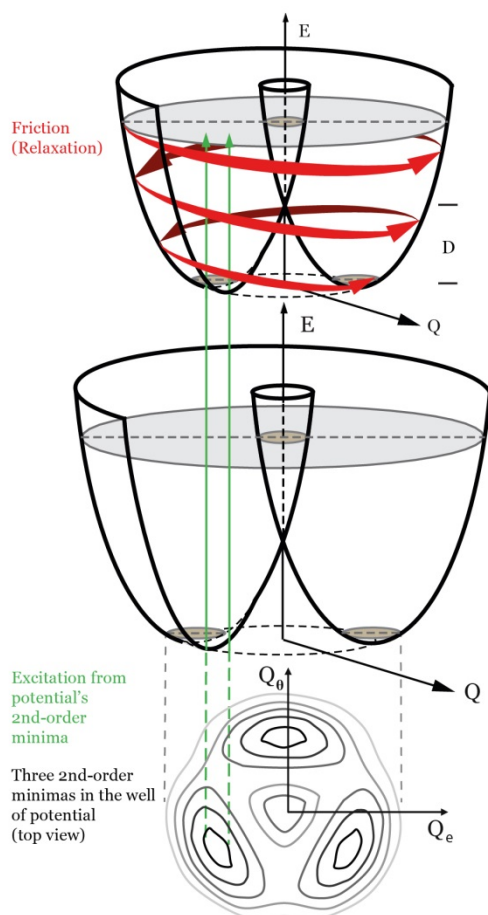
Relaxation through conical intersection: quantum friction of pseudorotation and Slonczewski resonances

Kaja Pae and Vladimir Hizhnyakov

Institute of Physics, University of Tartu, W.Ostwaldi 1, 50411 Tartu, Estonia

e-mail: kaja.pae@gmail.com

To the best of our knowledge first time a rigorous quantum-theoretical description of the relaxation of a vibronic system (impurity center or impurity molecule in a crystal or in solution) through the conical intersection of the potential surfaces is given with taking into account the motion of the system around the intersection. The process under consideration determines the speed of chemical and photochemical reactions and the rate of non-radiative de-excitation transitions from excited electronic states to the ground electronic state. We present here a novel theoretical study of the conceptually important E_xe-type Jahn-Teller effect with taking into account that phonons with non-zero momentum are causing the relaxation.



The dependence of the relaxation through the conical intersection on the rotational momentum of the vibronic system is elucidated for the first time. Also an analytical description of the quantum states of the conical intersection (Slonczewski resonances) is given. It is found that there is a finite probability of the speeding-up of the pseudorotation of the system at the intermediate stage of relaxation. In particular, this probability increases close to the Slonczewski resonances. During the relaxation, the system may change the direction of the pseudomomentum; the probability of such a change also increases near the resonances.

A number of features of the relaxation through the conical intersection of quantum origin resulting from these resonances are found. Although only the effects of phonons in E_xe-problem were considered here, our method [1-2] is quite general and it can be used for consideration of relaxation and other effects caused by phonons in any vibronic system with a finite number of degenerate or quasi-degenerate electronic levels.

References:

- [1] Hizhnyakov, V.; Pae, K.; Vaikjärv, T. (2012). Optical Jahn-Teller effect in the case of local modes and phonons. *Chem. Phys. Lett.*, 525–526, 64–68.
- [2] Pae, K.; Hizhnyakov, V. (2014). Time-dependent Jahn-Teller problem: Phonon-induced relaxation through conical intersection. *J. Chem. Phys.*, 141 (23).

Electroluminescence of PLZT Relaxor Ceramics at Fast-rising Electric Fields

S. A. Sadykov¹, S. N. Kallaev²,

¹Dagestan State University, 367000 Makhachkala, Russia

²Institute of Physics, Dagestan Scientific Center, Russian Academy of Sciences, 367003
Makhachkala, Russia

e-mail: ssadyk@yandex.ru

This work presents the results of an investigation on the temperature dependence of the electroluminescence intensity I_{EL} and its relationship with integral characteristics of the polarization switching in PLZT9/65/35 ceramics under the influence of unipolar high voltage pulses supplied at a controlled rate. The sample was of plate shape with dimensions of $10 \times 9 \times 1.1$ mm, on which silver electrodes were applied by fusion without edge protrusions. The experiments have been performed on a high voltage setup providing the rate of an electric field buildup of $E = 0.1$ kV/(mm· μ s). The emission pulses were detected by a photomultiplier with maximum spectral sensitivity in the 420–550 nm wavelength interval. The sample was oriented so that its rear side was facing the photomultiplier entrance window. The measurements were performed at sample temperatures in the 0–60°C interval, which included the point ($T_m \approx 60^\circ\text{C}$) corresponding to the maximum permittivity of ceramics.

Figure 1 presents the temperature dependences of a critical field E'_c (dynamic coercive field) for the start of domain reorientation, which corresponds to the onset of emission buildup, and the emission intensity amplitude I_{EL} (approximately determined by averaging the amplitude of separate peaks). A growth in the integral emission intensity I_{EL} with the temperature is related to the increase in both the amplitudes of separate flashes and their number during the switching time. The emission pulses also consisted of a discrete set of spectral lines and had multistep shapes related to a cascade growth and transformation of separate polar regions switched in strong increasing electric fields.

Similarly to the case of classical ferroelectrics, E'_c in PLZT 9/65/35 ceramics decreases when increasing the temperature, which is indicative of a decrease in the internal bias fields. An increase in the integral emission intensity I_{EL} is not proportional to a change in the value.

Moreover, the time of establishment of a polarized state in a strong field (at a switching time of $t_s \approx 50 \mu\text{s}$) determined from the duration of emission, shortens with temperature fall that is the formation and evolution of the domain structure gains strength (what, in turn, enhances the emission intensity).

It can be suggested that under the influence of a rapidly growing external field, separate microscopic regions with individual characteristic critical start fields are sequentially involved in the process of domain structure formation and rearrangement. The spread of these regions with respect to the internal and coercive fields determines the temporal scatter of separate emission peaks. The duration of each emission peak is about $0.1\text{--}0.5 \mu\text{m}$. If these periods correspond to the switching of nanodomains or nanopolar regions in ceramic grains, then we can speak for a domain mechanism of polarization switching, the dynamics of which is controlled by the nucleation rate.

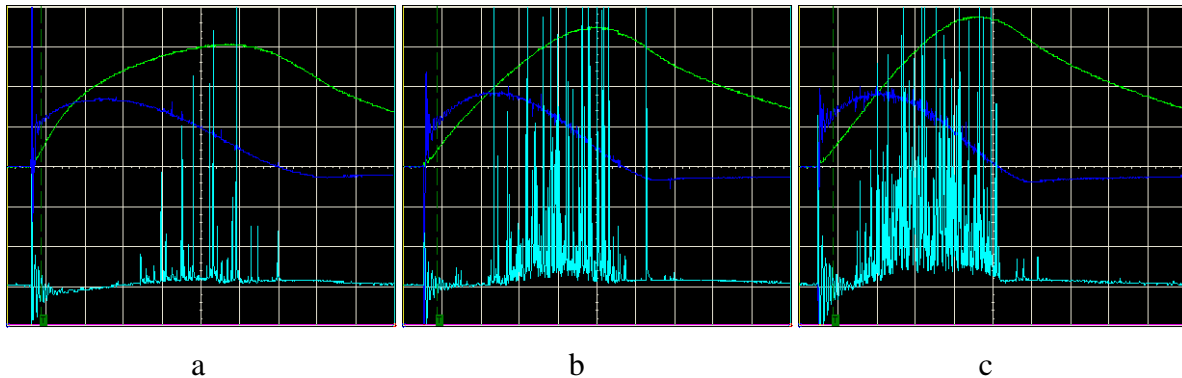


Fig. 1. Waveforms showing correlation of the electro luminescence pulses (lower curves) with the applied voltage (upper curves-green) and switching current (middle curves-blue) for PLZT 9/65/35 ceramics at 0°C (a), 40°C (b) and 60°C (c). Time (abscissa) scale, $10 \mu\text{s}/\text{div}$; voltage (ordinate) scale, $0.8 \text{ kV}/\text{mm}$.

Our experiments show that the electro luminescence intensity in relaxor ferroelectric ceramics increases with the period of time between sequential polarizing voltage pulses until reaching the initial level. Therefore a residual depolarizing field that is created by the charges bound at interfaces leads to a spontaneous decay of the polydomain state. The relaxation time of this process, as determined from measurements of the electro luminescence intensity and dielectric permittivity, amounts to $\sim 5 \text{ min}$.

Green Emission of U^{6+} activated Lithium based Tungstates

S.S. Pote

*Physics Department, St. Vincent Pallotti College of Engineering and Management,
GavsiManapur, Wardha Road, Nagpur-441 108*

E-mail: swapnilspote@gmail.com, swap_pote@yahoo.com

ABSTRACT

Rare earth activated lithium compounds with rocksalt lattice structure have received attention of several research workers specially working in the area of Solid state lighting. In this paper we have reported several hosts of Lithium based tungstates activated with various concentrations of uranium and photoluminescence spectra of U^{6+} was studied with reference to their crystal structure and X-ray diffraction studies of the prepared hosts.. The title compounds were prepared by usual high temperature ceramic procedures[1] with two step thermal annealing at 400° and 950° C. In the octahedral symmetry, the U(VI) luminescence originates from the ${}^4Y_{7u} \rightarrow {}^{12}Y_{8u}$ transition [2]. For 0.5 and 1 mol% U, highest intensity green emission was observed with a maximum at 524 and 517 nm respectively corresponding to near-UV excitation.

Therefore it is suggested that these characteristics can be useful for obtaining a low cost, green phosphor for the solid state lighting using near UV LEDs and Blue LEDs.

References:

- 1 J.Th.W.de Hair, G. Blasse J. Lumin. 1(1976) 307-323
2. H.O. Britfain and W.A. Mcallister J.Lumin. 101(1984) 29

I prefer poster presentation oral communication

Tunable and White-Light Emission nitride phosphors



Huan Jiao¹, Chao Li¹, Shijie Qiu¹, Kun Li¹

*School of Chemistry & Chemical Engineering, Shaanxi Normal University, Xi'an,
710119, PR China.*

E-mail: jiaohuan@snnu.edu.cn

Abstract:

Rare earth activated (oxy) nitride phosphors have been greatly attracted interest because of their structural diversity, chemical stability, small Stokes shift, small thermal quenching, and high conversion efficiency. For nitrids phosphors, most researches focus on monocolored phosphors and only few reports about different earth ions co-doping phosphors. $\text{M}_2\text{Si}_5\text{N}_8$ (M=Ca, Sr, Ba) is one of the most important host material in nitride phosphors. Realizing white light emission via energy transfer between different earth ions through down conversion in $\text{M}_2\text{Si}_5\text{N}_8$ (M=Ca, Sr, Ba) host has't been reported. $\text{Ca}_2\text{Si}_5\text{N}_8:\text{Eu}^{2+}$ phosphor emits orange red broad band light and $\text{Ca}_2\text{Si}_5\text{N}_8:\text{Ce}^{3+}$ gives bluish broad band light under the excitation of UV light. We co-doped Eu^{2+} with Ce^{3+} in $\text{Ca}_2\text{Si}_5\text{N}_8$ host in order to realize adjusting colour of nitride phosphors $\text{Ca}_2\text{Si}_5\text{N}_8:\text{Ce}^{3+}, \text{Na}^+, \text{Eu}^{2+}$ and emitting white light.

References:

- [1] C.W. Yeh, W.T. Chen, R.S. Liu, S.F. Hu, H.S. Sheu, J.M. Chen, H. T. Hintzen, *J. Am. Chem. Soc.*, 2012, 134, 14108-14117.
- [2] Y.Q. Li,; J.E.J. van Steen,; J.W. H. van Krevel, G.Botty, A.C.A. Delsing, F.J. Disalvo, G. de With, H.T. Hintzen, *J. Alloys Compounds.*, **2006**, 417, 273-279.

TDDFT study of thiocarbonyl compounds in RAFT polymerization

Nadia Ouddai^a, Salima Zekri^{a,b} and Nadjia Latelli^{a,c}

^aLaboratoire de chimie des matériaux et des vivants : activité, réactivité, Université Hadj Lakhdar, Batna 05000, Algeria

^b Faculté SESNV. département de chimie, Université Larbi Ben M'hidi, Oum El-Bouaghi 04000, Algeria

^c Faculté des sciences, département de chimie, Université de Msila, BP 166 Ichbilila, 28000 M'sila, Algeria

Abstract:

In the present study we analyze the reaction mechanisms involved by thionocarbonates (O-(C=S)-O) and thionoesters (Z-(C=S)-O) compounds in reversible addition fragmentation chain transfer (RAFT) polymerization. For the purpose, theoretical calculations have been performed by means of density functional theory (DFT), using B3LYP and 6-31G* basis sets. Absorption spectra have been simulated using the Time dependent density functional theory (TDDFT) calculations; to investigate their electronic structure and excited state properties. The two kinds of compounds detected different CT band and absorption spectra especially in M7. The lowest excitation energies (E_{gap}) and the maximal absorption wavelength (λ_{max}) of molecules are carried out at the optimized geometries of the ground states.

Key words: Thiocarbonyls Compounds, Density Functional Theory, Time-Dependant Density Functional Theory, Absorption Spectra.

Thermoluminescence of Novel Lanthanum Oxide Obtained by a Glycine-Based Solution Combustion Method

V. R. Orante-Barrón¹, B. M. Mothudi², C. Cruz-Vázquez¹, R. Bernal³

¹*Departamento de Investigación en Polímeros y Materiales de la Universidad de Sonora, Apartado Postal 130, Hermosillo, Sonora 83000 México*

²*Department of Physics, University of South Africa, P. O. Box 392, 0003 South Africa*

³*Departamento de Investigación en Física, Universidad de Sonora, Apartado Postal 5-088, Hermosillo, Sonora 83190 México*

It is well known, in a solution combustion process, that glycine fulfills two principal purposes: first, complexes with metal cations formed, which increases their solubility and prevents selective precipitation as water is evaporated; and second, it serves as fuel for the combustion reaction, being oxidized by the nitrate ions. The glycine molecule has a carboxylic acid group at one end and an amine group at the other end, both of which can participate in a selective complexation of metal ions of different ionic size [1]. Thus, novel La_2O_3 phosphor was obtained for the very first time by a glycine-based solution combustion synthesis (SCS) in which a redox combustion process between lanthanum nitrate and glycine at 500 °C was accomplished. The powder samples obtained were annealed at 900 °C during 2 h in air. X-ray diffraction (XRD) results showed the hexagonal phase of La_2O_3 for annealed powder samples. Thermoluminescence (TL) glow curves obtained after exposure to beta radiation of these samples, displayed three maxima located at ~ 112 °C, ~ 203 °C, and ~ 247 °C. Results from experiments such as dose response and thermoluminescence fading showed that annealed La_2O_3 powder obtained by SCS is a promising material for radiation dosimetry applications.

Keywords: Lanthanum oxide, thermoluminescence, glycine.

References:

- [1] Chick L. A., Pederson L. R., Maupin G. D., Bates J. L., Thomas L. E., Exarhos G. J. *Materials Letters* 10(1990) pp. 6-12.

Thermoluminescence of Novel Zinc Oxide Nanophosphors Obtained by Glycine-Based Solution Combustion Synthesis

V. R. Orante-Barrón¹, F. M. Escobar-Ochoa¹, C. Cruz-Vázquez¹, R. Bernal²

¹*Departamento de Investigación en Polímeros y Materiales de la Universidad de Sonora, Apartado Postal 130, Hermosillo, Sonora 83000 México*

²*Departamento de Investigación en Física, Universidad de Sonora, Apartado Postal 5-088, Hermosillo, Sonora 83190 México*

High-dose thermoluminescence dosimetry properties of novel zinc oxide nanophosphors synthesized by a solution combustion method in a glycine-nitrate process are presented for the very first time in this work. Sintered particles with sizes ranging between ~ 500 nm and ~ 2 μm were obtained by annealing the synthesized ZnO at 900 °C during 2h in air. X-ray diffraction patterns indicate the presence of the ZnO hexagonal phase, without any remaining nitrate peaks observed. Thermoluminescence glow curves of ZnO obtained after being exposed to beta radiation consists of two maxima: one located at ~ 149 °C and another at ~ 308 °C, the latter being the dosimetric component of the curve. Thermoluminescence decay curve fading displays an asymptotic behaviour for times longer than 16 h between irradiation and the corresponding TL readout, as well as a linear behaviour of the dose response without saturation in the studied dose interval (from 12.5 up to 400 Gy). Such features place synthesized ZnO as a promising material for high-dose radiation dosimetry applications.

Keywords: Lanthanum oxide, thermoluminescence, glycine.

Plasmon-assisted upconversion energy-transfer in $\text{Er}^{3+}, \text{Yb}^{3+}:\text{LiNbO}_3$

D. Hernández-Pinilla, P. Molina, J. L. Plaza, M. O. Ramírez and L.E. Bausá
Dept. Física de Materiales Universidad Autónoma de Madrid, 28049-Madrid, Spain

Plasmon-assisted luminescence enhancement and nanoscale laser operation of a trivalent rare earth (RE^{3+})-based solid-state gain medium have been reported on $\text{RE}^{3+}:\text{LiNbO}_3$ crystals [1,2].

Here we analyze the effect of arrays of silver nanoparticles deposited on the polar surface of LiNbO_3 on the upconversion energy transfer between pairs of optically active RE^{3+} ions embedded in the host crystal. In particular, the effect of the localized surface plasmons supported by the plasmonic nanostructures on the $\text{Yb}^{3+} \rightarrow \text{Er}^{3+}$ energy transfer upconversion is investigated.

The results reveal that under excitation in the f-f transition of Yb^{3+} ions located in the proximities of the metallic arrangements, the green upconverted Er^{3+} emission is enhanced by around 30%. The observed intensification can be explained by considering both the plasmonic spectral response supported by the metallic nanostructures and the two-photon character of the upconverted $\text{Yb}^{3+} \rightarrow \text{Er}^{3+}$ energy transfer process, which results into a quadratic boost on the local absorption under the influence of the metallic arrangements.

The results are of interest for different applications involving plasmon enhanced luminescence upconversion such as sensing, solar energy conversion, biological imaging or solid state nanolasers.

References:

- [1] E. Yraola, P. Molina, J.L. Plaza, M.O. Ramírez, L.E. Bausá. *Adv. Mater.* 25 (2013) 910.
- [2] P. Molina, E. Yraola, M.O. Ramírez, C. Tserkezis, J.L. Plaza, J. Aizpurua, J. Bravo-Abad and L.E. Bausá, *Nano Letters* 16 (2016) 895.

Investigation on Emission and Topological Phase Transition of Individual NaREF₄ Nanoparticle

Chun-Hua Yan, Wei Feng, Ling-Dong Sun

Beijing National Laboratory for Molecular Sciences, State Key Laboratory of Rare Earth Materials Chemistry and Applications, PKU-HKU Joint Laboratory in Rare Earth Materials and Bioinorganic Chemistry, Peking University, Beijing 100871, China

Upconversion luminescence of NaREF₄ (RE, rare earth elements) are supposed to close related to the phase and size of the nanoparticles. A lot of efforts has been devoted in obtaining different sized nanoparticle but the same crystal structure. In these studies, it is still challenge to obtain the nanoparticle with the same size but different structure. We selected two phased NaREF₄, hexagonal and cubic structure, which are typical for NaREF₄ and widely studied and imaged as upconversion nanocrystals. With electron beam irradiation, the *in-situ* hexagonal to cubic phase transition of NaREF₄ (RE=Y, Gd or Yb) nanocrystals were observed. Confirmed by the indexing of electron diffraction patterns and the central dark field images, the obtained cubic phase nanoparticles have three domains with different lattice orientations. The results show that the topological phase transition including two orientation relationships, $[0001]_{\text{hex}} \parallel [110]_{\text{cubic}}$ and $[10-10]_{\text{hex}} \parallel [200]_{\text{cubic}}$, occurs under electron beam irradiation.

The upconversion emission of individual nanoparticle (NaY/YbF₄: Yb, Er) was studied with dark field image correlated emission spectra. It is interesting that not all of the nanoparticle with the similar size gave out emission on the same level, and a few smaller nanoparticles gave out even brighter emission. The upconversion emission of individual single nanoparticle is measured before and after the phase transition. The emission branch ratio remained for a nanoparticle experienced hexagonal to cubic phase transition, but the emission intensity dropped a lot after the electron beam irradiation. A phase transition model and emission mechanism were proposed, and this phase transition process and single particle luminescence measurement provide a good model to figure out the emission behaviors of nanoparticles with different phases but the same size and luminescent centers.

References:

- [1] Du, Y. P.; Zhang, Y. W.; Sun, L. D.; Yan, C. H. *J. Phys. Chem. C* 112 (2008), 405.
- [2] Sun, L. D.; Wang, Y. F.; Yan, C. H. *Acc. Chem. Res.* 47 (2014), 1001.
- [3] Dong, H.; Sun, L. D.; Yan, C. H. *Chem. Soc. Rev.* 44 (2015), 1608.

Photon avalanche upconversion in rare-earth doped nanoparticles

Thomas Kornher, Roman Kolesov, Kangwei Xia, Rolf Reuter, Jörg Wrachtrup

3. Physikalisches Institut, University of Stuttgart, Pfaffenwaldring 57, 70569 Stuttgart, Germany

Since the discovery of photon avalanche upconversion in rare-earth doped crystals [1], it has been demonstrated in various materials [2,3], however, so far in bulk systems only. We present the first nanoscale photon avalanche upconversion study, conducted with Tm:YAG and Er:YAG nanoparticles.

In the experiment, Tm:YAG (5%) nanoparticles were pumped with 616.4 nm and their upconverted fluorescence was detected around 350 nm and between 450 nm and 500 nm. Er:YAG (20%) nanoparticles were pumped with 586.5 nm and their upconverted fluorescence was detected between 515 nm and 580 nm. Photon avalanche upconversion was confirmed by measuring characteristic avalanche curves featuring a delayed rise, shown in FIG. 1 (a). Additional ground state pumping at low powers down to 19 nW triggered the avalanche measurably for single shot measurements. The detected photon number up to a constant, avalanche specific rise time is used to distinguish between triggered and untriggered avalanches as shown in FIG. 1 (b).

These results suggest a low light detection scheme at nanoscale or even single photon detection to become feasible in such systems, provided the triggering mechanism can be enhanced further by utilizing optical cavities or by low temperature resonant excitation for example. Also, their application as upconverting biomarkers can be considered.

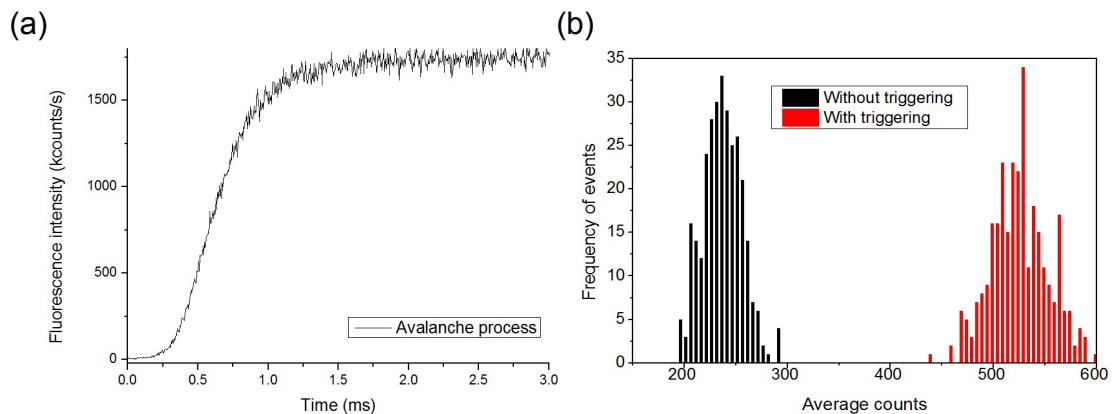


FIG. 1: (a) Measured avalanche process in Tm:YAG nanoparticles. (b) Average counts of 300 independent single shot read-outs with and without triggering beam of 19 nW power for Er:YAG nanoparticles at room temperature.

References:

- [1] Chivian et al., Appl. Phys. Lett. 35.2, 124-125 (1979)
- [2] Guy, S., et al. Radiat. Eff. Defect. S. 135:1-4, 65-68 (1995)
- [3] Auzelet al., J. Lumin. 65.1, 45-56 (1995)

Towards better understanding of the persistent luminescent properties of Cr-doped and Cr, Bi-doped ZnGa₂O₄ nanoparticles

**Morgane PELLERIN^{a, b}, Cristina COELHO-DIEGO^a, Christian BONHOMME^a,
Nadia TOUATI^b, Laurent BINET^b, Corinne CHANEAC^a, Bruno VIANA^b**

^a*Sorbonne Universités, UPMC Univ Paris 06, CNRS, Collège de France, Laboratoire de Chimie de la Matière Condensée de Paris, 11 place Marcelin Berthelot, 75005 Paris, France
morgane.pellerin@etu.upmc.fr, corinne.chaneac@upmc.fr*

^b*PSLResearchUniversity, Chimie ParisTech – CNRS, Institut de Recherche de Chimie Paris, 11 Rue Pierre et Marie Curie, 75005 Paris, France
bruno.viana@chimie-paristech.fr*

At the nanoscale, the ZnGa₂O₄ spinel doped with chromium (III) is an interesting material for *in vivo* optical imaging due to its bright near infrared persistent luminescence after UV and visible excitation.^[1] Moreover its persistent luminescent properties can be improved with the incorporation of bismuth (III) as a co-dopant without any structure or morphology changes.^[2]

The nanoparticles are synthesized by soft chemistry using microwave heating in aqueous media. These very small size nanophosphors (around 9nm) present interesting long lasting persistent luminescence after annealing at 1000°C and they can be excited both under UV and under visible LED excitation. After heating, the nanoparticles keep their small size as they are coated with a silica layer which limits the sintering and can then be removed by a chemical etching.

In this work we try to understand the origin of the persistent luminescent properties of the nanomaterial. First the chromium local environment is studied by electron paramagnetic resonance.^[3] Second, ⁷¹Ga nuclear magnetic resonance is used to get information on the gallium ions repartition (tetrahedral or octahedral site) in the structure.^[4] Finally, thermoluminescence is performed to investigate trapping and detrapping processes as well as trap distribution.

Comparison of these properties versus local structure increases the understanding of the persistent luminescence mechanism and gives insights to the new modalities for their used as nanoprobes for *in vivo* imaging.

References:

- [1] Maldiney T. et al. Nature Materials, 13 (2014), 418-426
- [2] Zhuang, Y. et al. Applied Physics Express, 6(5) (2013), 052602
- [3] Gourier D. et al. Journal of Physics and Chemistry of Solids, 75 (2014) 826-837
- [4] Allix M. et al. Chemistry of Materials, 25 (2013), 1600-1606

Influence of optical phonons on the electronic mobility in Al₂O₃/AlGa_{0.3}N/GaN double heterojunctions

Zhou Xiaojuan, Qu Yuan, Gu Zhuo, Zan Yuhai, Ban Shiliang, Wang Zhiping

Department of Physics, School of Physical Science and Technology, Inner Mongolia University, Hohhot 010021, China

Abstract: Based on the theory of force balance equation, a finite difference method and modified random-element-isodisplacement model, the mobility of the two dimensional electron gas in Al₂O₃/AlGa_{0.3}N/GaN heterojunctions is discussed in consideration of scattering from interface and half-space optical phonons. Considering the effect of ternary mixed crystals and built-in electric fields, the profiles of conduction bands and electronic wave function are obtained by solving Schrödinger equations. The results show that the interface optical phonons play a leading role for the mobility when Al component is small, the half-space optical phonons in GaN material become the main influence with the increasing of Al component, whereas the half-space phonons in AlGa_{0.3}N material are always a smaller factor. At the same time, the size effect on the mobility is also analyzed. It is found that the electron mobility decreases with the thickness of Al₂O₃ material, but increases with the thickness of AlGa_{0.3}N material. The contribution from the fixed charges at the Al₂O₃/AlGa_{0.3}N interface is also considered, the result shows that the mobility increases as the fixed charge density increases, and the expression of the two dimensional electron gas is given taking account of the fixed and the polarization charges. Some of our results are compared with the experimental data and this is helpful for designing HEMTs.

Key words: electronic mobility; optical-phonon scattering; Al₂O₃/AlGa_{0.3}N/GaN double-heterojunction

Optical Properties of CdTe Quantum Dot Superlattices Self-Organized with Electrostatic Interaction

Taichi Watanabe, Yong-Sin Lee, Kohji Takahashi, and DaeGwi Kim

Department of Applied Physics, Graduate School of Engineering, Osaka City University, Japan

So far, semiconductor quantum dots (QDs) have been intensively investigated to understand the size dependence of their physical and/or chemical properties [1, 2]. Randomly-dispersed QDs were samples in most of the studies so far. The periodic array structures of QDs, the so-called QD superlattices (QDSLs), have attracted much attention from the viewpoint of the fundamental physics and from the interest in the application to functional materials [3]. In the present work, we have investigated optical properties of QDSLs of CdTe self-organized with electrostatic interaction.

QDSLs of CdTe were prepared by mixing solutions of positively- and negatively-charged CdTe QDs. Charged CdTe QDs were obtained by modifying the QD surface with cationic and anionic thiol compounds. Cysteamine (CA) and thioglycolic acid (TGA) were used for the preparation of positively-charged CdTe (p-CdTe) and negatively-charged CdTe (n-CdTe) QDs, respectively.

From X-ray diffraction measurements, existence of the periodical ordering of QDs, that is, the formation of the three dimensional periodic QD superlattice was confirmed. Absorption spectra of p- and n-CdTe QDs exhibit clear peak structures at ~ 2.27 eV, indicating the formation of CdTe QDs with ~ 3.0 nm and the agreement of the mean diameter of both p- and n-CdTe QDs. We note that the agreement of the mean diameter and the uniformity of the size of p- and n-CdTe QDs are advantageous to the formation of ordered QDSLs. The absorption peak of the mixed solutions of p- and n-CdTe QDs is observed at ~ 2.23 eV and is red-shifted compared with the peak energy of p- and n-CdTe QDs. The red-shift of the absorption peak originates from the quantum resonance between the CdTe QDs which mutually interact [4]. Figure 1 shows PL decay profiles of CdTe QDSLs and of p- and n-CdTe QDs. It is noted that the PL decay profile of QDSLs exhibits a slower decay compared with that for p- and n-CdTe QDs. In QDSLs, the wave function is spatially extended by the quantum resonance, and the decrease in exciton oscillator strength would cause the prolonged decay of QDSLs.

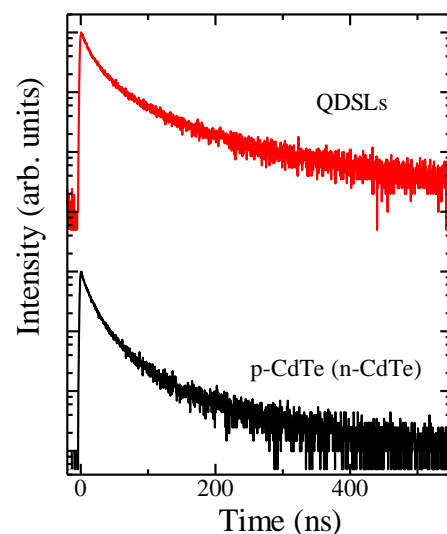


Figure 1

References:

- [1] J. Lumin. 70 (1996), edited by L. Brus, A. Efros, and T. Itoh.
- [2] A. Yoffe, Advances in Physics 50 (2001) 1.
- [3] C. Murray, C. Kagan, and M. Bawendi, Annu. Rev. Mater. Sci. 30 (2000) 545.
- [4] D. Kim, S. Tomita, K. Ohshiro, T. Watanabe, T. Sakai, I. Chang, and H. Kim, Nano Letters 15 (2015) 4343.

Single Donor-Acceptor Pair Attached to a Protein Molecule as a Tool for Studying Folding/Unfolding Fluctuations in the Protein

I.S.Osad'ko

Institute for spectroscopy, Russian Academy of Sciences, Troitsk, Moscow, Russia

Single donor-acceptor (D-A) pairs attached to a single protein molecule can be used for studying folding/unfolding processes in the protein molecule. Fig.1 shows scheme of such

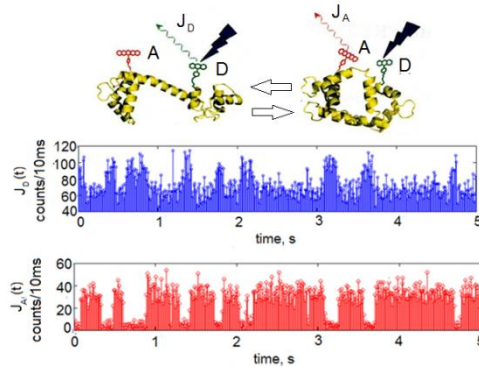


Fig.1 Fluctuations of single donor - acceptor pair fluorescence (panels) resulting from folding/unfolding processes in a protein molecule shown by black arrows..

experiment for a single protein molecule with attached D-A pair. Although CW-laser light excites only D-molecule we observe both D and A-fluorescence $J_{D,A}$. A-fluorescence emerges due to Förster resonance energy transfer (FRET) in the D-A pair. Efficiency

$$E(R_{DA}) = F(R_{DA}) / [F(R_{DA}) + D_0] \quad (1)$$

of FRET depends on the distance R_{DA} between D- and A-molecule in accordance with the equation: $F(R_{DA}) = D_0 / (R_{DA} / R_F)^6$ for Förster rate. Here D_0 is rate of deactivation of the excitation in D-molecule without presence of A-molecule and R_F is the Förster radius. Since folding/unfolding processes in the protein molecule change the distance, R_{DA} , the intensity of D- and A-fluorescence fluctuate as two panels in Fig.1 show. These fluctuations are the source of information about folding/unfolding processes in a protein molecule.

As a rule FRET efficiency is measured in an experiment with the help of the formula

$$E = \eta_A \Phi_A I_A / [\eta_A \Phi_A I_A + \eta_D \Phi_D I_D] \quad (2)$$

Here $\Phi_{D,A}$ are quantum yields of the donor and acceptor molecules, $\eta_{D,A}$ are efficiencies of photon detection in D and A channels and $I_{D,A}$ are fluorescence intensities measured in the experiment. However eq.(2) will not coincide with the eq.(1) for real FRET efficiency because measured intensities $I_{D,A}$ includes background fluorescence I_n and detection of a number of D-photons in A-channel (cross talk). The way the amplitude $E_{1,2}$ of FRET efficiency fluctuations and rate R of these fluctuations can be measured in real experiments with the help of fluctuating D- and A-fluorescence is discussed in the present talk.

The work was supported by the Russian Science Foundation via Grant No. 14-12-01415

Synthesis and spectroscopic properties of cage-like SrAl₂O₄:Eu²⁺ microspheres via a sol-gel method

J. Wan¹, Y. Zhang¹, Y. Wu¹, X. Qiao^{1,*}, F. Wang², X. Fan¹

¹State Key Laboratory of Silicon Materials, Department of Materials Science and Engineering, Zhejiang University, Hangzhou 310027, P.R. China

²Department of Physics and Materials Science, City University of Hong Kong, 83 Tat Chee Avenue, Hong Kong SAR, China

*Corresponding author: qiaoxus@zju.edu.cn

The cage-like SrAl₂O₄:Eu²⁺ microspheres has been synthesized via a rapid sol-gel process by epoxide adding method. AlCl₃·6H₂O, SrCl₂·6H₂O and EuCl₃·6H₂O dissolved in water and ethanol were used as inorganic source, then epoxide was added as trigger to initiate the sol-gel transition. All of the sol-gel transition completed within several minutes and no complicated facilities were essential. The obtained SrAl₂O₄:Eu²⁺ microspheres precursor have homogeneous spherical morphology with a diameter of 1~2 μm. The diameter of the SrAl₂O₄:Eu²⁺ precursor could be adjusted through varying different H₂O/ethanol ratio, AlCl₃·6H₂O, SrCl₂·6H₂O and epoxide molar ratio. The cage-like SrAl₂O₄:Eu²⁺ microspheres formed in a tube furnace heat-treated at 1200 °C for only 2 hours under the flow of NH₃. Compared with traditional solid phase reaction method, decarburization process was unnecessary by this means. The cage-like SrAl₂O₄:Eu²⁺ microspheres exhibit excellent spectrum with a strong luminescence peak at 520 nm under a broad band excitation peak at 315 nm. Luminescence quantum yields of the samples were determined for excitation at 315 nm, among which the highest value was nearly 95%. The mechanoluminescence property was also studied in this work with a significant peak at 520 nm observed. In summary, the whole fabrication of the cage-like SrAl₂O₄:Eu²⁺ microspheres was fast, cheap, convenient and energy saving, the synthesized SrAl₂O₄:Eu²⁺ microspheres have homogeneous cage-like morphology and excellent optical properties.

References:

- [1] Gash AE, Tillotson TM, Satcher JH, Hrubesh LW, Simpson RL (2001) New sol-gel synthetic route to transition and main-group metal oxide aerogels using inorganic salt precursors. *J Non-cryst Solids* 285 (1-3):22-28
- [2] Gash AE, Tillotson TM, Satcher JH, Poco JF, Hrubesh LW, Simpson RL (2001) Use of epoxides in the sol-gel synthesis of porous iron(III) oxide monoliths from Fe(III) salts. *Chem Mater* 13 (3):999-1007
- [3] Wan J, Qiao XS, Wu LA, Wu YM, Fan XP (2015) Facile synthesis of monodisperse aluminum nitride microspheres. *Journal of Sol-Gel Science and Technology* 76(3):658-665

Au Islands Enhanced Luminescence of Er³⁺/Yb³⁺ Co-Doped Gd₂(MoO₄)₃ Thin Films and Application in Temperature Sensing

Haoyue Hao^a, Yuxiao Wang^a, Xueru Zhang^a

^a*Department of Physics, Harbin Institute of Technology, Harbin 150001, PR China*

In our researches, Au modified Gd₂(MoO₄)₃:Er³⁺/Yb³⁺ thin films have been fabricated using the electrostatic layer-by-layer(LBL) technique. The analysis of luminescence intensity indicate that Au islands can greatly enhance the upconversion luminescence intensity of Gd₂(MoO₄)₃ thin films at 522 nm, 550 nm, and 660 nm. The corresponding results about the fluorescence lifetime and the number of photon responsible for the upconversion process confirm the luminescence intensity enhancement is induced by increased radiative decay rate and excitation rate. Furthermore, we study the temperature dependence of the luminescence intensity of Gd₂(MoO₄)₃ thin films. The sensitivity derived from the fluorescence intensity ratio(FIR) technique of Gd₂(MoO₄)₃:Er³⁺/Yb³⁺/Au thin films is approximately 0.017 K⁻¹ at 312 K, which is relatively higher than the sensitivity of thin films without Au island(0.009 K⁻¹). This result indicates that the fluorescent thin films with Au islands are more sensitive than those without Au islands in thermal sensing and thermal imaging.

Enhance the sensitivity of optical thermometer based on non-thermally coupled levels of Tm^{3+}

Hongyu Lu, Yuxiao Wang*, and Xueru Zhang*

Department of Physics, Harbin Institute of Technology, Harbin 150001, PR China

Abstract

A innovation for enhancing the sensitivity of optical temperature sensor is reported by using non-thermally coupled levels of Tm^{3+} . Under 980 nm laser excitation, the temperature-dependent luminescence of $\text{NaLuF}_4: \text{Yb}^{3+}, \text{Er}^{3+}, \text{Tm}^{3+}$ phosphor was investigated. The corresponding $^1\text{D}_2$ and $^1\text{G}_4$ level of Tm^{3+} were non-thermally coupled levels. Based on FIR method which is fitting by a polynomial function, the temperature sensing behavior is studied in the range of 300 - 600K. The obtained maximum sensitivity is $60.4 \times 10^{-3} \text{ K}^{-1}$ at 300 K. Meanwhile, luminescent colors can be precisely modulated by changing temperature. The $\text{Yb}^{3+}, \text{Er}^{3+}, \text{Tm}^{3+}$ co-doped NaLuF_4 material with the high sensitivity and the multicolor emissions indicated that it is promising for applications in optical temperature sensor and light display systems, respectively.

Metal transition ion implantation on Ga₂O₃ nanowires

A. Gonzalo¹, E. Nogales¹, B. Méndez¹ and J. Piqueras¹

¹*Departamento Física de Materiales, Facultad de CC Físicas, Universidad Complutense de Madrid, 28040 – Madrid, Spain*

K. Lorenz²

²*Campus Tecnológico e Nuclear, Instituto Superior Técnico, Estrada Nacional 10 (km 139,7), 2695-066 BobadelaLRS Portugal*

Undoped β -Ga₂O₃ nanowires have been obtained by a thermal evaporation method at 1100 °C under dynamic argon conditions. In order to get Cr and Mn doped Ga₂O₃ nanowires, an ion implantation process and subsequent thermal annealing were carried out. We have previously reported on the rare-earth ions implantation of Ga₂O₃ and GeO₂ nanowires and no significant damage appears in the nanowire morphology after the implantation process [1]. The metal transition ions used now are of interest because of their optical and magnetic properties. In this work, the structural and luminescence properties of the implanted nanowires were characterized by Raman and Cathodoluminescence (CL), which enables to study the evolution of the crystal lattice recovery and luminescence bands. The measurements have been conducted on as implanted samples as well as on 700 °C, 900 °C and 1100 °C annealed samples. For comparison, ion implantation and further annealing have also been carried out on bulk Ga₂O₃ crystals. The results show a nice correlation of the optical activation of luminescence centres with the sharpening of the Raman peaks of the beta-gallia structure. In the case of Cr doping, partial recrystallization occurs at 700 °C while 900 °C is needed to get the fully optical activation of Cr³⁺ ions. Even though Mn characteristic emission lines have not been resolved, the Raman spectra evolution has been used to monitor the recrystallization of the Ga₂O₃ lattice. In addition, the results show that the composed UV-blue band characteristic of native defects in bulk Ga₂O₃ experience changes when it comes to nanowires. CL measurements of Ga₂O₃ bulk and nanowires that have undergone the same ion implantation and annealing processes show a red-shift of the blue component and a blue-shift of the UV component in the case of nanowires. This suggests that the nanowire shape affects the native defect structure in the recrystallization process.

Acknowledgments:

The authors thank E.G. Villora and K. Shimamura for providing bulk Ga₂O₃ crystals.

References:

[1] E. Nogales, P. Hidalgo, K. Lorenz, B. Méndez, J. Piqueras and E. Alves, *Nanotechnology*, 22 (2011) 285706.

Formation of chelated rare earth clusters in porous sol-gel silicate materials

N. P. Arndt,¹ A.J. Silversmith,¹ D.M. Boye²

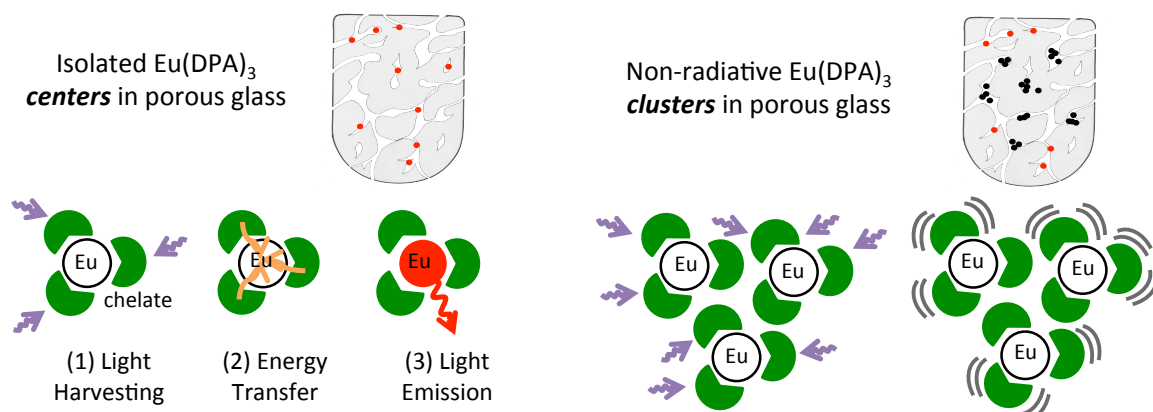
¹ Hamilton College, Clinton, NY 13323 USA 1

² Davidson College, Davidson, North Carolina, USA 2

*Corresponding author: asilvers@hamilton.edu

Chelation of rare earth (RE) ions provides a way to enhance emission in RE-based phosphors. Chelates absorb strongly in the near uv, and energy transfer (ET) to RE ions can yield bright RE emission in the visible. In this work we have incorporated a DPA(pyridinedicarboxylic acid)-RE complex into sol-gel glass using post-annealing-immersion (PAI). With the PAI technique, annealed porous glass is immersed in a solution containing RE(DPA)₃. The solution diffuses into the glass; subsequent drying results in transparent glass containing the chelated complexes. Emission spectra confirm that RE ions remain associated with the DPA molecules. Fluorescence decay dynamics indicate that chelation provides an isolated environment from the vibrational environment of the glass matrix which would quench fluorescence.

Single crystals of fully chelated Eu(DPA)₃ complexes were grown and incorporated into silicate glass. Excitation spectroscopy (monitoring 614nm; ⁵D₀→⁷F₂ emission) proved to be a sensitive probe of the distribution of dopants in the porous network, i.e. whether the glasses contain 1) single isolated centers in individual pores, or 2) clusters of Eu(DPA)₃ in pores. For the former, a strong excitation signal (peak intensity is ~200x the strongest peak excitation within the Eu 4f⁶ configuration) matches the broad DPA absorption between 250 and 350nm, indicating effective excitation of the Eu³⁺ ions via ET from excited DPA molecules. For the latter, excitation of Eu³⁺ fluorescence by chelate→RE ET diminishes markedly as dopant concentration increases, approaching the behavior of a Eu(DPA)₃ stoichiometric crystal: complete absence of ET from the chelate to Eu³⁺. In particular, for PAI concentrations ≤0.05M, doped sol-gels have pores with individual dopants. Above that cut-off concentration, the pores contain clusters of Eu(DPA)₃. The strikingly different optical behavior in the two regimes indicates that the PAI technique with chelated RE's can be a sensitive probe of pore size.



Transport and recombination of photo-injected electrons in Dye-sensitized solar cells based ZnO nanostructures

Baurzhan Ilyassov^{1,2}, Niyazbek Ibrayev¹

¹*Institute of Molecular Nanophotonics, E.A. Buketov Karaganda State University, 100028 Karagandy, Kazakhstan.*

²*Laboratory of Solar Energy, PI NLA, Nazarbayev University, 010000 Astana, Kazakhstan
Arial 11p italic*

Dye-sensitized solar cells (DSSCs) have attracted great attention of researchers in the recent last years [1-3]. Fabrication technology of DSSCs is much easier and cost-effective than solar cells based on p-n junction [4]. The power conversion efficiency (PCE) of DSSCs has reached a value of more than 10% [4], and the PCE of organic-inorganic perovskite solar cells, which are similar to DSSCs, has exceeded 20% [4].

One of the key components of the DSSCs is a metal oxide high energy-gap semiconductor which performs a double function: (1) It is a scaffold with a large specific surface needed for the dye loading, and (2) at the same time it is an electron transport material. In the DSSCs, the majority of electrons photo-injected from dyes to a semiconductor are located in trap states in the semiconductor film [4], leading to a trapped electron density that greatly exceeds the conduction electron density. Through these trapped states of semiconductors such as TiO₂ or ZnO photo-injected electrons can recombine with electrolyte species [3] and as result deteriorate photovoltaics performance of device.

In our work, we have studied an effect of the morphology and the defect density of ZnO on the transport and recombination of photo-injected electrons in ZnO nanostructured films. We obtained two different ZnO nanostructures, nanorods and nanosheets (Figure 1) and by Electrochemical Impedence Spectroscopy (EIS) technique investigated transport and recombination dynamics of photo-injected electrons.

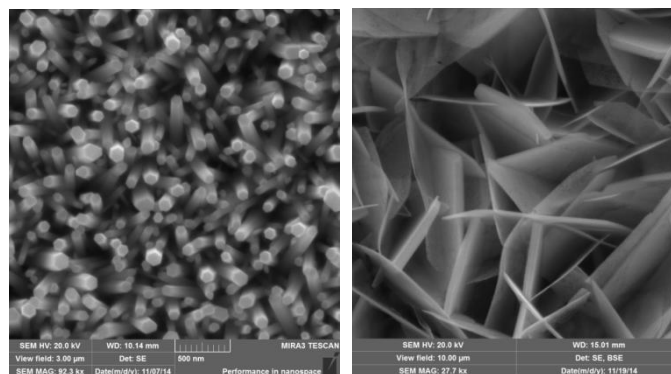


Figure 1. Arrays of ZnO nanorod (on the left) and nanosheet (on the right).

References:

- [1] N. Ibrayev, et al., Mater. Sci. Semiconduct. Process. 31 (2015) 358-362.
- [2] N. Nuraje, R. Asmatulu, S. Kudaibergenov, Curr. Inorg. Chem. 2 (2012) 124-146.
- [3] B. R. Ilyassov, N. Kh. Ibraev, D. B. Abzhanova, IOP Conf. Series: Materials Science and Engineering 81 (2015) 012046
- [4] B. Ilyassov, N. Ibrayev N. Nuraje, Mater. Sci. Semiconduct. Process. 40 (2015) 885-889

Study of surface effect on photoassisted field emission from Ta(112) and Ti(0001) by using the Transfer Hamiltonian method.

Rosangliana^{1*} and R.K. Thapa²

¹ Department of Physics, Govt. Zirtiri Residential Science College, Aizawl 976 001, Mizoram, India

² Department of Physics, Mizoram University, Aizawl 796 009, Mizoram, India

We will present here a model calculation of photoassisted field emission current (PFEC) by using transfer Hamiltonian method. Photoassisted field emission is a technique in which a metal is irradiated by an incident laser radiation of photon energy $\hbar\omega$. Photon energy is usually less than the work function (ϕ) of the metal under investigation. The incident radiation photo excites the electrons to a final state which lies below the vacuum level; hence these electrons are confined within the metal surface. A strong static electric field ($\approx 10^{11} \text{V/m}$), is then applied to the surface of the metal which causes the photoexcited electrons to tunnel through the surface potential barrier into the vacuum region and constitutes the photoassisted field emission current (PFEC). The incident radiation is usually a laser beam, causes the transition of electrons from the initial state $|i\rangle$ to the final state $|f\rangle$ and the matrix element for this transition can be written as $M_{fi} = \langle f | p.A + A.p | i \rangle$. PFEC is calculated in the case of Ta and Ti. The applied high static field causes the reduction of the work function of the metal causing Schottky effect which brings in the image potential effect. The formula used for calculation of PFEC as deduced by using transfer Hamiltonian method is given by

$$\left. \begin{aligned} \frac{dj(E)}{dE} &= \frac{2\pi e}{\hbar} |M_{fi}|^2 D(W) \\ &\times \delta(E_f - E_i) \delta(E - E_i) f(E_i) \end{aligned} \right\} \rightarrow (1)$$

$D(W)$ is the quantum mechanical transmission probability and W is the normal component of kinetic energy. We intend to calculate the initial state wavefunction for use in Eq. (1) by using Kronig-Penney potential model.

An appropriate dielectric model for the surface region of the metal will be used for the evaluation of vector potential A . PFEC will be calculated as a function of applied static field, photon energy, and the effect of the matrix element M_{fi} will also be studied.

FORTTRAN programme is written for the calculation of PFEC. The results will be checked with experimental data and the published theoretical results.

References :

- [1] R.K. Thapa, Gunakar Das, Lalthakimi Zadeng and R Bhattacharjee, Indian Jour. Phys. 78, (2004), 939.
- [2] R.K. Thapa and Gunakar Das, International Jour. Mod. Phys. B. 19, (2005), 3141.
- [3] R. K. Thapa, M.P. Ghimire, Gunakar Das, S.R. Gurung, B.I. Sharma and P.K.Patra, Mod. Phys. Lett B. 21, (2007), 1501.
- [4] Rosangliana, M.P. Ghimire, Lalmuanpuia, Sandeep and R.K. Thapa, Indian Jour. Phys. 84, (2010), 723-727.

Light induced toxicity of rare earth doped trifluoride crystalline nanoparticles

M S Pudovkin, S L Korableva, A O Krashenninnicova, A S Nizamutdinov, V V Semashko, P V Zelenihin, E. M. Alakshin, V.V Pavlov, A.Feraro

Kazan Federal University, 420008, Kremlevskaja str., 18, Kazan, Russian Federation

In recent years, great effort has been devoted to investigation of different properties of rare earth doped nanoparticles (REF₃ doped NPs) driven primarily by their potential biological application [1]. REF₃ doped NPs can be used in the field of bioimaging and in photodynamic therapy (PDT)[2]. For example infrared-emitting REF₃ doped CeF₃:Yb,Er and KY₃F₁₀:Er NPs are used in diagnostics and deep tissue imaging [3,4] because their emission in IR spectral range. There is also another class of NPs (TiO₂, ZnO) which can produce Reactive Oxygen Species (ROS)[4,5]. The ROS are very toxic for cells and those NPs can be used in PDT and waste water treatment. But REF₃ doped NPs can also produce ROS in water [2]. They can release their absorbed energy as luminescence and transfer the energy in molecular oxygen, generating ROS. So those NPs can be toxic and information about toxicity and about the mechanism of toxicity of those REF₃ doped NPs can be useful to create an optimal and safety method of bioimaging. Also the result of interaction between NPs and bacteria can reveal new physical properties of nanomaterials. In this work we present results of studying light induced toxicity of REF₃ doped NPs (under laser irradiation) toward bacteria. LaF₃, PrF₃, LaF₃:Pr, CeF₃, CeF₃:Yb,Er and KY₃F₁₀:Er NPs PrF₃ were synthesized by co-precipitation and hydrothermal methods. Microparticles of were synthesized by mechanical synthesis method. Then the experiments of light induced toxicity against bacteria (*Salmonella typhimurium* TA 98 bacteria) were conducted. The experiments showed that PrF₃ microparticles are not toxic toward *Salmonella typhimurium* TA 98 bacteria. But PrF₃ NPs are toxic toward *Salmonella typhimurium* TA 98 bacteria under the laser irradiation. Survival of the bacteria reduces while the power density of laser irradiation increases. Without laser irradiation the NPs don't demonstrate significant toxicity also NPs themselves are not toxic significantly. LaF₃ NPs are not toxic toward *Salmonella typhimurium* TA 98 bacteria. Previous experiments confirming presence of ROS showed presence of ROS. The presence of ROS was determined by special dye which illuminates light in presence of ROS. Photoconductivity experiments also were carried out and the results are being discussed.

References:

- [1] Min Lin, Ying Zhao, ShuQi Wang, Ming Liu, ZhenFeng Duan, YongMei Chen, Fei Li, Feng Xu, 30 (2012) 1551–1561
- [2] Sasidharan Swarnalatha Lucky, Khee Chee Soo, and Yong Zhang, (2014) A-BA
- [3] Laércio Gomes, Horácio Marconi da Silva M.D. Linhares, Rodrigo Uchida Ichikawa, 54 (2016) 57-66
- [4] Mei Chee Tan, G. A. Kumar, Richard E. Riman, 17 (2009) 1
- [5] Melissa F, José M, Amadeu M, Barata, 470 (2014) 379-389

Optical thermometry of Er³⁺-doped transparent NaYb₂F₇ glass-ceramics

Fangfang Hu¹, Xiantao Wei^{1,2}, Xinyue Li¹, Jiajia Cai¹, Yanguang Qin¹,
Zengpeng¹, Sha Jiang³, Yonghu Chen¹, Chang-Kui Duan^{1,*}, Min Yin^{1,*}

¹ *Department of Physics, University of Science and Technology of China, Hefei
230026, China*

² *Center of Physics Experiment, School of Physical Sciences, University of Science
and Technology of China, Hefei 230026, China*

³ *School of Science, Chongqing University of Post and Telecommunications,
Chongqing 400065, China*

⁴ *Department of Physics, Zhejiang Normal University, Jinhua, Zhejiang, 321004, China*

Er³⁺-doped transparent NaYb₂F₇ glass-ceramics (GC) were successfully fabricated using a conventional melt-quenching technique and subsequent heat treatment for the first time. The X-ray Diffraction patterns (XRD), transmission electron microscopy (TEM) images and stark splitting of Er³⁺ emissions indicate NaYb₂F₇ nanocrystals were well-formed. The decay curves and enhanced emission spectra after crystallization of the Er³⁺-doped NaYb₂F₇ GC upon 980 nm indicates more efficient spectra conversion in GC than precursor glass (PG). Furthermore, the temperature dependence green emissions of Er³⁺ doped GC were studied by the fluorescence intensity ratio of thermally coupled emitting states (⁴S_{3/2}, ²H_{11/2}) at 980 nm and 408 nm. The sensitivity is 1.35%K⁻¹ at 300 K and the obtained high energy difference (ΔE) is 843 cm⁻¹. This result suggests that the Er³⁺-doped GC may be a promising candidate for sensitive optical temperature sensor with high resolution and good accuracy.

References:

- [1] R. Dey, A. Pandey, V.K. Rai, Er³⁺-Yb³⁺ and Eu³⁺-Er³⁺-Yb³⁺ codoped Y₂O₃ phosphors as optical heater, *Sensors and Actuators B: Chemical*, 190 (2014) 512-515.
- [2] H. Suo, C. Guo, Z. Yang, S. Zhou, C. Duan, M. Yin, Thermometric and optical heating bi-functional properties of upconversion phosphor Ba₅Gd₈Zn₄O₂₁: Yb³⁺/Tm³⁺, *Journal of Materials Chemistry C*, 3 (2015) 7379-7385.
- [3] G. Canat, J.-C. Mollier, Y. Jaouën, B. Dussardier, Evidence of thermal effects in a high-power Er³⁺-Yb³⁺ fiber laser, *Optics letters*, 30 (2005) 3030-3032.

Enhanced near-infrared response of c-Si solar cell using YVO₄: Bi³⁺, Ln³⁺ (Ln = Yb and Nd) phosphors

R.A. Talewar ^{1*}, Charusheela Joshi ¹, S.V. Moharil ²

¹ Physics Department, Shri Ramdeobaba College of Engineering & Management, Katol Road,
Nagpur 440013, India

² Department of Physics, Rashtrasant Tukadoji Maharaj Nagpur University, Nagpur 440010,
India

Green and renewable energy is the only source capable of generating sufficient energy in order to meet the long-term energy demand world-wide, since the energy production from fossils fuels increasing the greenhouse gases^[1]. The photovoltaic cells are the prime candidates for this task, since it has capacity to convert the sunlight into electricity. Currently the commercial crystalline silicon solar cells with the conversion efficiency just above 15%^[2] although, theoretically the maximum efficiency can be reached upto 30%; this is known as Shockley-Queisser limit^[3]. Majority of the energy losses (over 70%) are related to the spectral mismatch of the incident solar photons energies to the energy gap ($E_g=1.12\text{eV}$ for c-Si solar cell) of a solar cell^[4].

The possibility of using luminescent materials for spectral modification can greatly eliminate the spectral mismatch phenomenon by improving the utilization of sunlight, thereby indirectly improving the efficiency and performance of solar cell^[4].

In the present work, we explored the efficient down-shifting phenomenon in YVO₄:Bi³⁺, Ln³⁺ (Ln = Yb & Nd) phosphors through efficient energy transfer.

An efficient ultraviolet to near infrared emitting YVO₄:Bi³⁺, Ln³⁺ (Ln = Yb & Nd) phosphors has been prepared by novel co-precipitation method followed by heat treatment. The prepared phosphors possesses a broadband absorption in the ultraviolet region of 250-400 nm and exhibits intense near-infrared emission around 1000 nm, which can be absorbed by crystalline silicon solar cells to overcome the thermalization losses. In YVO₄:Bi³⁺, Yb³⁺, the dependences of visible and NIR emissions, decay lifetime, energy transfer efficiency (η_{ETE}) and quantum efficiency were investigated in detail. As a result, it was found that the NIR emission of Ln³⁺ (Yb or Nd) was greatly enhanced through downconversion process, due to efficient energy transfer from Bi³⁺ to Ln³⁺ (Ln = Yb and Nd) in the YVO₄ phosphors. Photoluminescence excitation spectra reveals that incorporation of Nd³⁺ in YVO₄:Bi³⁺ phosphors red-shifted the excitation band by about 10 nm. Furthermore, excitation band can be easily tuned with partial replacement of VO₄³⁻ with PO₄³⁻ was also observed. This work shows the potential application of Bi³⁺, Ln³⁺ (Ln = Yb & Nd) co-doped yttrium vanadate as promising downconversion phosphors for the enhancement of performance and the efficiency of c-Si solar cells.

References:

1. O. Morton, Nature 443, (2006) 19
2. A. Goetzberger et al. Materials Science and Engineering R 40, (2003), 1–46
3. W. Shockley and H. Queisser J. Appl. Phys. 32, (1961) 510
4. B. Richards Solar Energy Materials & Solar Cells 90, (2006) 1189–1207

Photo-Physical Properties of Spin-Coated Lead Halide Perovskite Thin Films

Kien Wen Sun^{1,2}

¹*Department of Applied Chemistry, National Chiao Tung University, Hsinchu, Taiwan*

²*Department of Electronics Engineering, National Chiao Tung University, Hsinchu, Taiwan*

The recent development of lead halide (MAPbI₃) perovskite solar cells is remarkable after the first report by Miyasaka and co-workers in 2009 [1]. The performance of perovskite cells strongly depends on the crystallinity of the perovskite layer. Recent results show that only a minority of the perovskite in a mesoporous nanostructure has medium range crystalline order. It is considered that the grain structures have a major impact on the carrier diffusion and recombination in MAPbI₃. Physical and electrical characteristics of lead halide perovskites for solar cells were recently updated by Bretschneider et al. [2]. In this study, we reports results from studies on spin-coated lead halide perovskite thin films by using temperature dependent photoluminescence spectroscopy and x-ray diffraction techniques. The photoexcited emission peak positions, intensity, and full width at half maximum (FWHM) were recorded when the temperature was scanned from 300 K to 10 K.

From the XRD spectra, a phase transition from the tetragonal phase (at room temperature) to the orthorhombic phase begin to take place when the temperature of perovskite was cooled down to ~ 150 K. Clear PL signals originated from the orthorhombic phase were observed around 110 K ~ 120 K.

With increased temperature, the luminescence peak of the tetragonal phase first showed slightly blue-shifted from 1.596 eV to 1.598 eV at 40 K and then was red-shifted to 1.57 eV at 130 K. Above 130 K, the energy peak was again blue-shifted to 1.61 eV with temperature increased toward 300 K. The luminescence peak of the orthorhombic phase showed only slightly blue-shifted from 1.66 eV to 1.67 eV with temperature increased from 10 K to 120 K. Narrowing of the FWHM of the luminescence peak of the tetragonal phase from 105 meV to 49 meV was observed with increased temperature from 10 K to 120 K. Above 120 K, the FWHM began to broaden and reached 94 meV at 300 K. The FWHM of the luminescence peak of the orthorhombic phase decreased from 43 meV to 38 meV with decreased temperature from 100 K to 10 K.

In the scanning electron microscope images, nano scale grains with an average size of ~ 10 nm were observed in the MAPbI₃ thin film. We speculate that, due to the presence of the nano grains, localized states were induced within the energy gap of MAPbI₃ due to the quantum confinement effect. The observed temperature dependent behavior in photoluminescence spectra, which is similar to those observed in the self-assembly semiconductor quantum dots [3,4], can be attributed to the presence of localized states induced by the MAPbI₃ nano scale grains.

References:

- [1] A. Kojima, K. Teshima, Y. Shirai, T. Miyasaka, J. AM. Chem. Soc. 131 (2009), 6050-6051.
- [2] S.A. Bretschneider, J. Weichert, J.A. Dorman, L. Schmidt-Mende, APL Mater. 2 (2014), 040701
- [3] Y. Wang, N. Herron, J. Phys. Chem. 95 (1991), 525–532.
- [4] V. Popescu, G. Bester, A. Zunger, Appl. Phys. Lett. 95 (2009), 023108. 2009

Frequency selective transient and permanent spectral hole burning processes in Ce:YSO at liquid helium temperatures

Jenny Karlsson^{1,3}, Adam N. Nilsson¹, Diana Serrano², Andreas Walther¹, Lars Rippe¹, Stefan Kröll¹, Alban Ferrier^{3,4}, Philippe Goldner³

1 Department of Physics, Lund University, P.O. Box 118, SE-22100 Lund, Sweden

2 Department of Chemistry, University of Zürich, Winterthurerstrasse 190, 8057 Zürich, Switzerland

3 PSL Research University, ChimieParisTech - CNRS Institut de Recherche de Chimie Paris, 75005, Paris, France

4 Sorbonne Universités, UPMC Univ Paris 06, 75005, Paris, France

Because of their long coherence times[1] rare-earth-ion-doped crystals are an interesting route for quantum information and quantum computing hardware. Although single ensemble qubits have been realized [2], scalability of the system requires going towards the single ion level.

High-fidelity single ion readout is here a necessary requirement and the present work concerns a scheme relying on a dedicated readout ion, which can couple to nearby qubit ion through the permanent dipole-dipole interaction (dipole blockade effect) [3]. Due to a short excited state lifetime of the readout ion, fluorescence can rapidly be collected and the qubit state can thereby be determined.

Progress towards realizing such a scheme has been made by analysing cerium as a potential readout ion. To reach the required spatial and spectral resolution of single ion detection, a homebuilt scanning confocal microscope setup [4] and a 371 nm external cavity diode laser with a kHz-linewidth [5] is used.

So far, work has been carried out on a very low concentration Ce³⁺:Y₂SiO₅ crystal at the few-ion level. Spectral hole burning processes in the groundstate Zeeman levels of cerium has been analysed using an applied magnetic field[6]. Moreover, a permanent trapping mechanism is currently investigated[6, 7, 8].

This contribution will describe our work towards single Ce ion detection and our plans and continuing progress toward state selective qubit measurements.

References:

- [1] Zhong et al., Nature 517, 177-180 (2015).
- [2] Rippe et al., Phys. Rev. A 77, 022307 (2008).
- [3] Walther et al., Phys. Rev. A 92, 022319 (2015).
- [4] Karlsson et al. "A confocal optical microscope for detection of single impurities in a bulk crystal at cryogenic temperatures", Accepted for publication in Rev. Sci. Instr. (2016).
- [5] Zhao, Master thesis, Lund University, Lund Reports on Atomic Physics, LRAP-473 (2013).
- [6] Karlsson et al. "Narrow transient and permanent spectral hole burning in Ce³⁺:Y₂SiO₅ at liquid helium temperatures", Manuscript in preparation.
- [7] Xia et al., Phys. Rev. Lett. 115, 093602 (2015).
- [8] Kornher et al., Appl. Phys. Lett. 108, 053108 (2016).

Intersubband optical absorption between multi energy levels in InGaN/GaN spherical core-shell quantum dots

W. H. Liu, Y. Qu, S. L. Ban

School of Physical Science and Technology, Inner Mongolia University, Key Laboratory of Semiconductor Photovoltaic Technology at Universities of Inner Mongolia Autonomous Region, Hohhot 010021, PR China

Quasi zero-dimensional quantum dots (QDs), namely artificial atoms have exhibited unique quantum size effects on properties such as atom-like energy levels, tunable bandgap, etc.^[1, 2] Benefitting from the improvement of fabrication, core-shell quantum dots (CSQDs) can be realized and applied to many opto-electronic applications.^[3] Optical absorption coefficients (ACs) and refractive index changes (RICs) are important physical parameters characterizing the sensitive spectral range of opto-devices.

The intersubband optical absorption between multi energy levels in $\text{In}_x\text{Ga}_{1-x}\text{N}/\text{GaN}$ spherical core-shell quantum dots (CSQDs) and ternary mixed crystal and size effects have been investigated by using the principle of density matrix.^[4] Electronic eigenstates have been calculated by a finite element method. It is found that total optical absorption coefficients (ACs) and refractive index changes (RICs) decrease as increasing incident light intensity I . When I surpasses a certain value, the saturation of total AC and secondary peaks of RIC appears. For a given I , the maximum AC and zero RIC positions in $\text{In}_x\text{Ga}_{1-x}\text{N}/\text{GaN}$ CSQDs with a fixed shell size have a blue-shift when x increases or the radius R_1 of core $\text{In}_x\text{Ga}_{1-x}\text{N}$ decreases. The saturation of ACs or secondary peaks of RICs appears more likely in CSQDs with smaller x or larger R_1 .

These results are expected to be helpful both in the further theoretical and experimental study on optic devices consisting of CSQDs.

References:

- [1] H.-M.K. Alice Castan, and Jin Jang, All-Solution-Processed Inverted Quantum-Dot Light-Emitting Diodes, *Applied Materials and Interfaces*, 6 (2014) 2508-2515.
- [2] J. Vyskočil, P. Gladkov, O. Petříček, A. Hospodková, J. Pangrác, Growth and properties of IIIIV QD structures for intermediate band solar cells, *Journal of Crystal Growth*, 414 (2015) 172-176.
- [3] D. Yanover, R.K. Čapek, A. Rubin-Brusilovski, R. Vaxenburg, N. Grumbach, G.I. Maikov, O. Solomeshch, A. Sashchiuk, E. Lifshitz, Small-Sized PbSe/PbS Core/Shell Colloidal Quantum Dots, *Chemistry of Materials*, 24 (2012) 4417-4423.
- [4] I.b. Karabulut, S. Baskoutas, Linear and nonlinear optical absorption coefficients and refractive index changes in spherical quantum dots: Effects of impurities, electric field, size, and optical intensity, *Journal of Applied Physics*, 103 (2008) 073512.

Directionally solidified Ce:LaBr₃/ CaBr₂ eutectic scintillator for radiation imaging applications

Kei Kamada^{1,2}, Hiroyuki Chiba³, Shunsuke Kurosawa¹, Yasuhiro Shoji^{2,3}, Yuji Ohashi³, Yuui Yokota¹, and Akira Yoshikawa^{1,2,3}

¹Tohoku University, New Industry Creation Hatchery Center, Sendai, 980-8579, Japan

²C&A corporation, T-Biz, 6-6-10 Aoba, Aramaki, Aoba-ku, Sendai, 80-8579, Japan

³Tohoku University, Institute for Material Research, Sendai, 980-8577, Japan

Recently submicron-diameter phase-separated scintillator fibers (PSSFs) were reported and they possessed both the properties of an optical fiber and a radiation-to-light conversion. The PSSFs were fabricated using a directionally solidified eutectic (DSE) system. The DSE systems have been discovered in various materials for many applications. Up to now, CsI/NaCl and GdAlO₃/Al₂O₃[1] have been already reported as PSSFs for high resolution X-ray imaging application. Ce:LaBr₃ has attracted attention due to its high light yield of 61000photons/MeV and fast decay time of 25 ns with enough density of 5.1 g/cm³ for x-ray and g-ray detection [2]. In this research, exploration of PSSFs by directional crystal growth method will be reported. In this study, Ce doped LaBr₃/CaBr₂ eutectics were explored. Crystal growth was performed by Bridgeman (BZ) method at the eutectic point. Investigations of their crystal structure and eutectic phase were performed. Luminescence and scintillation properties were also evaluated.

Ce doped LaBr₃/CaBr₂ eutectics were grown by the BZ method in a quartz ampoule with 8mm inner diameter. Mixed powders were induced into the ampoule under high purity Ar atmosphere in a glove box. Growth rate was 0.3 mm/min. Circular samples with 1-mm thickness were obtained from the grown crystal. Fig.1 shows photographs of as-grown eutectic (a) and 1mm thick polished sample along transverse cross-section (b). The eutectic showed well aligned eutectic structure (Fig.2) with around 5 mm diameter Ce:LaBr₃ fibers and optically transparent like bundled optical fibers. Grown Ce doped LaBr₃/CaBr₂ eutectic shows 360 nm emission ascribed to Ce³⁺ 4f-5d transition under X-ray excitation. Pulse height spectra of the sample was showed in Fig.3. The light yield was around 60% of Ce:Lu₂SiO₄ (LYSO) scintillator standard and 20000 photon/MeV. Scintillation decay time under 662keV g -ray was 21.9 ns (61%) 175 ns 39%)

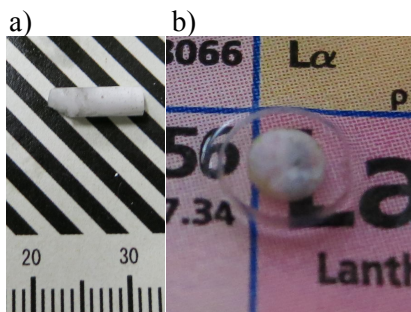


Fig. 1. Photographs of grown eutectic (a), as-grown (b) and 1mm thick polished sample along transverse cross-section.

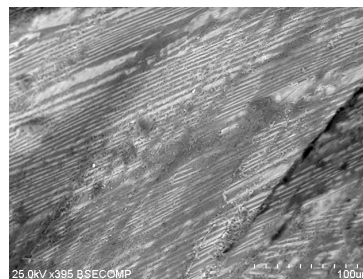


Fig. 2. Back scattered electron image of longitudinal cross-section. (White:LaBr₃, Black:CaCl₂)

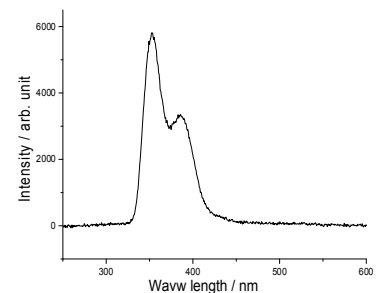


Fig. 3. Radioluminescence spectra of the grown eutectic. (x-ray from CuKα, 40mV 40mA)

References:

- [1] Y. Ohashi, et. al., App. Phys. Lett. 102, (2013) 051907.
- [2] E. V. D. van Loef et al., Nucl. Instr. Method A, 486 (2002) 254

Electronic Structure of Optical Properties of Host Material ($\text{Gd}_2\text{O}_2\text{S}$, Gd_2O_3 and $\text{Gd}_2\text{O}_{3-x}\text{S}_x$) for Upconversion Phosphor Computational Modeling

Fei Wang, Xiumin Chen, Bin Yang, DachunLiu, QingchunYu

1 National Engineering Laboratory for Vacuum Metallurgy, Kunming University of Science and Technology, Kunming 650093, People's Republic of China

2 Key Laboratory for Nonferrous Vacuum Metallurgy of Yunnan Province, Kunming, Yunnan, 650093, People's Republic of China

3 State Key Laboratory of Complex Nonferrous Metal Resources Clear Utilization in Yunnan Province, Kunming 650093, People's Republic of China

4 Department of Materials Engineering, KU Leuven, 3001 Leuven, Belgium

Solid state reaction in vacuum for the preparation of rare earth sulfide upconversion luminescent materials is proposed in this paper. Influence of vacuum on crystal growth and the formation mechanisms of impurity phase are investigated. The solid solution is formed by the host and impurity phase i.e. rare earth oxide which is ready to be produced in the solid-state reaction process in certain range, to realize wide band absorption, cooperative luminescence and highly enhanced upconversion efficiency. Thus, the choice of the host matrix is very crucial. Not only its structure should be amenable to accommodating the rare earth ion, but also, the local site symmetry should be appropriate for it to efficiently receive energy from host (in case if energy transfer) and show luminescence. It should also have wide band gap and low phonon energy to minimise the non-radiative energy loss. In this paper, we simulate geometry, electronic structure and spectroscopic properties of rare earth ions activated gadolinium oxysulfide and gadolinium oxide on the basis of substitution of oxygen and sulfur atoms, from the standpoint of the first-principles calculation to demonstrate effect of impurity atmos on microstructure of host, luminescence properties and internal energy transfer mechanism theoretically. The calculation has pointed out the theoretical basis and experimental possibility for luminescence regulation and enhancement, to explore the behavior of microstructure change on internal energy transfer mechanism. Meanwhile, the results aforementioned will be employed to guide the preparation and improvement of novel and high-efficiency upconversion luminescence materials.

Email: fei.wang@kuleuven.be

Giant negative magnetoresistance in oxygen-deficient Mn-substituted ZnO

X. L. Wang¹, Q. Shao¹, R. Lortz², J. N. Wang², A. Ruotolo¹

¹Department of Physics and Materials Science, City University of Hong Kong, Kowloon, Hong Kong, SAR China

²Department of Physics, Hong Kong University of Science and Technology, Kowloon, Hong Kong, SAR China

Magnetic thin films change their resistance under the application of a magnetic field. This magnetoresistive effect can be engineered to become *giant* by resorting to metallic multilayer devices [1,2]. An alternative route is the magnetically induced metal-insulator transition shown by strongly correlated semiconductors like mixed-valence manganites [3]. Yet, the application of these materials is limited by the difficulty and cost of fabrication. We here show that a negative magnetoresistance as large as several hundreds percent can be induced in simple zinc oxide (ZnO) doped with manganese (Mn) [4]. This anomalous effect was found to appear in oxygen-deficient films and to increase with the concentration of dopant. By combining magnetoresistive measurements with magneto-photoluminescence, we demonstrate that the effect can be explained as the result of a magnetically induced transition from hopping-type to metallic-type band conduction where the activation energy is caused by the *sp-d* exchange interaction.

The study was carried out on films of $Zn_{1-x}Mn_xO$ with $x = 0$ (pure ZnO), 0.02, 0.04 and 0.08. Oxygen vacancies (V_O 's) were introduced in the films by increasing the temperature of the substrate and decreasing the oxygen partial pressure during growth. A detailed characterization of our films showed that all the Mn is in valence 2+, therefore Mn-O-Mn double-exchange interaction can be ruled out [5]. As the temperature is reduced, the resistivity of the films increases with distinct signatures of a transition from band- to hopping-conduction. A sharp decrease of resistance of the Mn-substituted films was measured when an external magnetic field was applied. The change of resistivity was found to increase with the concentration of Mn.

Since ZnO is a transparent semiconductor, the magnetic activation of electrons to the band conduction can be probed by resorting to magneto-photoluminescence measurements. In fact, V_O 's are optically active defect centers that can form mono centric or pair exciton complexes at low temperatures. In our films, the oxygen vacancies form deep-level *F*-centres, where electrons are localized when the temperature is reduced. Electrons can hop between Mn- V_O complexes under the application of an electric field. An applied magnetic field reactivates the electrons in the conduction band, resulting in a sharp drop of resistivity.

References:

- [1] M. N. Baibich et al., Phys. Rev. Lett., **61**(1988) 2472.
- [2] G. Binasch et al., Phys. Rev. B **39**(1989) 4828.
- [3] A.-M. Haghiri-Gosnet et al., J. Phys. D: Appl. Phys. **36**(2003) R127.
- [4] X. L. Wang et al., Sci. Rep. **5**(2015) 9221.
- [5] Q. Shao, J. Appl. Phys. **115**(2014) 153902.

Epitaxial Seeded Growth of Rare Earth Nanocrystals with Efficient 800 nm Near-Infrared to 1525 nm Short-Wavelength Infrared Downconversion Photoluminescence for *in vivo* Bioimaging

Rui Wang, Xiaomin Li, Lei Zhou and Fan Zhang*

Department of Chemistry, Fudan University, Shanghai 200433, China

zhang_fan@fudan.edu.cn, (+86)21-51630322

Abstract

Photoluminescent (PL) labels have been widely used for biological applications, primarily in bioimaging and assays. Recently, much attention has been focused on the development of PL nanoprobes with excitation/emission maxima falling in the region between 650 and 1000 nm, an “imaging window”. However, the penetration depth of light in this “biological transparency window” only reaches several millimetres. Thus, a new imaging method incorporating high spatial resolution, fast feedback, and deep tissue penetration depth is desired to optimize the accuracy and sensitivity of PL-based biomedical imaging. Herein, we fabricated a novel kind of β -NaGdF₄/Na(Gd,Yb)F₄:Er/NaYF₄:Yb/NaNdF₄:Yb core/shell1/shell2/shell3 (C/S1/S2/S3) multi-shell nanocrystals (NCs) as an efficient 800 nm NIR to 1525 nm Short-Wavelength Infrared (SWIR) probe for *in vivo* bioimaging. 800 nm excitation is located in the “biological transparency window” with low water absorption and heat generation, and is considered to be the ideal excitation wavelength with the least impact on biological tissues. After phospholipids coating, the water soluble NCs showed good biocompatibility and low toxicity. With efficient SWIR 1525 nm emission, the probe is detectable in deep tissues up to 18 mm with low detection threshold concentration (5 nM for stomach of nude mice and 100 nM for stomach of SD rats). These results highlight the potential of the probe for specific detection and therapy monitoring of hard-to-detect areas.

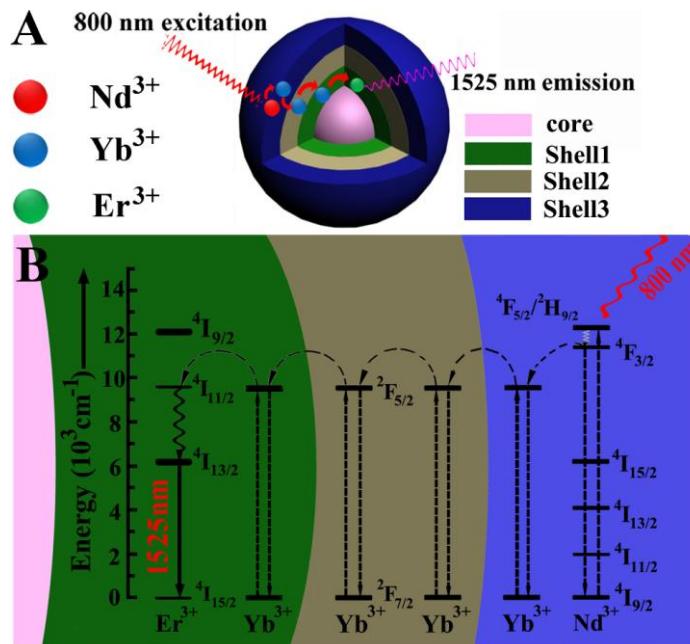


Figure 1 (A) Schematic design of the C/S1/S2/S3 NCs for 1525 nm luminescence. (B) Proposed energy transfer mechanisms in the multi-layer core/shell NCs.

References

1. R. Wang, X. Li, L. Zhou, F. Zhang*, *Angew. Chem.-Int. Edit.* **2014**, *53*, 12086-12090.
2. R. Wang, F. Zhang*, *J. Mater. Chem. B* **2014**, *2*, 2422-2443.

Poster Session II -70

3. X. Li, R. Wang, F. Zhang*, L. Zhou, D. Shen, C. Yao, D. Zhao*, *Sci. Rep.* **2013**, *3*, 3536.
4. L. Zhou, R. Wang, C. Yao, X. Li, C. Wang, X. Zhang, C. Xu, A. Zeng, D. Zhao, F. Zhang*, *Nat. Commun.* **2015**, *6*, 6938.
5. X. Li, R. Wang, F. Zhang*, D. Zhao*, *Nano Lett.* **2014**, *14*, 3634– 3639.

Single-band upconversion nanoprobe for multiplexed simultaneous in situ molecular mapping of cancer biomarkers

Lei Zhou, Rui Wang, Dongyuan Zhao and Fan Zhang*

Department of Chemistry, Fudan University, Shanghai 200433, China
zhang_fan@fudan.edu.cn, (+86)21-51630322

Abstract

The identification of potential diagnostic markers and target molecules among the plethora of tumour oncoproteins for cancer diagnosis requires facile technology that is capable of quantitatively analysing multiple biomarkers in tumour cells and tissues. Diagnostic and prognostic classifications of human tumours are currently based on the western blotting and single-colour immunohistochemical methods that are not suitable for multiplexed detection. Herein, we report a general and novel method to prepare single-band upconversion nanoparticles with different colours. The expression levels of three biomarkers in breast cancer cells were determined using single-band upconversion nanoparticles, western blotting and immunohistochemical technologies with excellent correlation. Significantly, the application of antibody-conjugated single-band upconversion nanoparticle molecular profiling technology can achieve the multiplexed simultaneous in situ biodetection of biomarkers in breast cancer cells and tissue specimens and produce more accurate results for the simultaneous quantification of proteins present at low levels compared with classical immunohistochemical technology.

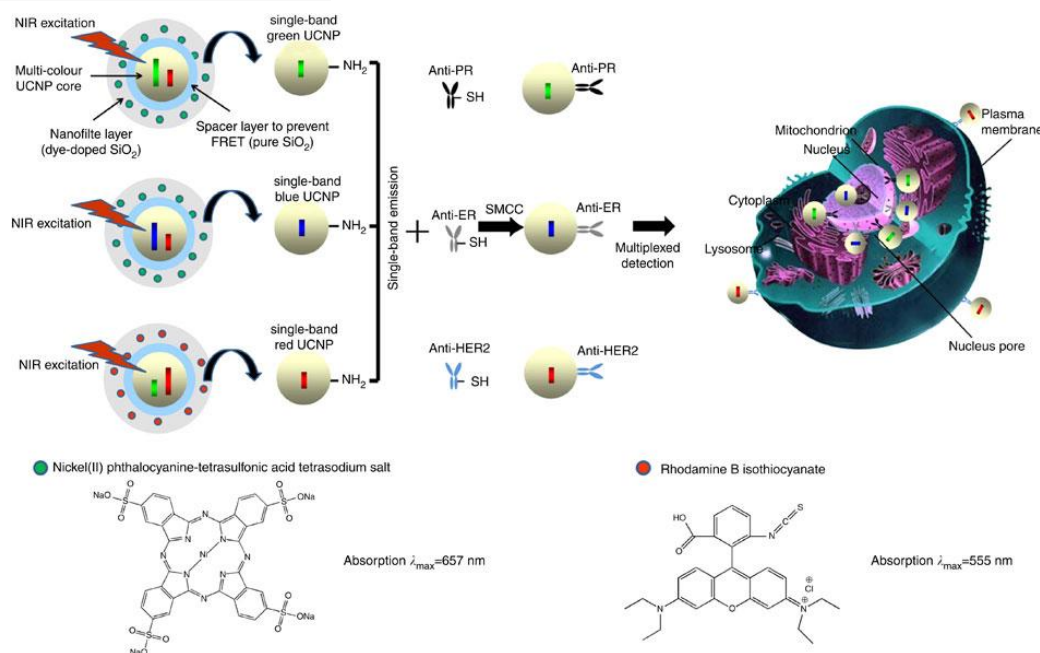


Figure 1 Schematic diagram of the single band upconversion nanoprobe fabrication for multiplexed in situ molecular mapping of breast cancer biomarkers.

References

1. Lei Zhou, Rui Wang, Chi Yao, Xiaomin Li, Chengli Wang, Xiaoyan Zhang, Congjian Xu, Aijun Zeng, Dongyuan Zhao, Fan Zhang* *Nat. Commun.*, **2015**, 6, 6938.
2. Xiaomin Li, Lei Zhou, Yong Wei, Ahmed Mohamed El-Toni, Fan Zhang*, Dongyuan Zhao* *J. Am. Chem. Soc.*, **2014**, 136, 15086-15092.
3. Xiaomin Li, Lei Zhou, Yong Wei, Ahmed Mohamed El-Toni, Fan Zhang*, Dongyuan Zhao* *J. Am. Chem. Soc.*, **2015**, 137, 5903-5906.

A many-particle quantum-kinetic formalism for describing emission properties of single quantum objects in frozen environments

Maxim G. Gladush^{1,2,3}, **Andrei V. Naumov**^{1,2,3}

¹ *Institute for Spectroscopy of Russian Academy of Sciences, Troitsk Moscow, Russia*

² *Moscow State Pedagogical University, Moscow, Russia*

³ *Moscow Institute of Physics and Technology, Moscow, Russia*

www.single-molecule.ru

We demonstrate methodological notes that are essential in the theory of light emission by a single quantum system when dynamics of its excited states and radiative properties are strongly dependent on both – its macroscopic host and the nearby environment on the nanoscale. Although most experimental data suggest that the properties of a light emitter are determined by its interaction with other quantum objects and the host medium at the micro, meso and macro scales the existing theories have been either model dependent or limited to some particular situations. The majority of the theoretical approaches are aimed at determining the change in the rate of spontaneous decay of an excited single particle in a given environment compared to its spontaneous emission in a vacuum. In the literature, these approaches are conventionally divided into "microscopic" and "macroscopic" models. The common points in the models are to take into account the following: modifications of intrinsic properties of the emitting center, the structure of the local field and the change in density of photonic states.

Of particular interest is the problem of studying the properties of optical centers in a host medium in the presence of an external laser radiation. The mathematical apparatus used in laser physics, nonlinear and quantum optics, and other research in the area of interaction of radiation with the matter is largely based on an analysis of Maxwell-Bloch (MB) equations. To date, there is limited number of papers giving MB equations, which take into account in a consistent manner the effective values of all parameters: Rabi frequency, frequency shifts and the rates of relaxation/excitation mechanisms (including spontaneous emission and energy transfer in pairs). In this work, we derived a generalized master equation emitters forming an ensemble of motionless optical centers in a dielectric medium, transparent for the external light. The master equation was used to build the material part of MB, i.e., the system of optical Bloch equations. It takes into account the effective rates of individual and collective radiative damping of optical centers, the Rabi frequencies, and frequency shifts of the optical transitions caused by the presence of a dielectric host and other quantum objects. The MB parameters were found to be functions of the real and imaginary parts of the host permittivity. The lifetimes of the excited state of the emitters were shown to be functions of the effective refractive index n of the host around the emitter and be in agreement with the experimental data.

Finally, we discuss the possibility of nanoscale mapping of effective n -values in frozen dye-doped solutions by single-molecule spectromicroscopy.

This work was supported by RFBR (14-29-07270; 16-02-01174).

References:

- [1] D.V. Kuznetsov, V.K. Roerich, M.G. Gladush, *J. Exp. Theor. Phys.*, 113, 647 (2011).
- [2] T.A. Anikushina, M.G. Gladush et al., *Faraday Discussions*, 184, 263 (2015).

Author Index

- Abashev R., 128
Abashev Rinat, 205
Afanasyev Dmitriy, 110, 153
Afzelius Mikael, 51, 67
Aguilo Magdalena, 22
Agullo-Lopez Fernando, 47, 131
Ahlefeldt Rose, 50
Aimaganbetova Zuhra, 116
Aizpurua Javier, 20, 22
Akahane Kouichi, 162, 163
Akhtyamov Oleg, 191
Akimoto Ikuko, 64
Alakshin Egor, 236
Alvarez Angel Luis, 98
Alvarez-Fraga Leo, 21
Alyatkin Sergei, 152
Amer Mariam, 212
Andrey Naumov, 31
Anikushina Tatiana, 31
Anisimov P., 87
Aonuma Naoto, 162
Arndt Nathan, 233
Asai Keisuke, 193
Awater Roy, 107
- Bachiller-Perea Diana, 47, 131
Baltabekov Askhat, 124, 182
Ban Shi-Liang, 241
Ban Shiliang, 192
Bao Yupan, 72
Baran Anna, 122
Barandiarán Zoila, 76
Barclay Paul, 57, 58
Barmina Alexandra, 116
Barreda-Argueso Antonio, 121
Barros Anthony, 46
Bartholomew John, 145, 159
Barzowska Justyna, 114, 179, 206
Basche Thomas, 33
Bausa Luisa, 22, 221
Bawitlung Zoliana, 207
Beck Franziska, 144
Beeler Mark, 83
Belsky A., 128
- Bercha Artem, 77
Berkowski Marek, 112
Bernal Rodolfo, 219, 220
Bettinelli Marco, 94, 180
Biner Daniel, 76
Binet Laurent, 225
Bingfu Lei, 96
Bitam Adel, 119
Blankenship Robert, 18
Bliznjuk Olga, 210
Blower Philip, 27
Bondzior Bartosz, 59, 111
Bonhomme Christian, 225
Bonvalet Adeline, 15
Borysiuk Jolanta, 83
Bos Adrie, 42, 43
Bottger Thomas, 69
Boutinaud Philippe, 46, 212
Boye Daniel, 233
Broyer Michel, 24
Bunzli Jean-Claude, 25
Burner Pauline, 186
- Cai Jiajia, 237
Cai Peiqing, 117, 118
Camarillo Enrique, 121
Camarillo Ignacio, 121
Campidelli Stephane, 151
Camy Patrice, 41
Cao Zhongmin, 198
Carminati Remi, 56
Carrasco Irene, 180
Carvajal Joan, 22
Casabone Bernardo, 144
Cefalas Alciviadis-Constantinos, 191
Chadeyron Genevieve, 46, 174
Chamma Didier, 17
Chaneac Corinne, 185, 225
Chaneliere Thierry, 70
Chauvet Anne, 70
Chawngthu Rosangliana, 235
Chen Cuili, 117, 118
Chen Jincan, 155
Chen Xueyuan, 26

Chen Yonghu, 211, 237
 Chen Yu-Hui, 71
 Chen Zhuo, 155
 Chiba Hiroyuki, 242
 Chin Wutharath, 17
 Cho Youngmin, 102
 Choi Heelack, 102–104, 143
 Chronister Eric, 84
 Climent-Pascual Esteban, 21, 98
 Coelho-Diego Cristina, 225
 Cone Rufus, 57, 58, 69
 Cordier Stephane, 39
 Costuas Karine, 39
 Coya Carmen, 98
 Crepin Claudine, 17
 Crut Aurelien, 24
 Cruz-Vazquez Catalina, 219, 220
 Cruzeiro Emmanuel, 51
 Cui Xianjin, 27

 Dai Z., 141
 Daniault Louis, 15
 De Andres Alicia, 21, 98
 De Jong Mathijs, 76
 De Oliveira Lima Karmel, 145
 De Riedmatten Hugues, 68, 144
 Deboo Gabriele, 52
 Dedic Roman, 157
 Del Fatti Natalia, 24
 Delpont Geraud, 150, 151
 Deren Przemyslaw, 12, 59, 99–101, 111, 122
 Deshko Yury, 49
 Diaf Madjid, 119
 Diaz Elena, 156
 Diaz Francesc, 22
 Dixon Ned, 200
 Dobrovolsky Alexander, 35, 147
 Dominguez-Adame Francisco, 156
 Dong Hao, 28
 Dorenbos Pieter, 42, 43, 106, 107, 196
 Dreyer E.f.c., 87
 Duan Chang-Kui, 211, 237
 Dyu Valeriya, 130

 Eisfeld Alexander, 34
 Eremchev Ivan, 31
 Escobar-Ochoa Flor, 220
 Esparza J. U., 23
 Eurov Daniil, 149

 Fan Zhang, 247
 Fang Hongwei, 211

 Farukhshin Ilnur, 127
 Fedorenko Stanislav, 30
 Fedorov N., 128
 Fei Wang, 243
 Feldbach Eduard, 123
 Feng Wei, 222, 223
 Feng Xinlinag, 151
 Feofilov Sergey, 11
 Fernandez-Gonzalvo Xavier, 71
 Ferraro Angelo, 236
 Ferrier Alban, 70, 113, 144, 145, 159, 186, 240
 Fisher A.a., 87
 Flores Cristina, 121
 Fritz Linda, 200
 Fujimoto Yutaka, 184, 193
 Fukuda Kentaro, 184
 Furukawa Yoshiaki, 81, 195, 203

 Galaup Jean-Pierre, 17
 Gautier-Luneau Isabelle, 186
 Georgescu Serban, 202
 Gheorghe Cristina, 187–189
 Gillin William, 27
 Giorgis Valentina, 154
 Gisin Nicolas, 51
 Gladush Maxim, 31, 248
 Glais Estelle, 185
 Glowacki Michal, 112
 Gold Alfred, 82
 Goldner Philippe, 70, 113, 144, 145, 159, 240
 Golovanova Alina, 31
 Golubev Valerii, 149
 Gonzalez-Fernandez J. V., 142
 Gonzalo Alicia, 232
 Gorbenko Galina, 194
 Gorbenko Vitaliy, 194
 Gorecka Natalia, 179, 206
 Gorokhovskiy Anshel, 49
 Gorshelev Alexey, 31
 Grasset Fabien, 39
 Green Mark, 27
 Grinberg Marek, 44, 97, 114, 122, 178, 179, 206
 Grzanka Ewa, 83
 Grzeszkiewicz Karina, 199
 Guimarães Vinicius, 186

 Haiyong Ni, 204
 Hala Jan, 157
 Han T. P. J., 158
 Hansch Theodor, 144
 Hao Haoyue, 230
 Hartmann Thomas, 86

Hau Stefania, 187–189
 Hernandez Ignacio, 27
 Hernandez Jose Manuel, 121
 Hernandez-Pinilla David, 221
 Hillenkamp Matthias, 24
 Hinze Gerald, 33
 Hizhnyi Yuriy, 132
 Hongbin Liang, 204
 Horvath Sebastian, 52, 160
 Hreniak Dariusz, 199
 Hu Fangfang, 237
 Hu Ping, 155
 Hu Yunbin, 151
 Huang Lihui, 137
 Huang Mingdong, 155
 Huang Ping, 26
 Huang Yan, 196
 Hummer Thomas, 144
 Hunger David, 144
 Hush Michael, 50

 Ibanez Alain, 186
 Ibrayev Niazbek, 153
 Ibrayev Niyazbek, 110, 234
 Ihor Syvorotka, 109
 Ikesue Akio, 159, 187–189
 Ilyassov Baurzhan, 234
 Inoue Jun-Ichi, 166
 Ishchenko A., 128
 Ishida Kunio, 126
 Ivanov S., 175
 Ivanovskikh K., 128
 Ivanovskikh Konstantin, 120
 Iyer Muley Aarti, 197

 Jang Der-Jun, 129
 Jankowiak Ryszard, 18
 Jankowski Dawid, 77, 83
 Jansen Thomas, 123
 Jaque F., 158
 Jaque Francisco, 121
 Jayasankar C K, 133, 134
 Jelezko Fedor, 48
 Jeon Byungjoo, 102–104, 143
 Jeong Youngwoo, 102
 Jiao Huan, 217
 Jimenez-Rey David, 47, 131
 Jimenez-Villacorta Felix, 21
 Jin Ye, 44, 178
 Joffre Manuel, 15
 Jongsu Kim, 102, 103
 Jorg Wrachtrup, 224

 Joshi Charusheela, 183, 238
 Juarez-Perez Emilio, 98
 Junko Ishi-Hayase, 162, 163
 Justel Thomas, 123

 Kabanau Dzmitry, 138, 139
 Kabanava Volha, 138
 Kador Lothar, 31
 Kaldvee Kaarel, 30
 Kallaev Suleyman, 214, 215
 Kamada Kei, 242
 Kamenskikh Irina, 175
 Kaminska Agata, 83
 Kanemitsu Yoshihiko, 38
 Kang Taewook, 102–104, 143
 Kargin Yury, 130
 Karlsson Jenny, 145, 240
 Karlsson Maths, 180
 Kawano Naoki, 193
 Kell Adam, 18
 Kemlin Vincent, 15
 Khaidukov Nikolai, 123
 Khaydukov Evgeniy, 152
 Khiari Saidi, 119
 Khudyakova Elena, 130
 Kiisk Valter, 108
 Kim Daegwi, 227
 Kim Daehan, 102, 143
 Kim Gotaek, 102, 103
 Kim Hyojun, 102–104, 143
 Kim Jongsu, 104, 143
 Kim Sun Il, 117, 118
 Kim Taehoon, 102–104
 Kirm Marco, 60, 123
 Kisteneva Marina, 130, 173
 Kleshchev Nikolaj, 210
 Kohler Jurgen, 31
 Kohlmann Holger, 115
 Koketai Temirgaly, 124, 182
 Kolesov Roman, 224
 Kong Xianggui, 73
 Korableva Stella, 127, 236
 Kornher Thomas, 224
 Kornienko Tatiana, 173
 Korona Krzysztof, 83
 Koshimizu Masanori, 184, 193
 Kramer Karl, 75, 76
 Krashenninovicova Alina, 236
 Kravets Oleg, 109
 Krebs John, 200
 Kroll Stefan, 72, 240
 Krukowski Stanislaw, 83

Krutyak Nataliya, 175
 Kunkel Nathalie, 115, 159
 Kurdyukov Dmitrii, 149
 Kurosawa Shunsuke, 242

 Lakhdar Guerbous, 174
 Lalov Ivan, 86
 Lapierre Ray, 82
 Laplane Cyril, 51
 Lastusaari Mika, 181
 Laudereau Jean-Baptiste, 70
 Lauret Jean-Sebastien, 151
 Lavin Victor, 133, 134
 Lavoie Jonathan, 51
 Lazarowska Agata, 44, 97
 Lebiadok Yahor, 138, 139
 Ledoux Gilles, 37
 Lee Wunho, 102–104, 143
 Lee Yong-Sin, 227
 Lei Zhou, 247
 Lemanski Karol, 59
 Lenhard Andreas, 68
 Leon-Luis Sergio Fabian, 133, 134
 Lesniewski Tadeusz, 44, 114, 178
 Li Chao, 217
 Li Kun, 217
 Li Linsen, 155
 Li Liyi, 95
 Li Qian, 72
 Li Ruxin, 165
 Li Xiaomin, 245, 246
 Li Xinyue, 237
 Li Yang, 28
 Liang Hongbin, 196
 Lin Yuan-Chih, 180
 Liu Chunmeng, 196
 Liu Guokui, 13
 Liu Jiansheng, 165
 Liu Ru-Shi, 44, 97, 178
 Liu Wen-Hao, 241
 Liu Xiaogang, 74
 Liu Xiaomin, 73
 Longdell Jevon, 71
 Look David, 66
 Lorenz Katharina, 232
 Lu Haizhou, 27
 Lu Hongyu³²¹, 231
 Lucheckho Andriy, 109
 Lukyashin K., 128
 Luo Hongde, 43
 Lupei Aurelia, 187–189
 Lupei Voicu, 187–189

 Lutz Thomas, 57, 58

 Macfarlane Roger, 69
 Maestro L. M., 158
 Magi Henri, 123
 Mahiou Rachid, 46, 174
 Mahlik Sebastian, 44, 97, 122, 178
 Maia Lauro, 186
 Maioli Paolo, 24
 Makhov Vladimir, 123
 Maksimov R., 128
 Malyshev Andrey, 154
 Malyshev Victor, 154
 Mamytbekov Zhayloo, 205
 Marisov Mikhail, 125, 127
 Marquardt Christian, 34
 Marques Gilmar, 82
 Marques M. I., 158
 Martin P., 128
 Martin Patrick, 65
 Matsuda Kazunari, 79
 Matsunaga Ryusuke, 61
 Mazzer Margherita, 68
 Meijerink A., 140
 Meijerink Andries, 42, 76, 115, 136
 Mendez Bianchi, 232
 Michalik Daniel, 114
 Milman Igor, 205
 Miniajluk Natalia, 100, 101
 Mohamed Kechouane, 174
 Moharil S., 197
 Molina Pablo, 22, 221
 Mongin Denis, 24
 Monroy Eva, 83
 Monteseuro Virginia, 133, 134
 Monty Claude, 108
 Mothudi Bakang, 219
 Mukhurov Mikolai, 177
 Mullen Klaus, 151
 Muller Markus, 34
 Munoz-Martin Angel, 47, 131
 Munoz-Santiuste Juan E., 176
 Munuera Carmen, 98
 Murakami Hiroshi, 146
 Murakami Katsuya, 81
 Murrieta Hector, 121
 Mussenova Elmira, 124
 Myasnikova Lyudmila, 116

 Nadilko Sergii, 132
 Nagirnyi Vitali, 60, 123
 Nagirnyi Vitaly, 175

Naka Nobuko, 64
 Nakaike Yumi, 38
 Nakayama Masaaki, 81, 164, 195, 203
 Nakayama Sho, 161
 Narita Akimitsu, 151
 Nasu Keiichiro, 126
 Naumov Andrey, 248
 Nechaev Andrei, 152
 Nelson Dmitrii, 149
 Ni Haiyong, 208
 Nilsson Adam, 72, 240
 Ning Lixin, 190
 Nizamutdinov Alexey, 191, 236
 Nizamutdinov Alexey, 125, 127
 Nogales Emilio, 232
 Norrbo Isabella, 181

 Ogurtsov Alexander, 210
 Ohashi Naoki, 39
 Ohashi Yuji, 242
 Okada Go, 184
 Omelkov Sergey, 60
 Orante-Barron Victor, 219, 220
 Orlovskaya Elena, 30
 Orlovskii Yurii, 30
 Orrit Michel, 32
 Osad'ko Igor, 228
 Osipov V., 128
 Ouddai Nadia, 218

 Pae Kaja, 213
 Park Jaehyoung, 102, 104
 Park Kwangwon, 102–104, 143
 Pars Martti, 30
 Paulheim Alexander, 34
 Pavlov Vitaliy, 236
 Pazik Robert, 122
 Pellarin Michel, 24
 Pellerin Morgane, 185, 225
 Peng Mingying, 45, 95
 Peng Yu, 27
 Peng Zeng, 237
 Phuong Le Quang, 38
 Piqueras Javier, 232
 Pisarev Roman, 62, 63
 Platnitskaya Katsiaryna, 138, 139
 Platonov V., 128
 Plaza Jose L., 221
 Potdevin Audrey, 174
 Pote Swapnil, 216
 Prieto Carlos, 21
 Przybylinska Hanka, 114
 Przybylinska Hanna, 112
 Puchalska Margorzata, 77
 Pudovkin Maksim, 236
 Pusep Yuri, 82
 Puust Laurits, 30, 108

 Qian Shan, 137
 Qiao Xusheng, 229
 Qin Yanguang, 237
 Qiu Shijie, 217
 Qu Yuan, 241

 Rabouw Freddy, 136
 Ramaz François, 70
 Ramirez Maria O, 22
 Ramirez Mariola, 221
 Ramirez-Jimenez Rafael, 21
 Rancic Milos, 52
 Rand Stephen, 87
 Reid Michael, 52, 53, 160
 Reineker Peter, 86
 Rielander Daniel, 68
 Rippe Lars, 72, 240
 Robitaille Sarah, 200
 Rodriguez Fernando, 121
 Rodroguéz-Mendoza Ulises, 133, 134
 Roemer Rudolf, 156
 Rogge Sven, 52, 71
 Rolf Reuter, 224
 Rondin Loic, 151
 Ruotolo Antonio, 244

 Saadatkia Pooneh, 66
 Sadykov Sadyk, 214, 215
 Sagymbaeva Shynar, 116
 Saito Norio, 39
 Sakowski Konrad, 83
 Salaun Mathieu, 186
 Salkeyeva Aizhan, 182
 Sanchez-Alejo Marco, 121
 Sanchez-Garcia Laura, 22
 Sarantopoulou Evangelia, 191
 Sarychev M., 128
 Sarychev Maksim, 205
 Sato Yoshitaka, 162
 Savchenko Elena, 85
 Sayaka Kitazawa, 163
 Scheblykin Ivan, 35, 147
 Scherzinger Kerstin, 148
 Scholz Marek, 157
 Seijo Luis, 76
 Selim Farida, 66

Seliverstova Evgeniya, 110
 Sellars Matthew, 50, 52
 Semashko Vadim, 125, 127, 191, 236
 Seo Hyo Jin, 117, 118
 Seraiche Mourad, 174
 Sergejev Daulet, 116
 Seri Alessandro, 68
 Serrano Diana, 240
 Setsuhisa Tanabe, 42
 Shandarov Stanislav, 130, 173
 Sharma Suchinder, 180
 Shavelev Alexey, 125
 Sheik-Bahae Mansoor, 10
 Shi Q., 128
 Shiliang Ban, 209
 Shitov V., 128
 Shoji Yasuhiro, 242
 Shu Kangying, 137
 Shulgin B., 128
 Shunkeyev Kuanyshbek, 116
 Shunkeyev Saginbek, 116
 Shyichuk Andrii, 132
 Sildos Ilmo, 30, 108
 Silversmith Ann, 233
 Sokolowski Moritz, 34
 Sontakke Atul, 95, 186
 Sopicka-Lizer Margorzata, 114
 Spassky Dmitry, 175
 Starukhin Anatolii, 149
 Stefan Angela, 202
 Stefanska Dagmara, 99
 Stoll Tatjana, 24
 Stottinger Sven, 33
 Stovpiaga Ekaterina, 149
 Strak Pawel, 83
 Streck Wieslaw, 199
 Suchocki Andrzej, 77, 112, 114
 Sumioka Takahiro, 164
 Sun Kien Wen, 239
 Sun Ling-Dong, 222, 223
 Sun Lingdong, 28
 Syurdo Aleksandr, 205
 Szczodrowski Karol, 114, 179, 206

 Takahashi Kohji, 227
 Takeuchi Hideo, 164
 Tao Ye, 196
 Tauber Daniela, 35
 Teodoro Marcio, 82
 Thapa Ram, 207
 Thiel Charles, 57, 58, 69
 Thon Raphael, 17

 Thuresson Axel, 72
 Tian Yuxi, 35
 Tiranov Alexey, 51
 Tito Marco, 82
 Tittel Wolfgang, 57, 58
 Toldsepp Eliko, 123
 Tolstik Alexei, 173
 Toma Octavian, 202
 Touati Nadia, 225
 Trzeciakowski Witold, 77
 Tserkezis Christos, 22
 Tu Datao, 26
 Tu Langping, 73
 Tuerxun Aidilibike, 135
 Turmukhambetova Elizaveta, 124
 Tussupbekova Ainura, 124, 182

 Ueda Jumpei, 42
 Unger Eva, 147
 Usmani Imam, 51

 Vacha Martin, 14
 Vainer Yuri, 152
 Valiente Rafael, 75
 Vallee Fabrice, 24
 Van Der Meer Alexander, 160
 Van Hulst Niek F., 16
 Vanetsev Alexander, 30
 Veissier Lucile, 57, 58
 Venkatramu Vemula, 133, 134
 Viana Bruno, 95, 185, 186, 225
 Vielhauer Sebastian, 123
 Viktor Borysiuk, 132
 Villanueva-Delgado Pedro, 75
 Vinklerek Ivo, 157
 Voinov Viktor, 205

 Wada Yoshiki, 39
 Wakamiya Atsushi, 38
 Walther Andreas, 240
 Wang Buguo, 66
 Wang Lingli, 208
 Wang Rui, 245, 246
 Wang Wentao, 165
 Wang Yuxiao, 230, 231
 Wang Z. J., 140
 Warns Christoph, 86
 Watanabe Taichi, 227
 Watras Adam, 100, 101, 122
 Wei Xiantao, 237
 Weiping Qin, 135
 Welinski Sacha, 113

Wells Jon-Paul, 160
Wolos Agnieszka, 112
Wolszczak Weronika, 106
Woodburn Philip, 57, 58
Wu Fei, 73
Wyatt Peter, 27

Xia Kangwei, 224
Xia Zhiguo, 190
Xiao Fangming, 208
Xiaoxiao Huang, 190
Xu Jin, 26
Xu Shiqing, 137
Xu Zhizhan, 165

Yakovlev Dmitri, 55
Yamaoka Suguru, 203
Yan Chun-Hua, 28, 222, 223
Yan Jing, 196
Yanagida Takayuki, 184
Yartsev Arkady, 147
Ye Huanqing, 27
Yin Chunming, 52, 71
Yin Min, 211, 237
Yokota Yuui, 242
Yoshikawa Akira, 242
Yoshioka Kosuke, 80
Yuan Qu, 192, 209
Yuto Arai, 163

Zan Yuhai, 192
Zeinidenov Aslbek, 153
Zelenihin Pavel, 236
Zhang Bingbing, 196
Zhang Fan, 29, 245, 246
Zhang Hong, 73
Zhang Qi, 52
Zhang Qiuhong, 208
Zhang Xueru, 230, 231
Zhang Yaxin, 155
Zhang Yong, 36
Zhanturina Nurgul, 116
Zhao Jialong, 105
Zhao Shen, 151
Zheng Wei, 26
Zhong Jiuping, 201
Zhou Jianbang, 196
Zhou Lei, 245, 246
Zhou Shanyong, 26
Zhou Xiaojuan, 226
Zhu Haiming, 9
Zhuo Gu, 209

Zhydachevskii Yaroslav, 112
Zhydachevskyy Yaroslav, 114
Zuo Jing, 73